



Measurement of W bosons in p-Pb at 8.16 TeV and of charmonia in Pb-Pb at 5.02 TeV with the CMS detector at the LHC

André Govinda Ståhl Leiton

Rapporteurs: Boris Hippolyte

Lydia Roos

Examinateurs: Albert de Roeck

Begoña de la Cruz Martínez

Carlos A. Salgado

Sophie Henrot-Versillé

Directeur de thèse: Raphaël Granier de Cassagnac

Outline

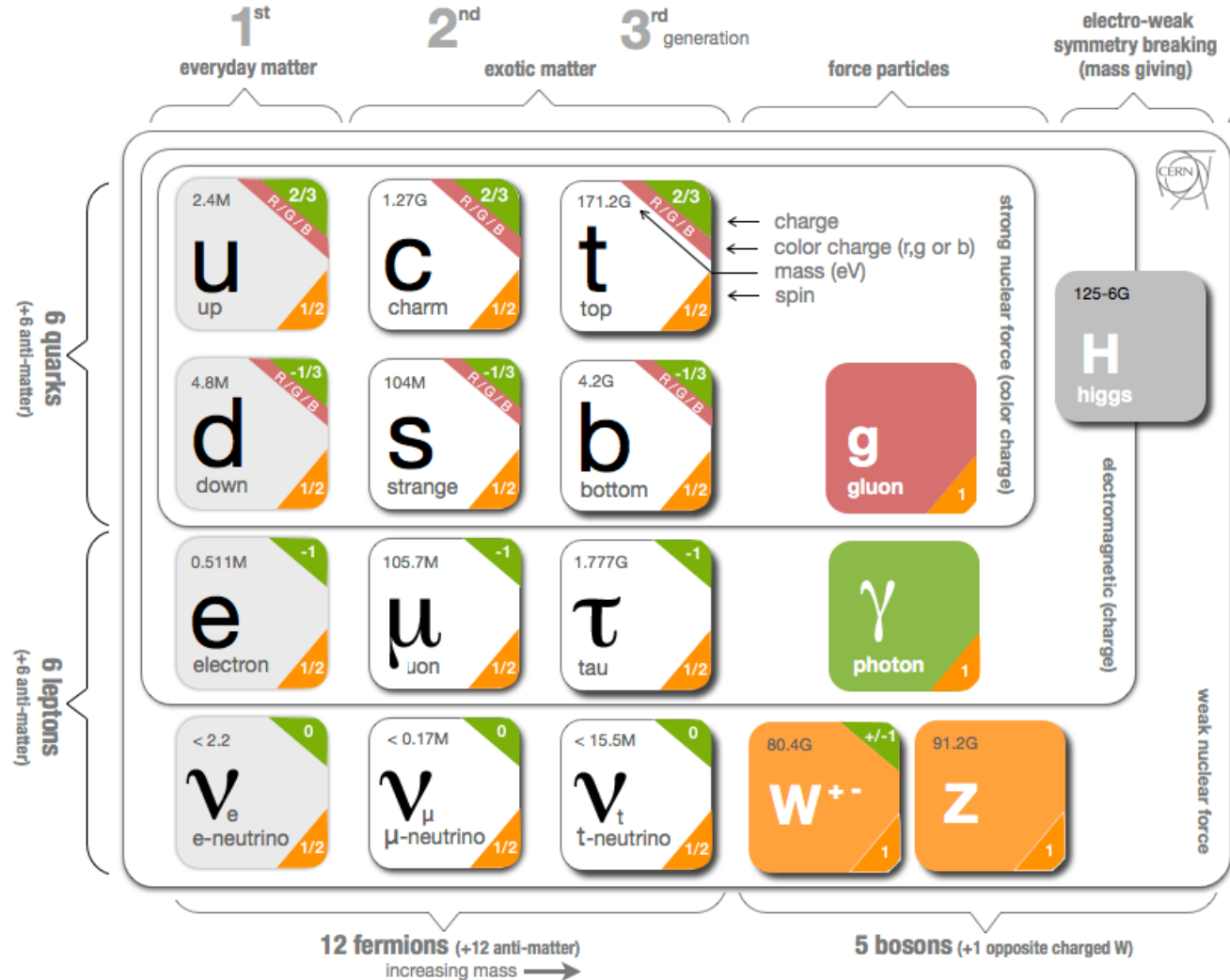
- Theoretical context
- The CMS detector at the LHC
- W-boson production in p-Pb at 8.16 TeV
 - Introduction
 - Analysis
 - Results
- Charmonium production in Pb-Pb at 5.02 TeV
 - Introduction
 - Analysis
 - Results
- Conclusions

Outline

- **Theoretical context**
- The CMS detector at the LHC
- W-boson production in p-Pb at 8.16 TeV
 - Introduction
 - Analysis
 - Results
- Charmonium production in Pb-Pb at 5.02 TeV
 - Introduction
 - Analysis
 - Results
- Conclusions

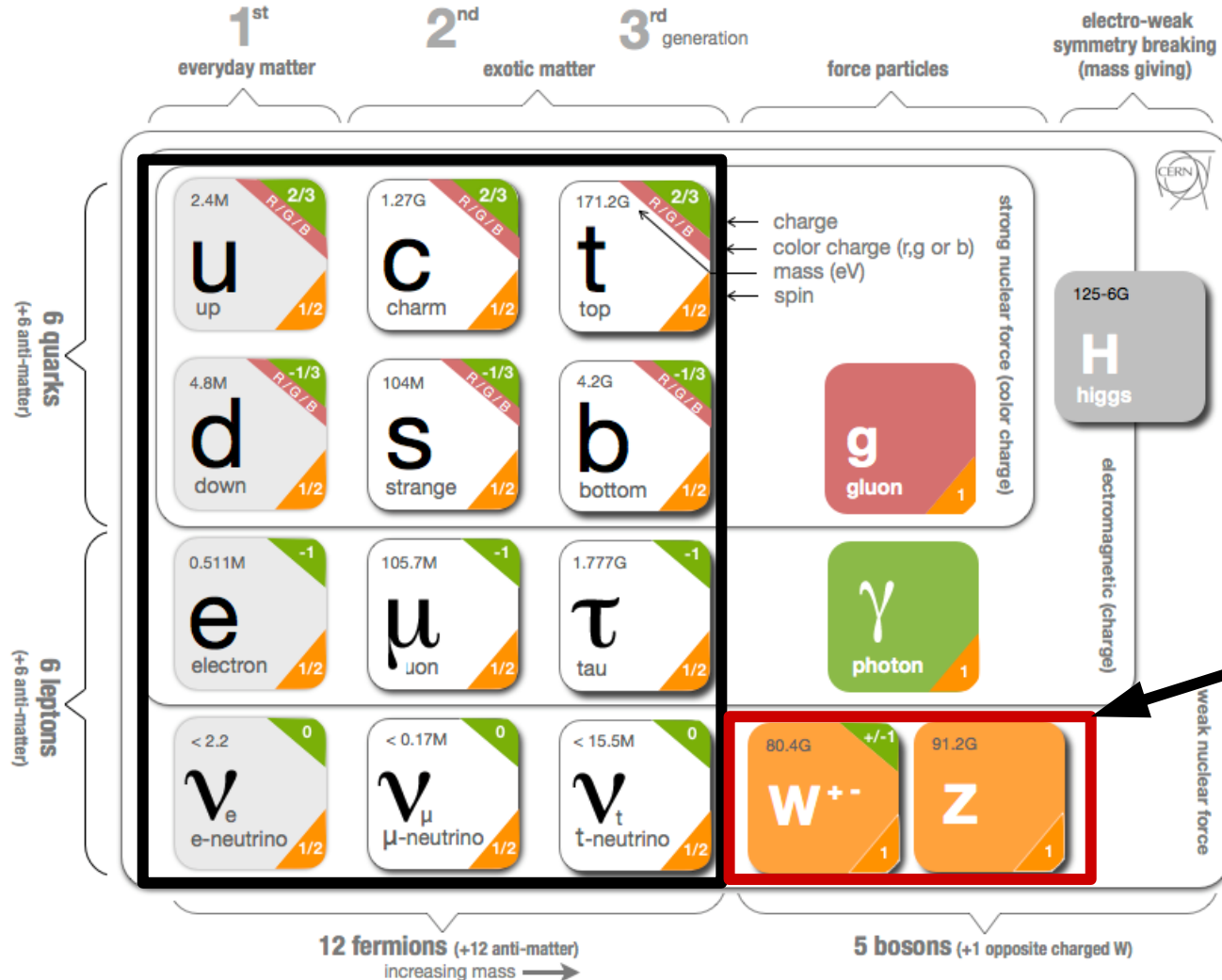
Standard Model of particles

The standard model describes three fundamental interactions



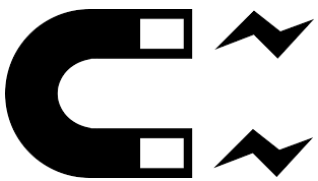
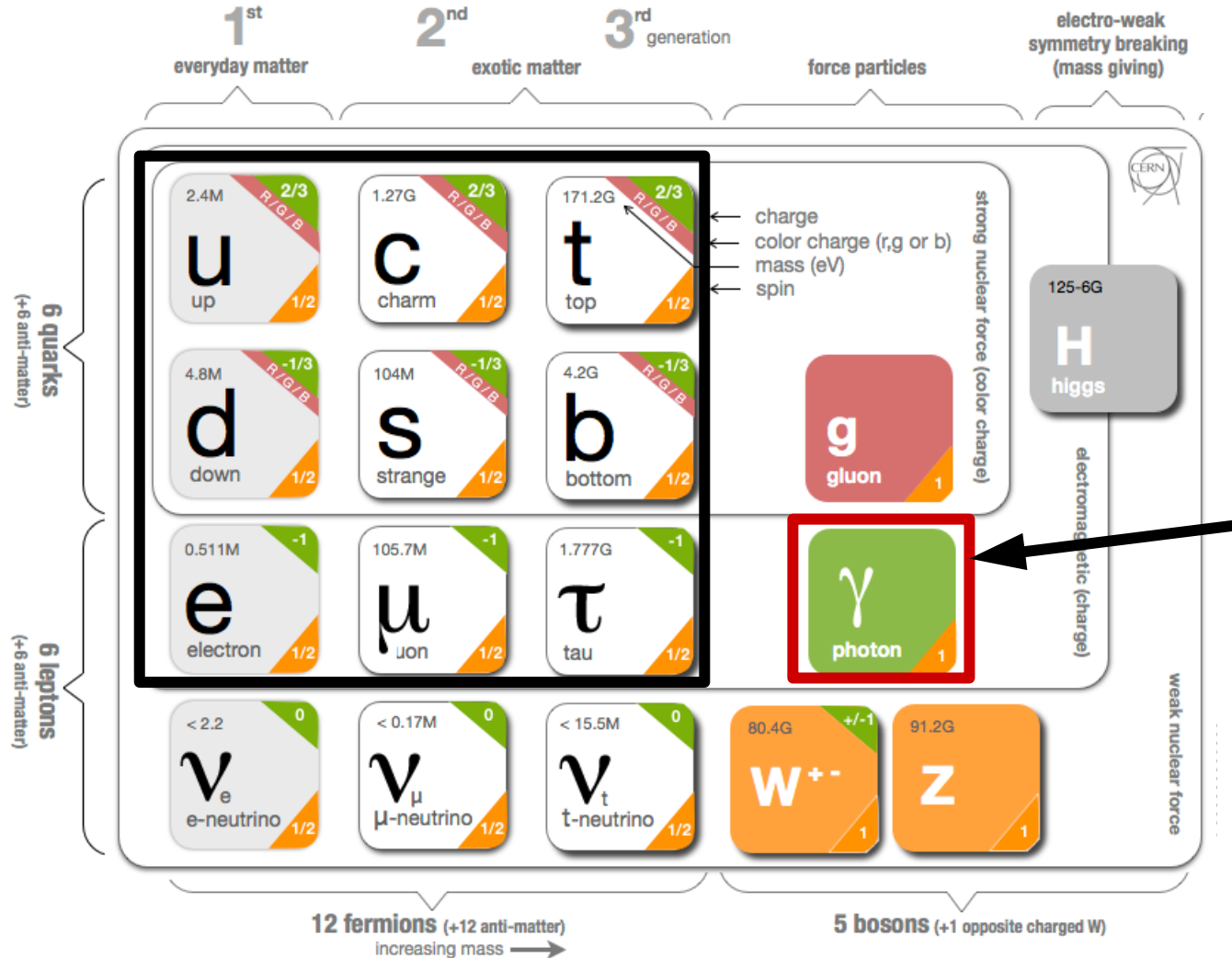
Standard Model of particles

The weak interaction



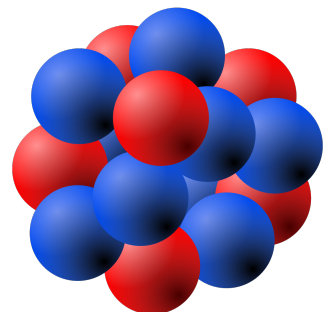
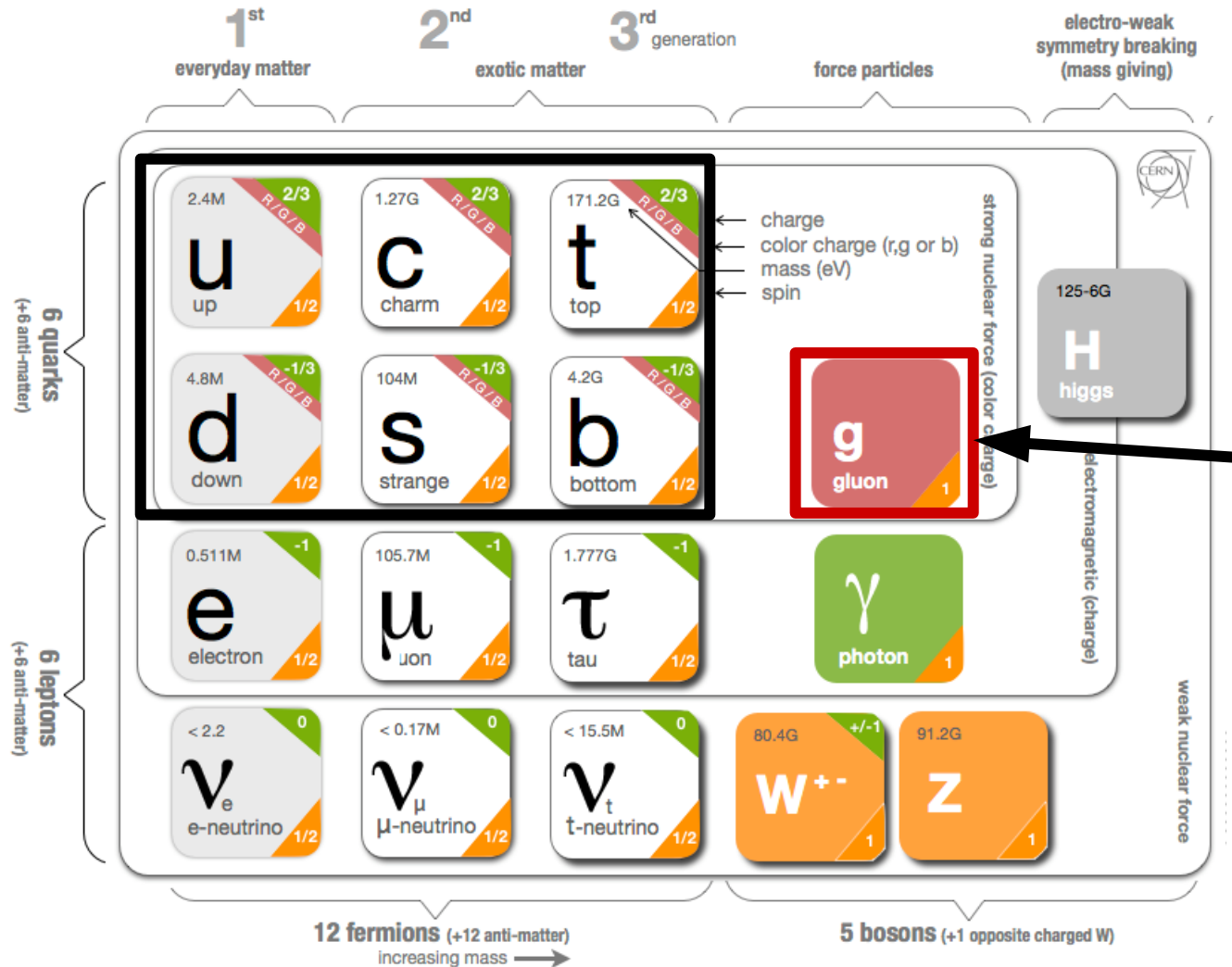
Standard Model of particles

The electromagnetic interaction



Standard Model of particles

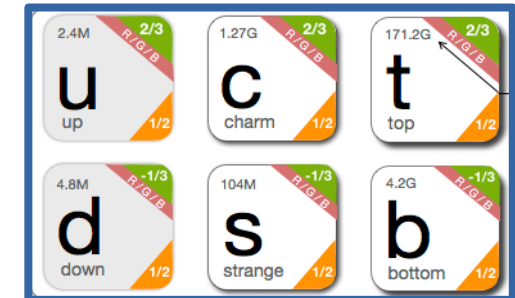
The strong interaction



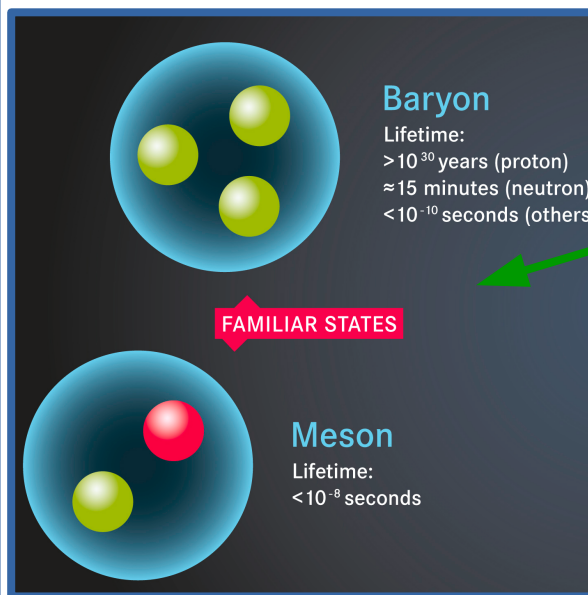
Mediators
Gluons

Quantum Chromodynamics (QCD)

- QCD is the theory of the strong force
- Describes the interactions between quarks and gluons

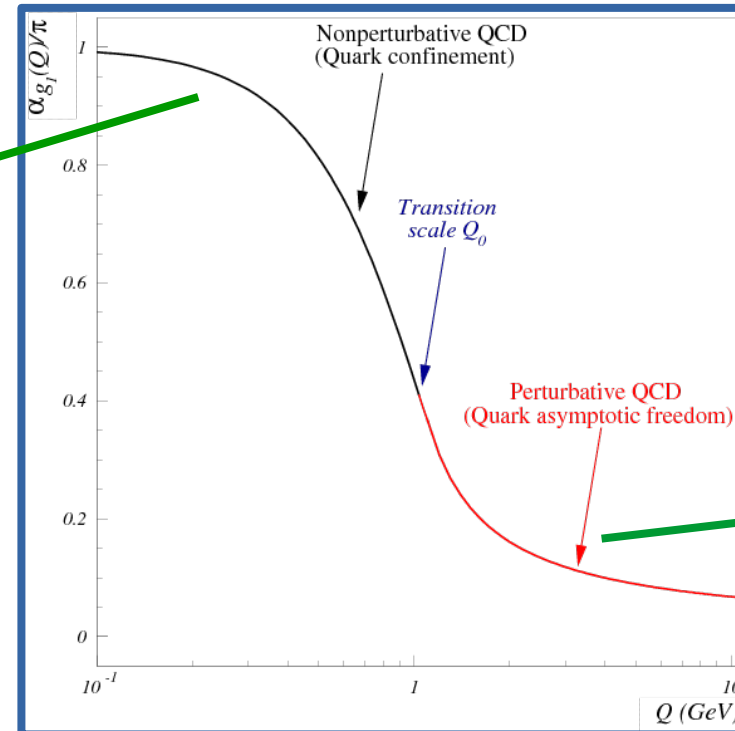


Hadrons

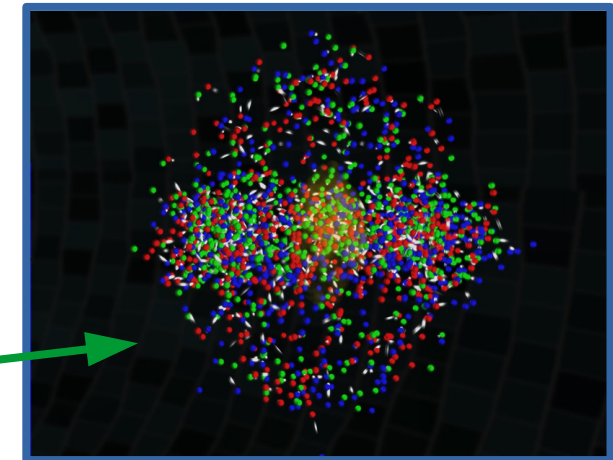


Confinement

Coupling Strength vs Energy

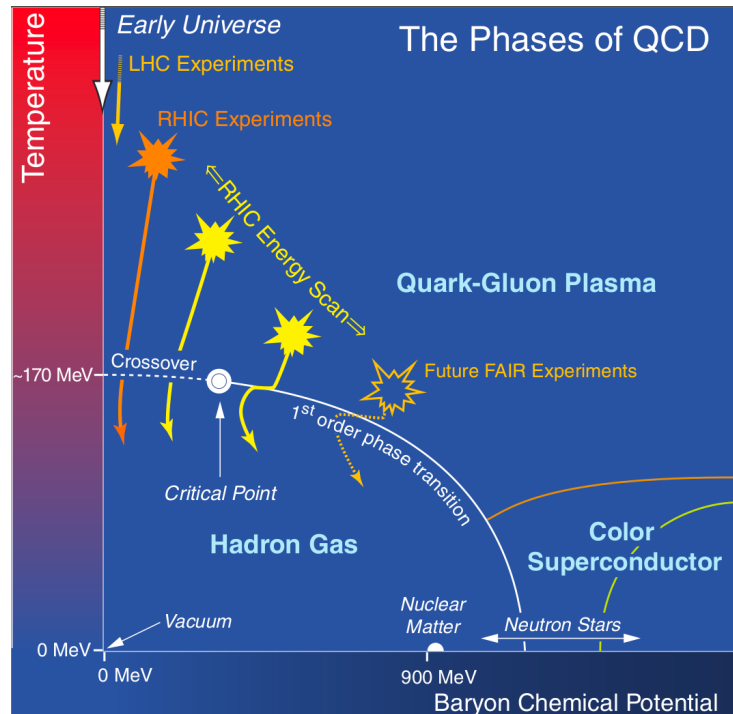


Asymptotic Freedom



Deconfined matter

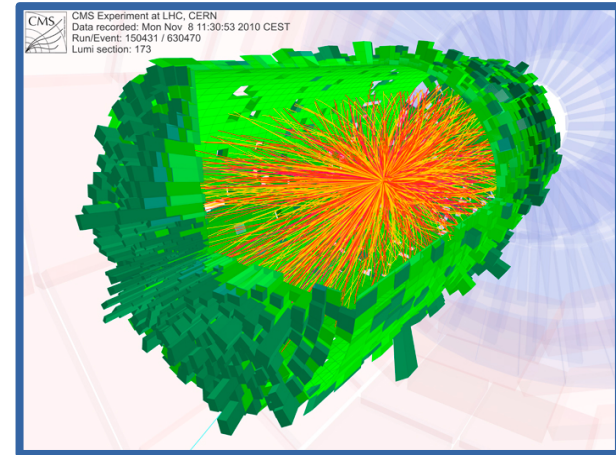
Quark-Gluon Plasma (QGP)



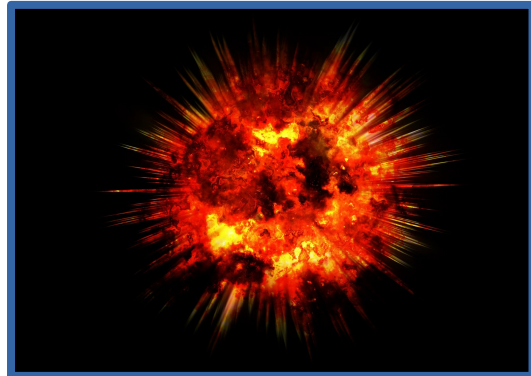
A state of matter where quarks and gluons are deconfined is predicted by QCD at high temperature



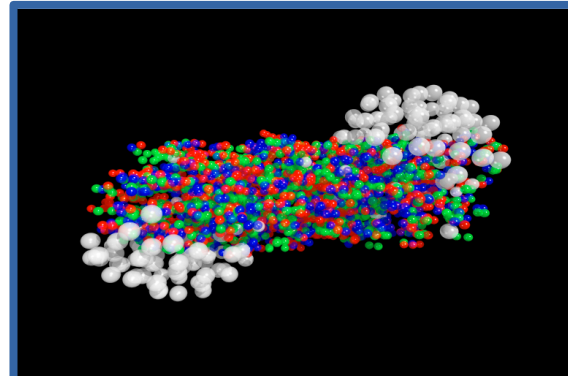
QGP is formed in relativistic heavy ion collisions



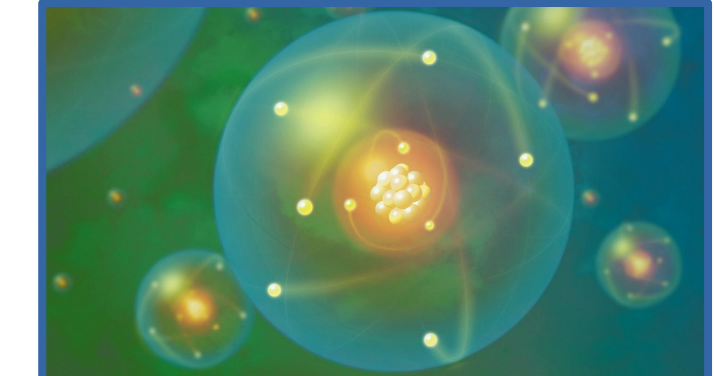
Experiment



Early Universe



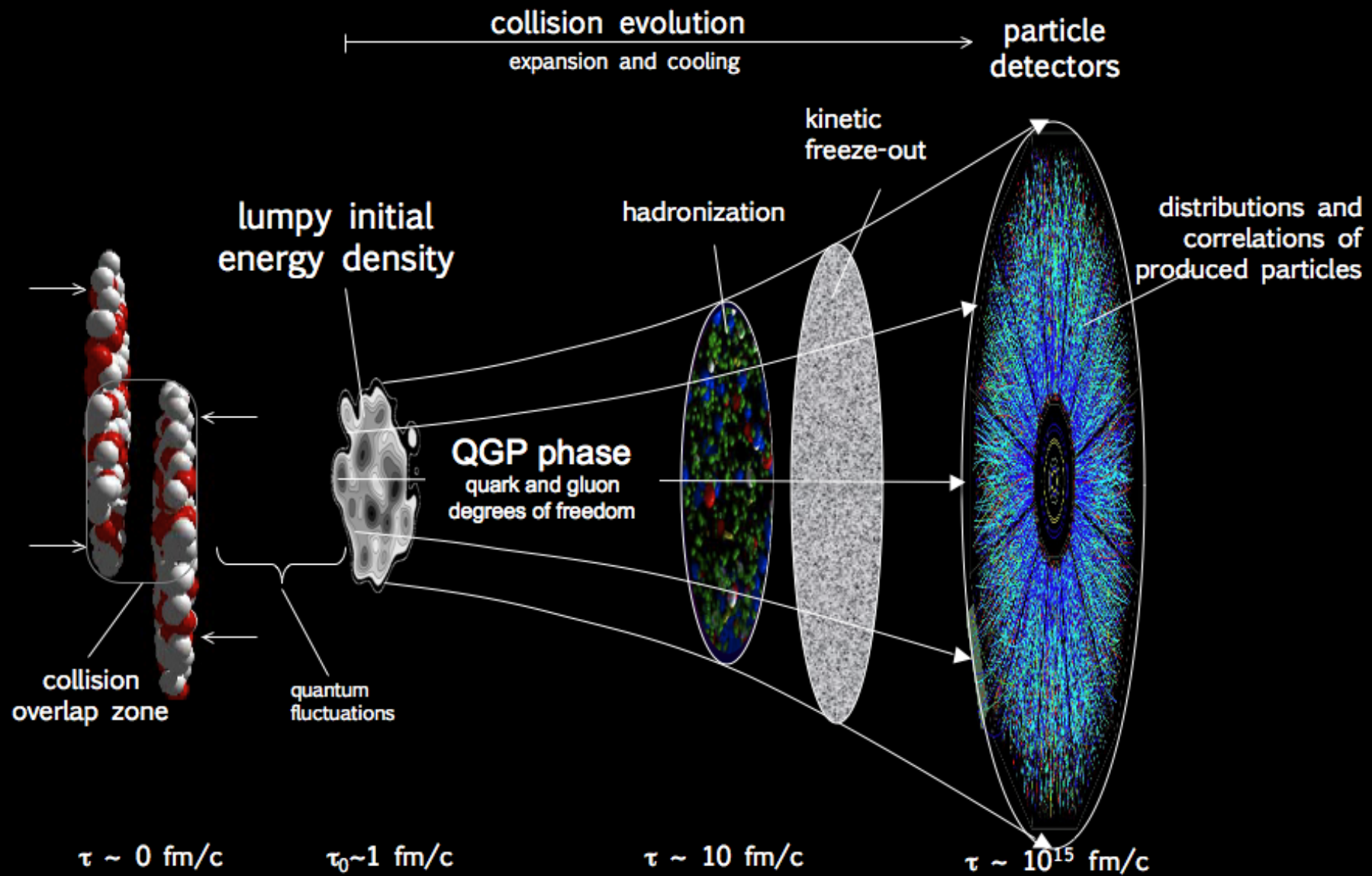
Quark-Gluon Plasma



Nuclear Matter

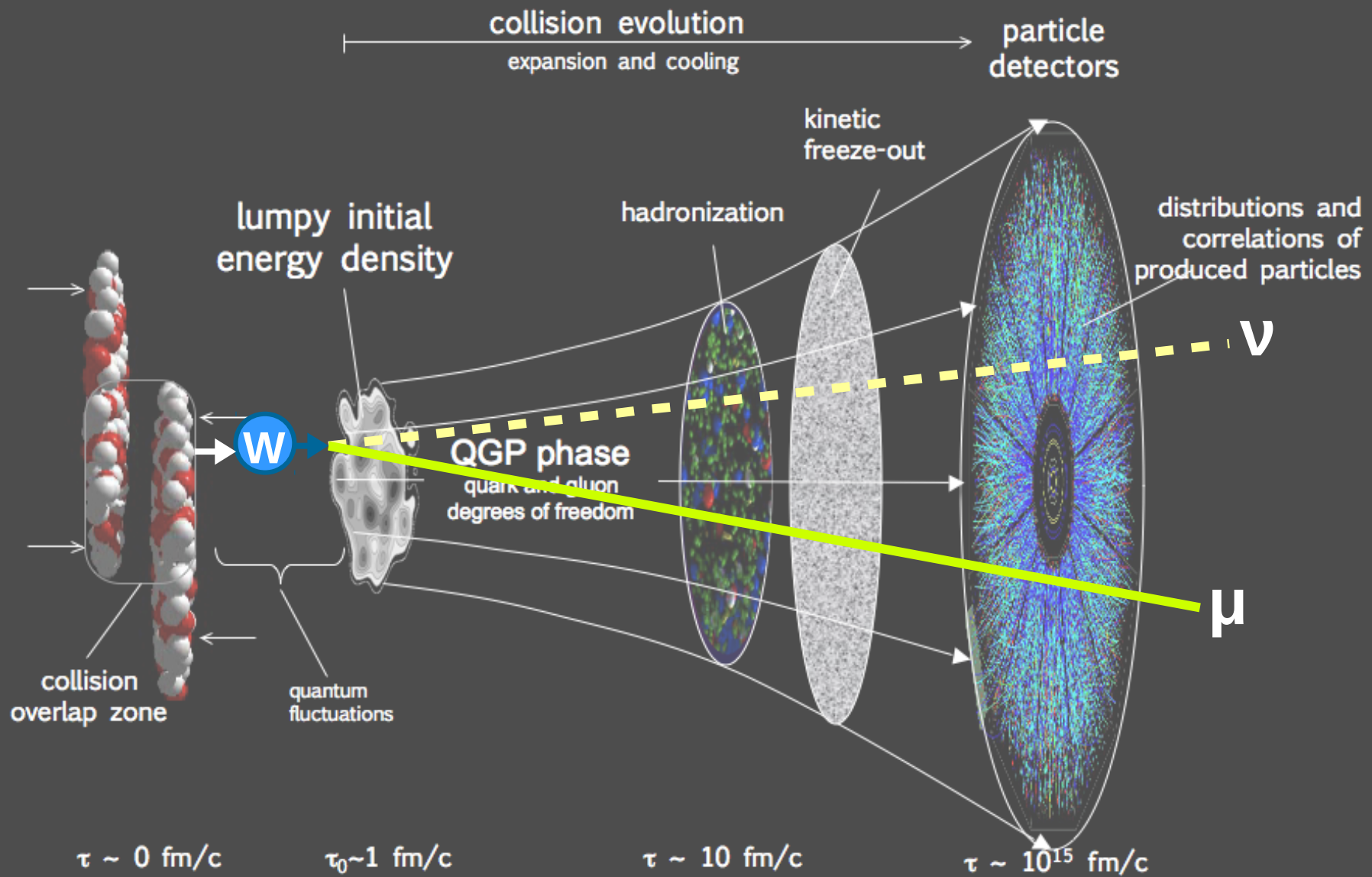
Heavy-ion collisions

Nuclear collisions and the QGP expansion



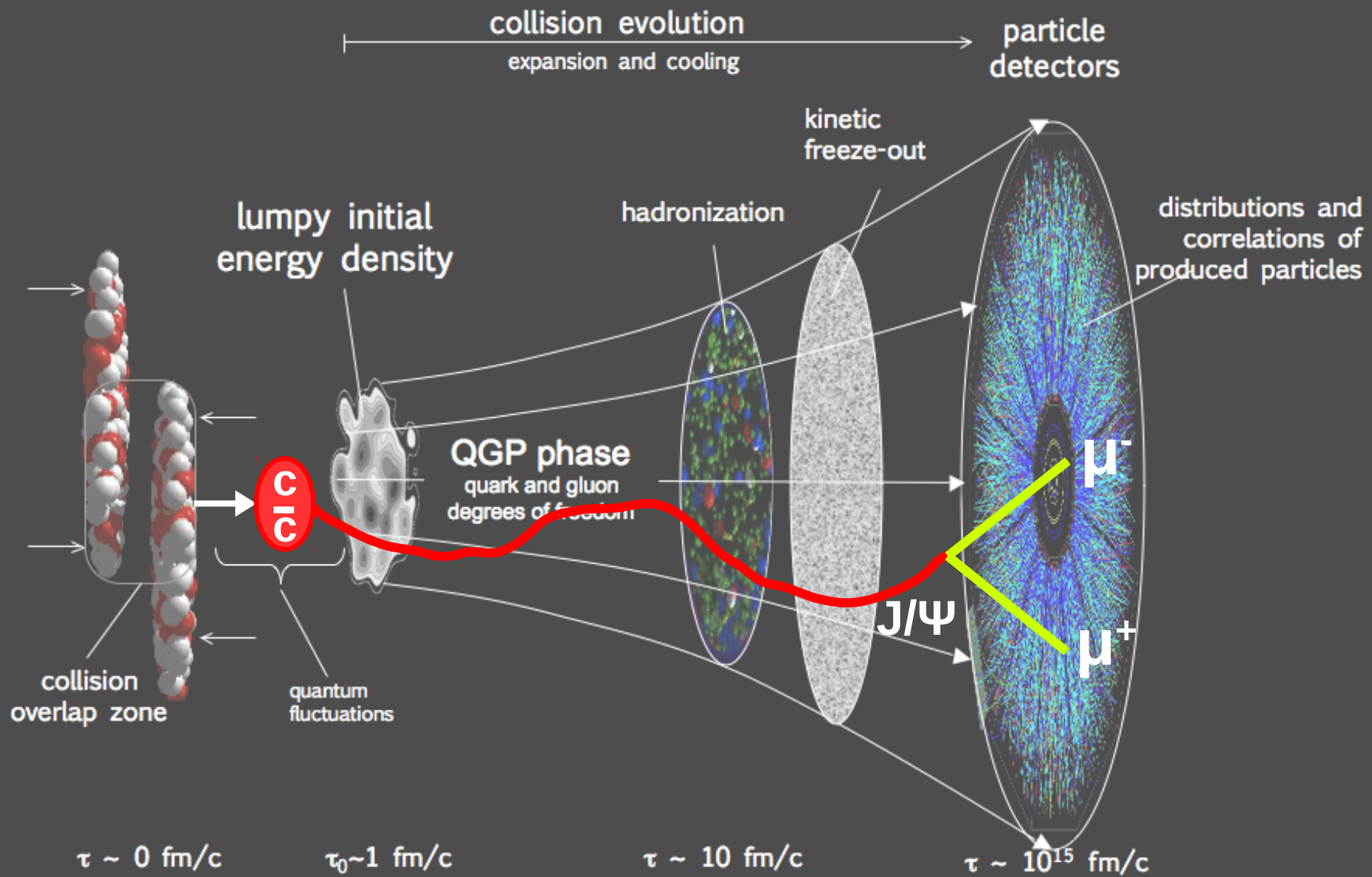
Heavy-ion collisions

Nuclear collisions and the QGP expansion



Heavy-ion collisions

Nuclear collisions and the QGP expansion



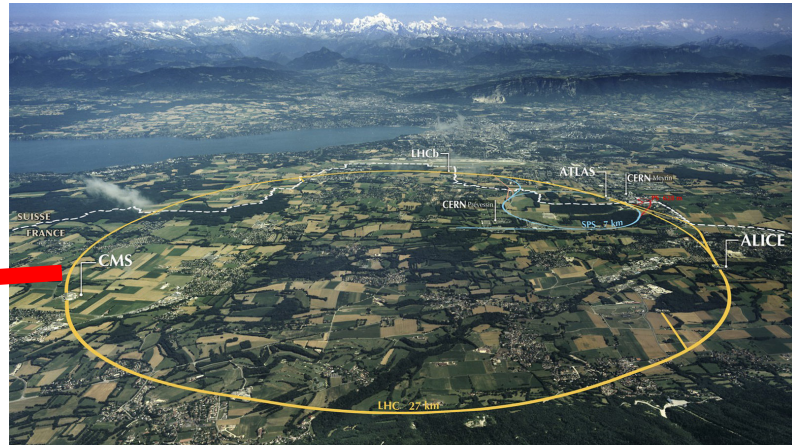
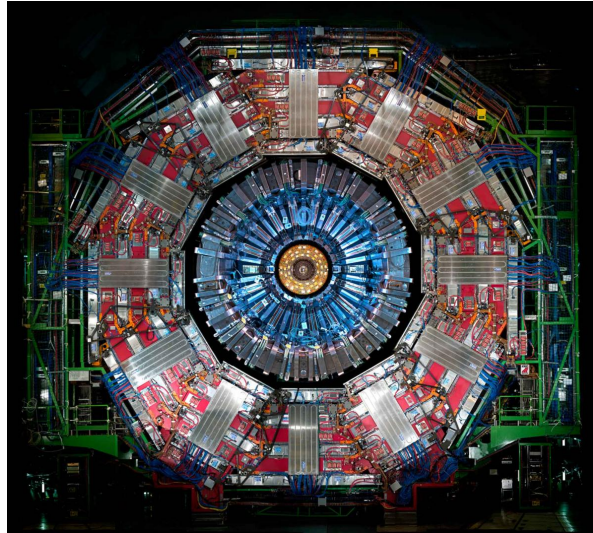
Outline

- Theoretical context
- **The CMS detector at the LHC**
- W-boson production in p-Pb at 8.16 TeV
 - Introduction
 - Analysis
 - Results
- Charmonium production in Pb-Pb at 5.02 TeV
 - Introduction
 - Analysis
 - Results
- Conclusions

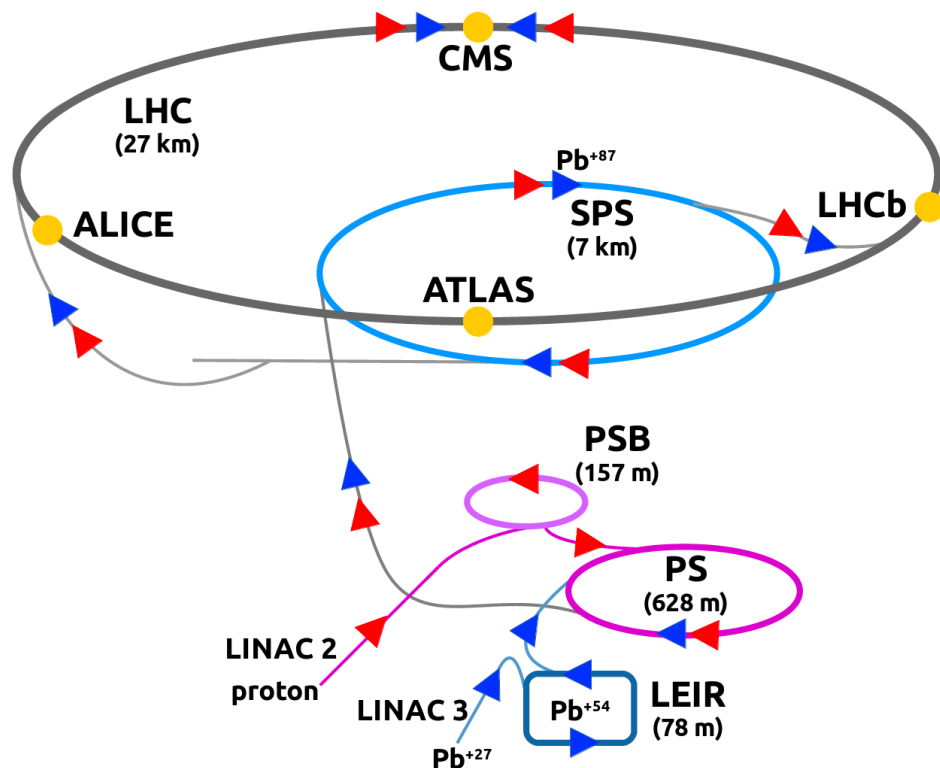


Large Hadron Collider

Detector



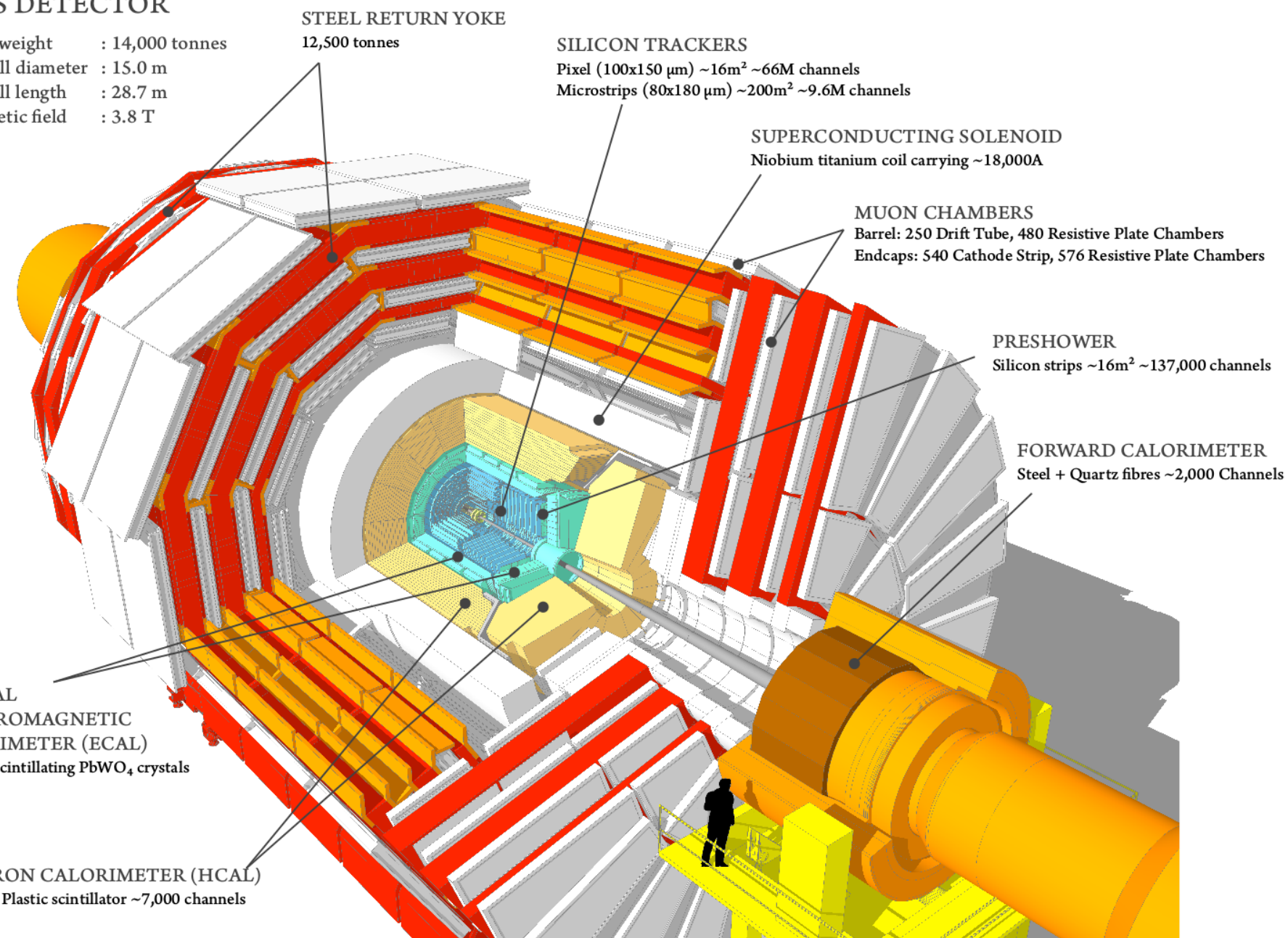
Compact Muon Solenoid



Compact Muon Solenoid

CMS DETECTOR

Total weight : 14,000 tonnes
Overall diameter : 15.0 m
Overall length : 28.7 m
Magnetic field : 3.8 T



Compact Muon Solenoid

CMS DETECTOR

Total weight : 14,000 tonnes
Overall diameter : 15.0 m
Overall length : 28.7 m
Magnetic field : 3.8 T

STEEL RETURN YOKE
12,500 tonnes

SILICON TRACKERS
Pixel ($100 \times 150 \mu\text{m}$) $\sim 16\text{m}^2 \sim 66\text{M}$ channels
Microstrips ($80 \times 180 \mu\text{m}$) $\sim 200\text{m}^2 \sim 9.6\text{M}$ channels

SUPERCONDUCTING SOLENOID
Niobium titanium coil carrying $\sim 18,000\text{A}$

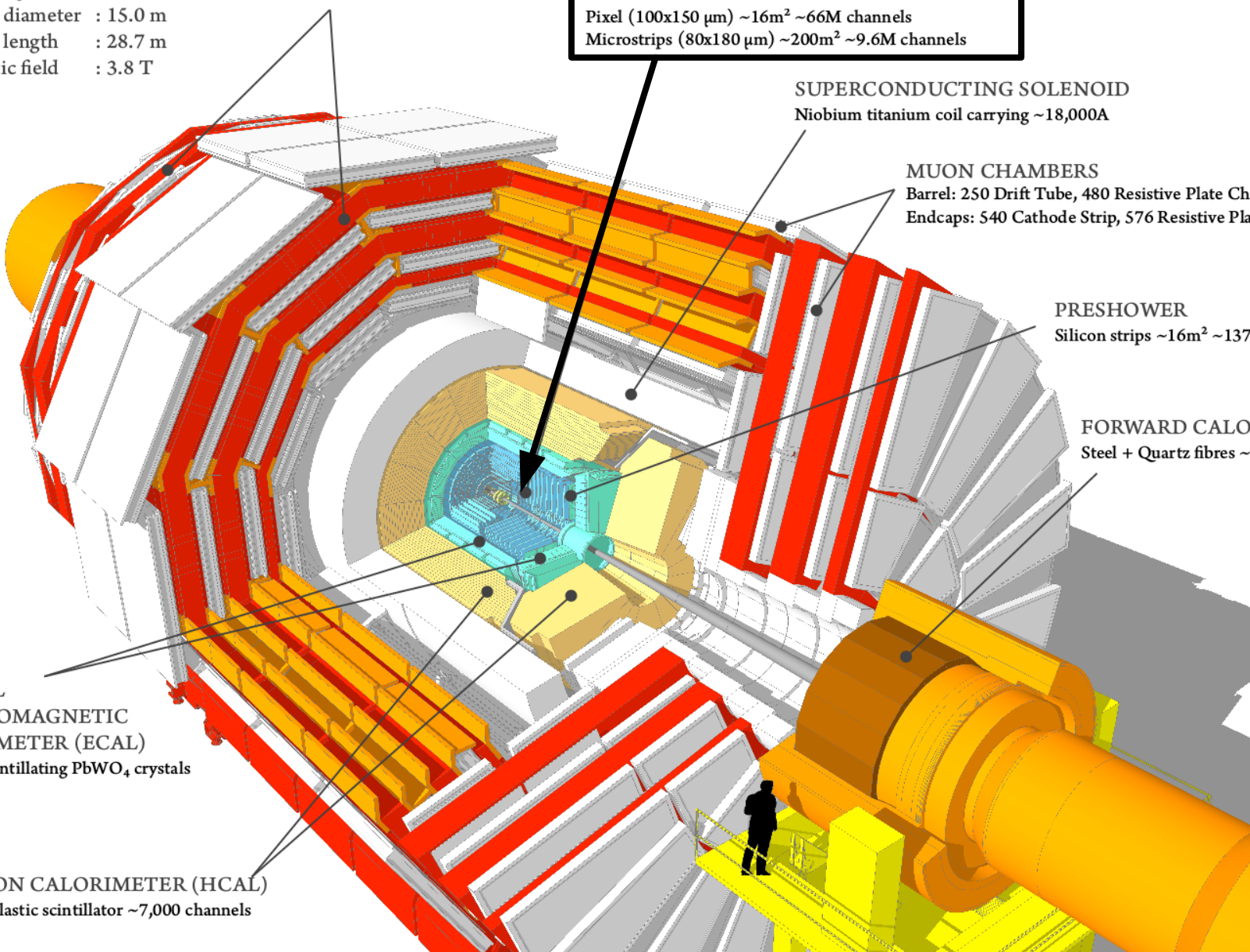
MUON CHAMBERS
Barrel: 250 Drift Tube, 480 Resistive Plate Chambers
Endcaps: 540 Cathode Strip, 576 Resistive Plate Chambers

PRESHOWER
Silicon strips $\sim 16\text{m}^2 \sim 137,000$ channels

FORWARD CALORIMETER
Steel + Quartz fibres $\sim 2,000$ Channels

CRYSTAL
ELECTROMAGNETIC
CALORIMETER (ECAL)
 $\sim 76,000$ scintillating PbWO₄ crystals

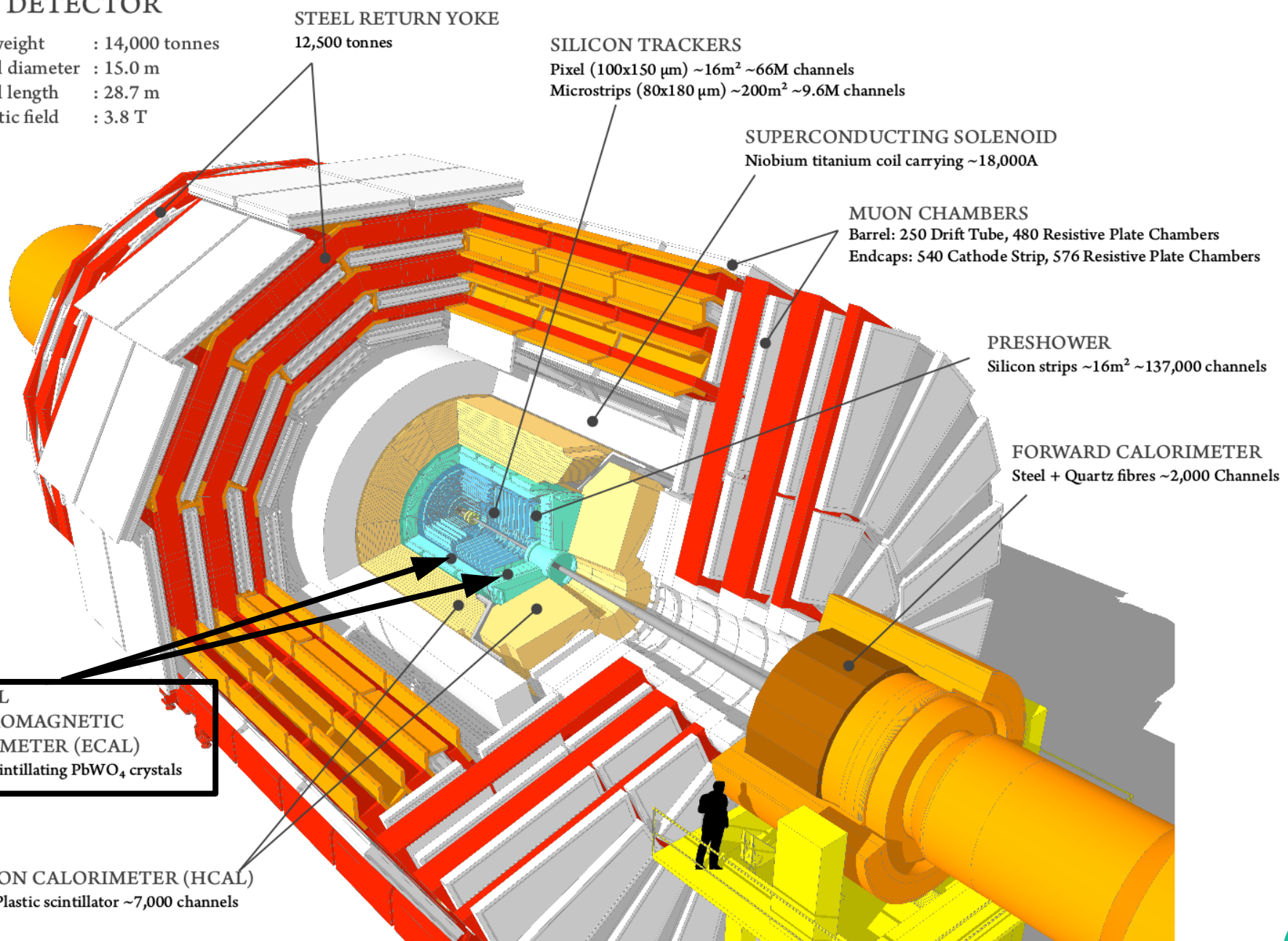
HADRON CALORIMETER (HCAL)
Brass + Plastic scintillator $\sim 7,000$ channels



Compact Muon Solenoid

CMS DETECTOR

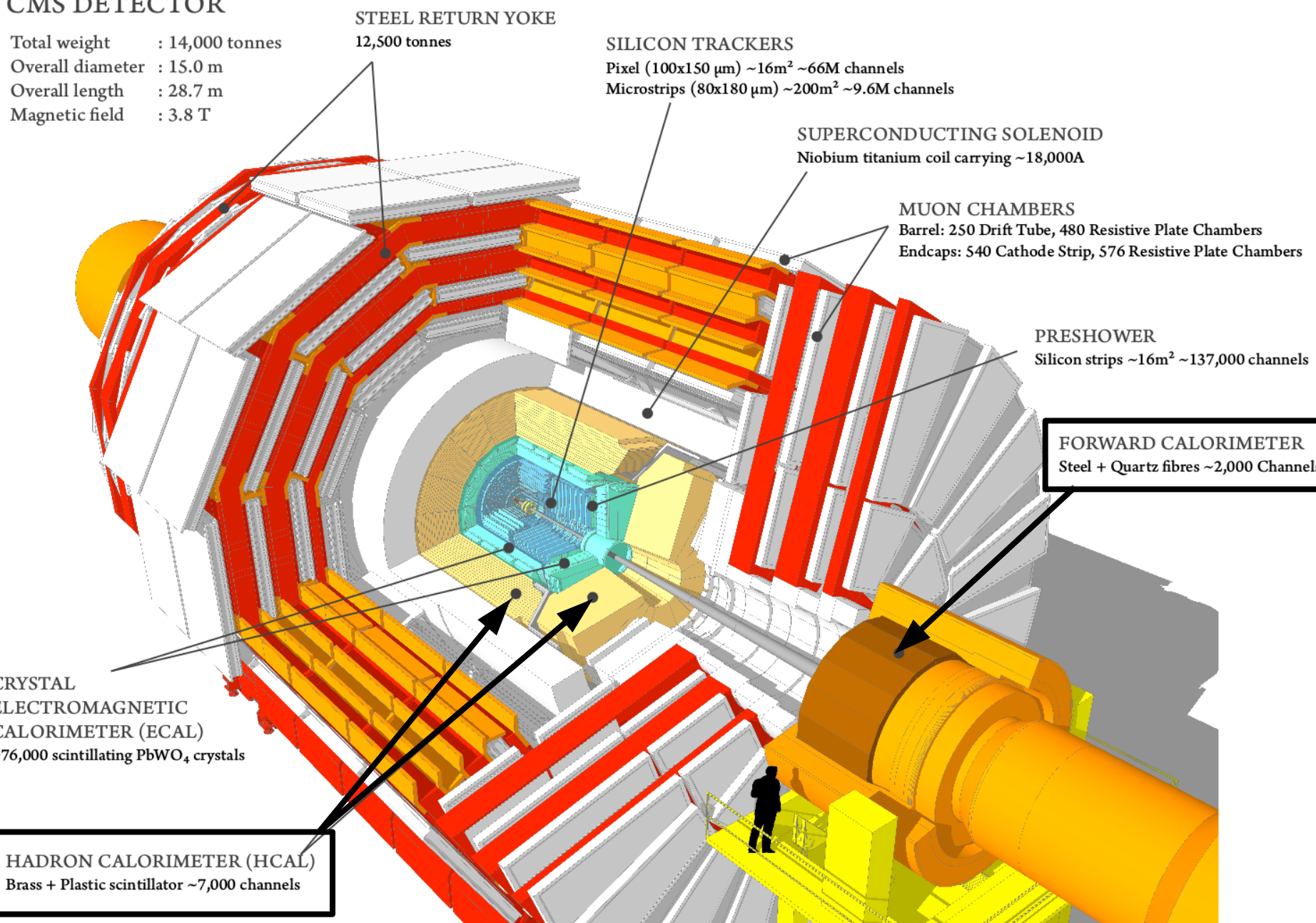
Total weight : 14,000 tonnes
Overall diameter : 15.0 m
Overall length : 28.7 m
Magnetic field : 3.8 T



Compact Muon Solenoid

CMS DETECTOR

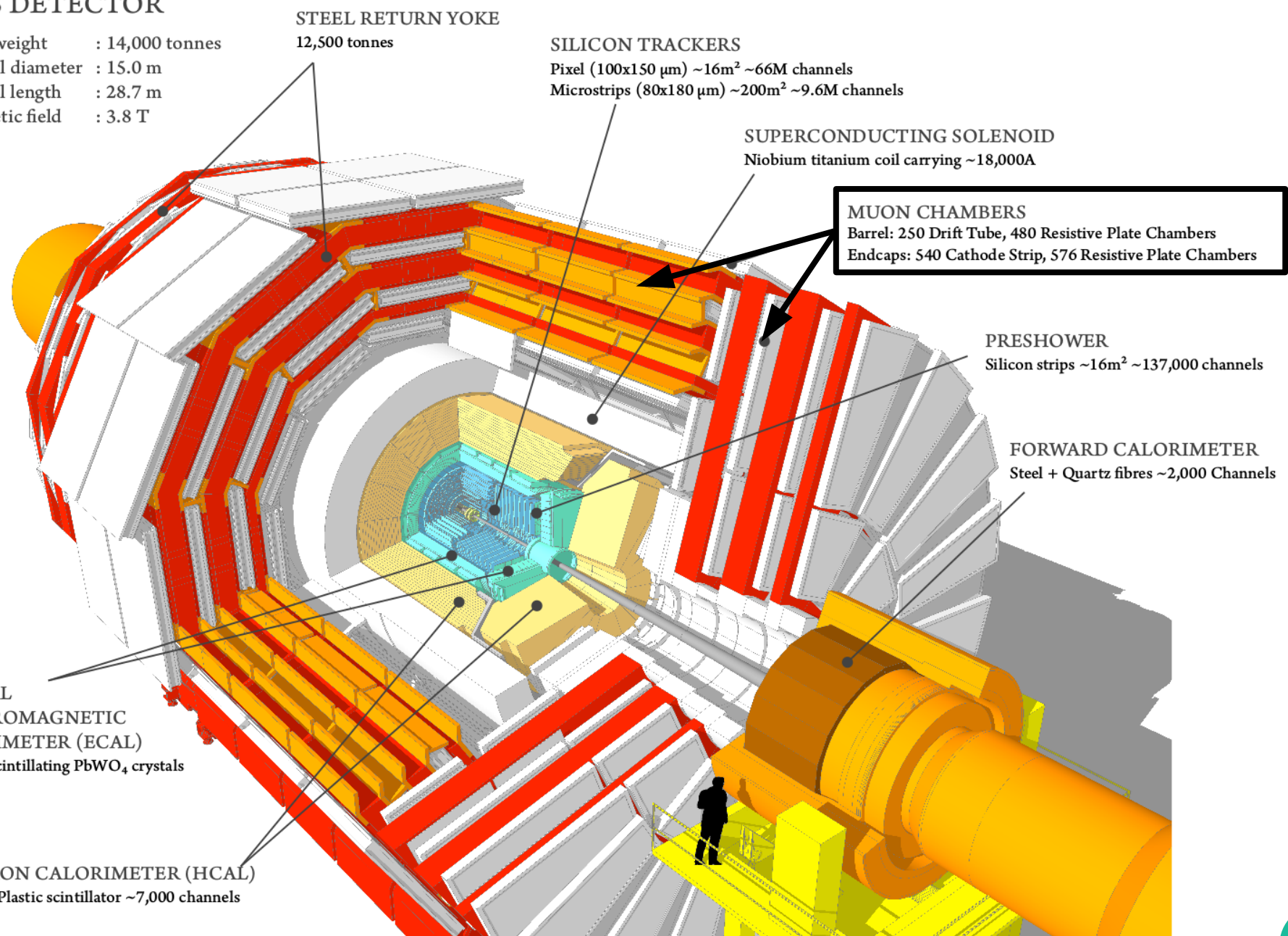
Total weight : 14,000 tonnes
Overall diameter : 15.0 m
Overall length : 28.7 m
Magnetic field : 3.8 T



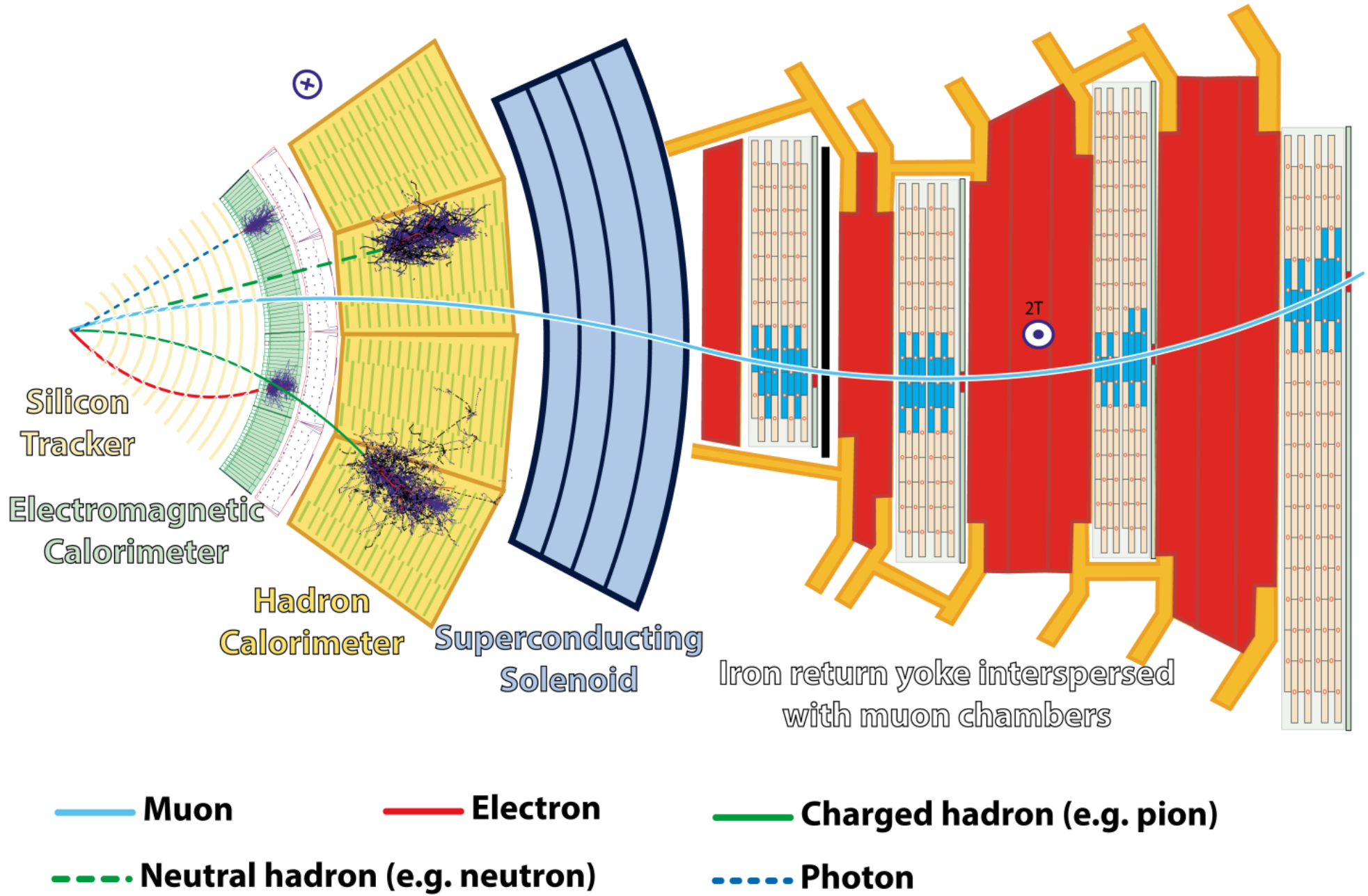
Compact Muon Solenoid

CMS DETECTOR

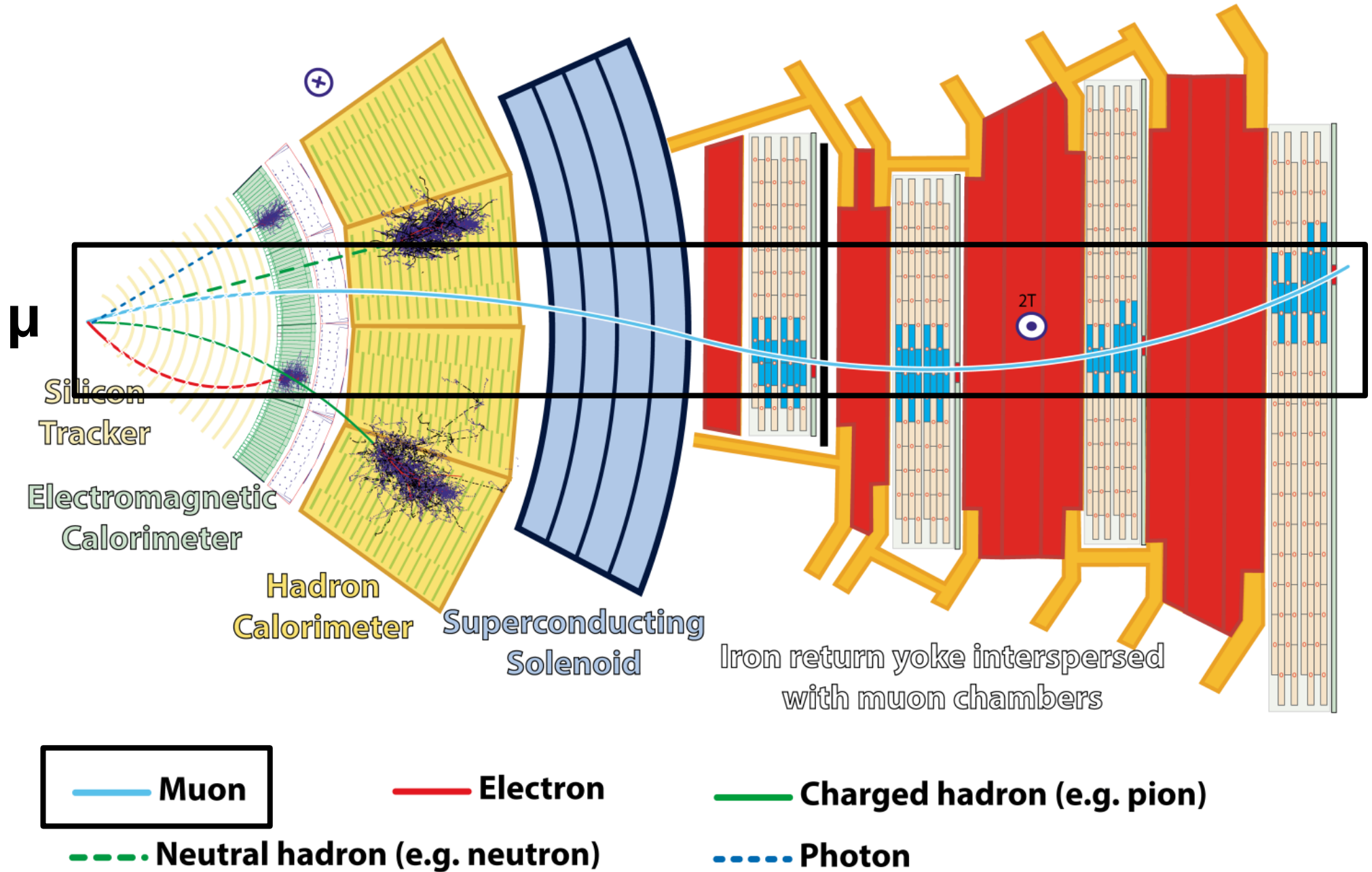
Total weight : 14,000 tonnes
Overall diameter : 15.0 m
Overall length : 28.7 m
Magnetic field : 3.8 T



Particle reconstruction

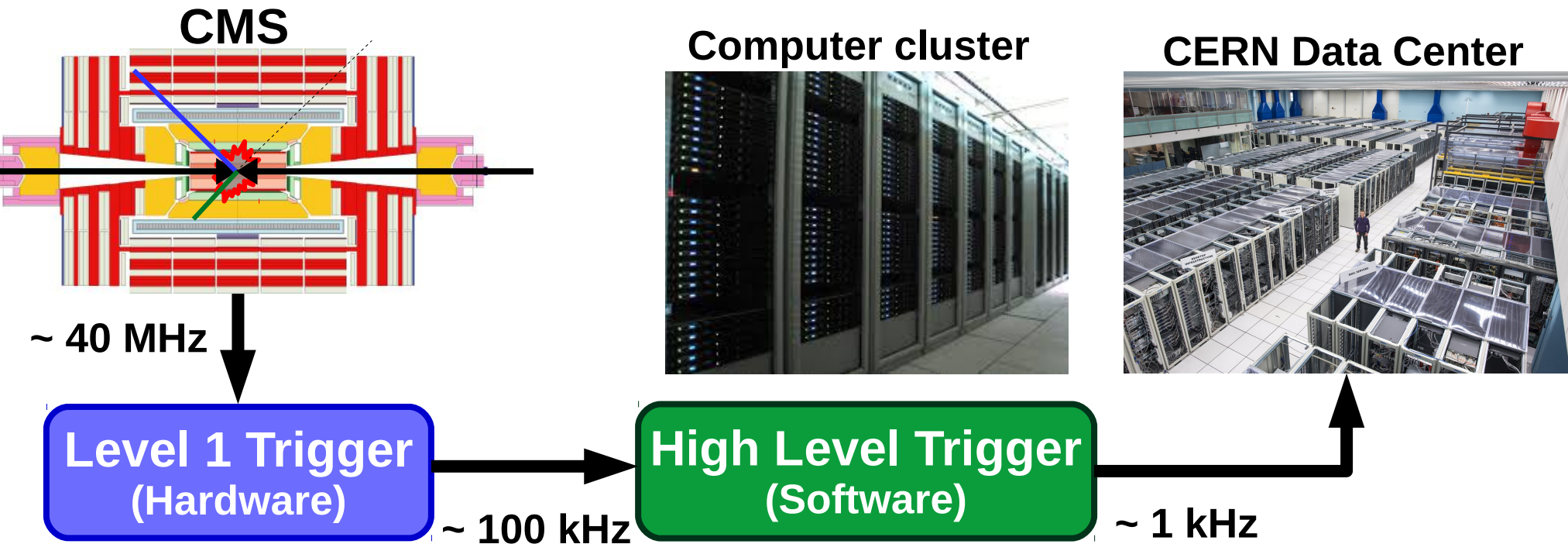


Particle reconstruction



CMS trigger system

CMS uses a two-tier trigger system to select events of interest



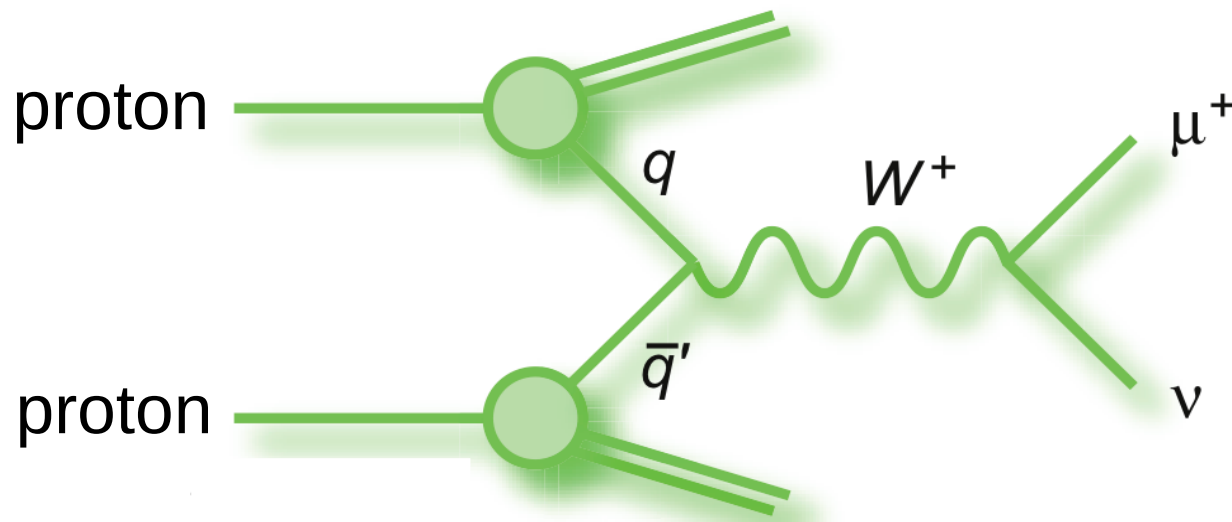
I was responsible for implementing the muon trigger selections for:

- proton-lead collisions at 8.16 TeV in 2016
- proton-proton collisions at 5.02 TeV in 2017

Outline

- Theoretical context
- The CMS detector at the LHC
- **W-boson production in p-Pb at 8.16 TeV**
 - Introduction
 - Analysis
 - Results
- Charmonium production in Pb-Pb at 5.02 TeV
 - Introduction
 - Analysis
 - Results
- Conclusions

How are W bosons produced at LHC?

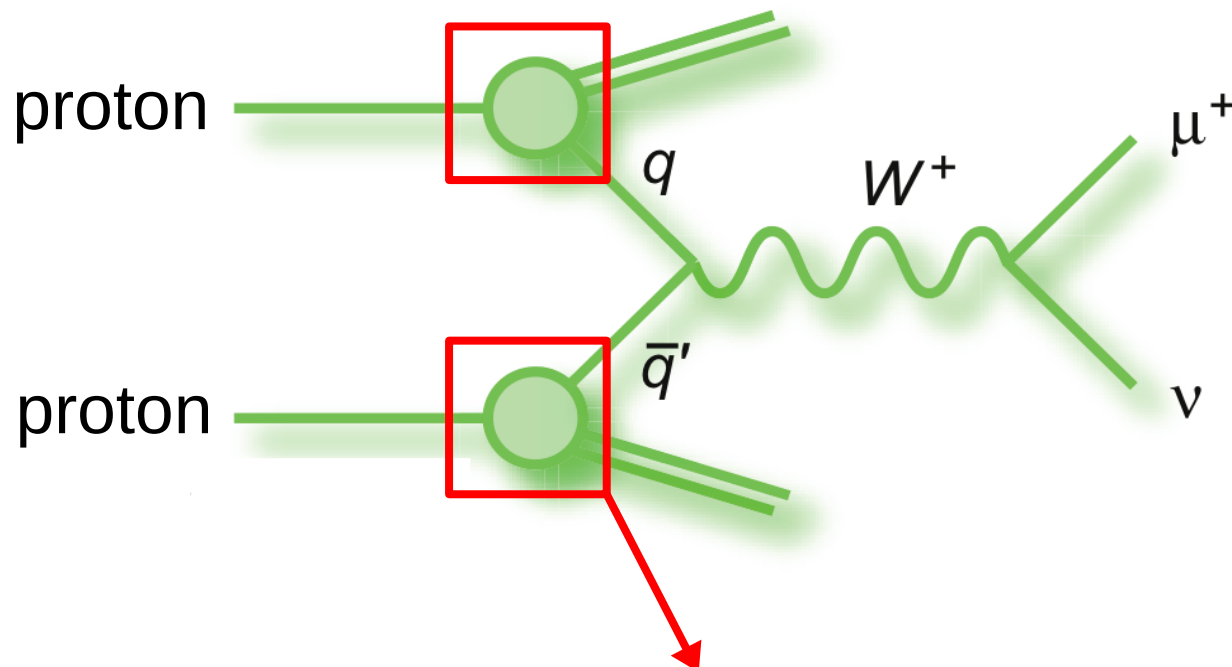


$$\sigma_W(s, M_W^2) = \sum_{a,b} \int_0^1 dx_1 dx_2 f_a^{h_1}(x_1, M_W^2) f_b^{h_2}(x_2, M_W^2) \hat{\sigma}_{ab \rightarrow W}(x_1 x_2 s, M_W^2)$$

Hadronic cross section **Parton distribution function (PDF)** **Partonic cross section**

- Dominant production mode: $u \bar{d} \rightarrow W^+$, $d \bar{u} \rightarrow W^-$
- W bosons is sensitive to quark PDFs

How are W bosons produced at LHC?

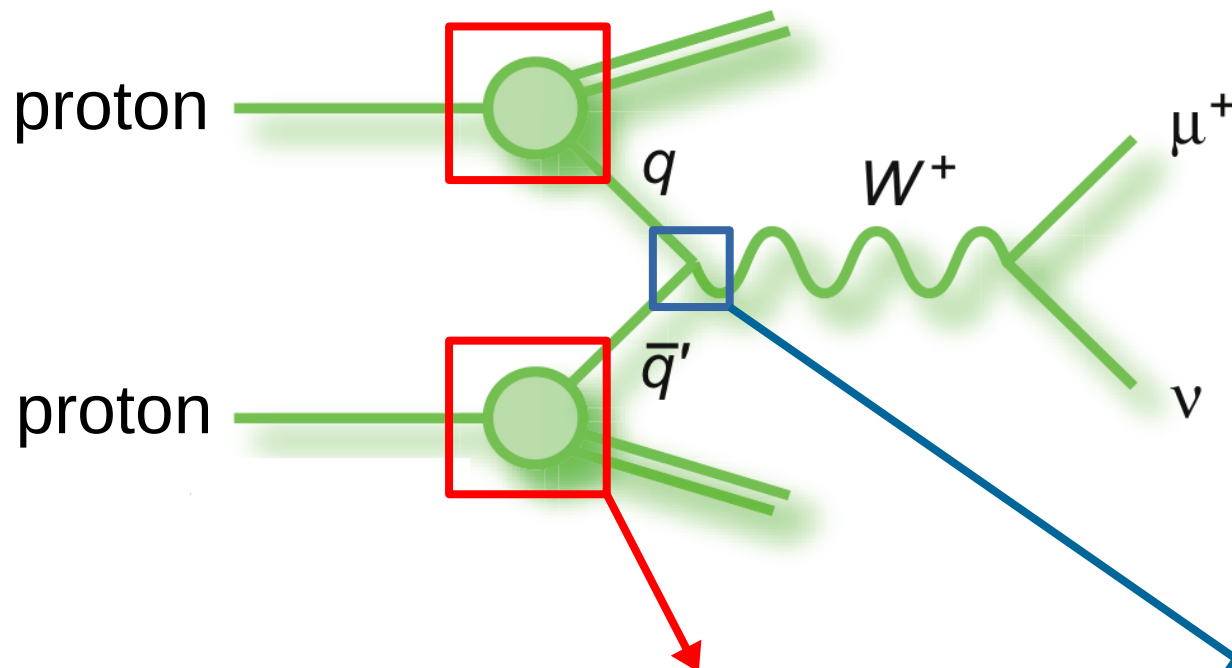


$$\sigma_W(s, M_W^2) = \sum_{a,b} \int_0^1 dx_1 dx_2 f_a^{h_1}(x_1, M_W^2) f_b^{h_2}(x_2, M_W^2) \hat{\sigma}_{ab \rightarrow W}(x_1 x_2 s, M_W^2)$$

Hadronic cross section **Parton distribution function (PDF)** **Partonic cross section**

- Dominant production mode: $u \bar{d} \rightarrow W^+$, $d \bar{u} \rightarrow W^-$
- W bosons is sensitive to quark PDFs

How are W bosons produced at LHC?

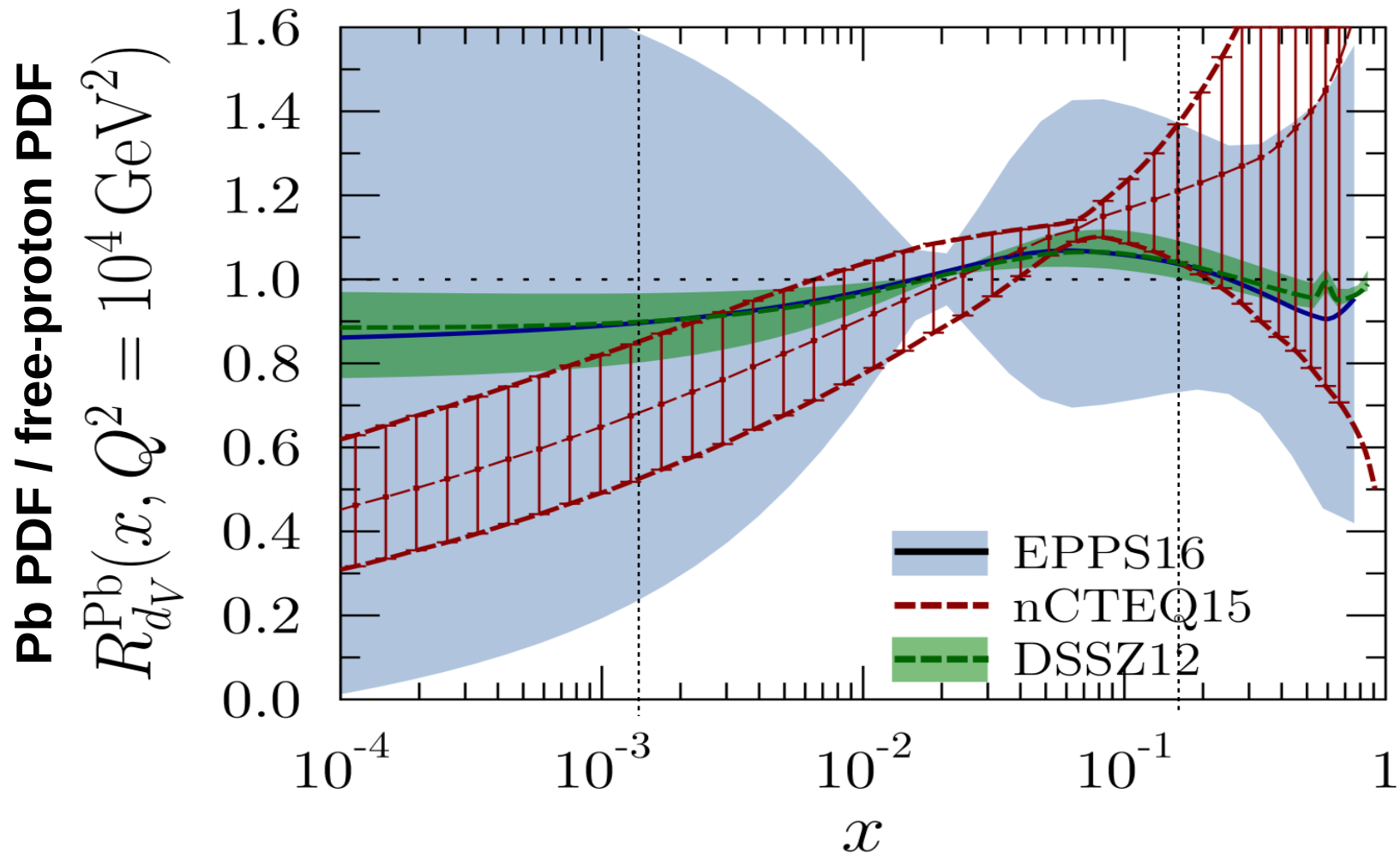


$$\sigma_W(s, M_W^2) = \sum_{a,b} \int_0^1 dx_1 dx_2 f_a^{h_1}(x_1, M_W^2) f_b^{h_2}(x_2, M_W^2) \hat{\sigma}_{ab \rightarrow W}(x_1 x_2 s, M_W^2)$$

Hadronic cross section **Parton distribution function (PDF)** **Partonic cross section**

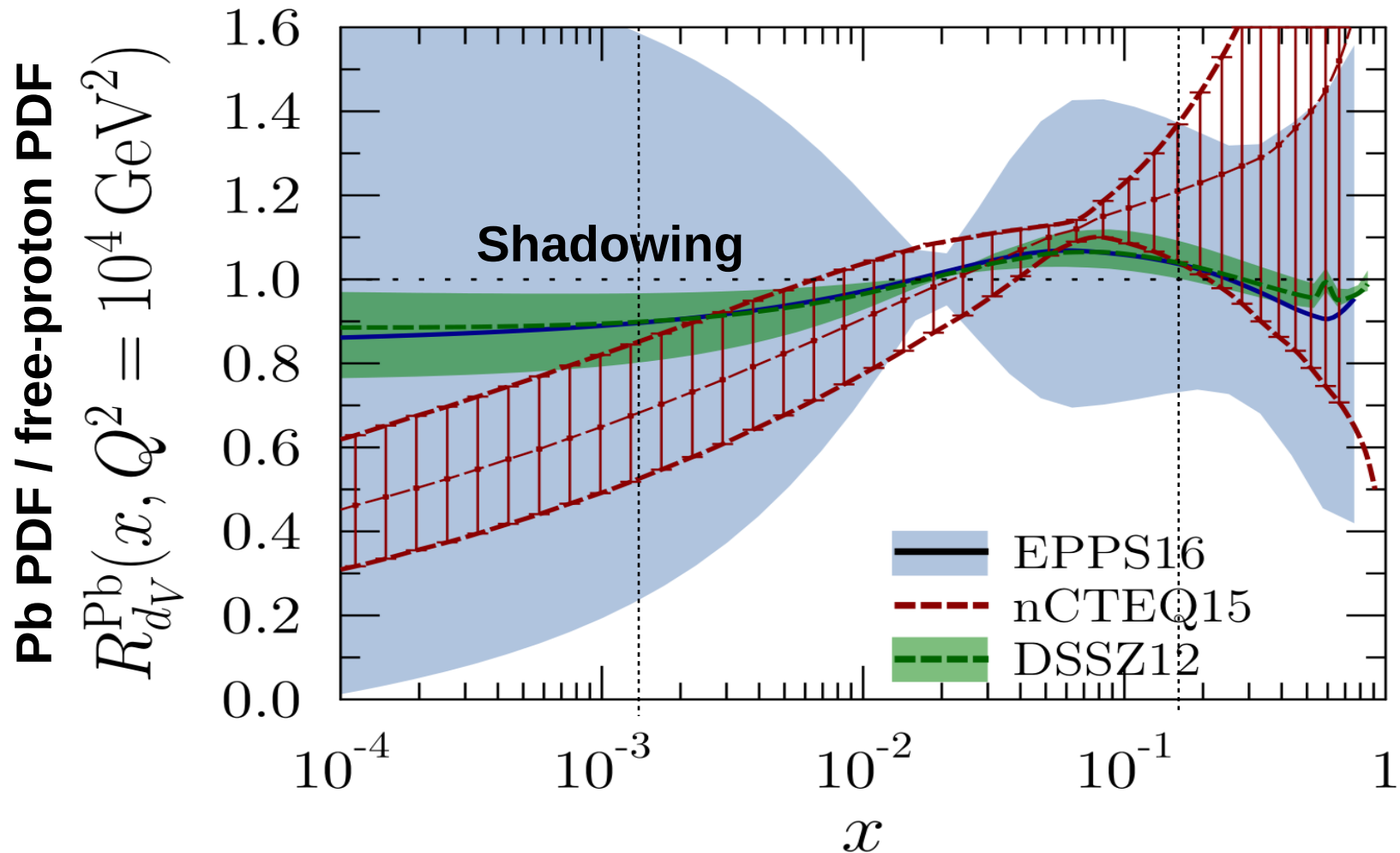
- Dominant production mode: $u \bar{d} \rightarrow W^+$, $d \bar{u} \rightarrow W^-$
- W bosons is sensitive to quark PDFs

Nuclear modification of PDF



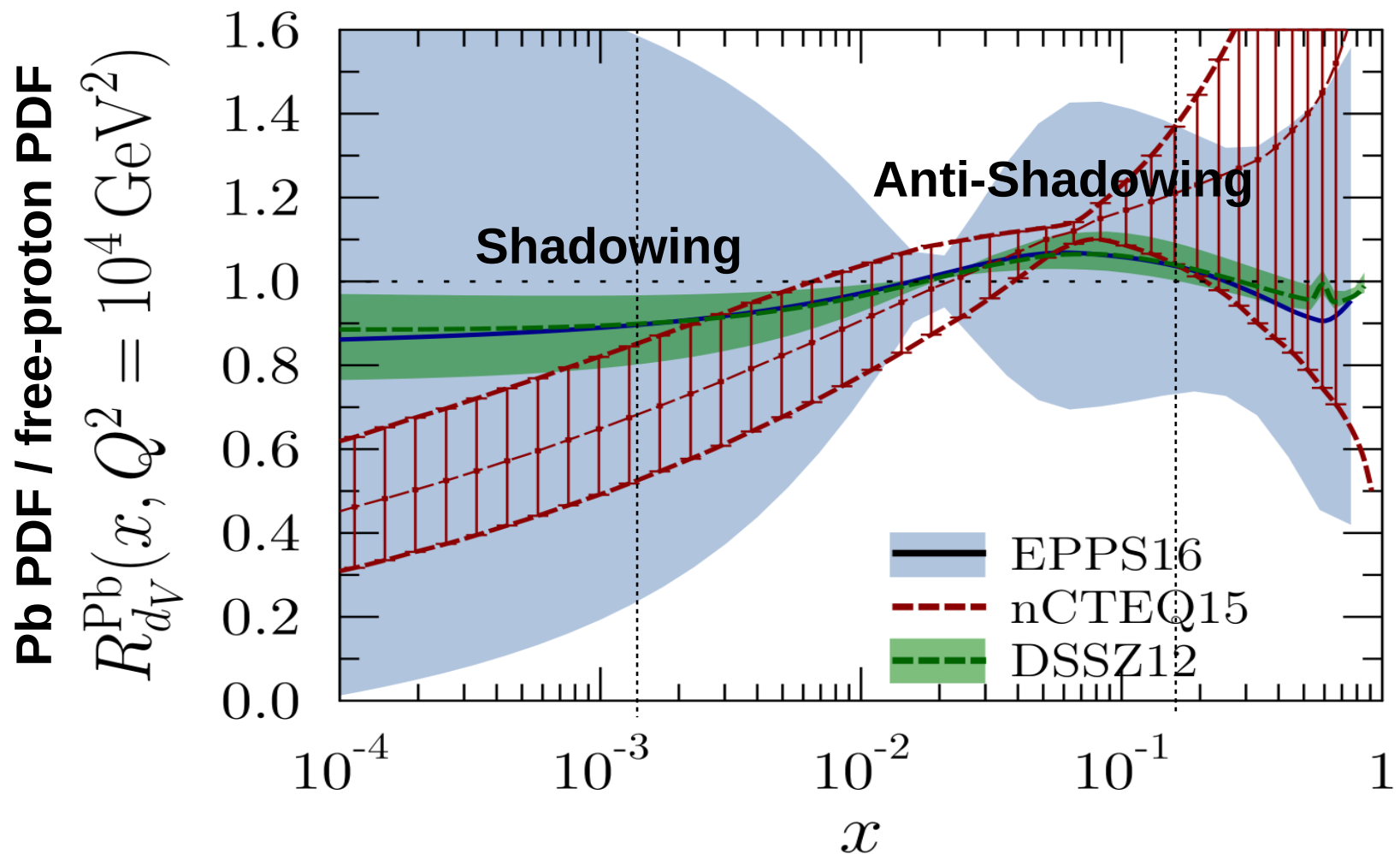
- PDFs of nucleons inside nuclei are modified compare to free proton PDFs

Nuclear modification of PDF



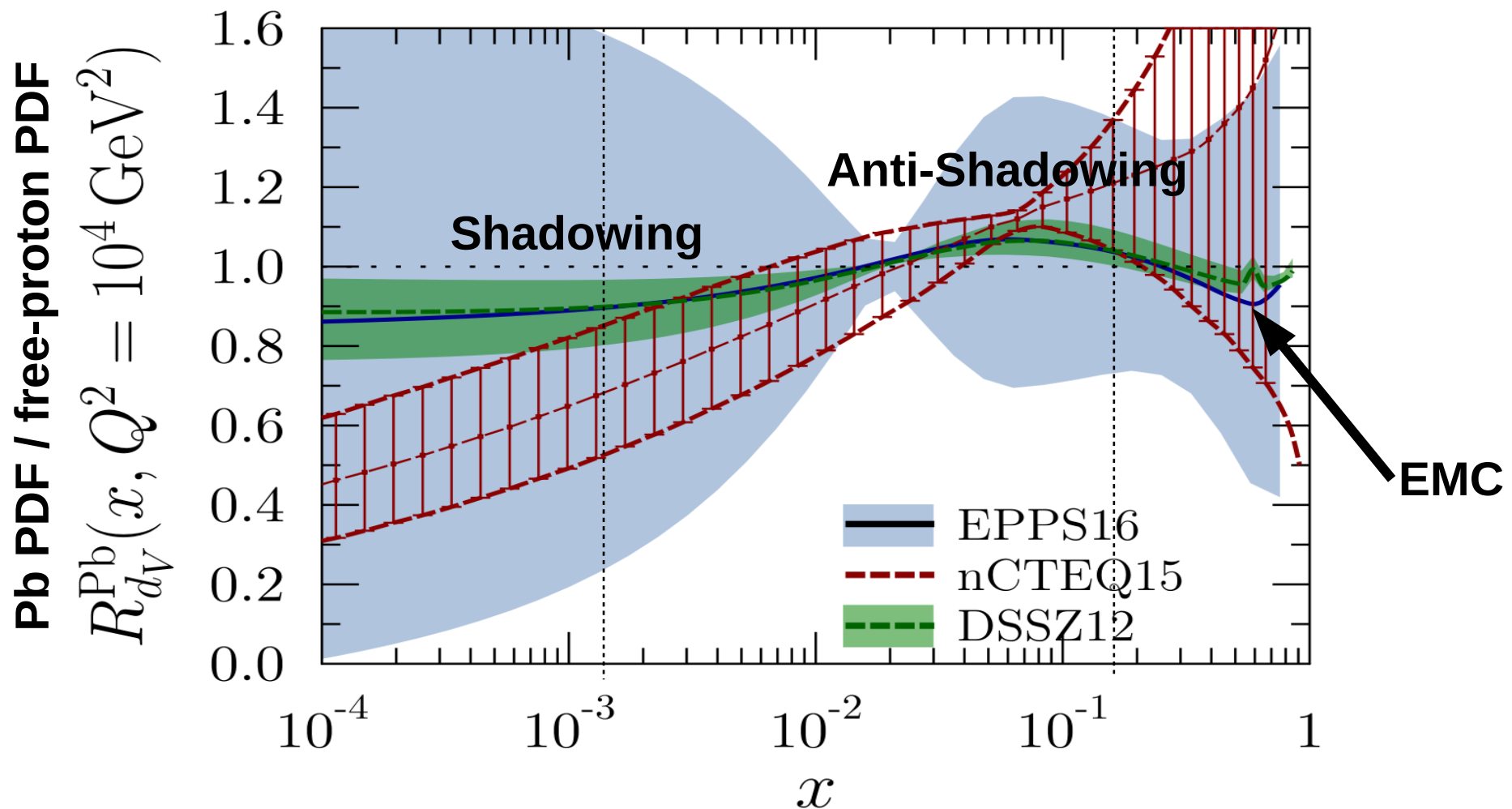
- PDFs of nucleons inside nuclei are modified compare to free proton PDFs

Nuclear modification of PDF



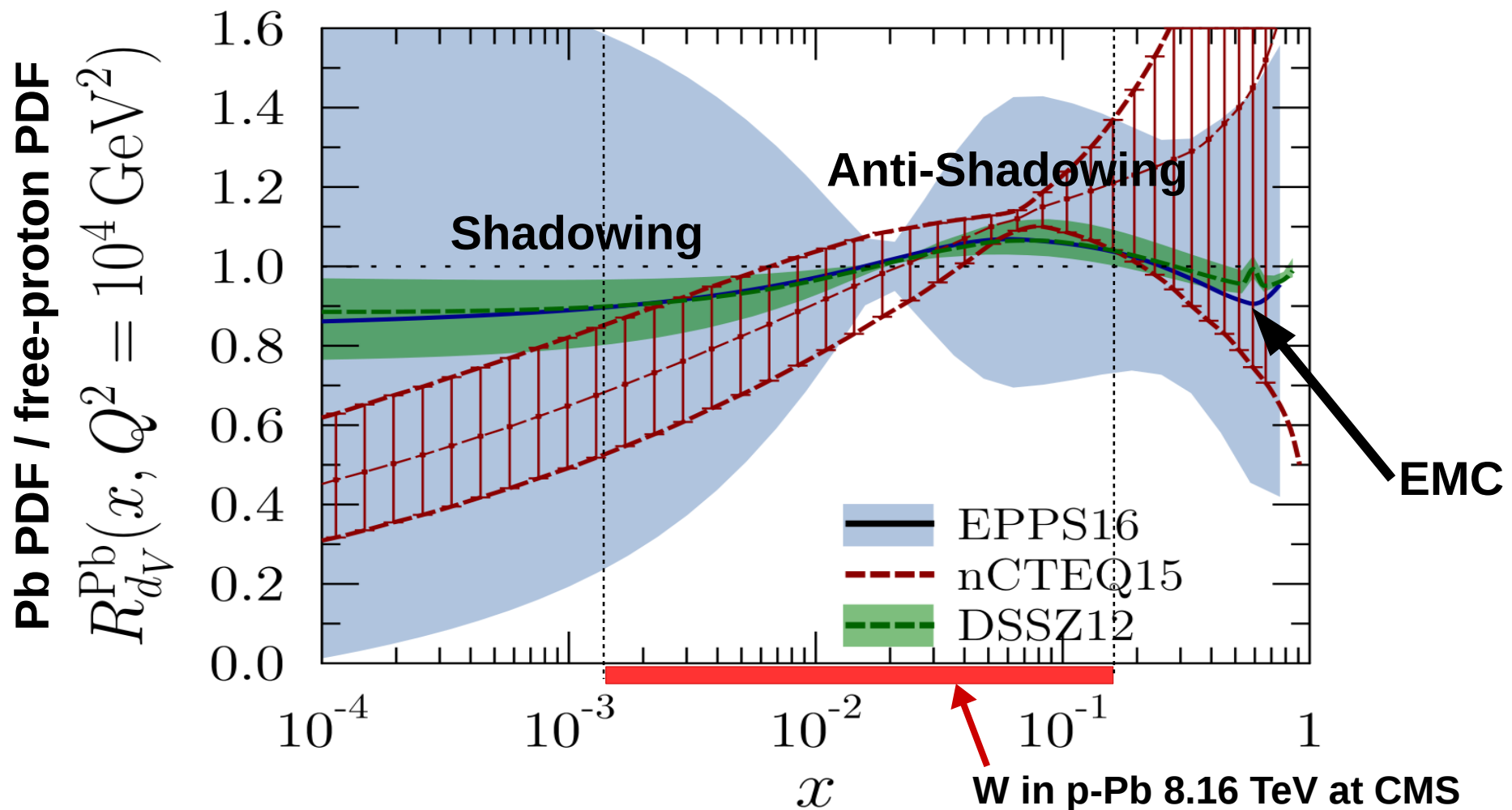
- PDFs of nucleons inside nuclei are modified compare to free proton PDFs

Nuclear modification of PDF



- PDFs of nucleons inside nuclei are modified compare to free proton PDFs

Nuclear modification of PDF



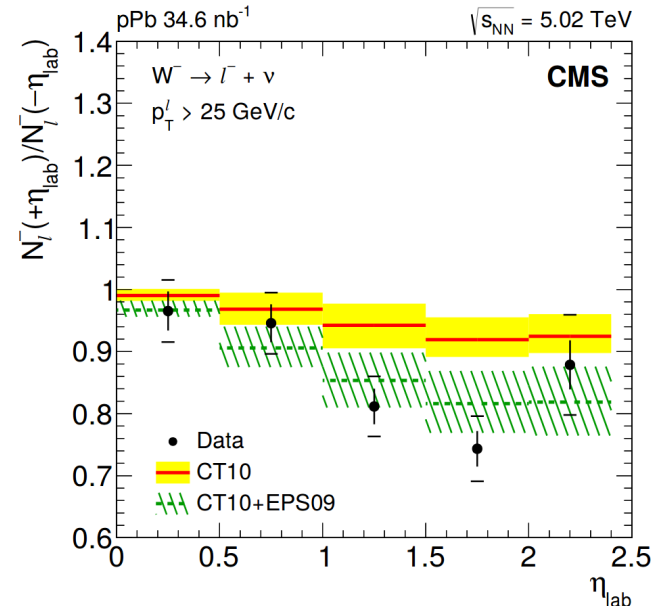
- PDFs of nucleons inside nuclei are modified compare to free proton PDFs
- W boson production in $p\text{-Pb}$ collisions at CMS probe nuclear PDFs in $10^{-3} < x < 0.17$

W bosons in p-Pb collisions

- Previous measurement of **W production at 5.02 TeV** by CMS helped to improve nPDF sets
- Provided a hint of nuclear modifications with poor significance

Alice Florent, PhD thesis (LLR)

Phys. Lett. B750 (2015)

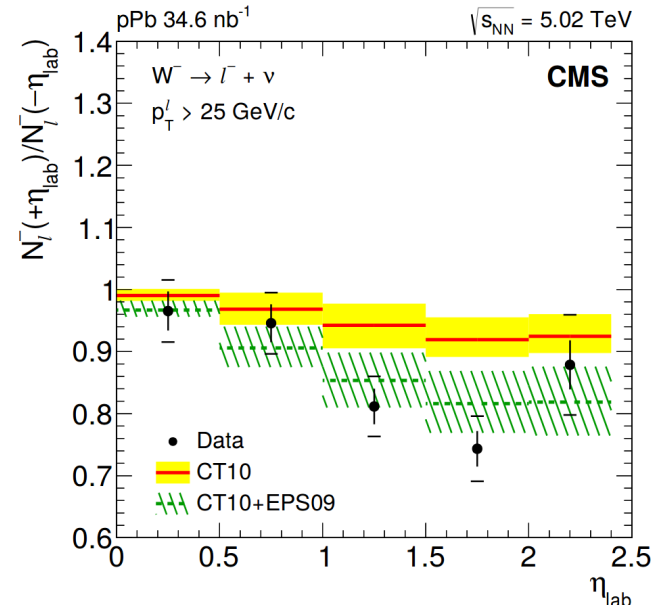


W bosons in p-Pb collisions

- Previous measurement of **W production at 5.02 TeV** by CMS helped to improve nPDF sets
- Provided a hint of nuclear modifications with poor significance

Alice Florent, PhD thesis (LLR)

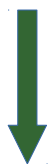
Phys. Lett. B750 (2015)



Phys. Lett. B750 (2015)

This thesis: proton-lead collisions at 8.16 TeV

W boson yield increased by $\sim 10x$
in 2016 data w.r.t. 2013



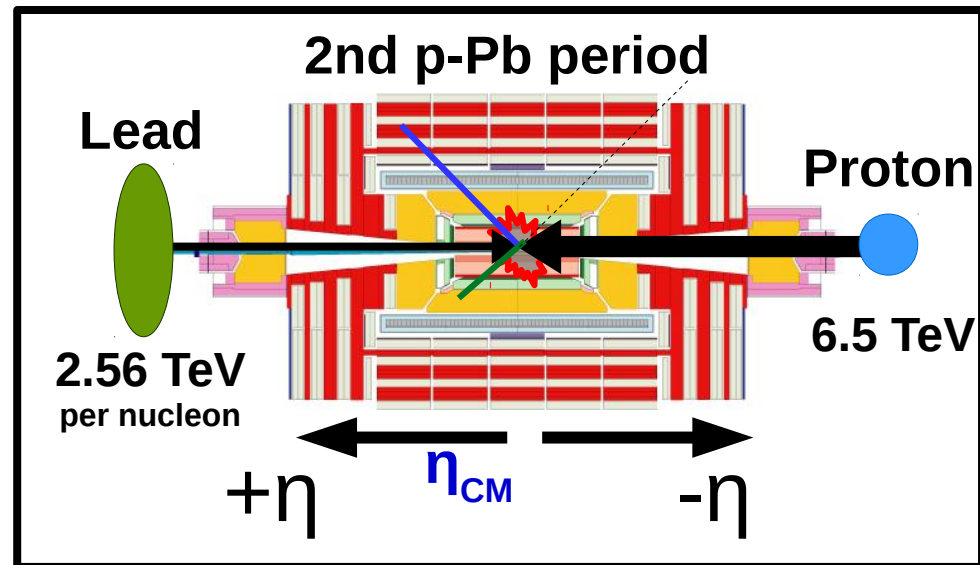
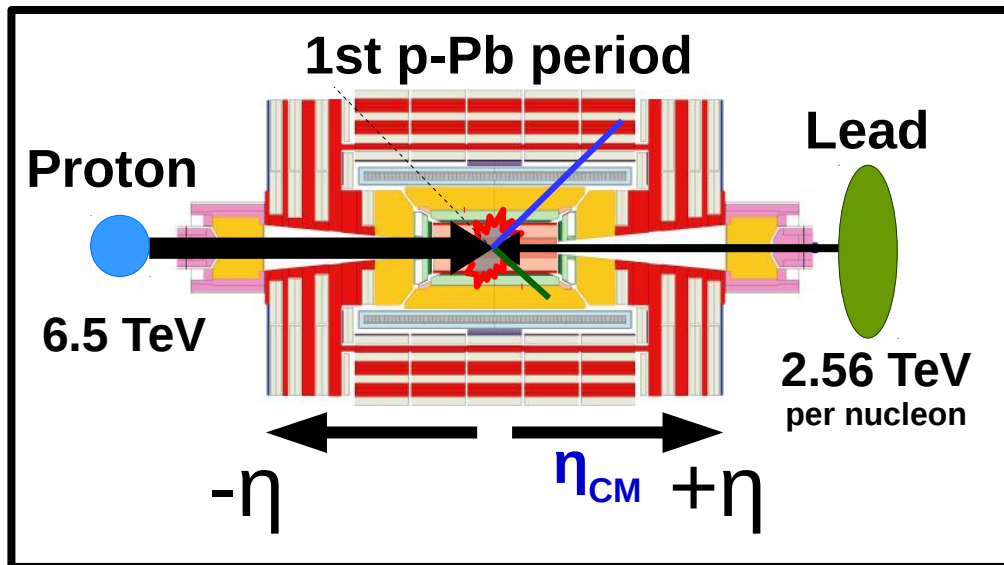
Year	$\sqrt{s_{NN}}$	Luminosity (CMS)
2013	5.02 TeV	35 nb ⁻¹
2016	8.16 TeV	174 nb ⁻¹

Outline

- Theoretical context
- The CMS detector at the LHC
- **W-boson production in p-Pb at 8.16 TeV**
 - Introduction
 - **Analysis**
 - Results
- Charmonium production in Pb-Pb at 5.02 TeV
 - Introduction
 - Analysis
 - Results
- Conclusions

Proton-lead collisions

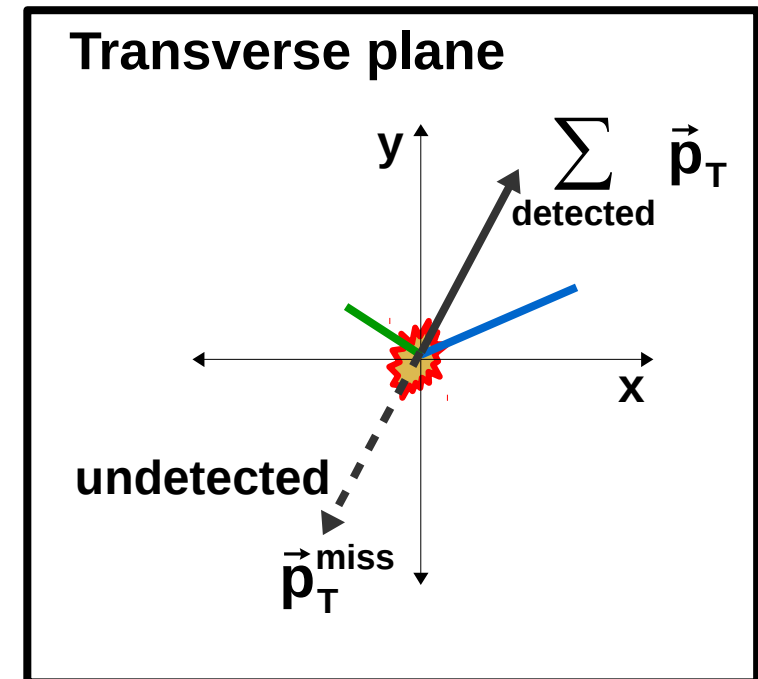
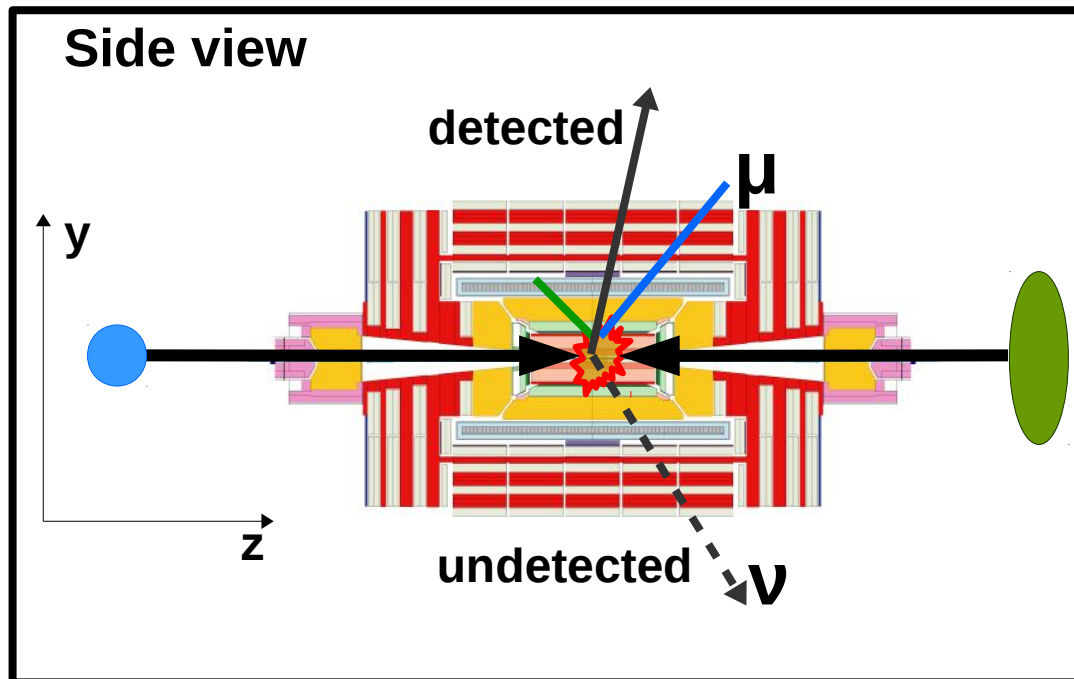
Proton-lead asymmetric collisions:



- Positive pseudorapidity ($+\eta$) defined along the proton-going direction
- Center-of-mass frame boosted by 0.465 units of rapidity

Missing transverse momentum

- Muonic decays of W bosons produce a high p_T muon and neutrino ($p_T \sim 40 \text{ GeV}/c$)
- Neutrinos are not detected, but their p_T can be inferred from the missing p_T



- Missing transverse momentum is the imbalance in p_T of all observed particles:

$$\vec{p}_T^{\text{miss}} = - \sum_{\text{detected}} \vec{p}_T$$

Background

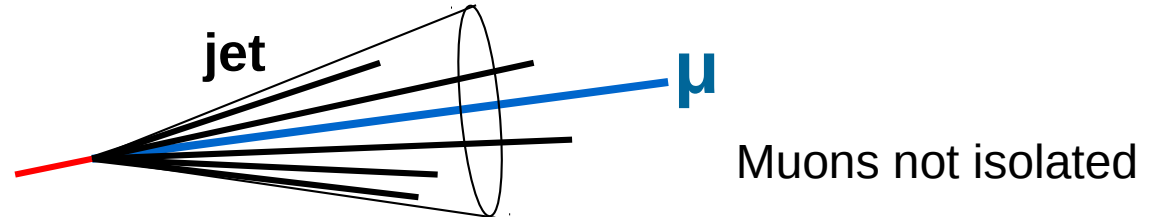
Several sources of background events can produce p_T^{miss} and high p_T muons

Background

Several sources of background events can produce p_T^{miss} and high p_T muons

QCD jet background: Muon decays of heavy-flavour quarks or light hadrons (π or K)

- Large cross section at LHC
- Muons produced in jets

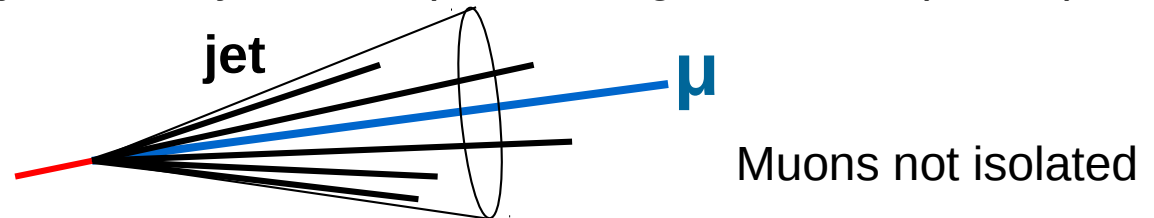


Background

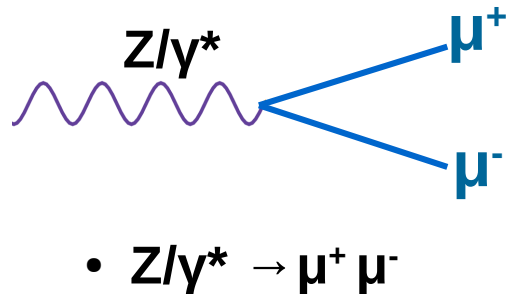
Several sources of background events can produce p_T^{miss} and high p_T muons

QCD jet background: Muon decays of heavy-flavour quarks or light hadrons (π or K)

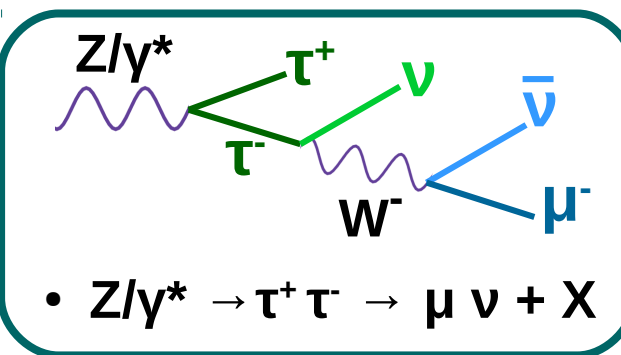
- Large cross section at LHC
- Muons produced in jets



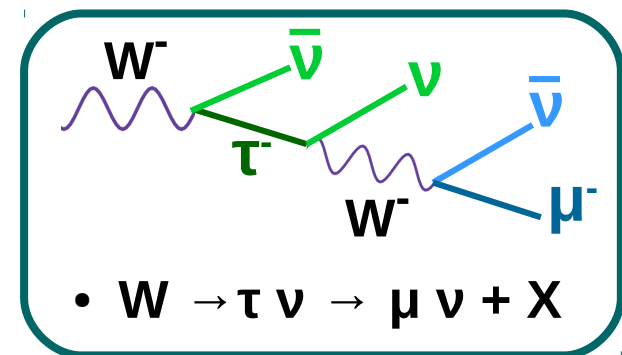
Electroweak background: Muon decays of Z bosons, virtual photons or tau leptons



$$\bullet \ Z/\gamma^* \rightarrow \mu^+ \mu^-$$



$$\bullet \ Z/\gamma^* \rightarrow \tau^+ \tau^- \rightarrow \mu \nu + X$$



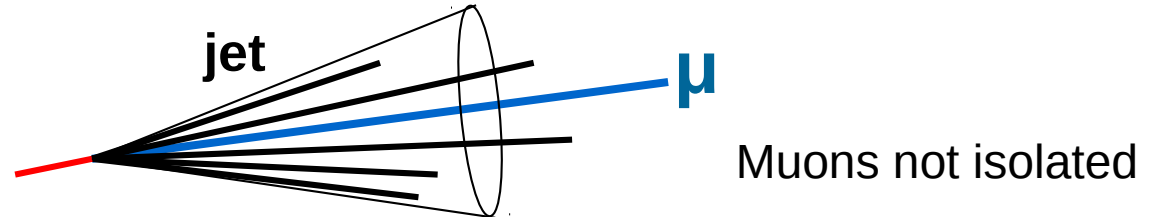
$$\bullet \ W \rightarrow \tau \nu \rightarrow \mu \nu + X$$

Background

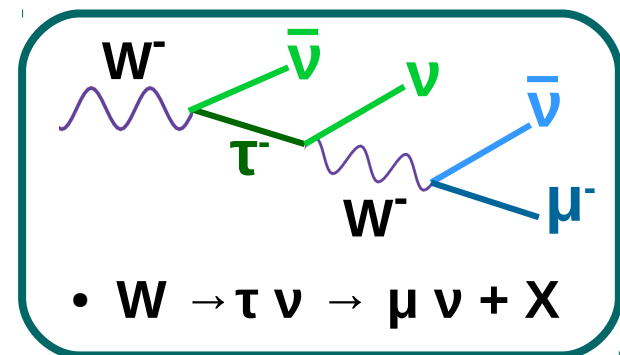
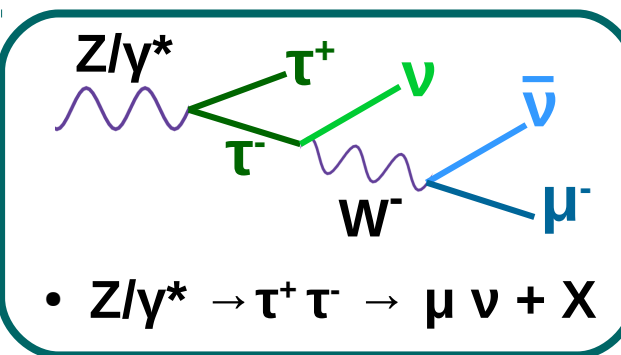
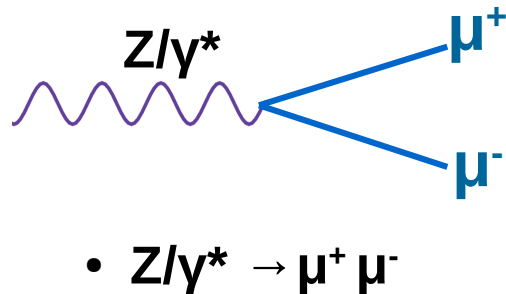
Several sources of background events can produce p_T^{miss} and high p_T muons

QCD jet background: Muon decays of heavy-flavour quarks or light hadrons (π or K)

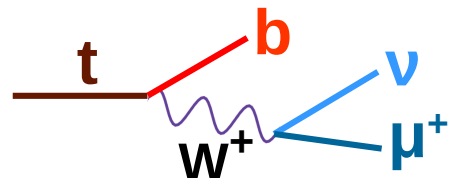
- Large cross section at LHC
- Muons produced in jets



Electroweak background: Muon decays of Z bosons, virtual photons or tau leptons



Top-quark background: Muon decays from top quark and anti-quark pairs



Data selection

Events in data are selected using the following criteria:

Data selection

Events in data are selected using the following criteria:

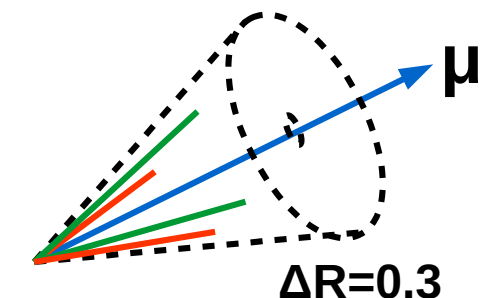
- **Trigger:** requires the presence of a muon with $p_T > 12 \text{ GeV}/c$
- **Analysis selection:** muon $p_T > 25 \text{ GeV}/c$ and $|\eta_{\text{LAB}}| < 2.4$

Data selection

Events in data are selected using the following criteria:

- **Trigger:** requires the presence of a muon with $p_T > 12 \text{ GeV}/c$
- **Analysis selection:** muon $p_T > 25 \text{ GeV}/c$ and $|\eta_{\text{LAB}}| < 2.4$
- **Muon isolation:** requires isolated muons

$$I^\mu = \left(\sum_{\substack{\Delta R < 0.3 \\ \text{charged hadrons}}} p_T + \sum_{\substack{\Delta R < 0.3 \\ \text{neutral hadrons}}} p_T + \sum_{\substack{\Delta R < 0.3 \\ \text{photons}}} p_T \right) / p_T^\mu < 0.15$$



- Sum of p_T of particles (γ , h^\pm & h^0) around the muon $< 15\%$ of muon p_T
- Suppress muons from jets

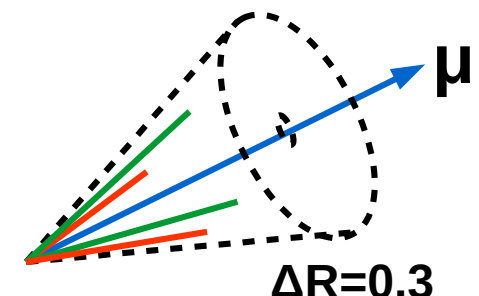
Data selection

Events in data are selected using the following criteria:

- **Trigger:** requires the presence of a muon with $p_T > 12 \text{ GeV}/c$
- **Analysis selection:** muon $p_T > 25 \text{ GeV}/c$ and $|\eta_{\text{LAB}}| < 2.4$

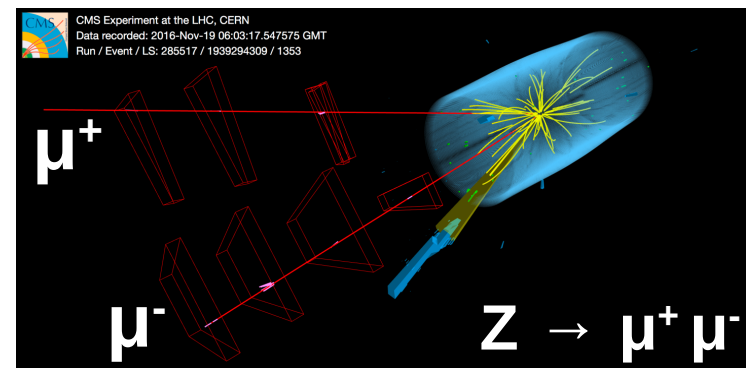
- **Muon isolation:** requires isolated muons

$$I^\mu = \left(\sum_{\substack{\Delta R < 0.3 \\ \text{charged hadrons}}} p_T + \sum_{\substack{\Delta R < 0.3 \\ \text{neutral hadrons}}} p_T + \sum_{\substack{\Delta R < 0.3 \\ \text{photons}}} p_T \right) / p_T^\mu < 0.15$$

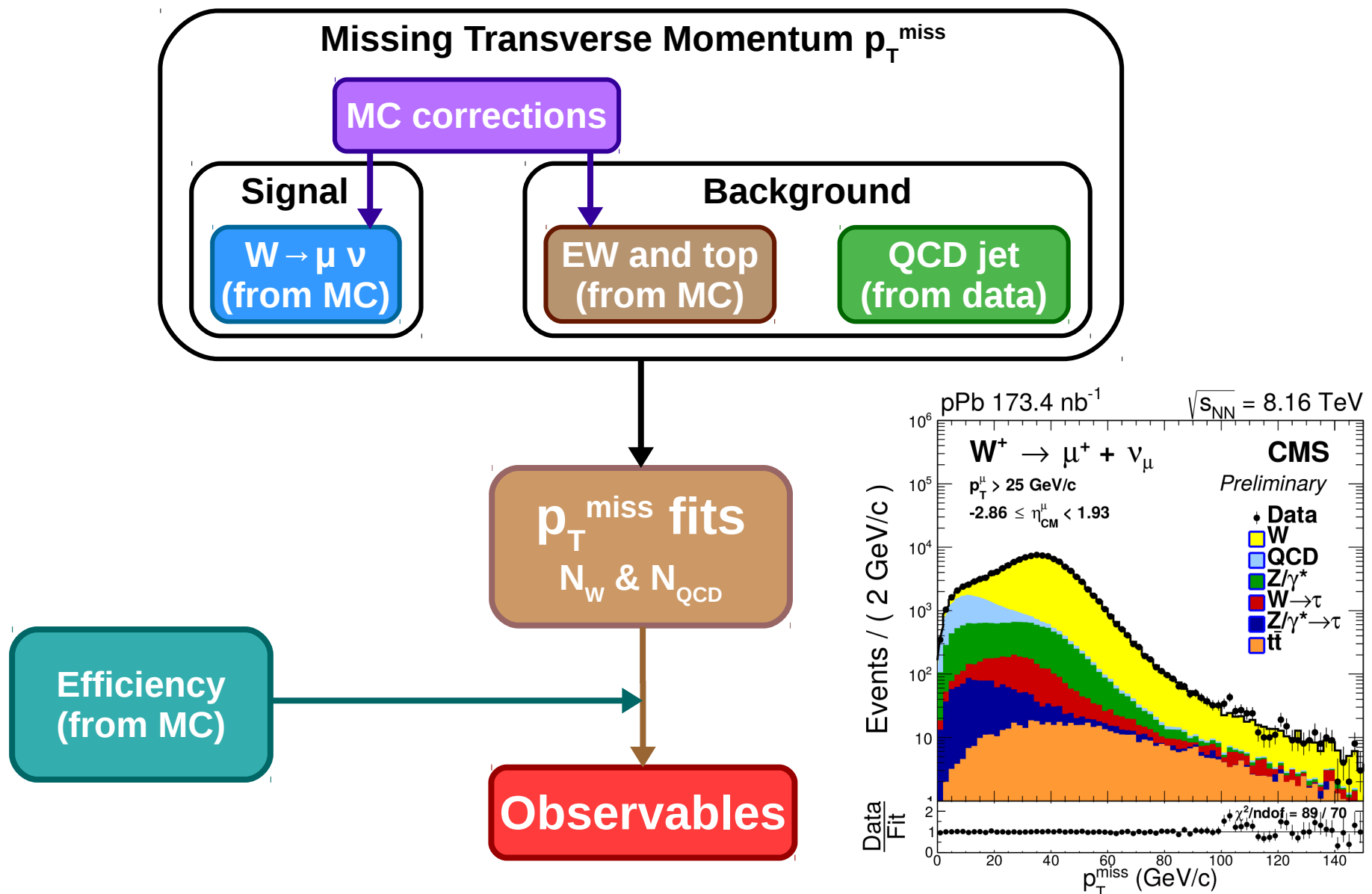


- Sum of p_T of particles (γ , h^\pm & h^0) around the muon $< 15\%$ of muon p_T
- Suppress muons from jets

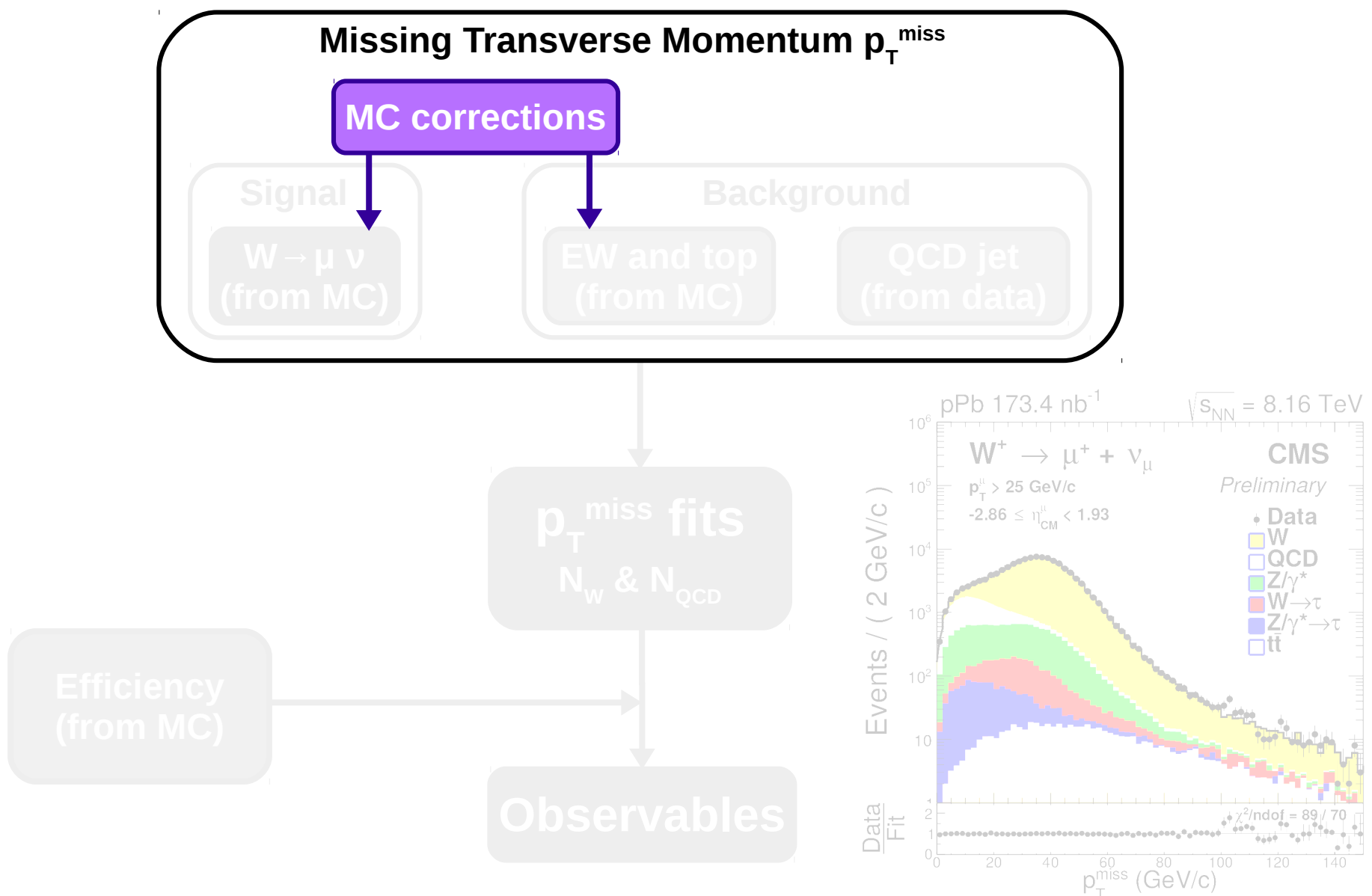
- $Z/\gamma^* \rightarrow \mu^+ \mu^-$ veto: rejects events containing $\mu^- \mu^+$ pairs, each muon with $p_T > 15 \text{ GeV}/c$



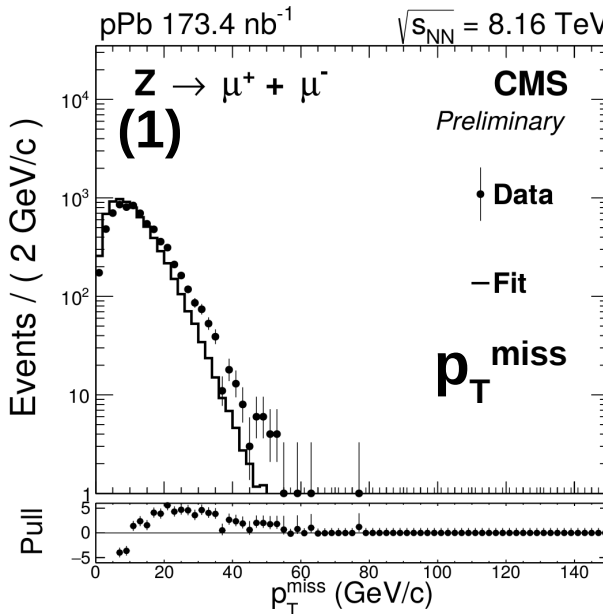
Extraction of W-boson yields



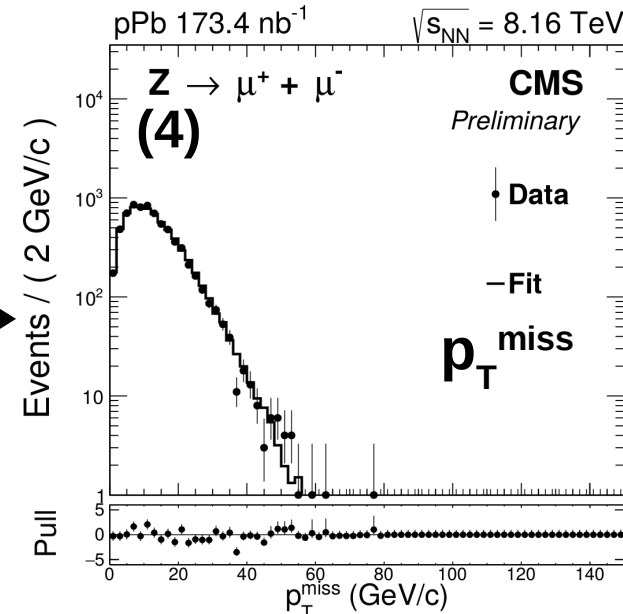
Extraction of W-boson yields



MC corrections

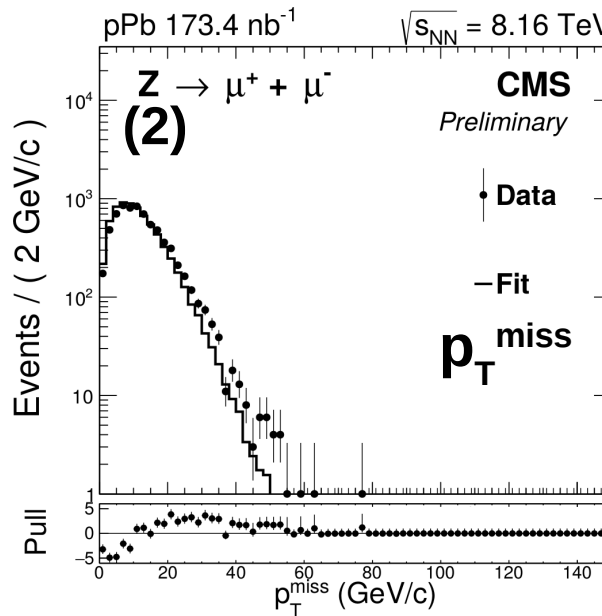
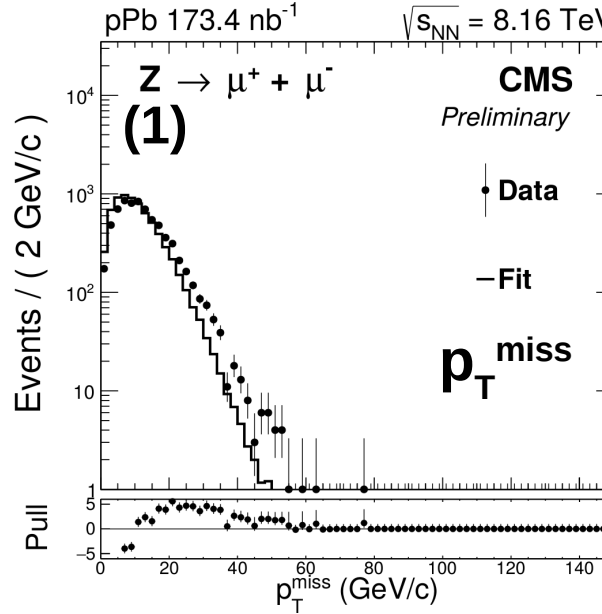


MC corrections

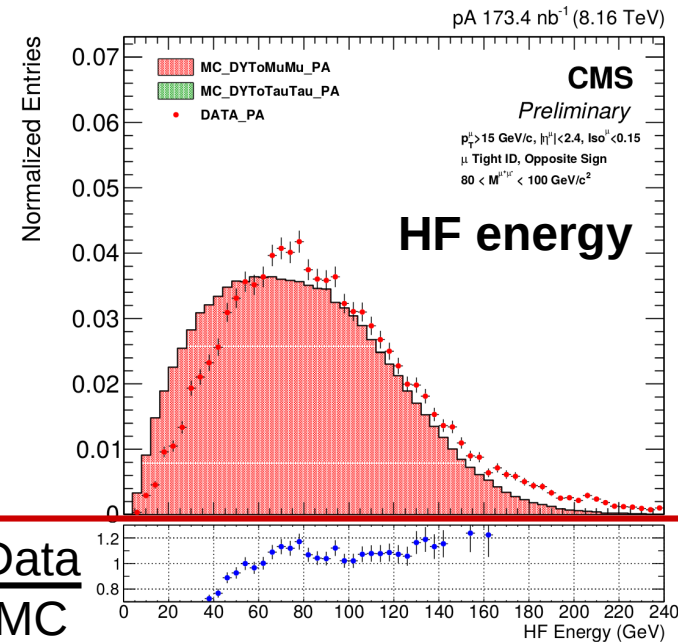
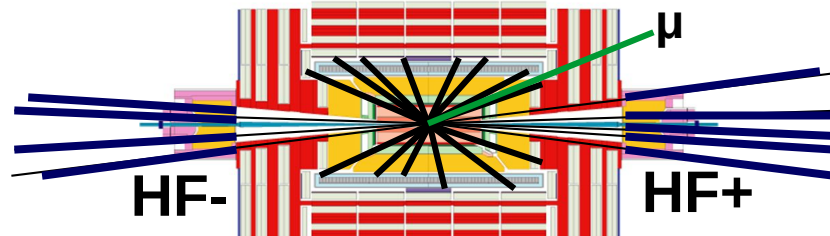


- Simulations are used to describe $p_{\text{T}}^{\text{miss}}$ shape of signal and (EW, top) background events
- At first, the simulated $p_{\text{T}}^{\text{miss}}$ distribution does not describe data → correct the simulations
- Use a $Z \rightarrow \mu^+ \mu^-$ sample to derive the corrections (similar to the W but background-free)
- **Three corrections** are implemented:
 - Event activity weighing
 - Weak boson p_{T} weighing
 - Recoil calibration

Event activity weighing

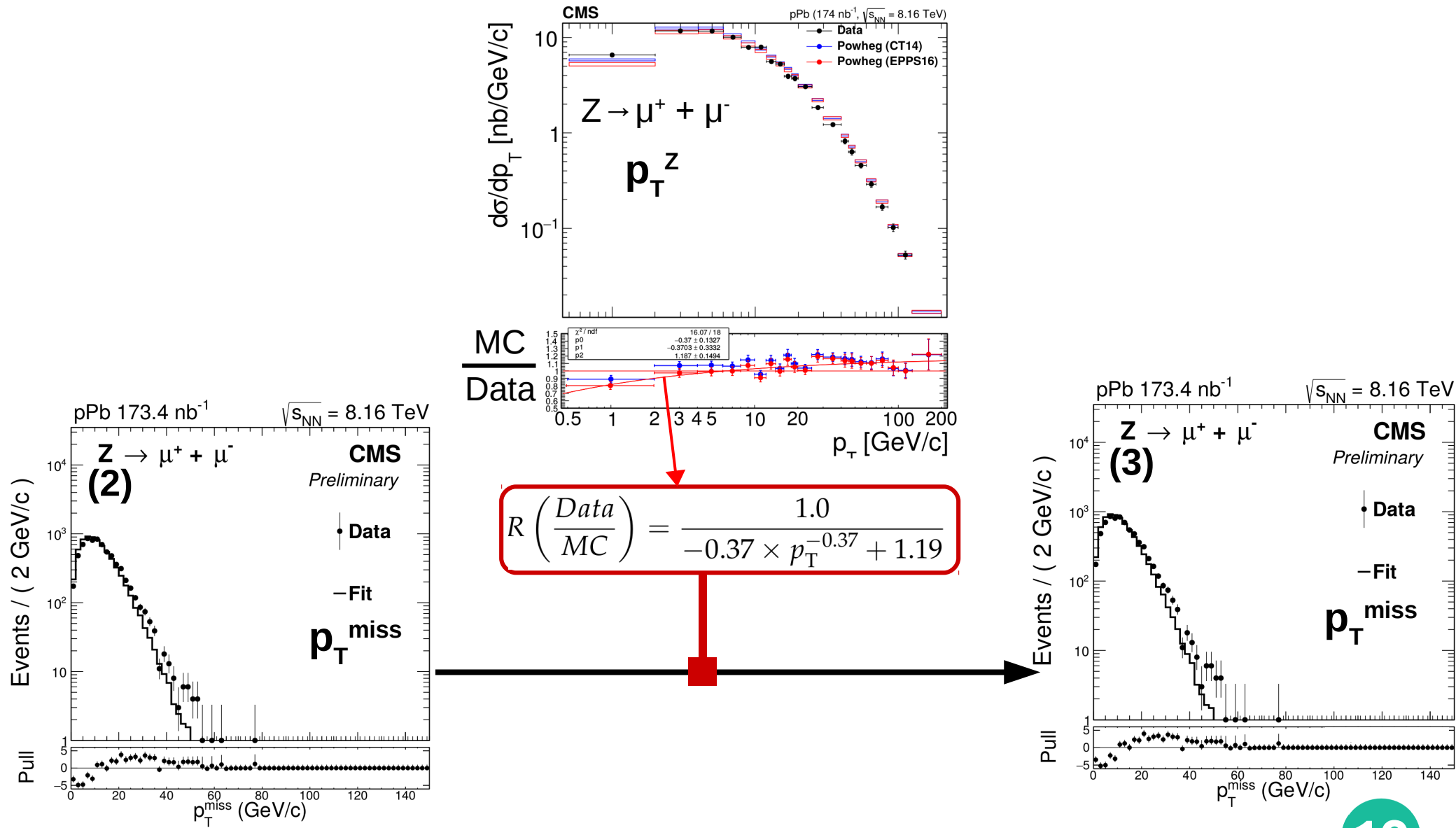


Energy in forward calorimeter (HF) correlated with event activity



Weak boson p_T weighing

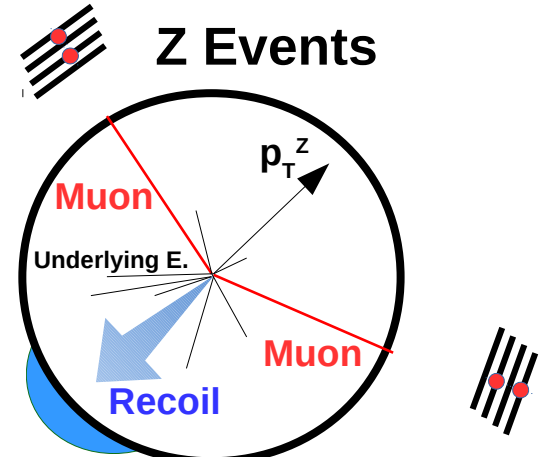
Simulated weak boson p_T does not match data \rightarrow affects p_T^{miss} and muon p_T



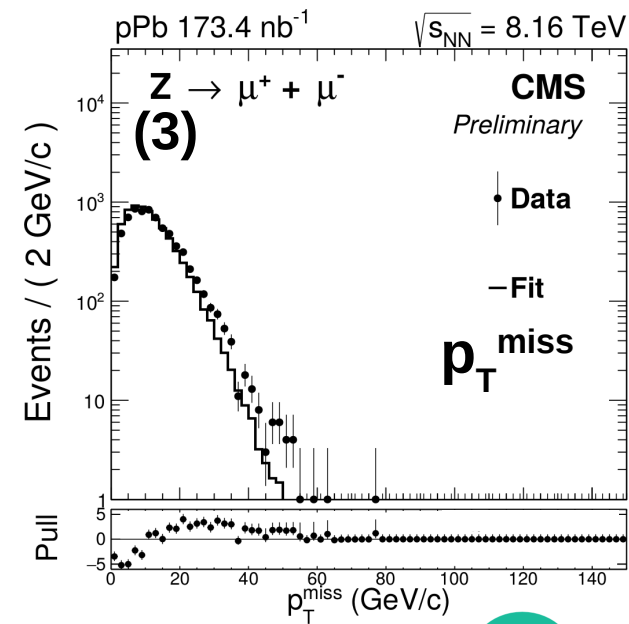
Recoil calibration

Recoil is the p_T sum of all observed particles excluding the Z boson p_T

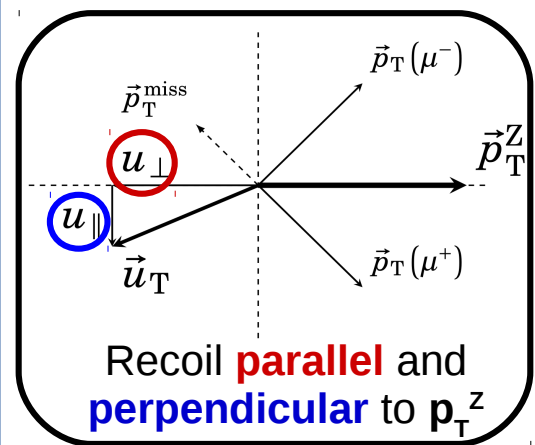
$$\vec{u}_T = \left(\sum_{\text{detected}} \vec{p}_T \right) - \vec{p}_T^Z$$



- Use data-driven technique to calibrate the recoil considering correlation between underlying events and weak boson p_T

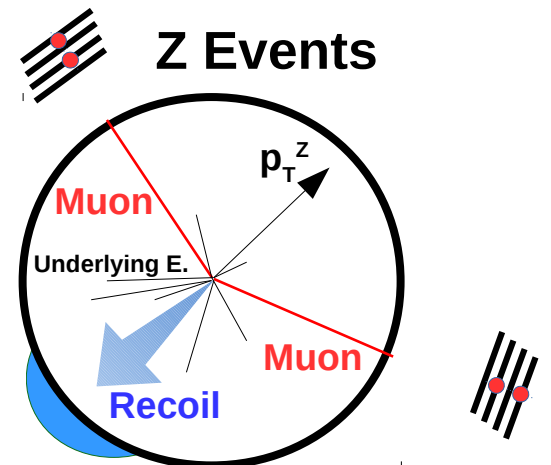


Recoil calibration

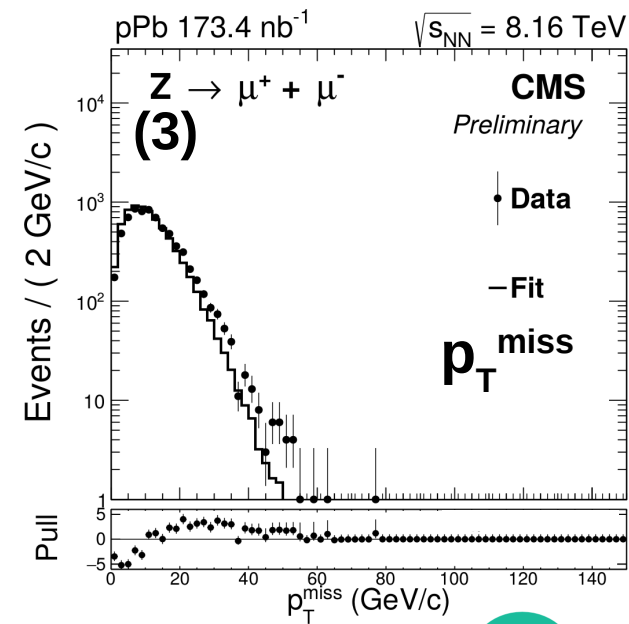
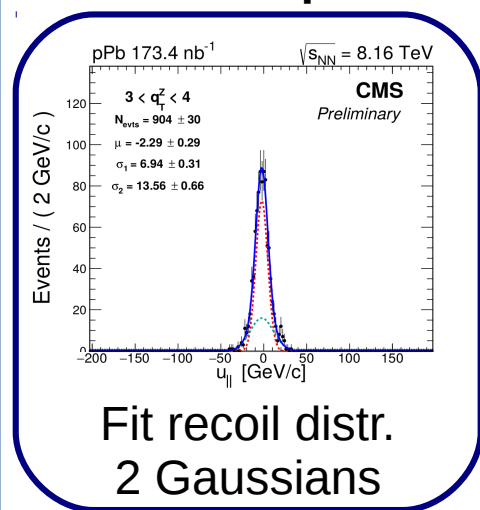


Recoil:

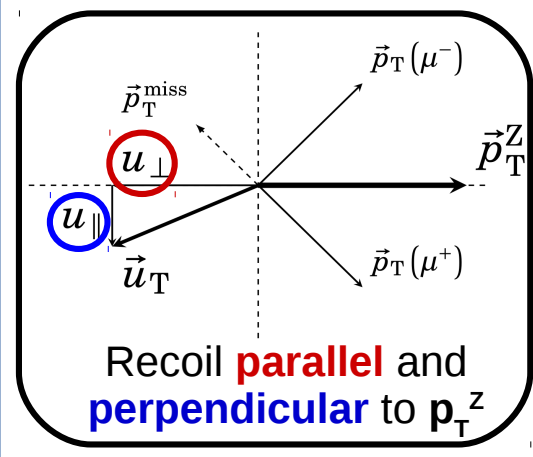
$$\vec{u}_T = \left(\sum_{\text{detected}} \vec{p}_T \right) - \vec{p}_T^Z$$



1st step

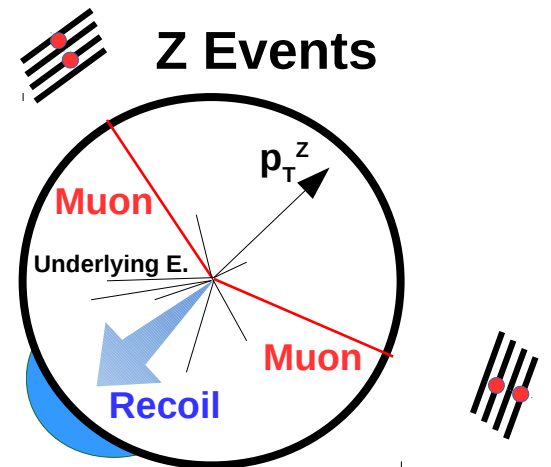


Recoil calibration

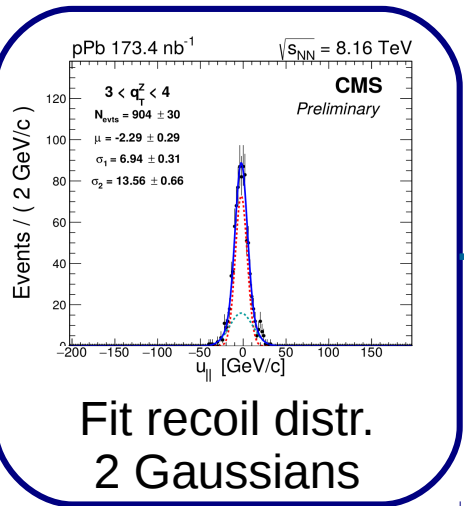


Recoil:

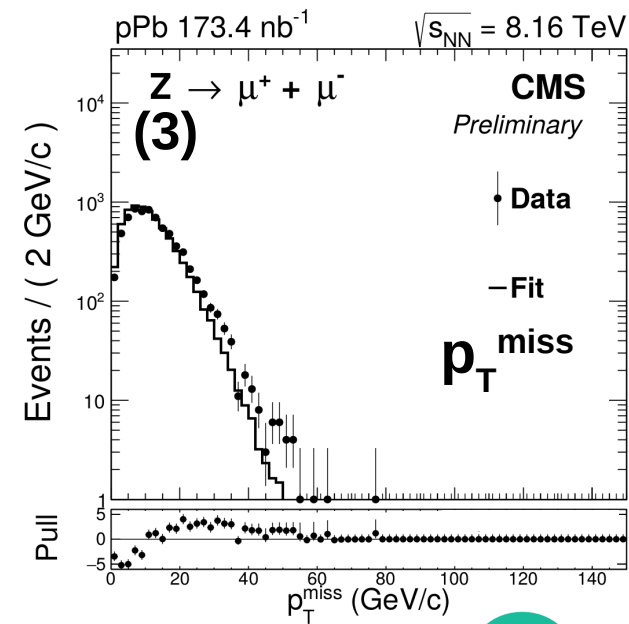
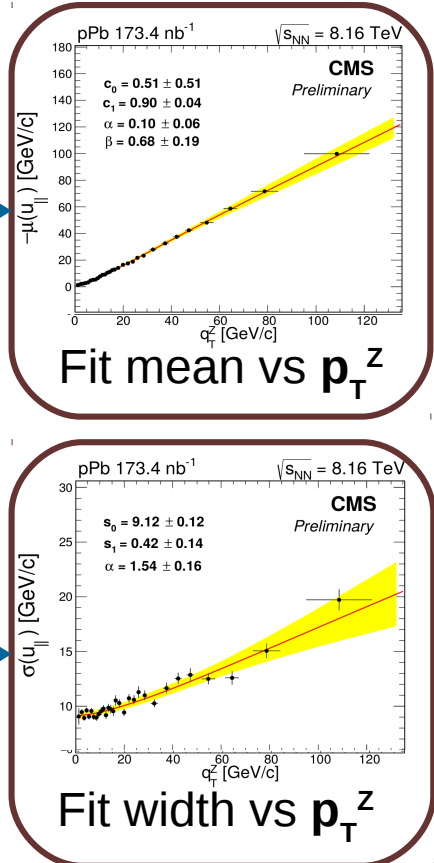
$$\vec{u}_T = \left(\sum_{\text{detected}} \vec{p}_T \right) - \vec{p}_T^Z$$



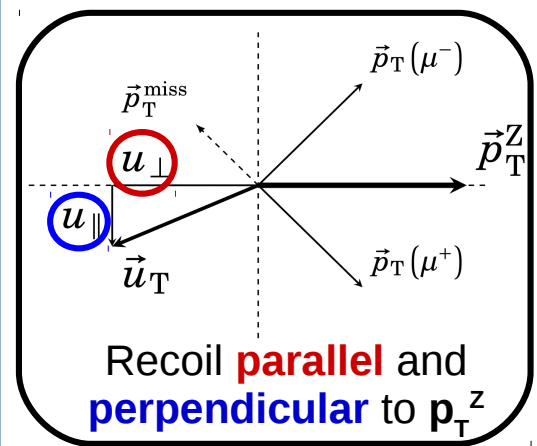
1st step



2nd step

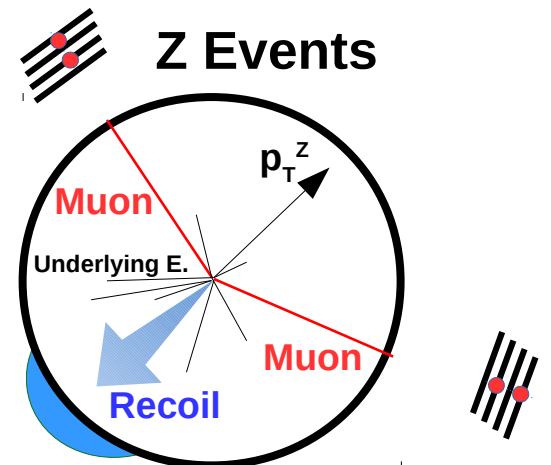


Recoil calibration

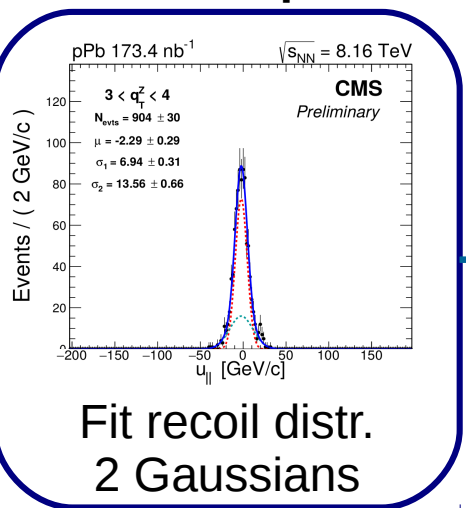


Recoil:

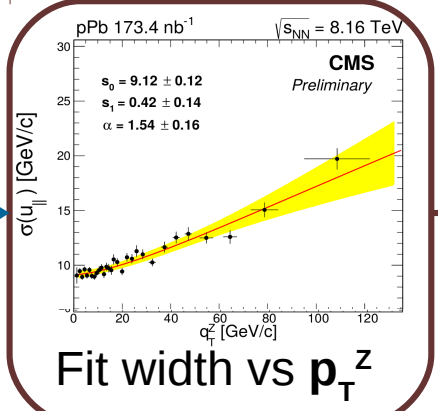
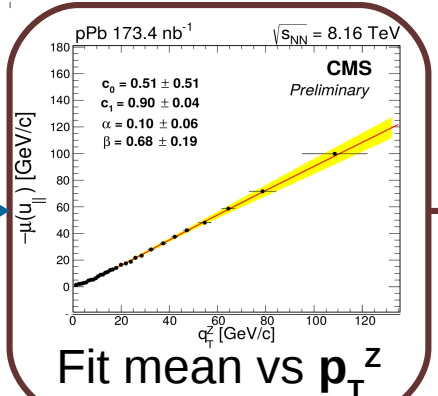
$$\vec{u}_T = \left(\sum_{\text{detected}} \vec{p}_T \right) - \vec{p}_T^Z$$



1st step



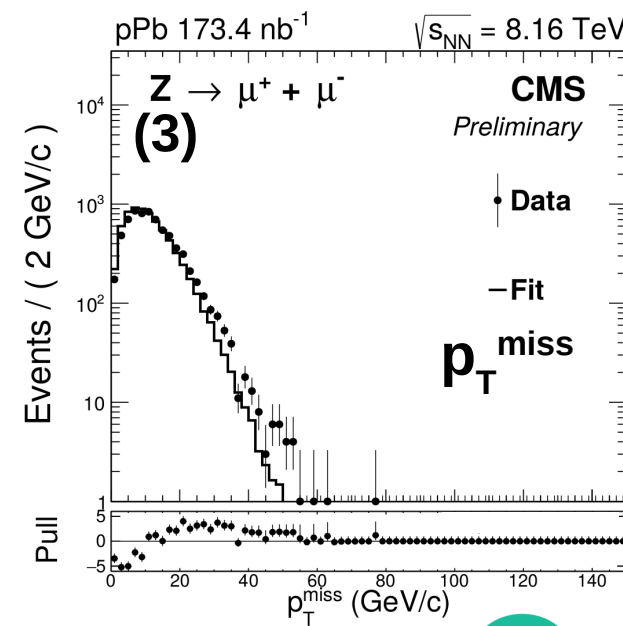
2nd step



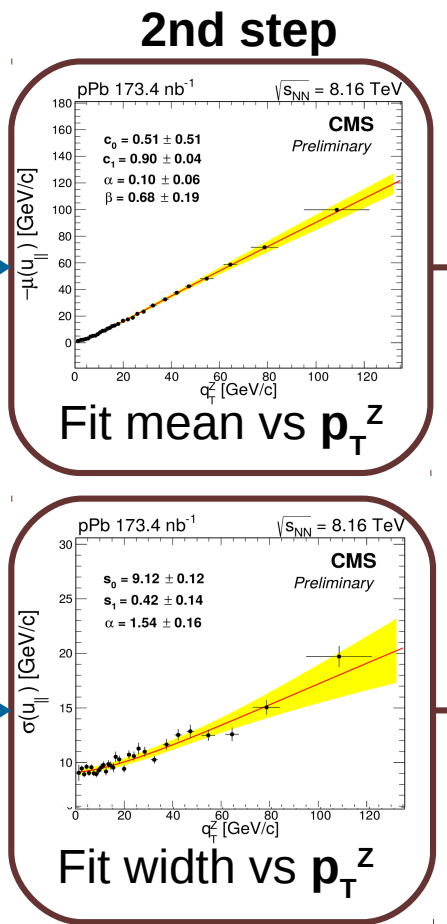
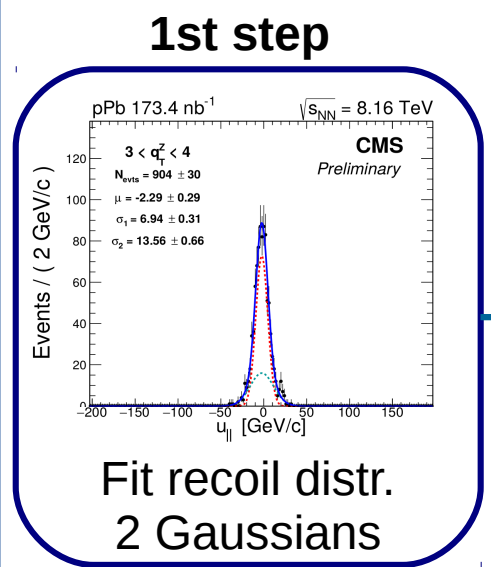
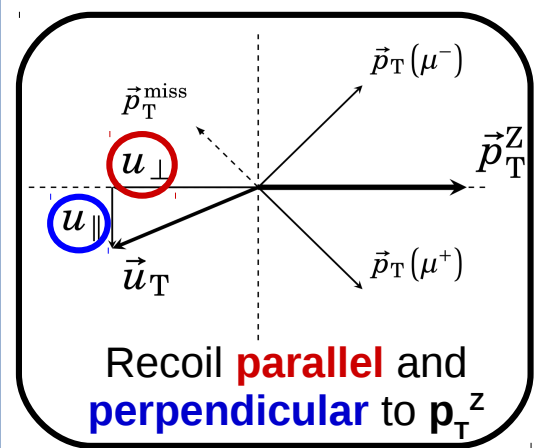
3rd step

Scale recoil
in simulation
using boson p_T

average mean and
width match data



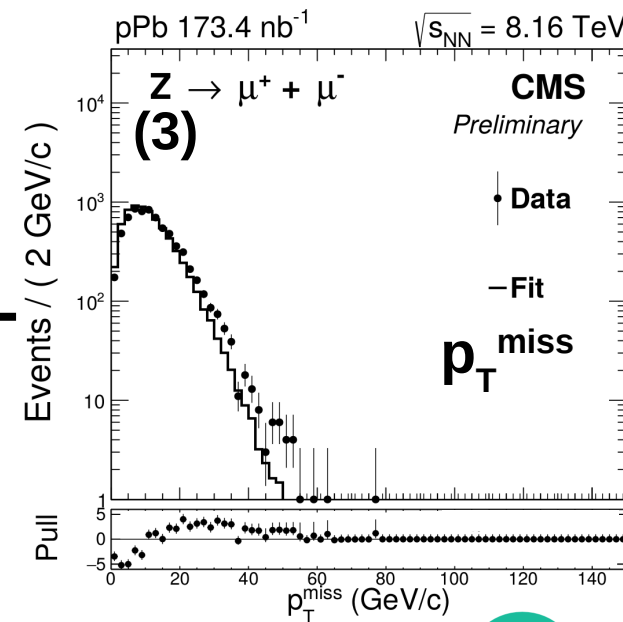
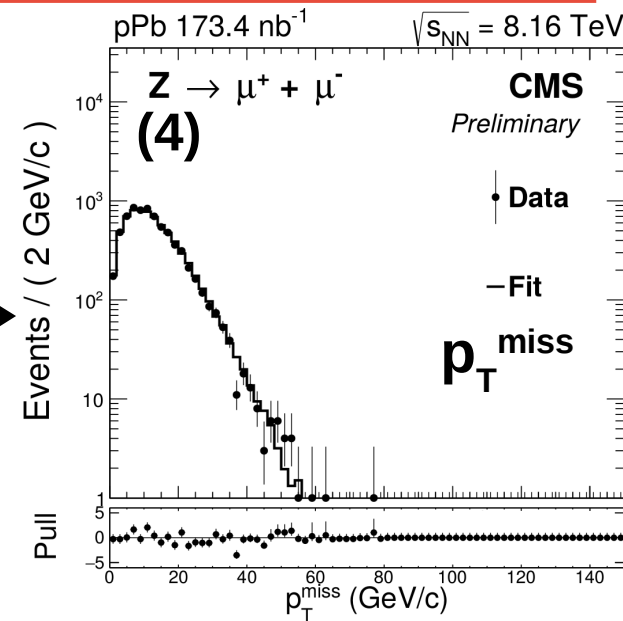
Recoil calibration



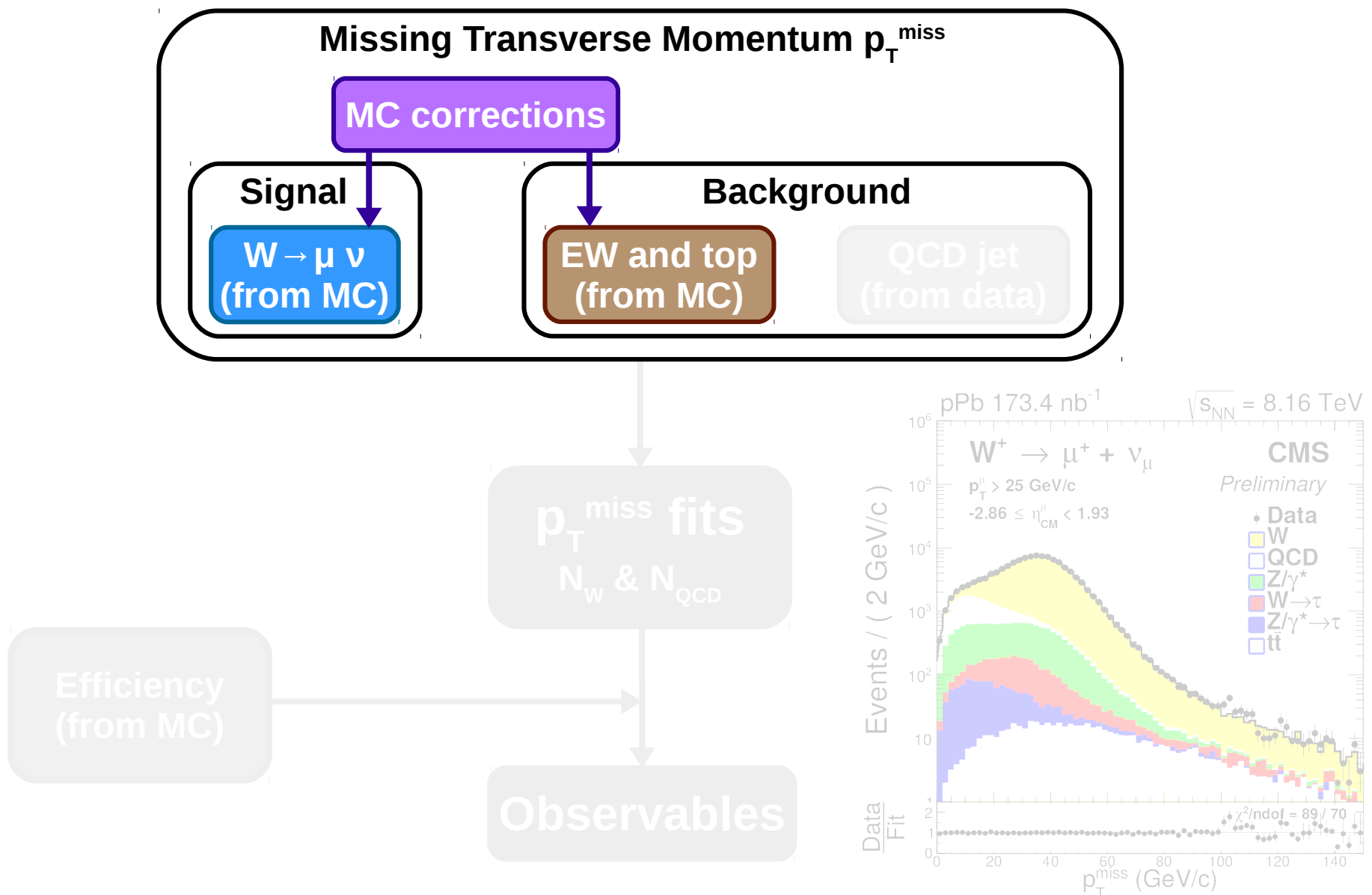
3rd step

Scale recoil in simulation using boson p_T

average mean and width match data

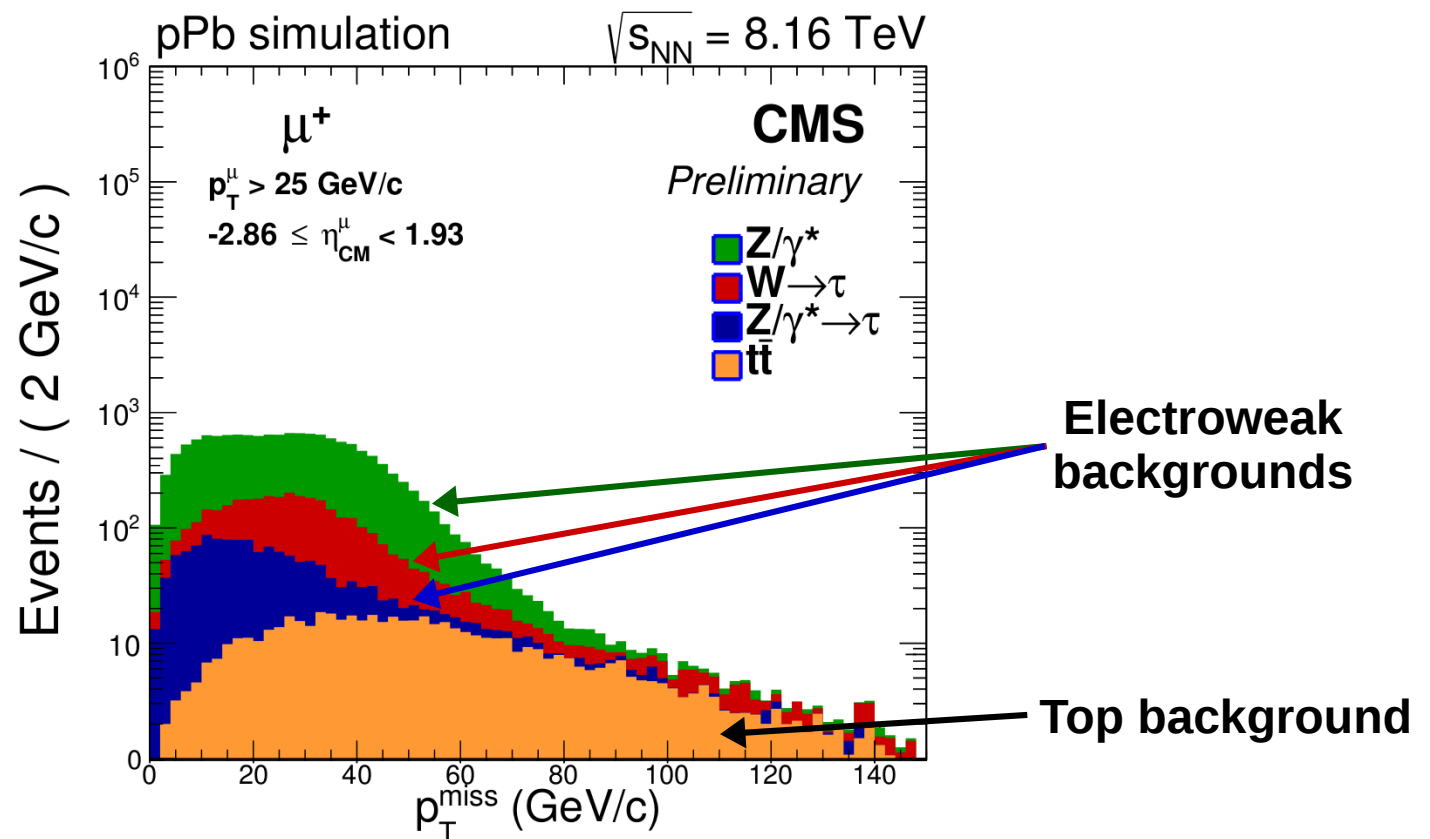


Extraction of W-boson yields

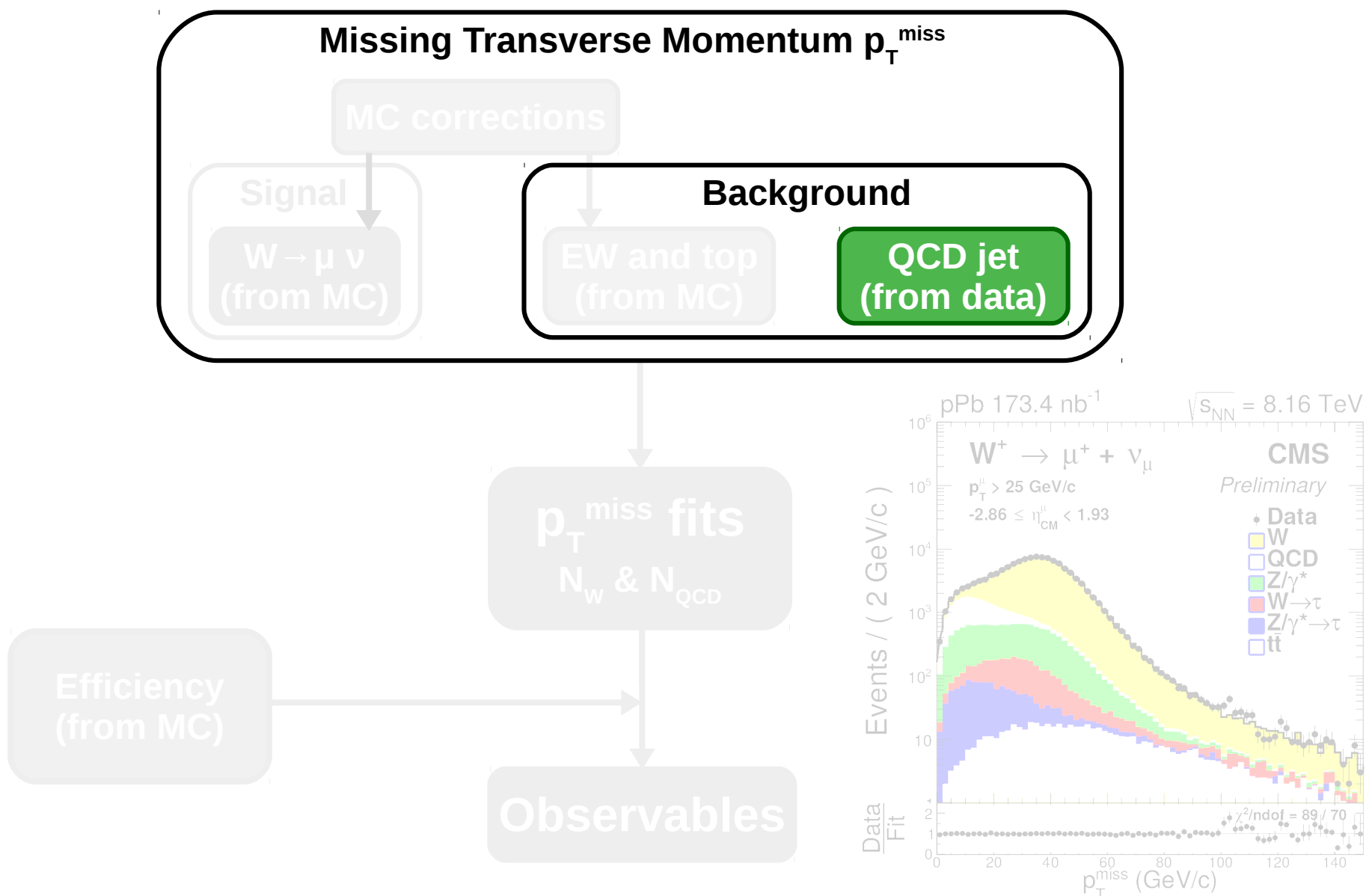


p_T^{miss} templates from simulation

The p_T^{miss} distribution of signal, electroweak background and top background is described with simulations (next-to-leading order + EPPS16 nPDF)

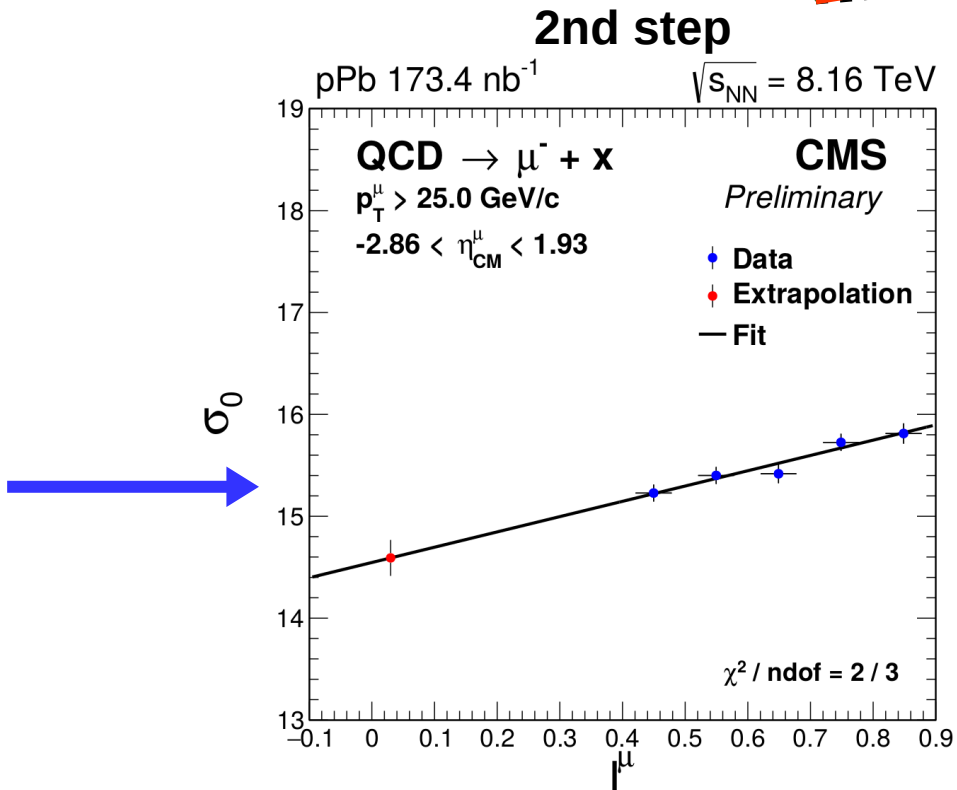
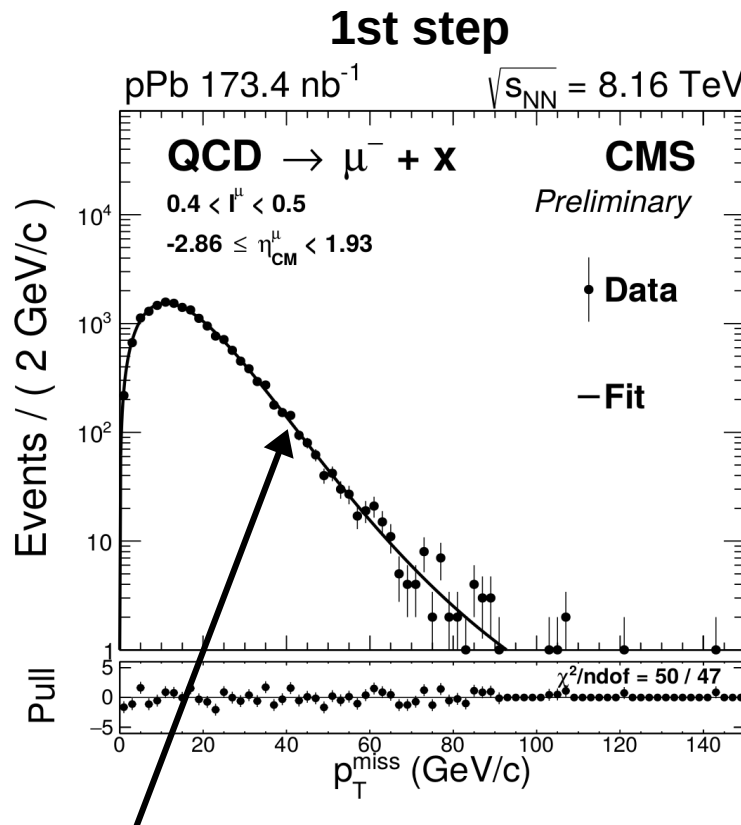
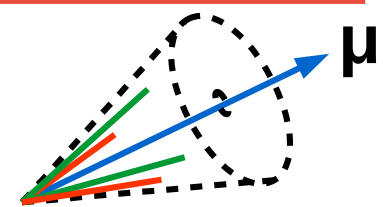


Extraction of W-boson yields



QCD jet p_T^{miss} function

Derived using a sample of non-isolated muons from data ($|l^\mu| > 0.4$)

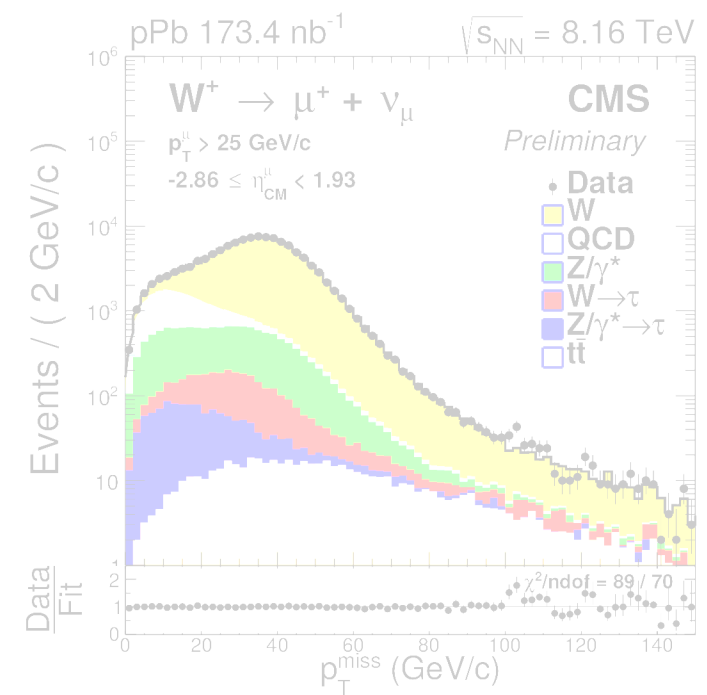
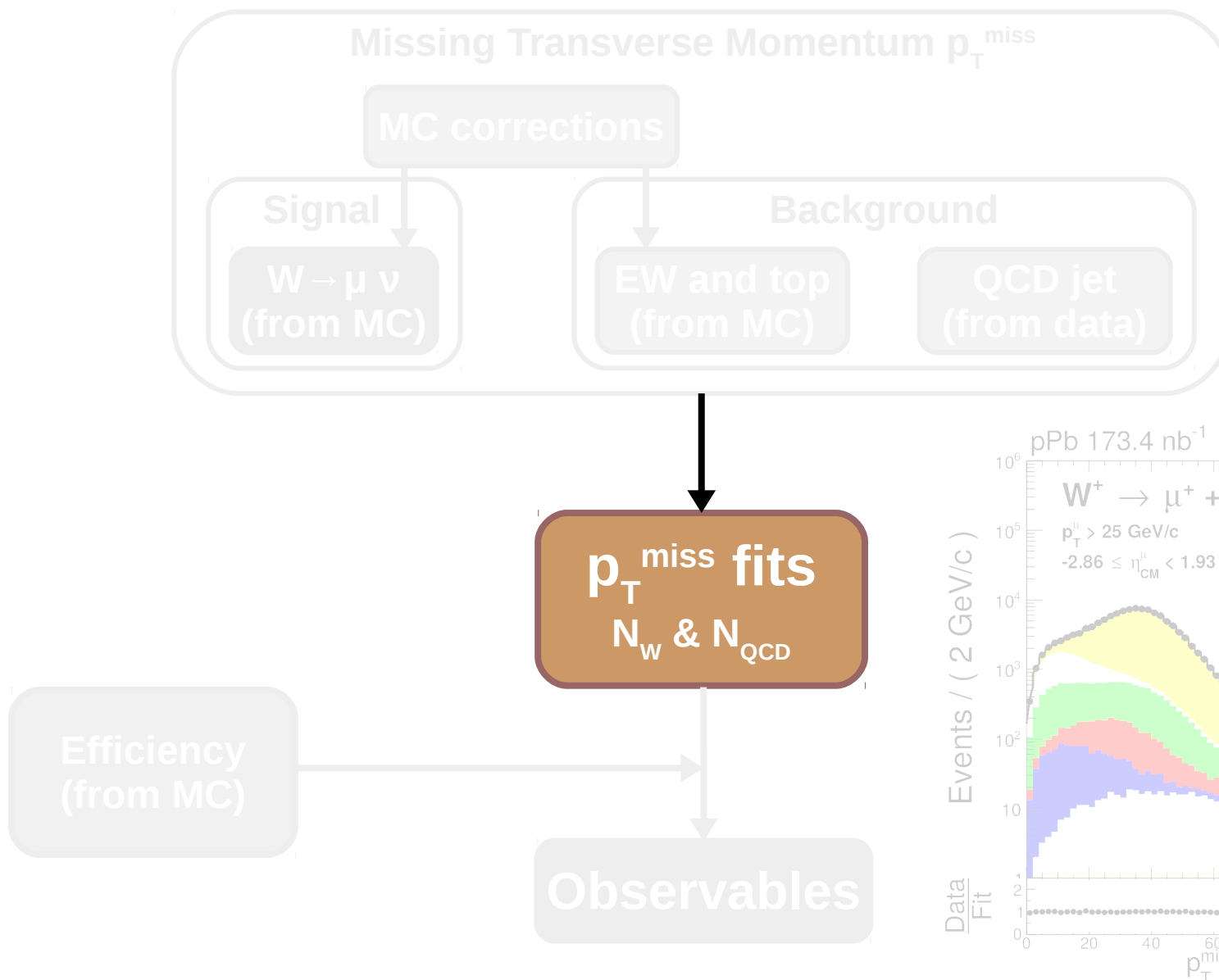


Modified Rayleigh distribution

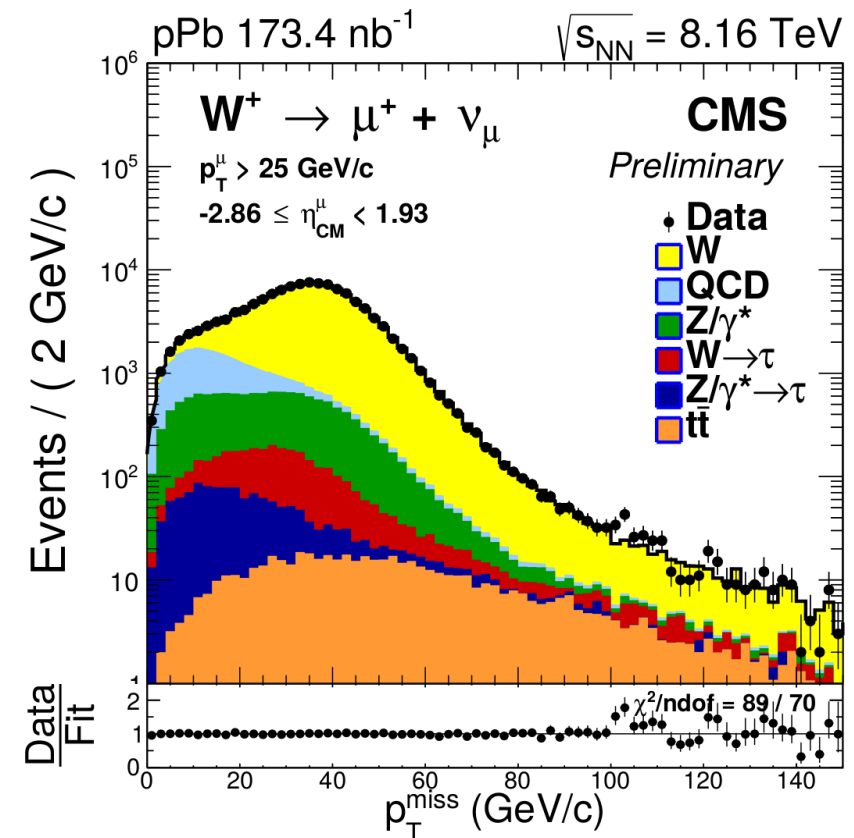
$$p_T^{\text{miss}} \cdot \exp \left(-\frac{(p_T^{\text{miss}})^2}{2(\sigma_0 + \sigma_1 \cdot p_T^{\text{miss}} + \sigma_2 \cdot (p_T^{\text{miss}})^2)^2} \right)$$

Extrapolate p_T^{miss} parameters (σ_0 , σ_1 and σ_2) to low muon isolation (signal region)

Extraction of W-boson yields



- W yields extracted from fits to the p_T^{miss} distribution
- The relative fractions of the EW and top backgrounds w.r.t the signal ($r = N_{\text{bkg}} / N_W$) are fixed to simulation, assuming similar modification of their yields



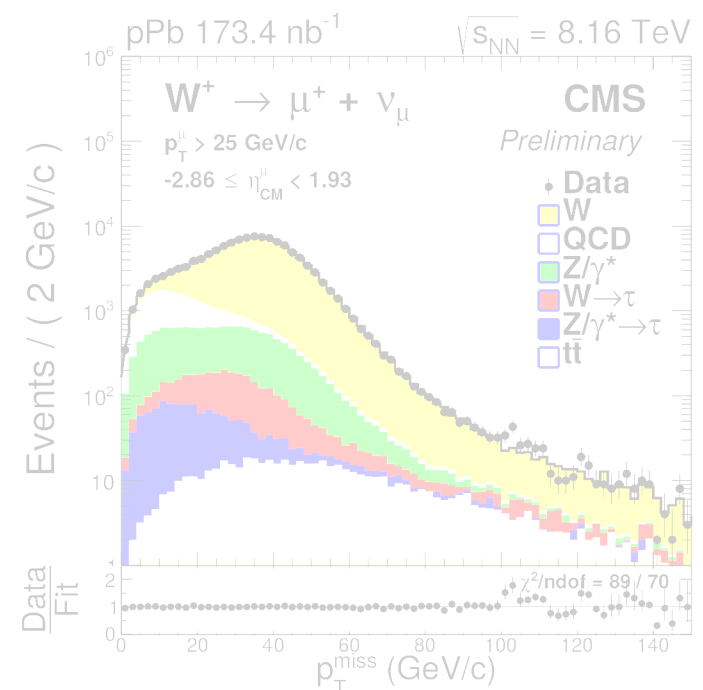
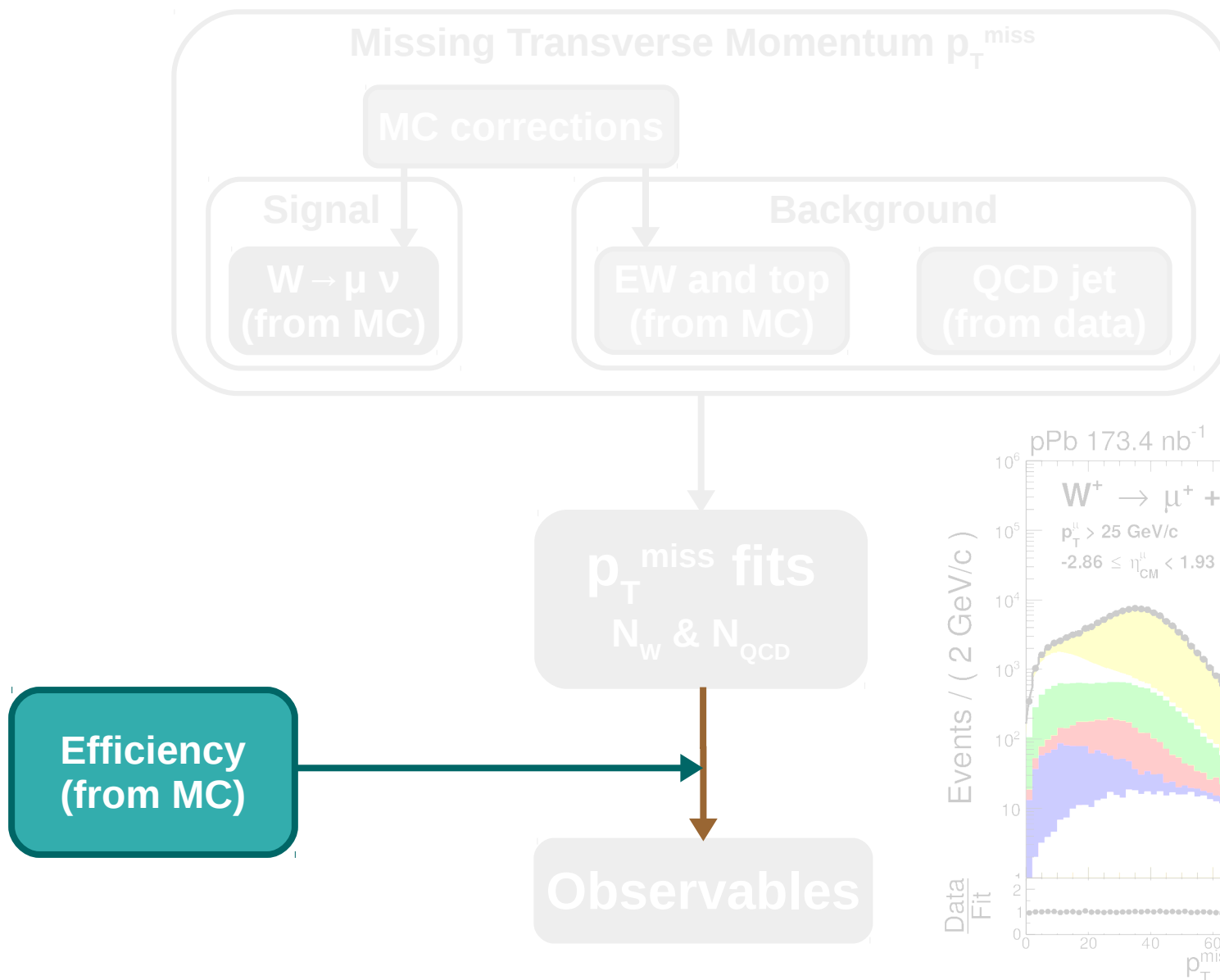
Free parameters:

- N_W : Number of signal events
- N_{QCD} : Number of QCD jet events

Background Sources :

QCD jet (~13%) , Z/ γ^* $\rightarrow \mu$ (~9%), W $\rightarrow \tau$ (~2%), Z/ γ^* $\rightarrow \tau$ (~1%) and tt (~0.5%)

Extraction of W-boson yields



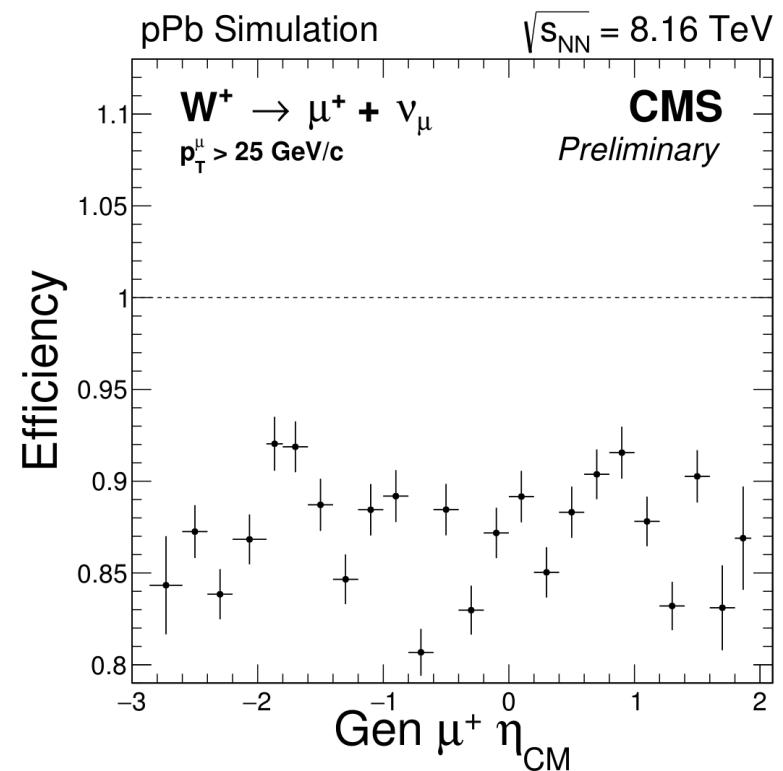
Muon efficiency

Muon efficiency computed from $W \rightarrow \mu\nu$ simulation:

Number of muons passing analysis selection

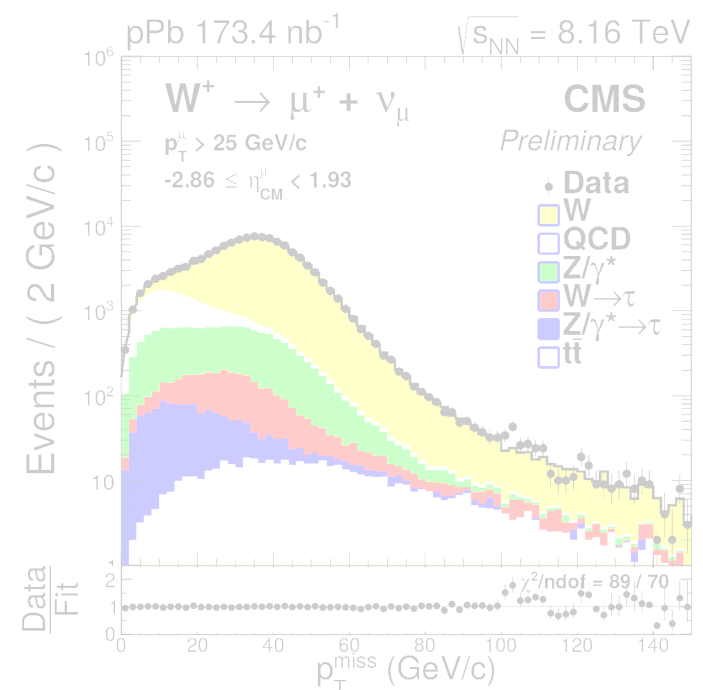
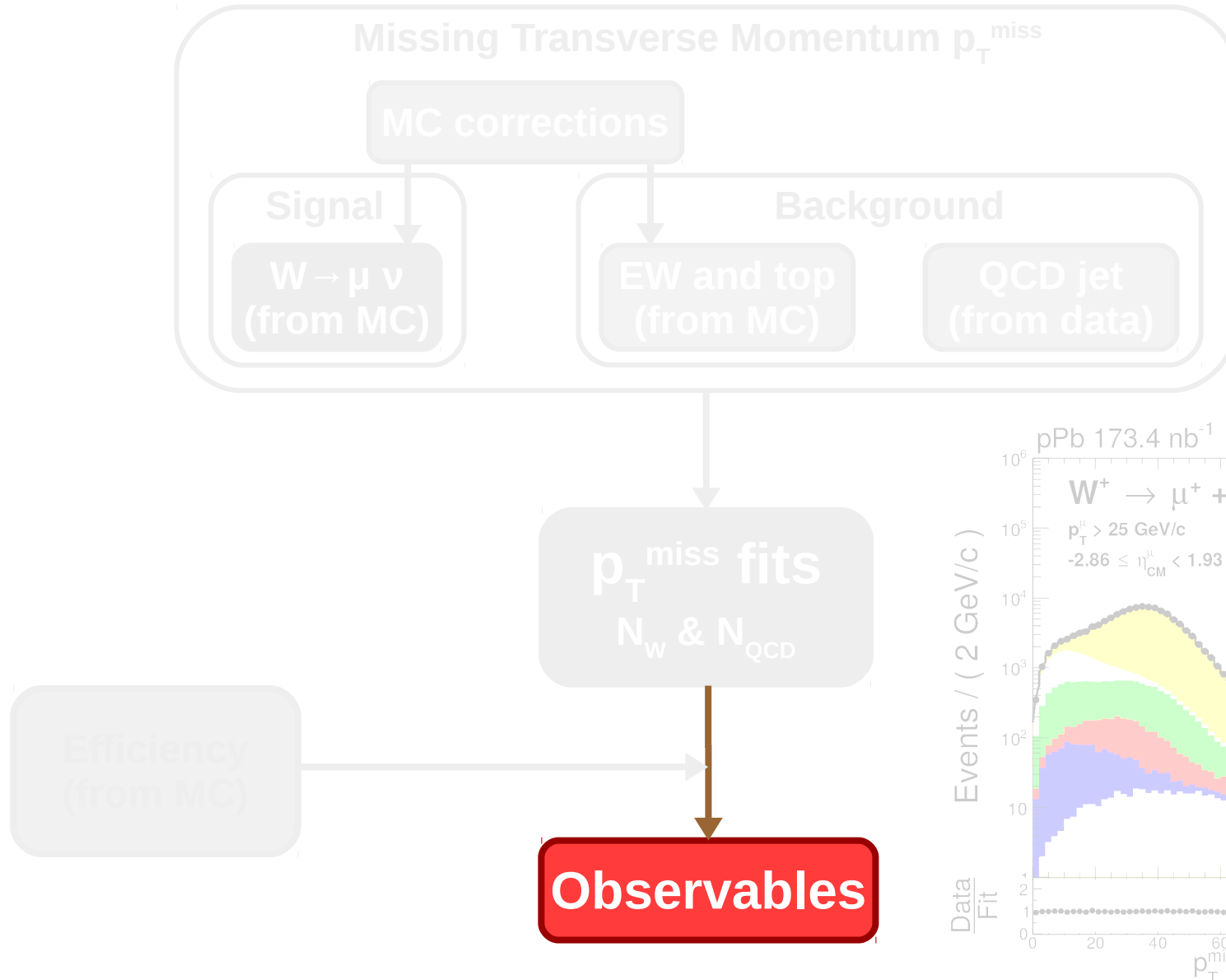
$$\epsilon^{\mu^\pm}(\eta^\mu) = \frac{N_{\text{ana}}^{\mu^\pm}[\eta^\mu]}{N_{\text{gen}, p_T > 25 \text{ GeV}/c}^{\mu^\pm}[\eta^\mu]}$$

Number of muons with $p_T > 25 \text{ GeV}/c$



Muon efficiency between 80% and 95%, corrected with data-driven method (Tag-and-Probe)

Extraction of W-boson yields



Observables

Measured number of signal events:

$$N_{\mu}^{\pm}(\eta_{CM}^{\mu}) = \frac{N_{\mu,raw}^{\pm}(\eta_{CM}^{\mu})}{\epsilon^{\pm}(\eta_{CM}^{\mu})}$$

Extracted from p_T^{miss} fit

Observables

Measured number of signal events:

$$N_{\mu}^{\pm}(\eta_{\text{CM}}^{\mu}) = \frac{N_{\mu,\text{raw}}^{\pm}(\eta_{\text{CM}}^{\mu})}{\epsilon^{\pm}(\eta_{\text{CM}}^{\mu})}$$

Extracted from p_T^{miss} fit

Cross section of $W \rightarrow \mu\nu$:

$$\frac{d\sigma(W^{\pm} \rightarrow \mu^{\pm}\nu_{\mu})}{d\eta_{\text{CM}}^{\mu}}(\eta_{\text{CM}}^{\mu}) = \frac{N_{\mu}^{\pm}(\eta_{\text{CM}}^{\mu})}{\mathcal{L} \cdot \Delta\eta_{\text{CM}}^{\mu}}$$

Observables

Measured number of signal events:

$$N_{\mu}^{\pm}(\eta_{\text{CM}}^{\mu}) = \frac{N_{\mu,\text{raw}}^{\pm}(\eta_{\text{CM}}^{\mu})}{\epsilon^{\pm}(\eta_{\text{CM}}^{\mu})}$$

Extracted from p_T^{miss} fit

Cross section of $W \rightarrow \mu\nu$:

$$\frac{d\sigma(W^{\pm} \rightarrow \mu^{\pm}\nu_{\mu})}{d\eta_{\text{CM}}^{\mu}}(\eta_{\text{CM}}^{\mu}) = \frac{N_{\mu}^{\pm}(\eta_{\text{CM}}^{\mu})}{\mathcal{L} \cdot \Delta\eta_{\text{CM}}^{\mu}}$$

p-Pb integrated luminosity ($173.4 \pm 6.1 \text{ /nb}$)

Observables

Measured number of signal events:

$$N_{\mu}^{\pm}(\eta_{\text{CM}}^{\mu}) = \frac{N_{\mu,\text{raw}}^{\pm}(\eta_{\text{CM}}^{\mu})}{\epsilon^{\pm}(\eta_{\text{CM}}^{\mu})}$$

Extracted from $p_{\text{T}}^{\text{miss}}$ fit

Cross section of $\text{W} \rightarrow \mu\nu$:

$$\frac{d\sigma(\text{W}^{\pm} \rightarrow \mu^{\pm}\nu_{\mu})}{d\eta_{\text{CM}}^{\mu}}(\eta_{\text{CM}}^{\mu}) = \frac{N_{\mu}^{\pm}(\eta_{\text{CM}}^{\mu})}{\mathcal{L} \cdot \Delta\eta_{\text{CM}}^{\mu}}$$

p-Pb integrated luminosity ($173.4 \pm 6.1 \text{ /nb}$)

η_{CM} bin width

Observables

Measured number of signal events:

$$N_{\mu}^{\pm}(\eta_{\text{CM}}^{\mu}) = \frac{N_{\mu,\text{raw}}^{\pm}(\eta_{\text{CM}}^{\mu})}{\epsilon^{\pm}(\eta_{\text{CM}}^{\mu})}$$

Extracted from $p_{\text{T}}^{\text{miss}}$ fit

Cross section of $\text{W} \rightarrow \mu\nu$:

$$\frac{d\sigma(\text{W}^{\pm} \rightarrow \mu^{\pm}\nu_{\mu})}{d\eta_{\text{CM}}^{\mu}}(\eta_{\text{CM}}^{\mu}) = \frac{N_{\mu}^{\pm}(\eta_{\text{CM}}^{\mu})}{\mathcal{L} \cdot \Delta\eta_{\text{CM}}^{\mu}}$$

p-Pb integrated luminosity ($173.4 \pm 6.1 \text{ /nb}$)

η_{CM} bin width

Forward-backward ratio:

$$R_{\text{FB}}^{\pm}(\eta_{\text{CM}}^{\mu}) = \frac{N_{\mu}^{\pm}(+\eta_{\text{CM}}^{\mu})}{N_{\mu}^{\pm}(-\eta_{\text{CM}}^{\mu})}$$

Observables

Measured number of signal events:

$$N_{\mu}^{\pm}(\eta_{\text{CM}}^{\mu}) = \frac{N_{\mu,\text{raw}}^{\pm}(\eta_{\text{CM}}^{\mu})}{\epsilon^{\pm}(\eta_{\text{CM}}^{\mu})}$$

Extracted from $p_{\text{T}}^{\text{miss}}$ fit

Cross section of $\text{W} \rightarrow \mu\nu$:

$$\frac{d\sigma(\text{W}^{\pm} \rightarrow \mu^{\pm}\nu_{\mu})}{d\eta_{\text{CM}}^{\mu}}(\eta_{\text{CM}}^{\mu}) = \frac{N_{\mu}^{\pm}(\eta_{\text{CM}}^{\mu})}{\mathcal{L} \cdot \Delta\eta_{\text{CM}}^{\mu}}$$

p-Pb integrated luminosity ($173.4 \pm 6.1 \text{ /nb}$)

η_{CM} bin width

Forward-backward ratio:

$$R_{\text{FB}}^{\pm}(\eta_{\text{CM}}^{\mu}) = \frac{N_{\mu}^{\pm}(+\eta_{\text{CM}}^{\mu})}{N_{\mu}^{\pm}(-\eta_{\text{CM}}^{\mu})}$$

proton-going ($\eta_{\text{CM}} > 0$)

Observables

Measured number of signal events:

$$N_{\mu}^{\pm}(\eta_{\text{CM}}^{\mu}) = \frac{N_{\mu,\text{raw}}^{\pm}(\eta_{\text{CM}}^{\mu})}{\epsilon^{\pm}(\eta_{\text{CM}}^{\mu})}$$

Extracted from $p_{\text{T}}^{\text{miss}}$ fit

Cross section of $\text{W} \rightarrow \mu\nu$:

$$\frac{d\sigma(\text{W}^{\pm} \rightarrow \mu^{\pm}\nu_{\mu})}{d\eta_{\text{CM}}^{\mu}}(\eta_{\text{CM}}^{\mu}) = \frac{N_{\mu}^{\pm}(\eta_{\text{CM}}^{\mu})}{\mathcal{L} \cdot \Delta\eta_{\text{CM}}^{\mu}}$$

p-Pb integrated luminosity ($173.4 \pm 6.1 \text{ /nb}$)

η_{CM} bin width

Forward-backward ratio:

$$R_{\text{FB}}^{\pm}(\eta_{\text{CM}}^{\mu}) = \frac{N_{\mu}^{\pm}(+\eta_{\text{CM}}^{\mu})}{N_{\mu}^{\pm}(-\eta_{\text{CM}}^{\mu})}$$

proton-going ($\eta_{\text{CM}} > 0$)

Pb-going ($\eta_{\text{CM}} < 0$)

Observables

Measured number of signal events:

$$N_{\mu}^{\pm}(\eta_{\text{CM}}^{\mu}) = \frac{N_{\mu,\text{raw}}^{\pm}(\eta_{\text{CM}}^{\mu})}{\epsilon^{\pm}(\eta_{\text{CM}}^{\mu})}$$

Extracted from $p_{\text{T}}^{\text{miss}}$ fit

Cross section of $\text{W} \rightarrow \mu\nu$:

$$\frac{d\sigma(\text{W}^{\pm} \rightarrow \mu^{\pm}\nu_{\mu})}{d\eta_{\text{CM}}^{\mu}}(\eta_{\text{CM}}^{\mu}) = \frac{N_{\mu}^{\pm}(\eta_{\text{CM}}^{\mu})}{\mathcal{L} \cdot \Delta\eta_{\text{CM}}^{\mu}}$$

p-Pb integrated luminosity ($173.4 \pm 6.1 \text{ /nb}$)

η_{CM} bin width

Forward-backward ratio:

$$R_{\text{FB}}^{\pm}(\eta_{\text{CM}}^{\mu}) = \frac{N_{\mu}^{\pm}(+\eta_{\text{CM}}^{\mu})}{N_{\mu}^{\pm}(-\eta_{\text{CM}}^{\mu})}$$

proton-going ($\eta_{\text{CM}} > 0$)

Pb-going ($\eta_{\text{CM}} < 0$)

Muon charge asymmetry:

$$\mathcal{A}_{\mu}(\eta_{\text{CM}}^{\mu}) = \frac{N_{\mu}^{+}(\eta_{\text{CM}}^{\mu}) - N_{\mu}^{-}(\eta_{\text{CM}}^{\mu})}{N_{\mu}^{+}(\eta_{\text{CM}}^{\mu}) + N_{\mu}^{-}(\eta_{\text{CM}}^{\mu})}$$

Uncertainties

Source of uncertainty	Max. relative uncertainty	
	$\sigma(W^- \rightarrow \mu^-\bar{\nu}_\mu) [\%]$	$\sigma(W^+ \rightarrow \mu^+\nu_\mu) [\%]$
Luminosity	3.5	3.5
Efficiency	3.0	3.2
QCD jet background	1.2	0.7
EW and top backgrounds	0.4	0.3
Weak boson p_T	0.5	0.4
Event activity	0.6	0.4
Recoil calibration	0.2	0.3
W-boson generator	0.9	0.5
Total systematic uncertainty	4.8	4.8
Statistical uncertainty	2.4	2.0

- Dominant sources of uncertainties: luminosity (cross section) and efficiency
- Correlations in muon charge and η_{CM} considered in the uncertainties of the muon charge asymmetry and forward-backward ratios

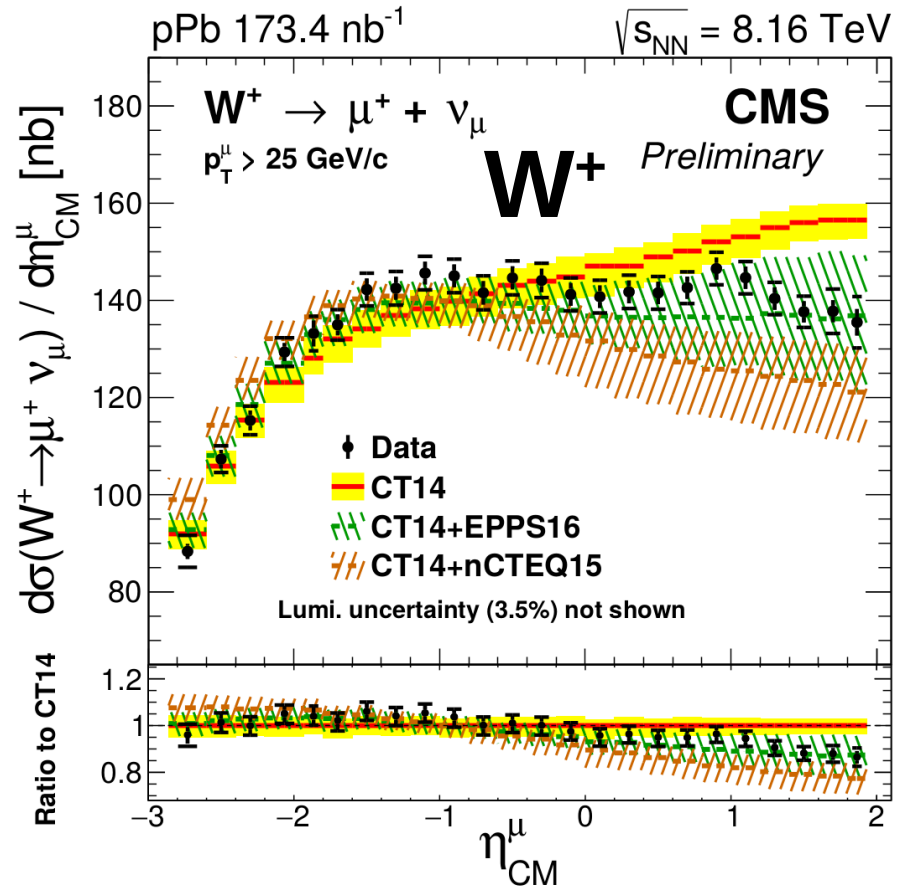
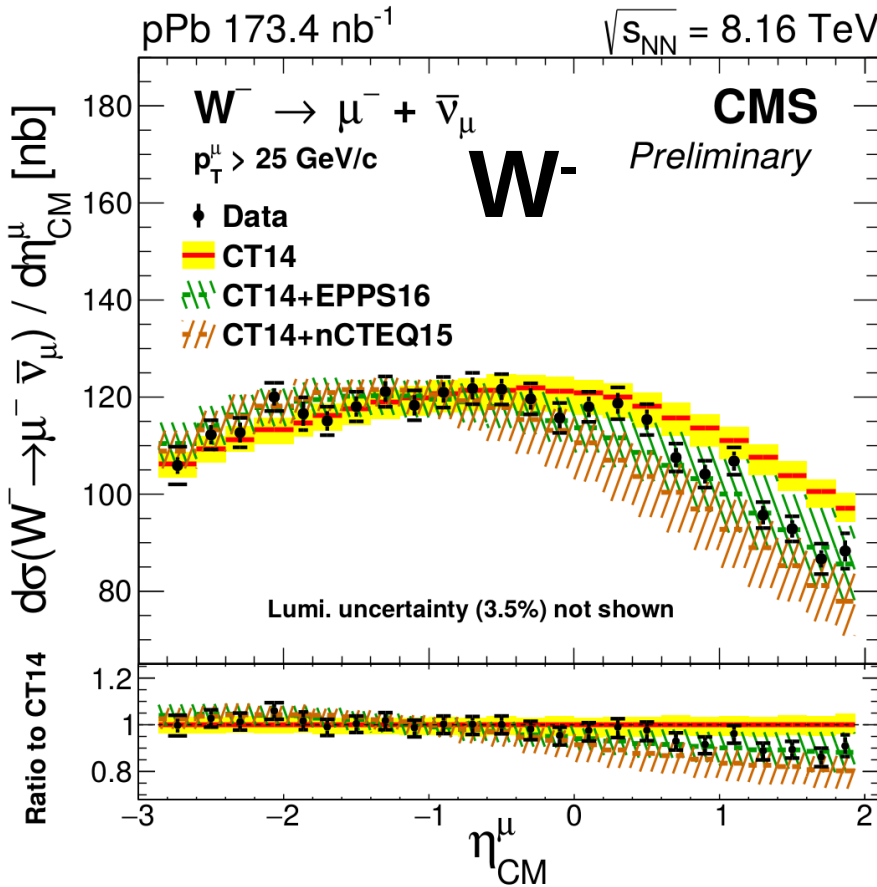
Outline

- Theoretical context
- The CMS detector at the LHC
- **W-boson production in p-Pb at 8.16 TeV**
 - Introduction
 - Analysis
 - **Results**
- Charmonium production in Pb-Pb at 5.02 TeV
 - Introduction
 - Analysis
 - Results
- Conclusions



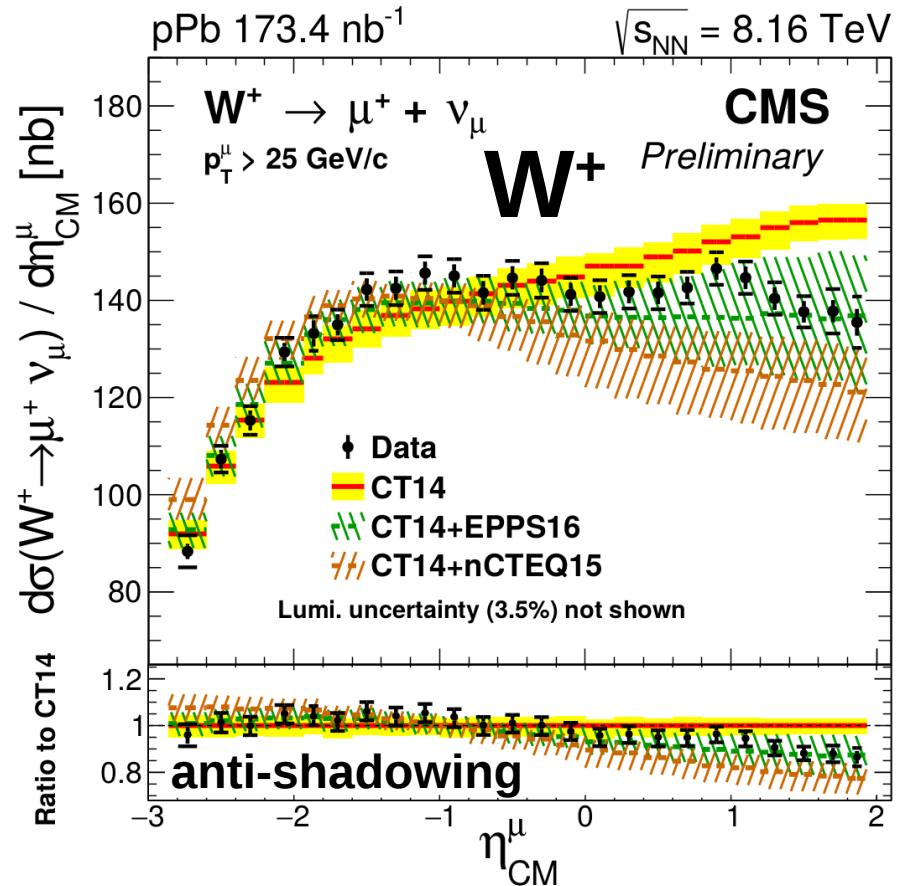
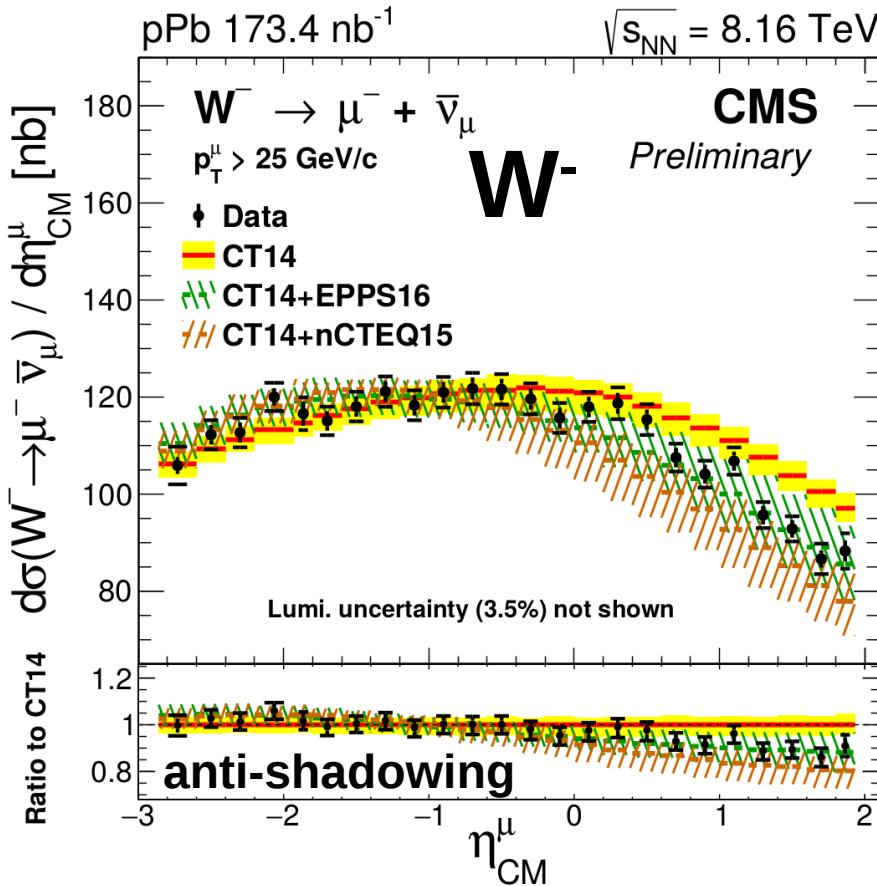
W-boson cross sections

$$P(\chi^2) = <0.01\% \text{ CT14} , 79\% \text{ nCTEQ15} , 96\% \text{ EPPS16}$$



W-boson cross sections

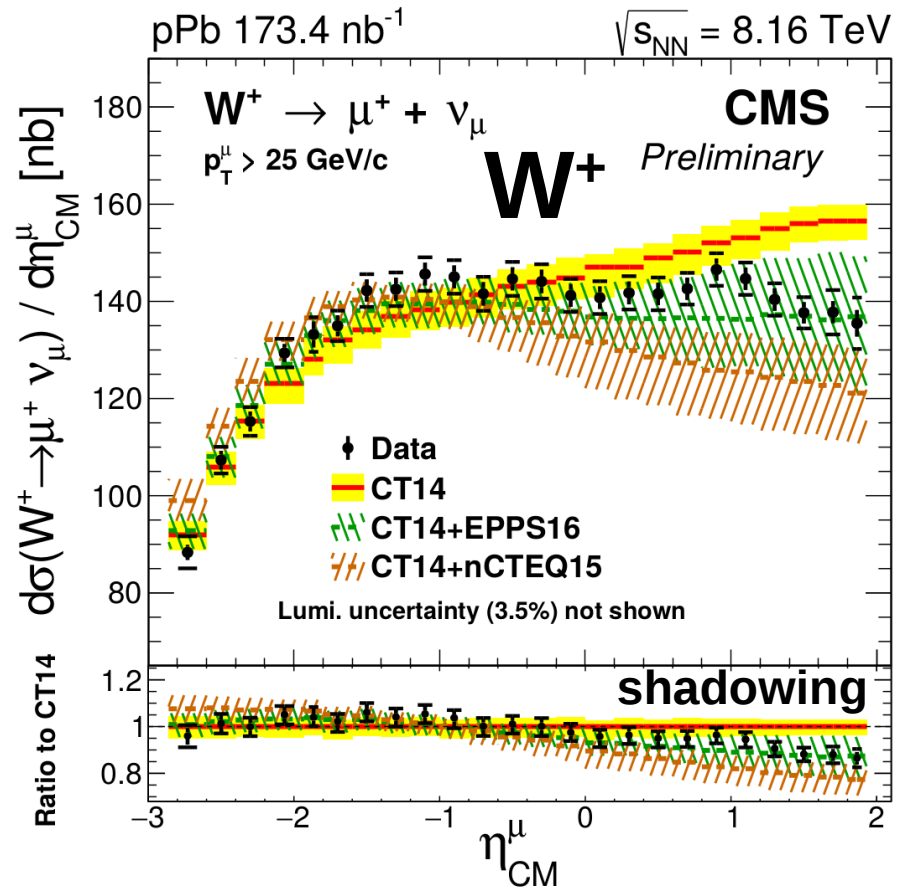
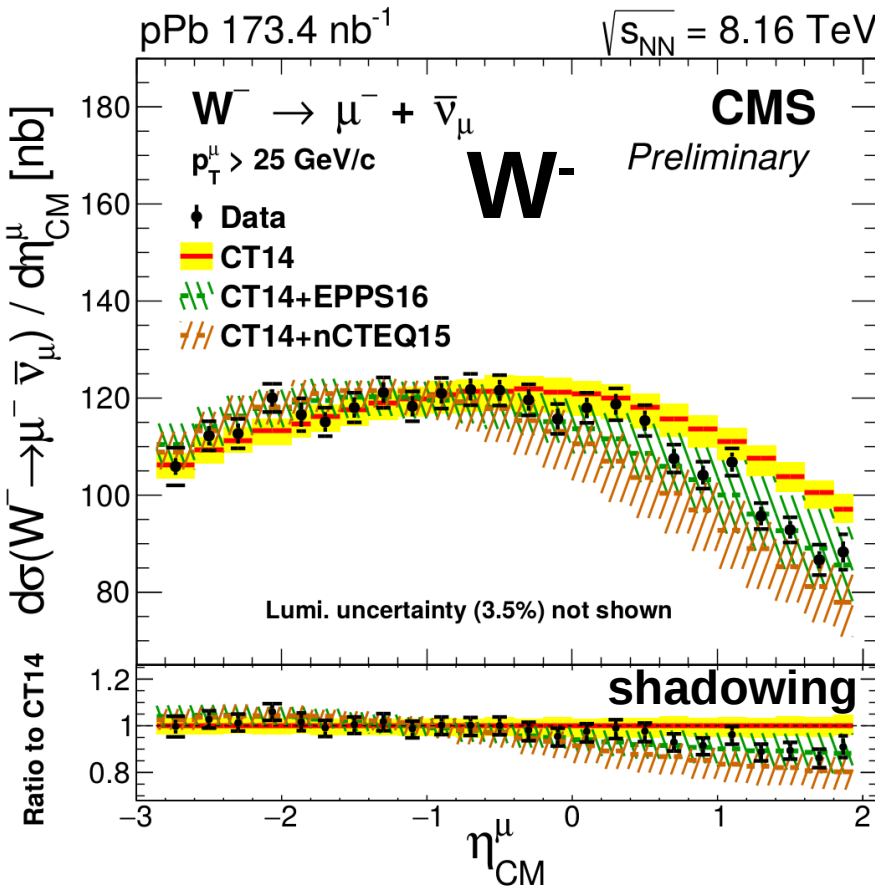
$$P(\chi^2) = <0.01\% \text{ CT14} , 79\% \text{ nCTEQ15} , 96\% \text{ EPPS16}$$



- $\eta_{CM} < 0$ (large x_{Pb}): Results **agree** with **PDF** and **nPDF** calculations

W-boson cross sections

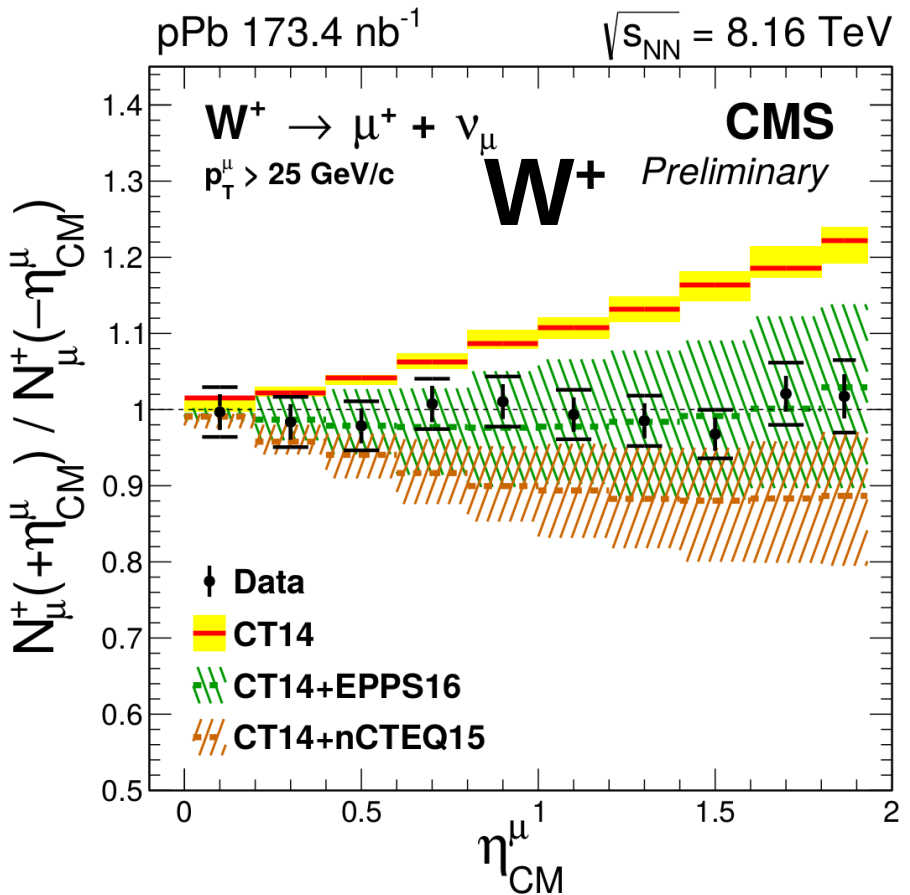
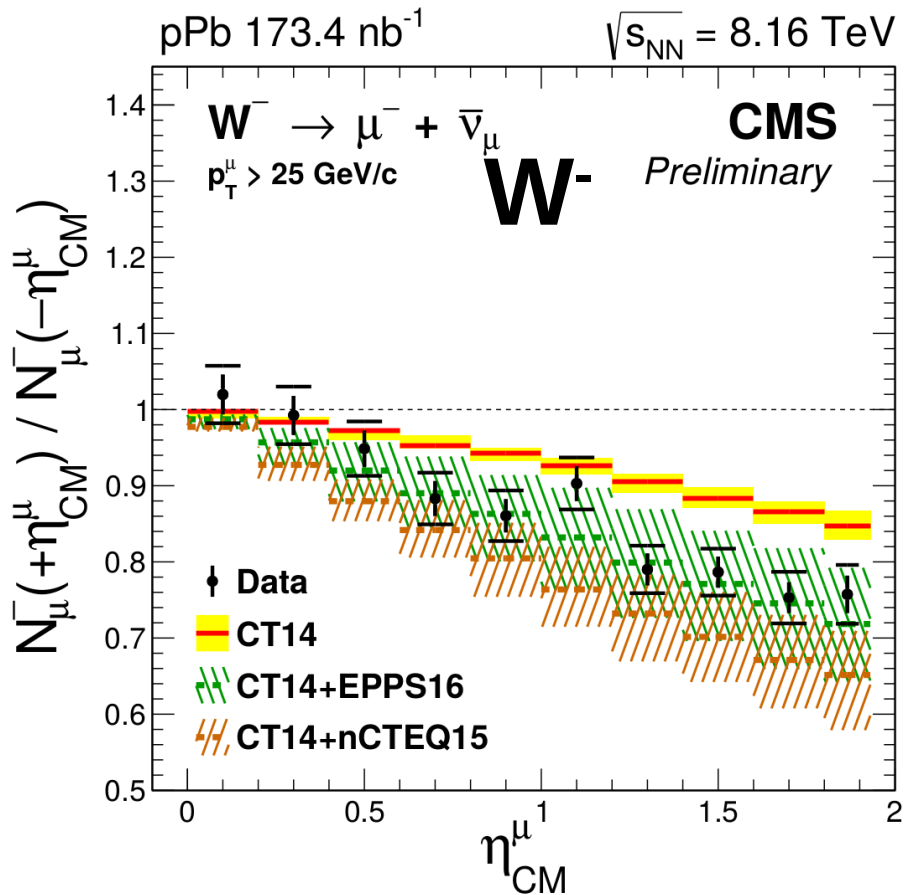
$$P(\chi^2) = <0.01\% \text{ CT14 , } 79\% \text{ nCTEQ15 , } 96\% \text{ EPPS16}$$



- $\eta_{CM} < 0$ (large x_{Pb}): Results **agree** with **PDF** and **nPDF** calculations
- $\eta_{CM} > 0$ (small x_{Pb}): Results **favor** the **nuclear PDF** calculations

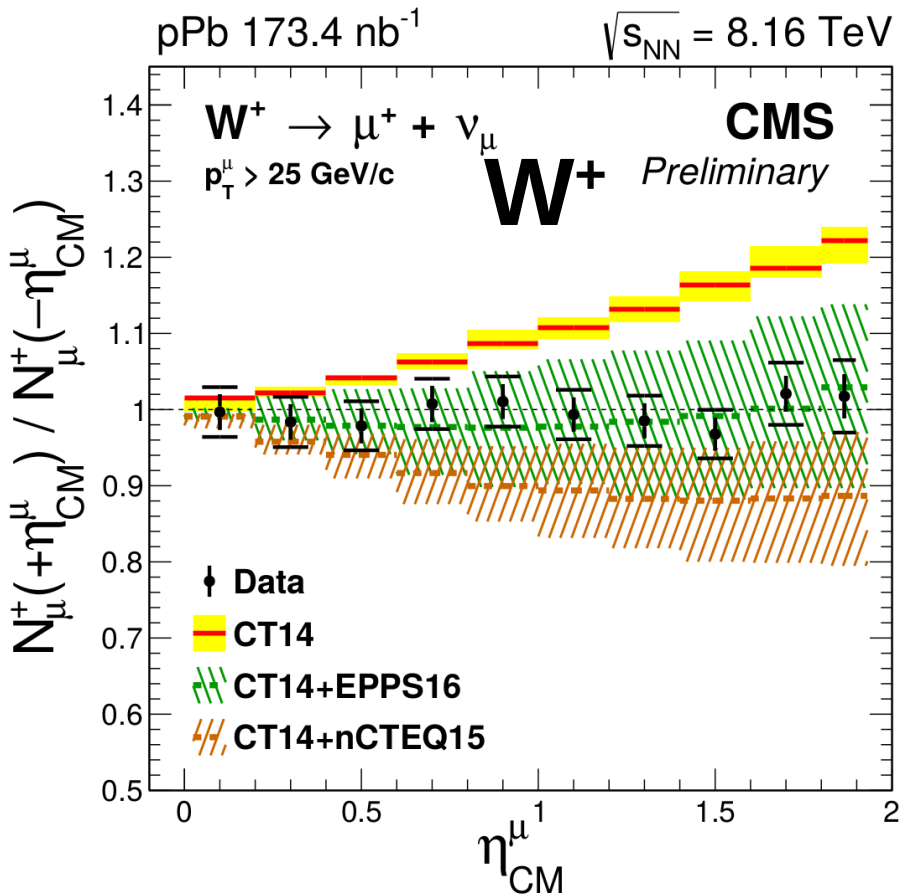
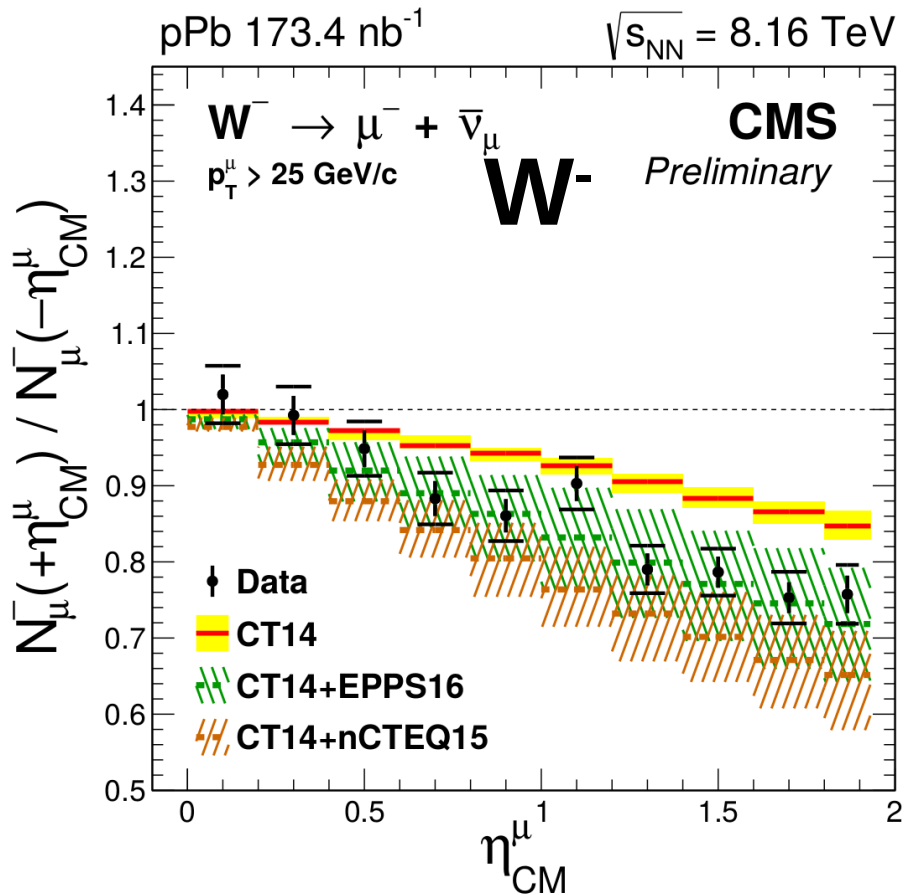
Muon forward-backward ratio

$$P(\chi^2) = <0.01\% \text{ CT14} , 83\% \text{ nCTEQ15} , 95\% \text{ EPPS16}$$



Muon forward-backward ratio

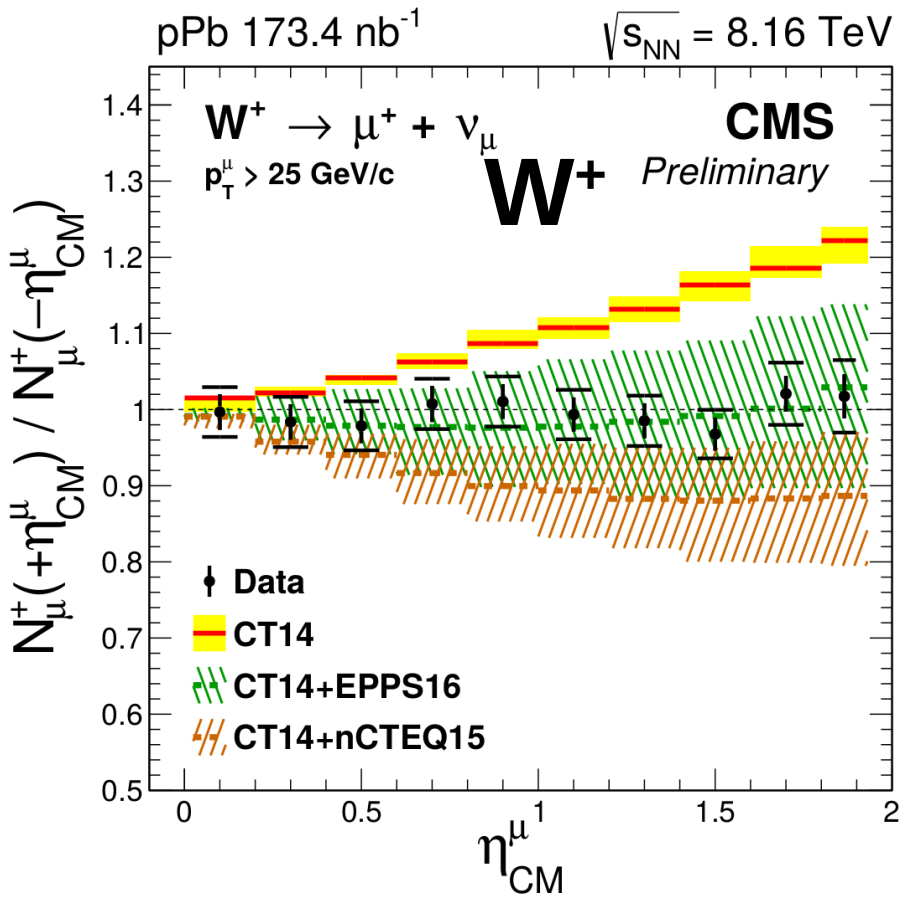
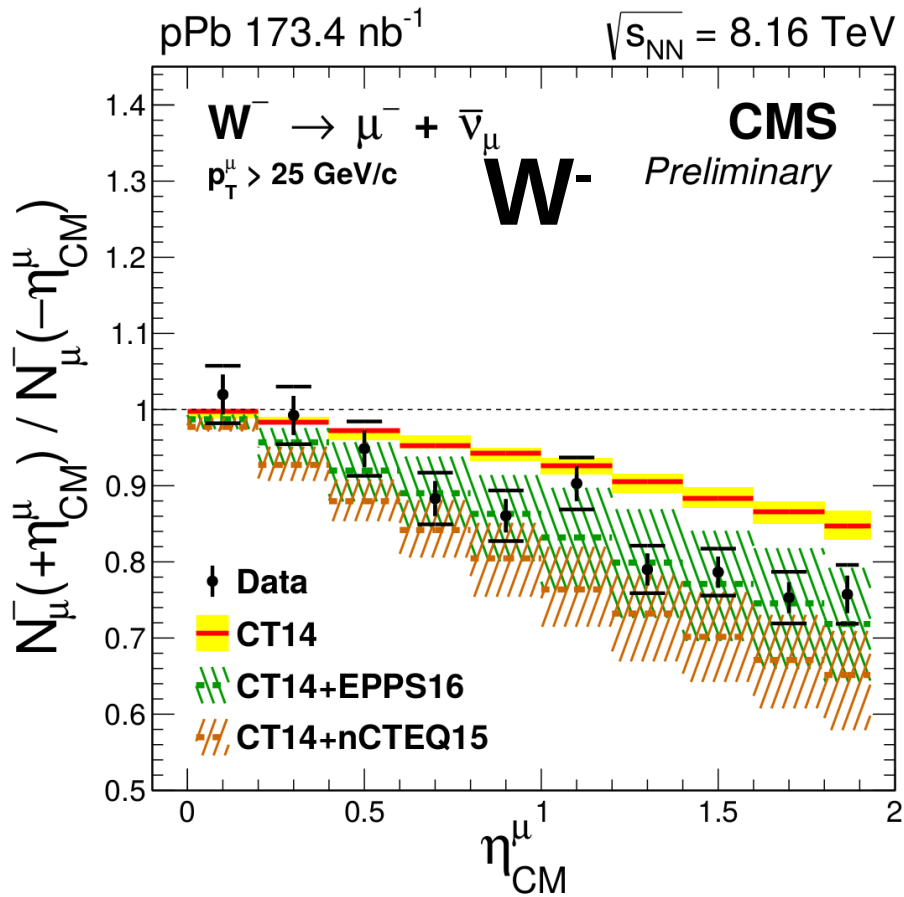
$$P(\chi^2) = <0.01\% \text{ CT14} , 83\% \text{ nCTEQ15} , 95\% \text{ EPPS16}$$



- Deviate ($>7\sigma$) from free-nucleon PDF calculations

Muon forward-backward ratio

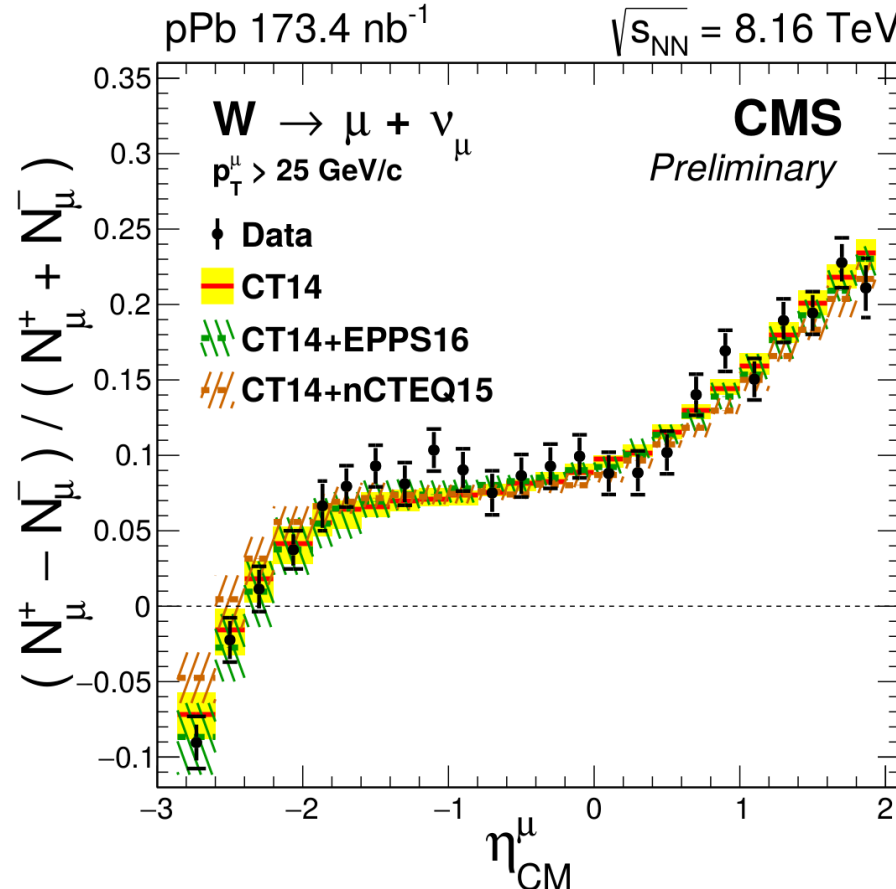
$$P(\chi^2) = <0.01\% \text{ CT14} , 83\% \text{ nCTEQ15} , 95\% \text{ EPPS16}$$



- Deviate ($>7\sigma$) from free-nucleon PDF calculations
- Experimental uncertainties smaller than nPDF uncertainties

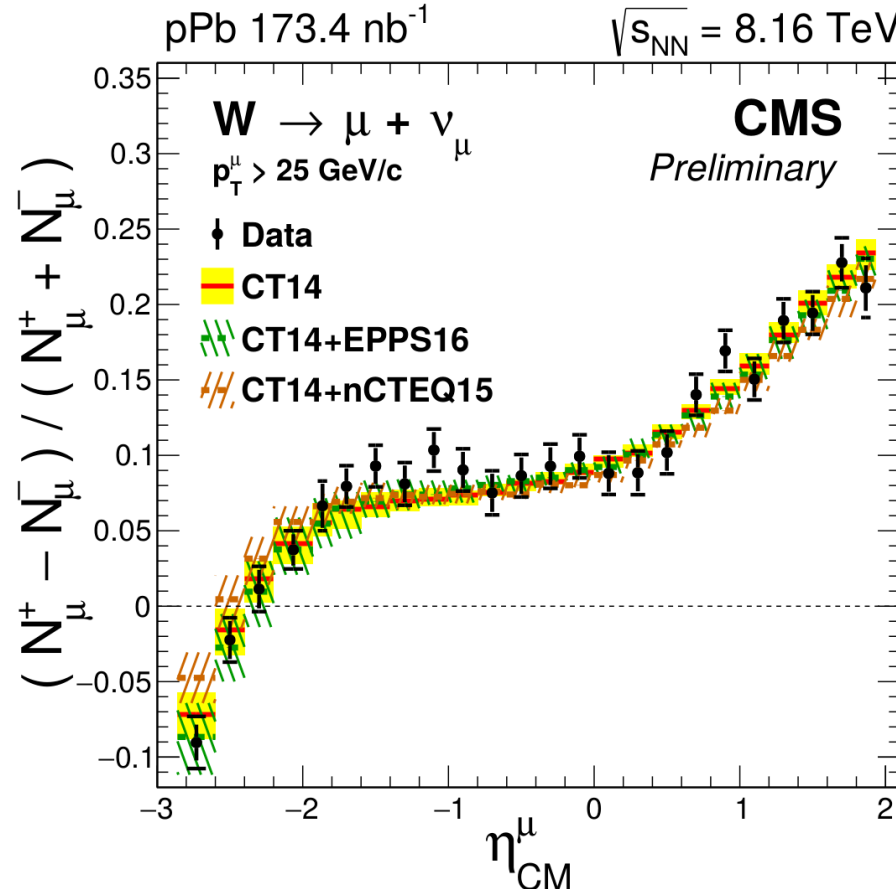
Muon charge asymmetry

$$P(\chi^2) = 54\% \text{ CT14}, 23\% \text{ nCTEQ15}, 80\% \text{ EPPS16}$$



Muon charge asymmetry

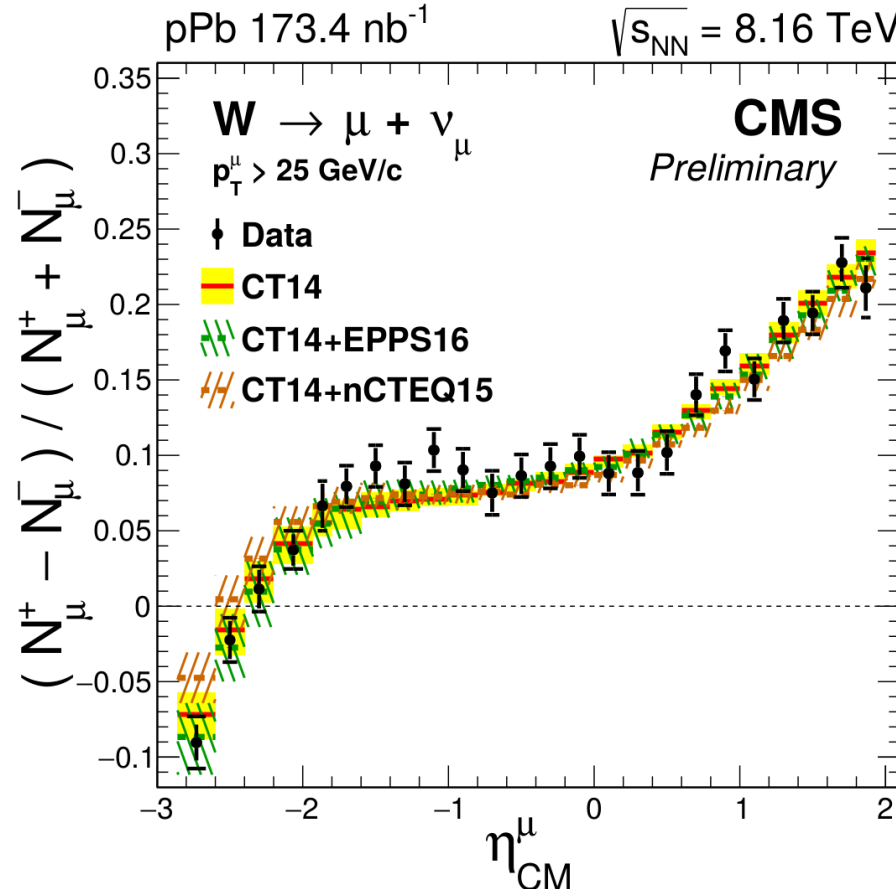
$$P(\chi^2) = 54\% \text{ CT14}, 23\% \text{ nCTEQ15}, 80\% \text{ EPPS16}$$



- Sensitive to isospin effect (neutrons and protons in Pb ion)

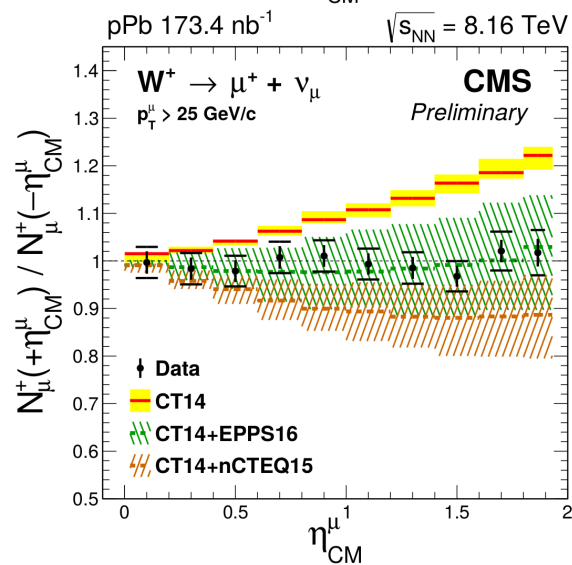
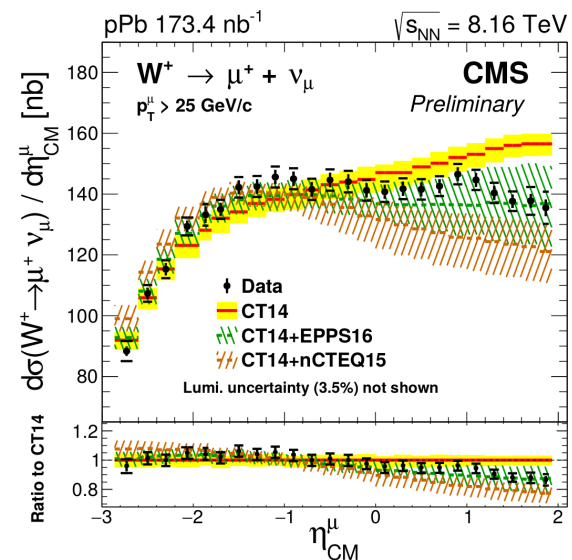
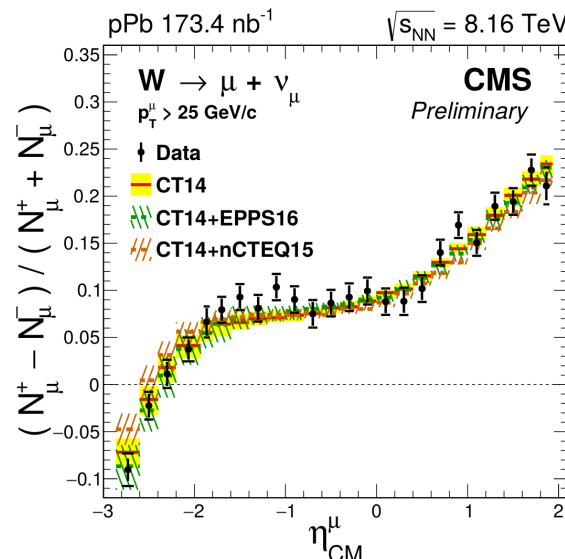
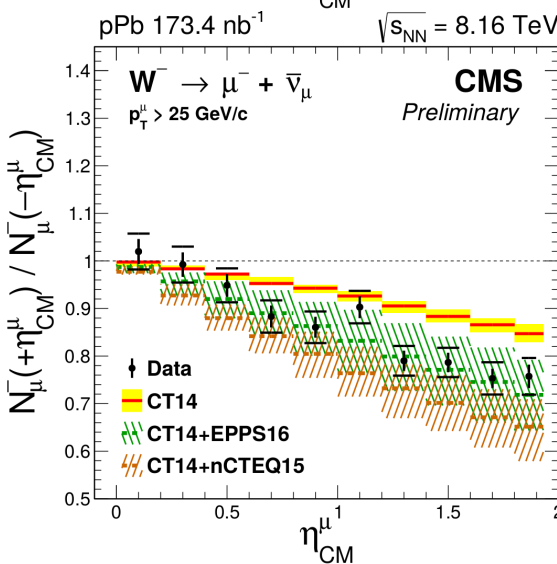
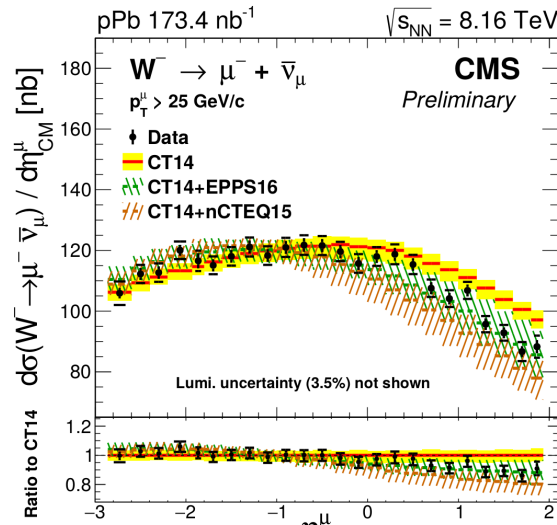
Muon charge asymmetry

$$P(\chi^2) = 54\% \text{ CT14}, 23\% \text{ nCTEQ15}, 80\% \text{ EPPS16}$$



- Sensitive to isospin effect (neutrons and protons in Pb ion)
- All (n)PDF calculations reproduce the measurements

Summary of W-boson measurement



- Observation of nuclear modifications of the (anti) quark PDFs
- Experimental uncertainties smaller than nuclear PDF uncertainties

Outline

- Theoretical context
- The CMS detector at the LHC
- W-boson production in p-Pb at 8.16 TeV
 - Introduction
 - Analysis
 - Results
- Charmonium production in Pb-Pb at 5.02 TeV
 - Introduction
 - Analysis
 - Results
- Conclusions

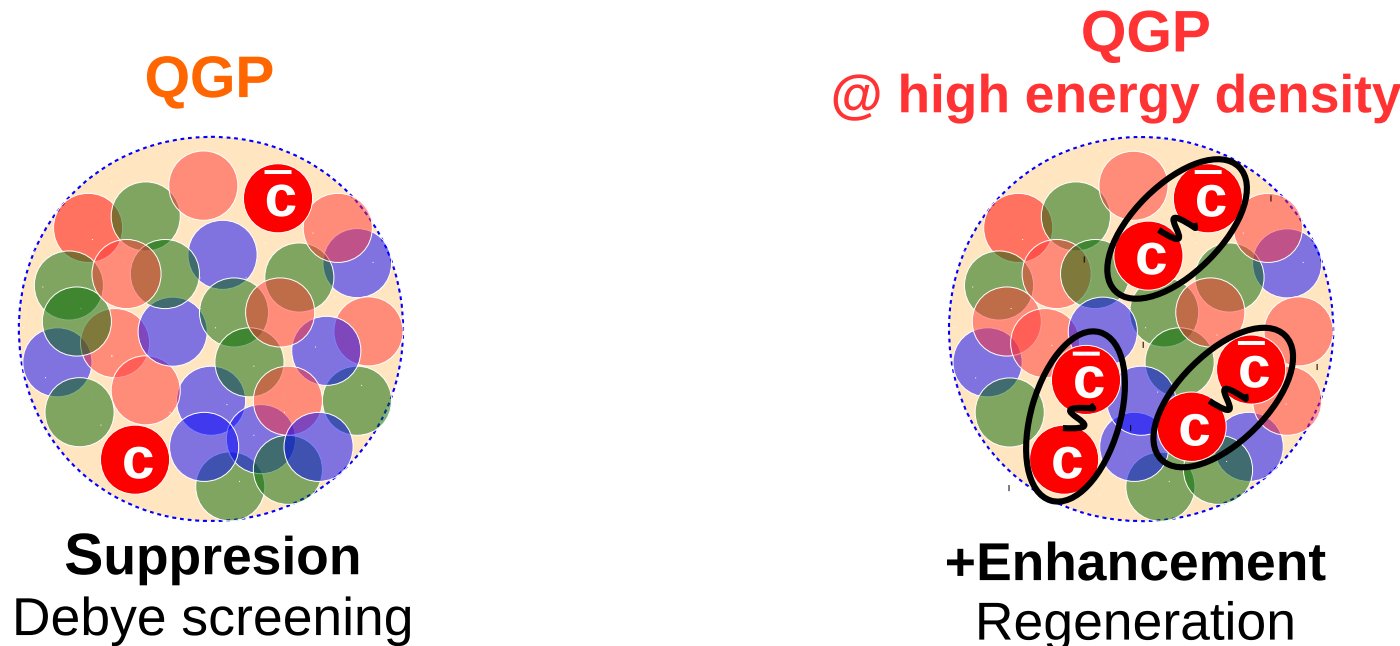


Charmonia in Pb-Pb collisions

Charmonia ($cc\bar{c}$ mesons) are produced in the early stages of the collision

$$\tau_{formation}^{Charmonia} \lesssim \tau_{formation}^{QGP} < \tau_{lifetime}^{QGP} < \tau_{decay}^{Charmonia}$$

The Quark-Gluon Plasma is expected to modify the charmonia production



Charmonia are good probes of the medium evolution

Prompt and nonprompt J/Ψ

Inclusive J/Ψ

Prompt J/Ψ

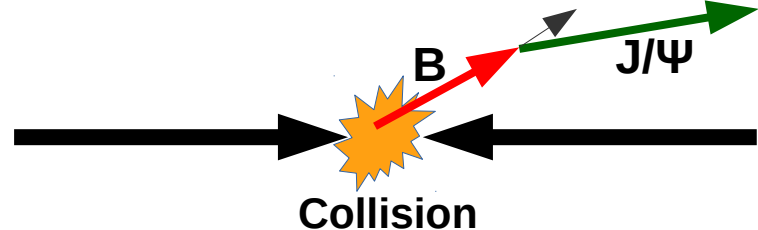
Direct
J/Ψ

Feed-down from
 $\Psi(2S)$ and χ_c



Nonprompt J/Ψ

From B hadron decays



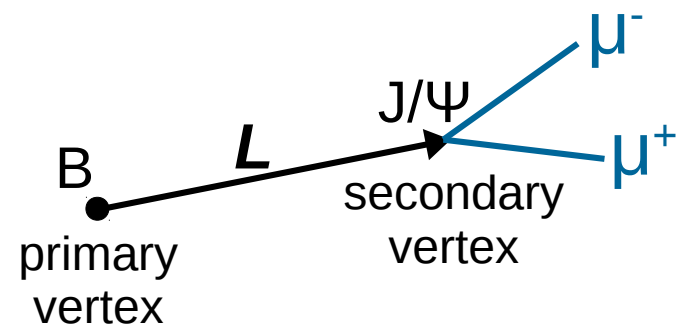
- **Prompt J/Ψ:**

Directly affected by the QGP

- **Nonprompt J/Ψ:**

Reflects energy loss of b quarks in the QGP

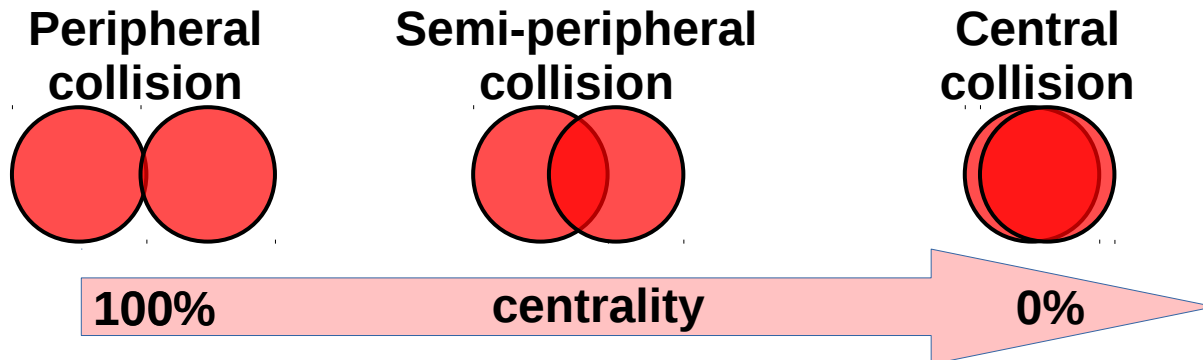
Separation based on **pseudo-proper decay length** ($\ell_{J/\psi}$)



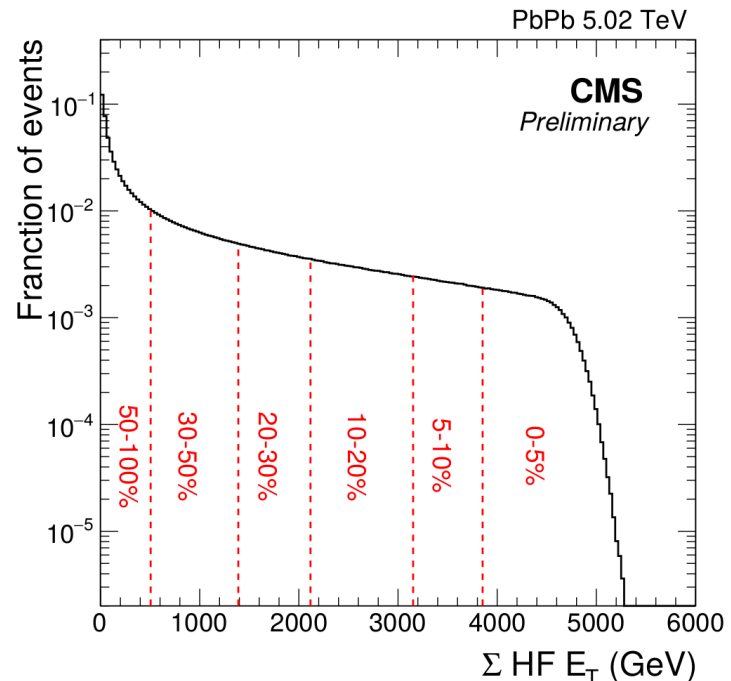
$$\ell_{J/\psi} = \frac{m_{J/\psi}}{p_{\mu\mu}} L$$

decay length in the laboratory frame

Centrality

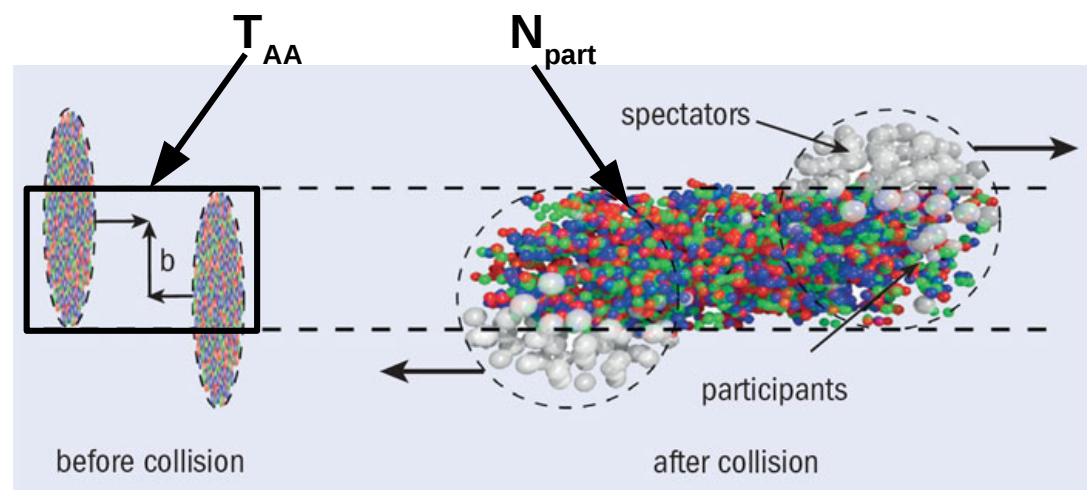


Centrality percentile determined from the energy distribution in the hadron forward calorimeter



Geometry of the heavy-ion collision:

Glauber model relates centrality to number of participants (N_{part}) and the nuclear overlap function (T_{AA})



Outline

- Theoretical context
- The CMS detector at the LHC
- W-boson production in p-Pb at 8.16 TeV
 - Introduction
 - Analysis
 - Results
- Charmonium production in Pb-Pb at 5.02 TeV
 - Introduction
 - Analysis
 - Results
- Conclusions



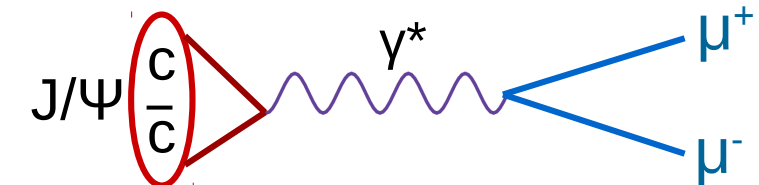
Data selection

Events in data are selected using the following criteria:

Data selection

Events in data are selected using the following criteria:

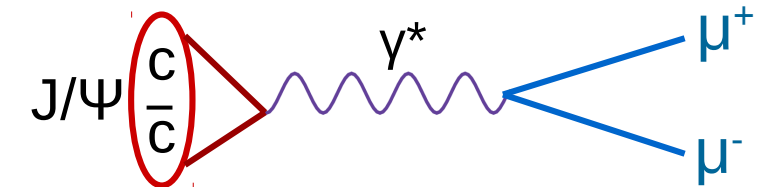
- **Dimuon L1 trigger:** requires the presence of two muons



Data selection

Events in data are selected using the following criteria:

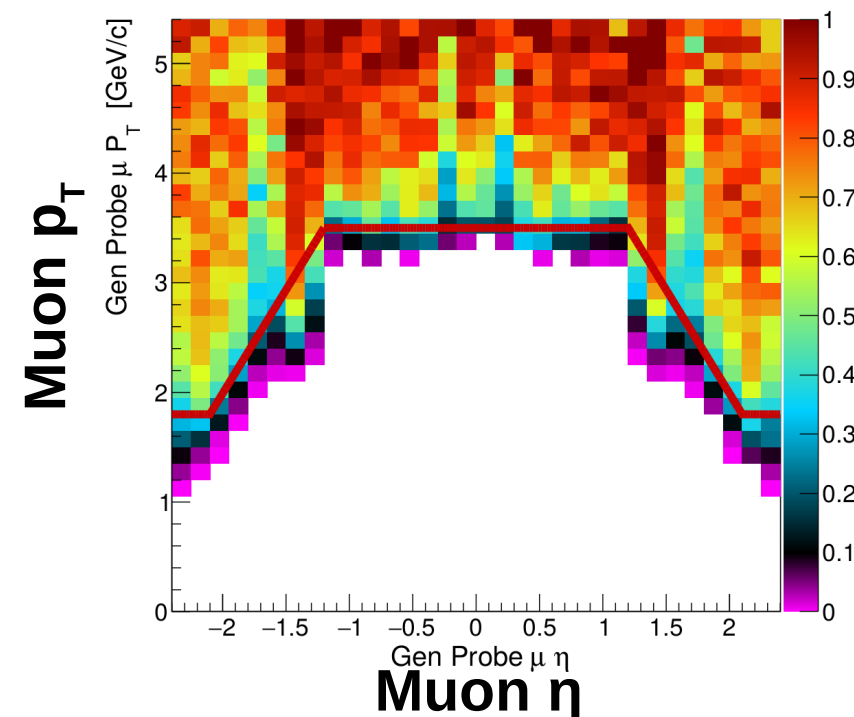
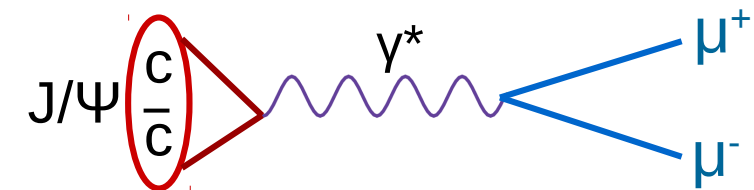
- **Dimuon L1 trigger:** requires the presence of two muons
- **Dimuon vertex selection:** requires the probability that the two muons derive from the same vertex to be larger than 1%



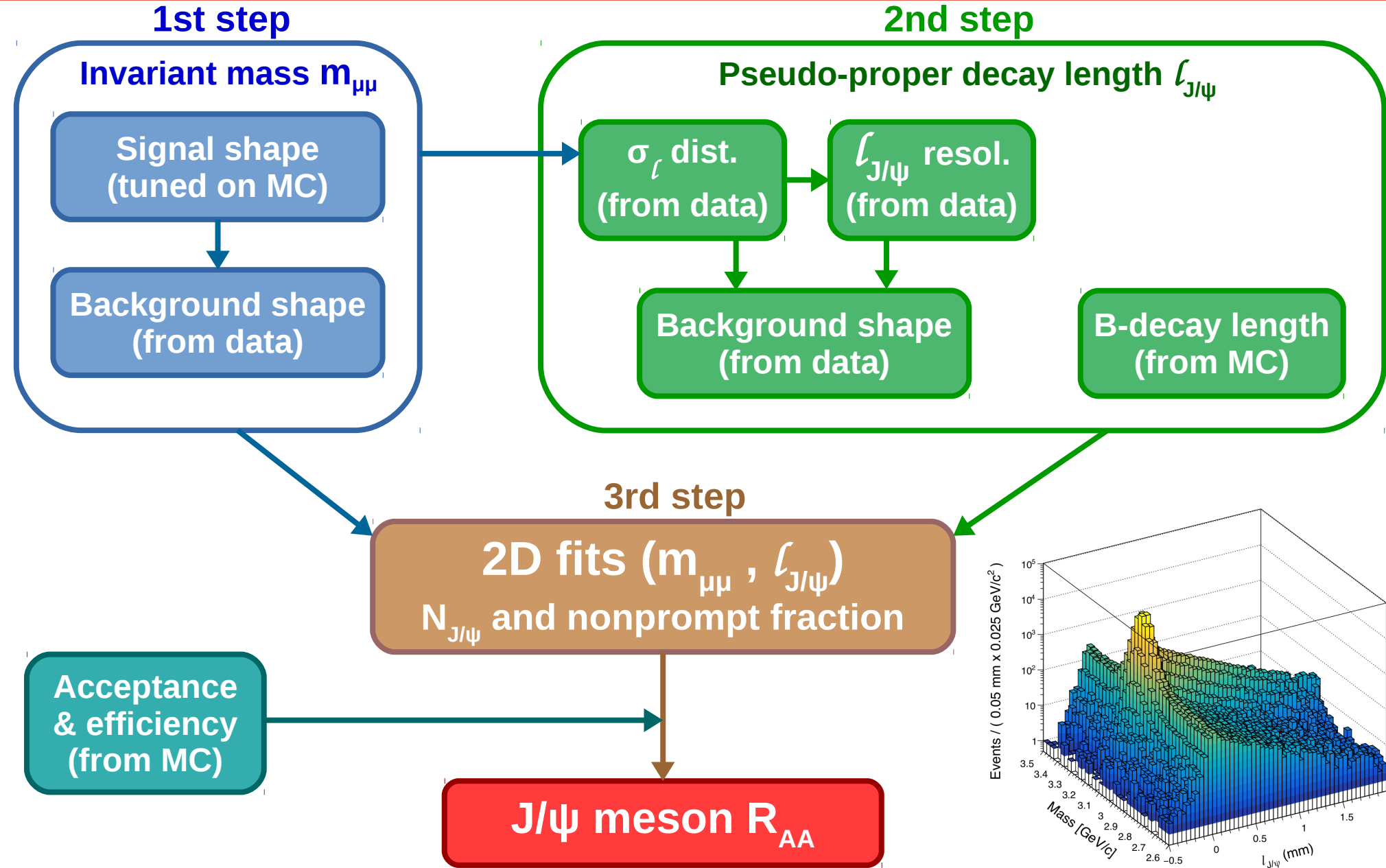
Data selection

Events in data are selected using the following criteria:

- **Dimuon L1 trigger:** requires the presence of two muons
- **Dimuon vertex selection:** requires the probability that the two muons derive from the same vertex to be larger than 1%
- **Muon kinematic selection:** requires muons to be within the CMS kinematic acceptance



Measurement of J/ ψ R_{AA}



Measurement of J/ ψ R_{AA}

1st step

Invariant mass m _{$\mu\mu$}

Signal shape
(tuned on MC)

Background shape
(from data)

2nd step

Pseudo-proper decay length $\ell_{J/\psi}$

σ_ℓ dist.
(from data)

$\ell_{J/\psi}$ resol.
(from data)

Background shape
(from data)

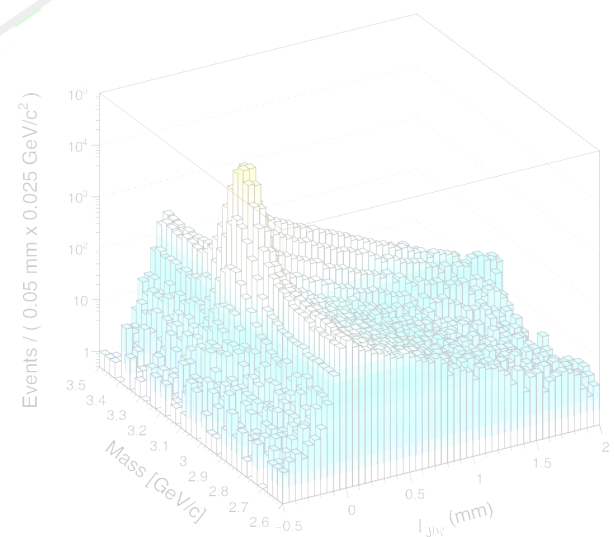
B-decay length
(from MC)

3rd step

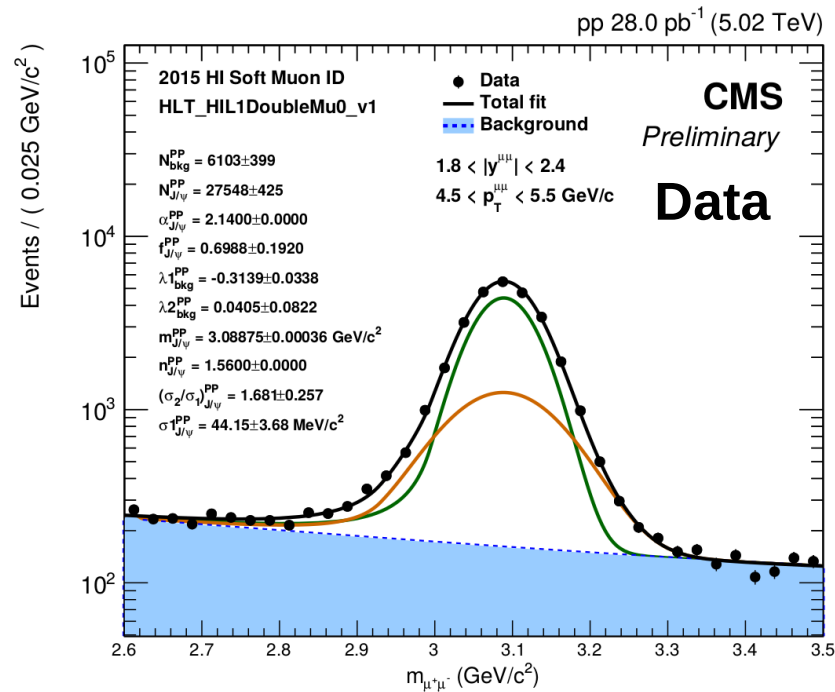
2D fits (m _{$\mu\mu$} , $\ell_{J/\psi}$)
N_{J/ ψ} and nonprompt fraction

Acceptance
& efficiency
(from MC)

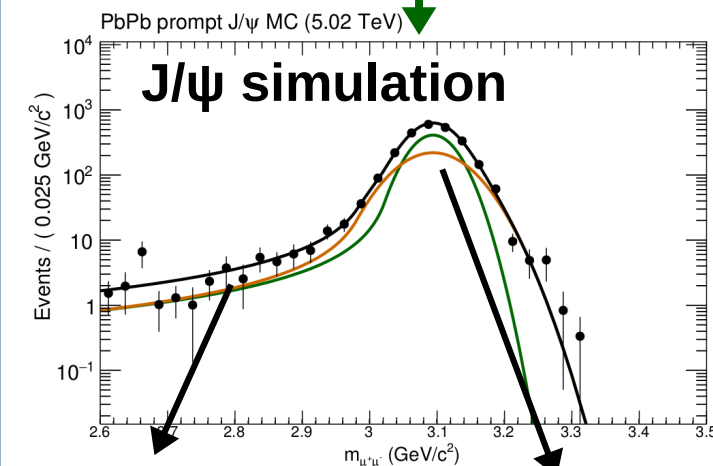
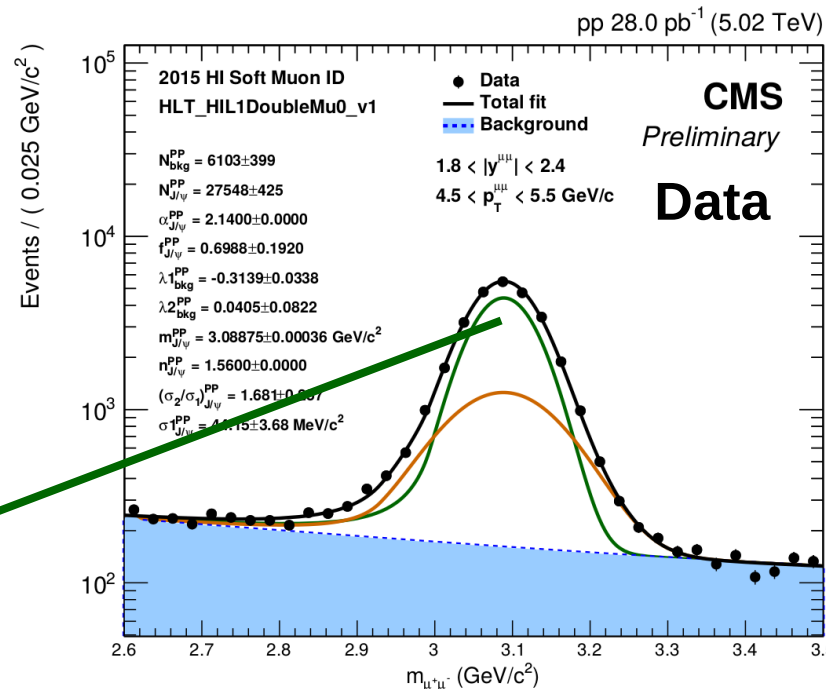
J/ ψ meson R_{AA}



Invariant mass fit



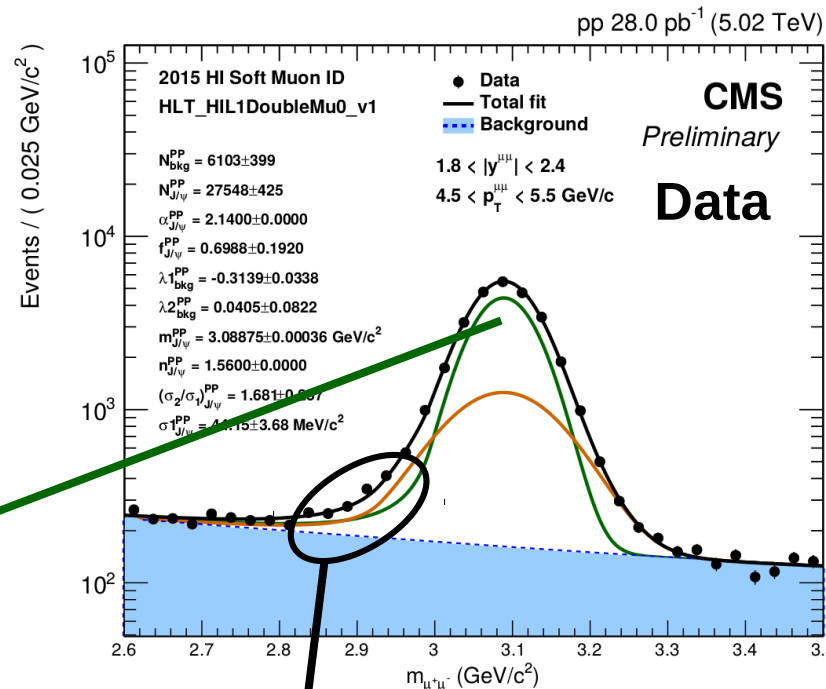
Invariant mass fit



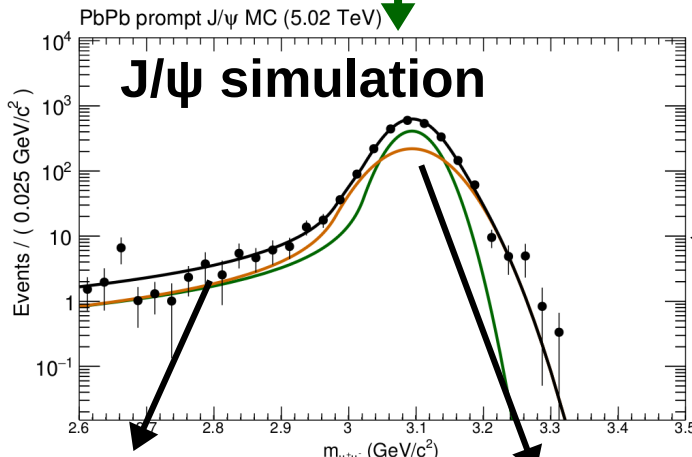
Power-law tail
FS radiation

Gaussian core
mass resolution

Invariant mass fit



Signal shape:
2 Crystal Balls

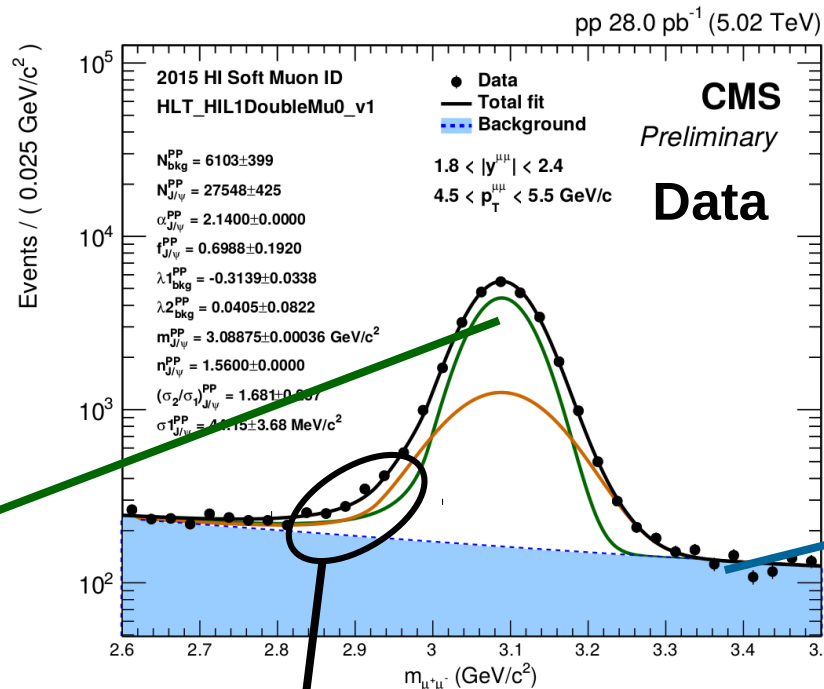


Power-law tail
FS radiation

Gaussian core
mass resolution

Tail parameters tuned on
 J/ψ simulation and fixed
on data

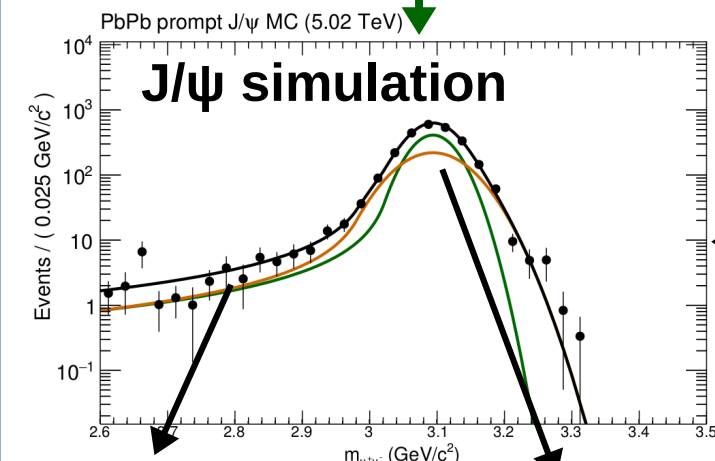
Invariant mass fit



Signal shape:
2 Crystal Balls

Background shape:
Chebyshev polynomial

Best order selected with
Log-Likelihood-ratio test

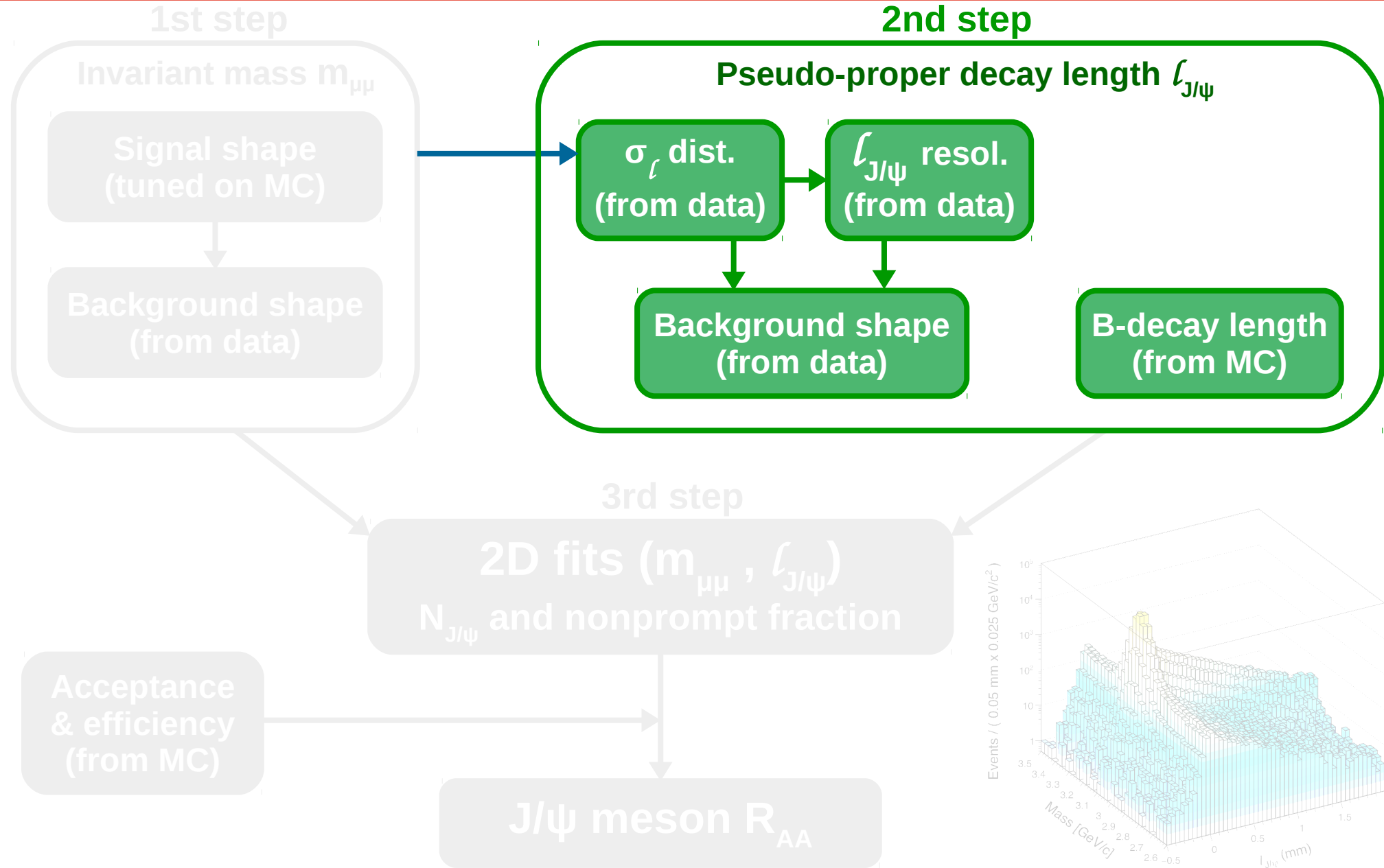


Power-law tail
FS radiation

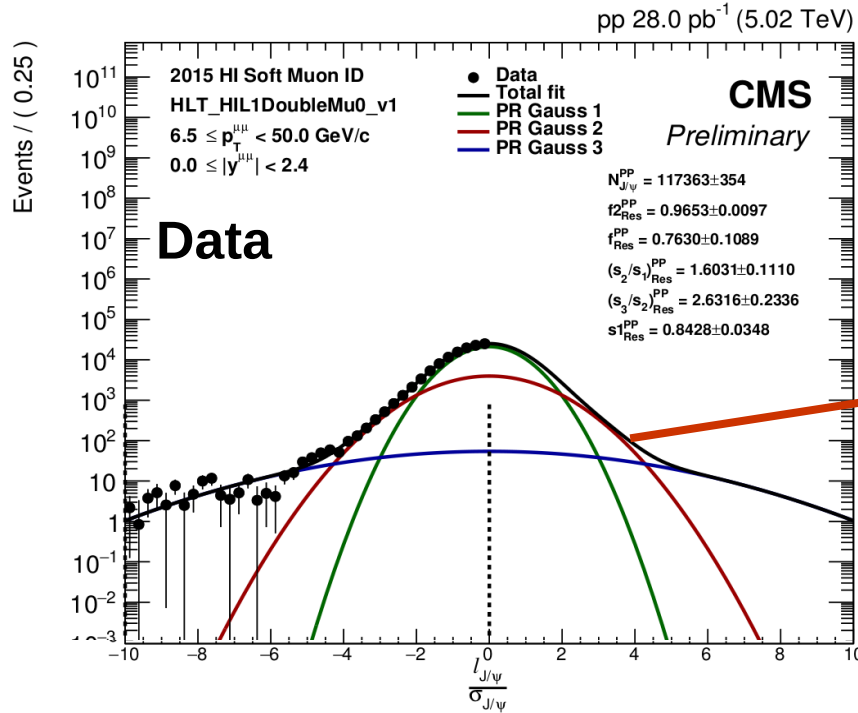
Gaussian core
mass resolution

Tail parameters tuned on
 J/ψ simulation and fixed
on data

Measurement of J/ ψ R_{AA}



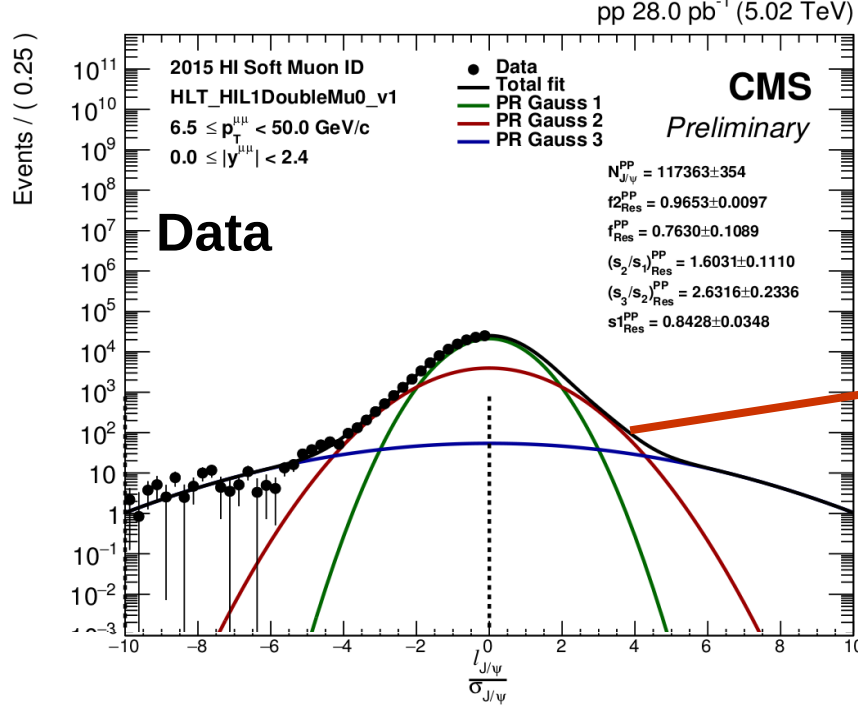
$\ell_{J/\psi}$ resolution



Parametrized from $\ell_{J/\psi} < 0$ distribution from a signal data sample

$\ell_{J/\psi}$ resolution shape:
3 Gaussians

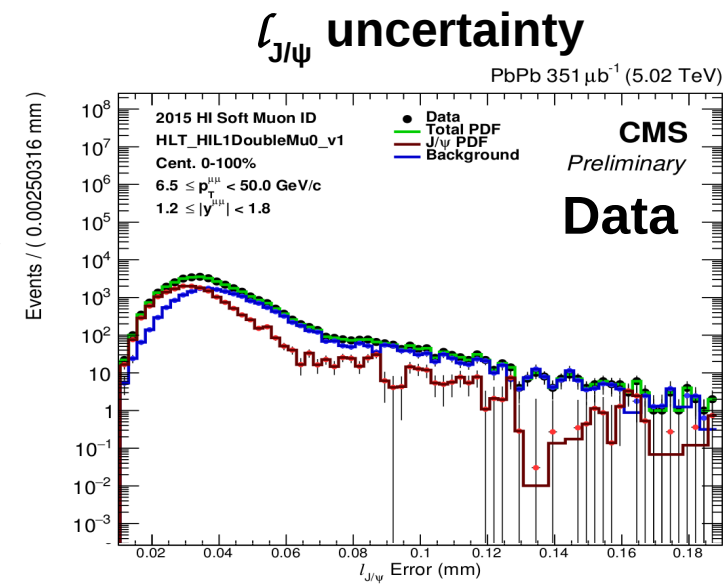
$\ell_{J/\psi}$ resolution



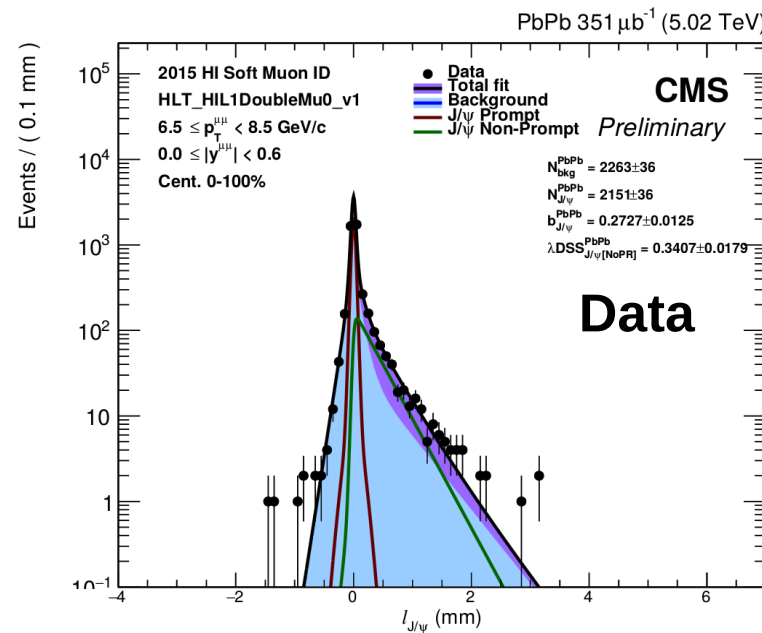
Parametrized from $\ell_{J/\psi} < 0$ distribution from a signal data sample

$\ell_{J/\psi}$ resolution shape:
3 Gaussians

Gaussian resolution model adjusted per event to $\ell_{J/\psi}$ uncertainty provided by the vertex reconstruction algorithm

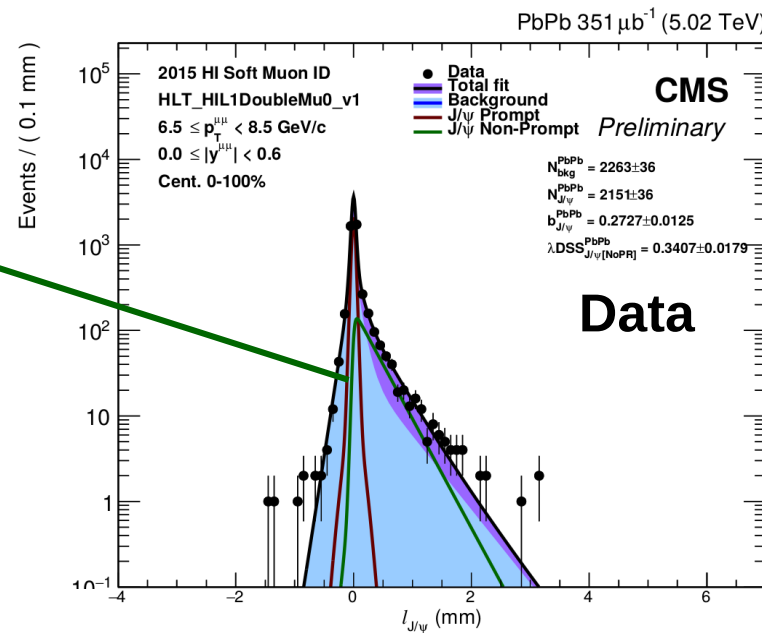


J/ψ parametrisation



$\ell_{J/\Psi}$ parametrisation

Signal $\ell_{J/\Psi}$ shape:
• **Prompt:** delta $\otimes \ell_{J/\Psi}$ res.
• **Nonprompt:** exp.

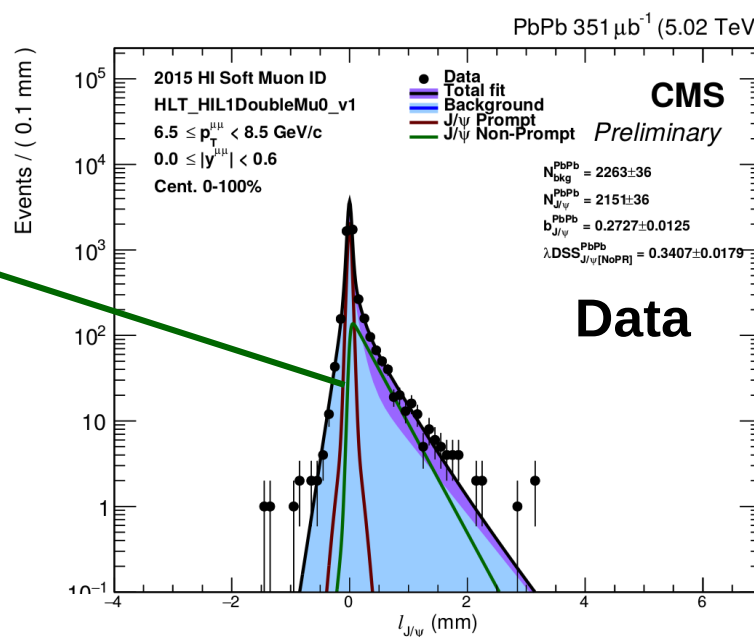
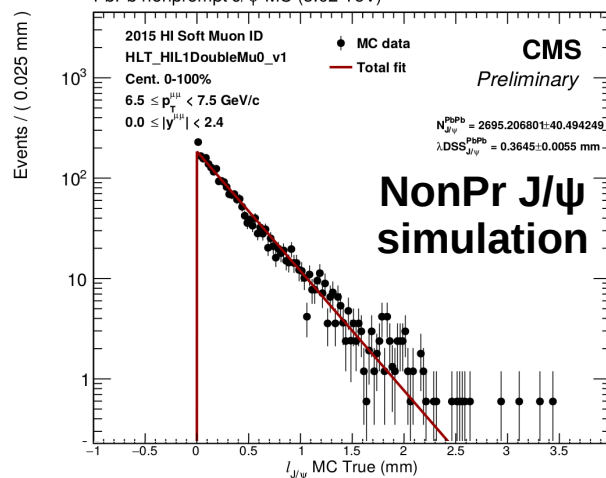


$\ell_{J/\psi}$ parametrisation

Signal $\ell_{J/\psi}$ shape:

- Prompt: delta
- Nonprompt: exp. $\otimes \ell_{J/\psi}$ res.

B-hadron decay length tuned on nonprompt J/ψ simulation



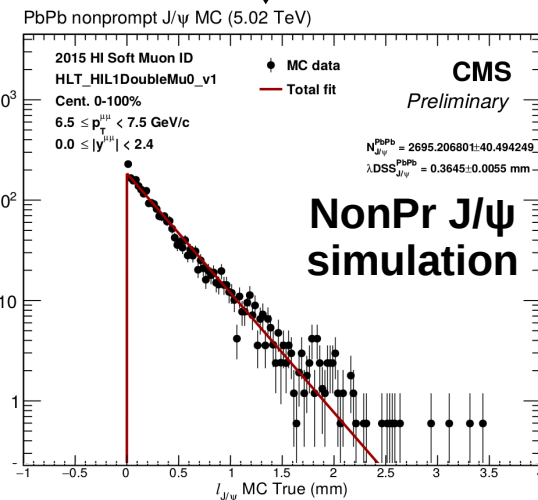
$\ell_{J/\Psi}$ parametrisation

Signal $\ell_{J/\Psi}$ shape:

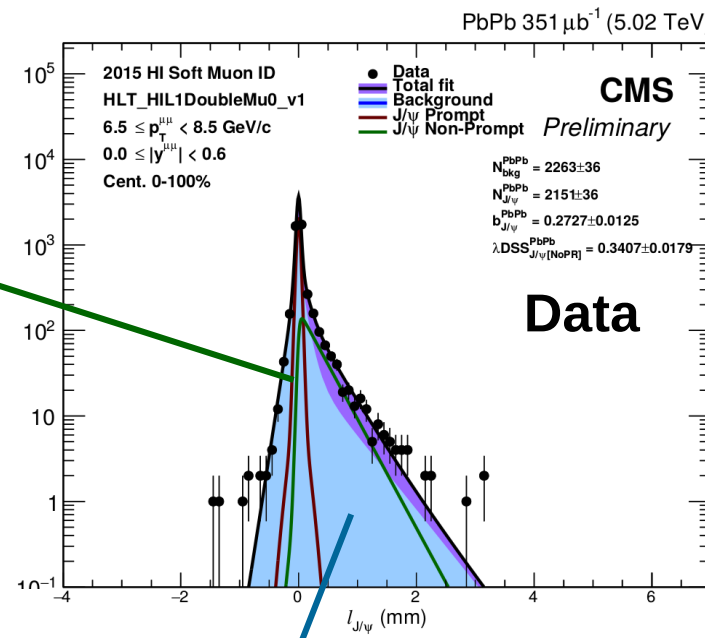
- **Prompt:** delta $\otimes \ell_{J/\Psi}$ res.
- **Nonprompt:** exp.

B-hadron decay length tuned on nonprompt J/ ψ simulation

Events / (0.025 mm)



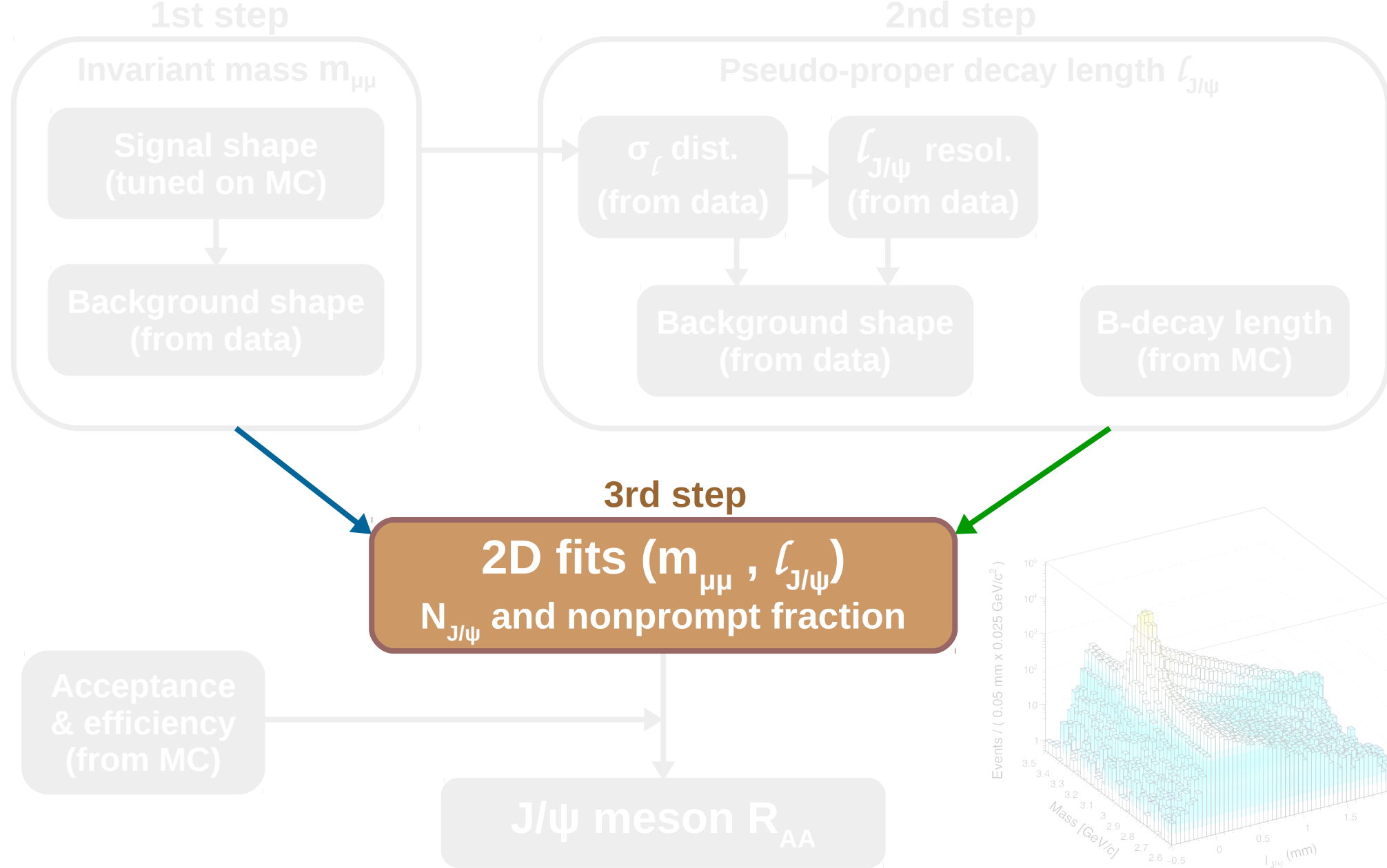
Events / (0.1 mm)



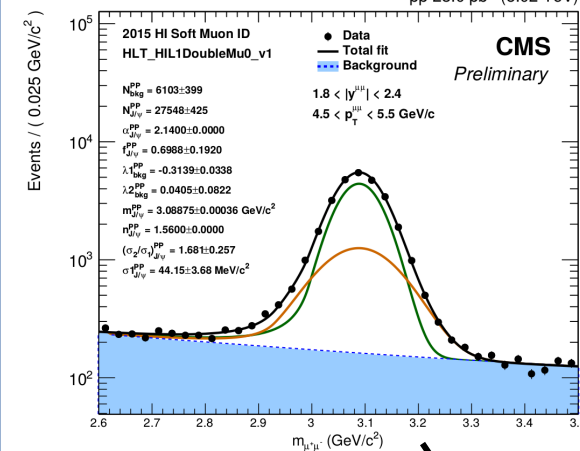
Background $\ell_{J/\Psi}$ shape:

- **Prompt:** delta
- **Nonprompt:** 3 exp. $\otimes \ell_{J/\Psi}$ res.

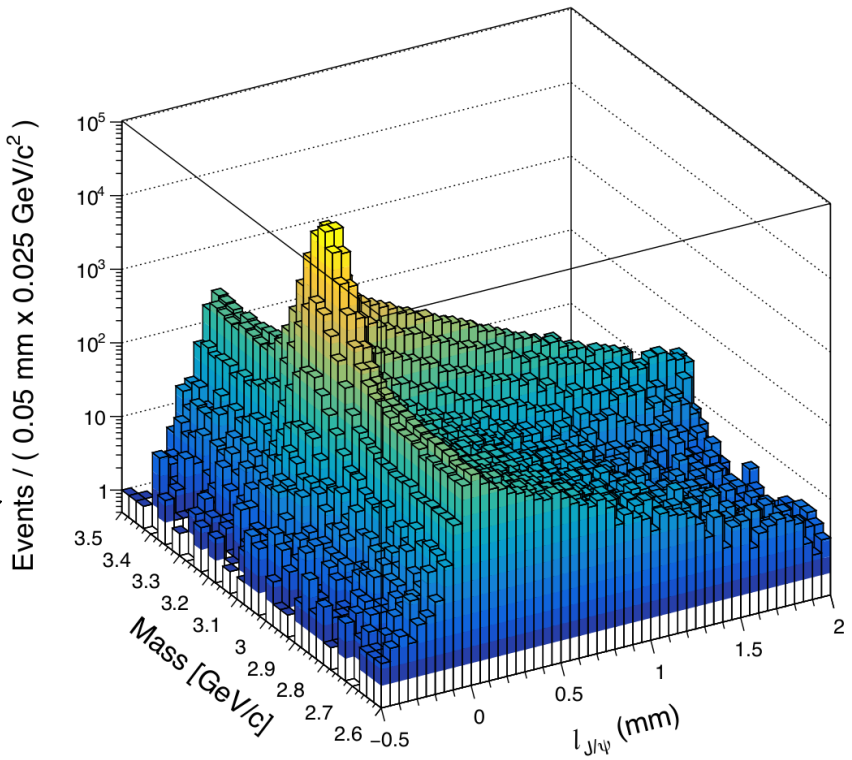
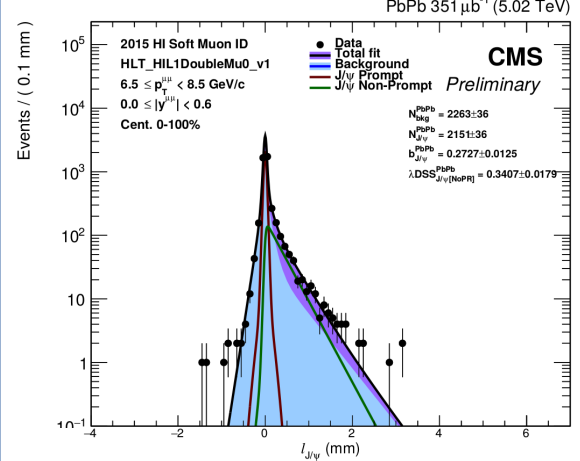
Measurement of J/ ψ R_{AA}



2D ($m_{\mu\mu}$, $\ell_{J/\Psi}$) fit



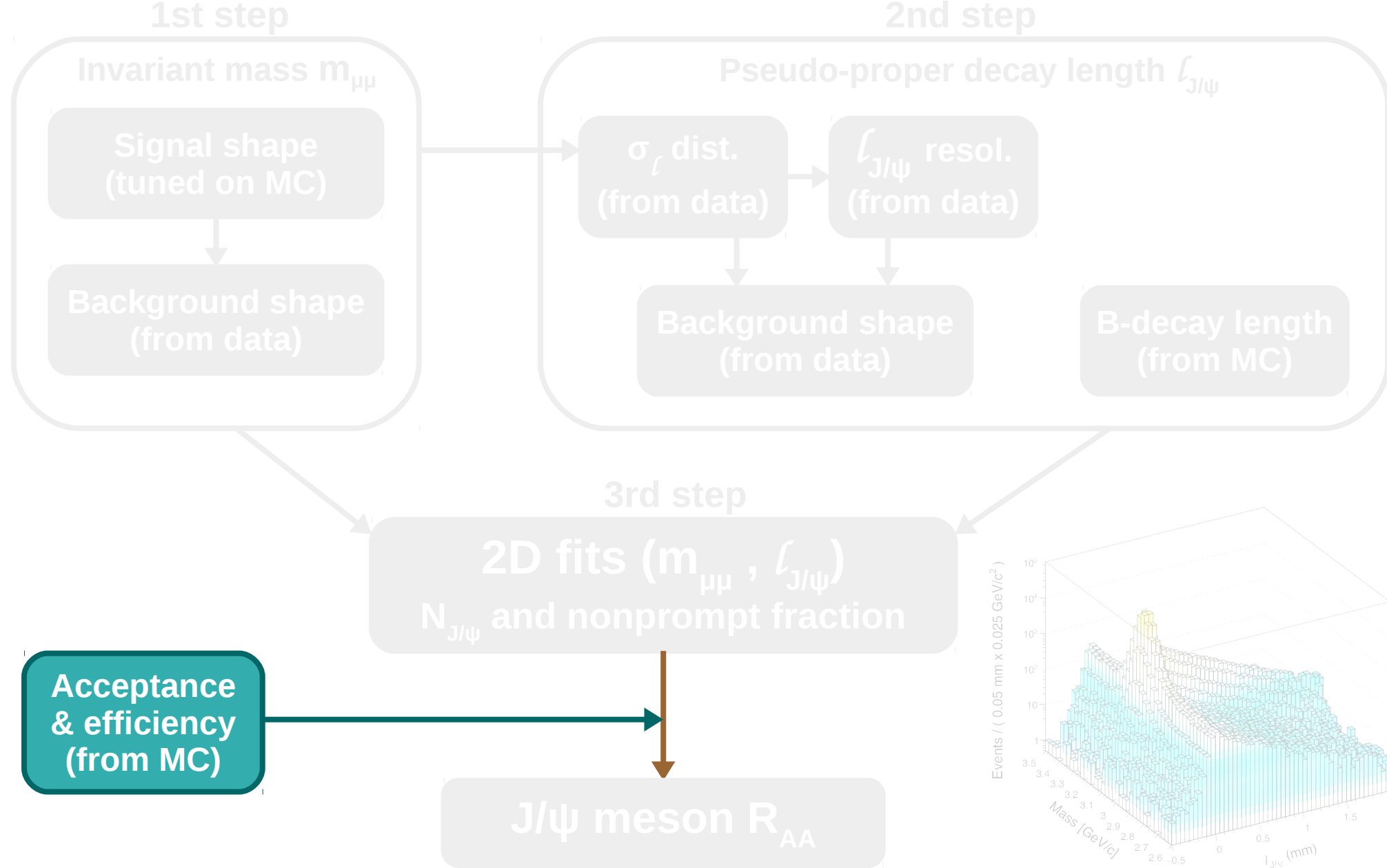
Fix the invariant mass and $\ell_{J/\Psi}$ shapes derived in previous steps



Fit the 2D ($m_{\mu\mu}$, $\ell_{J/\Psi}$) distribution:

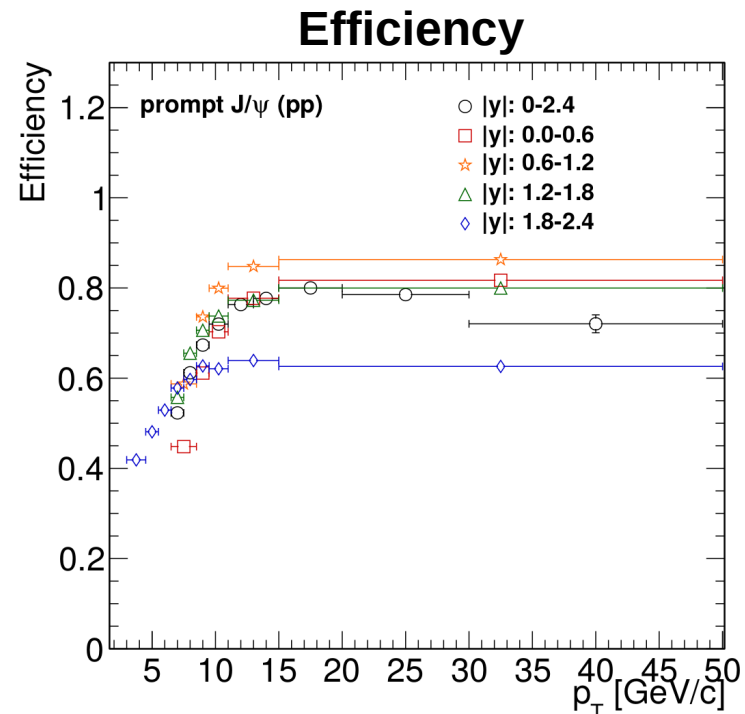
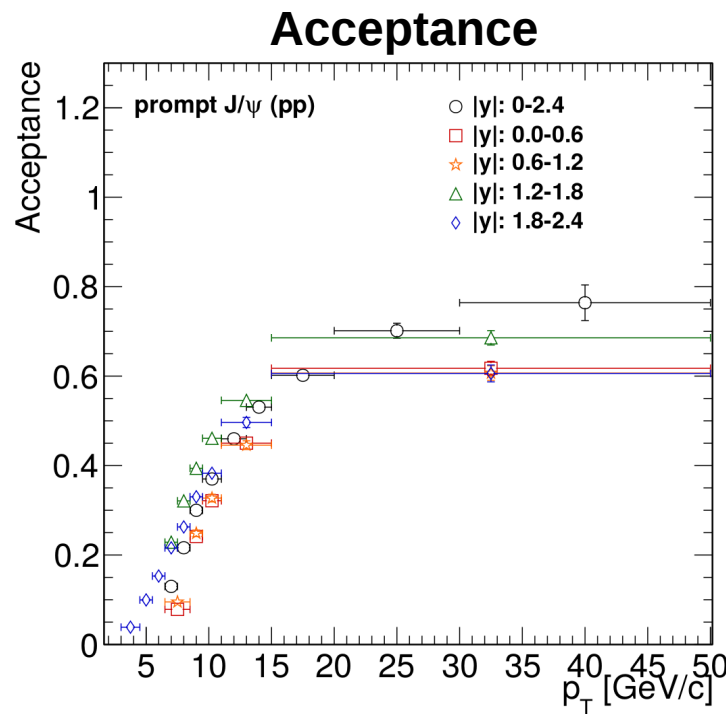
- $N_{J/\Psi}$ and N_{bkg}
- $b_{J/\Psi}$: J/ψ nonprompt fraction
- λ : b-hadron decay length

Measurement of J/ ψ R_{AA}

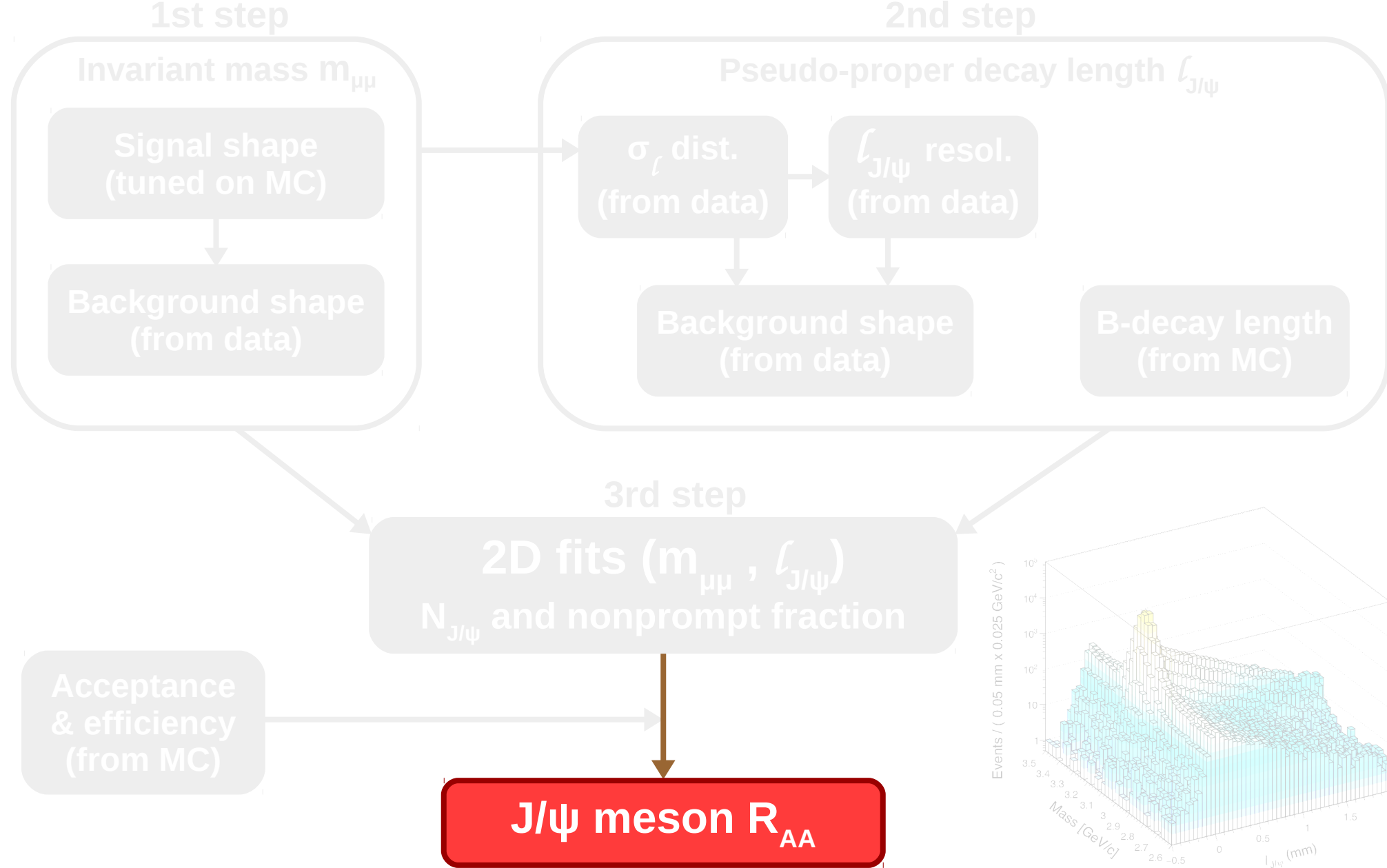


Acceptance and Efficiency

- Signal acceptance and efficiency derived using simulations



Measurement of J/ ψ R_{AA}



Measurement of J/ ψ R_{AA}

Measured number of signal events:

$$N_{J/\psi} = \frac{N_{J/\psi}^{\text{raw}}}{(\mathcal{A}_{J/\psi} \times \epsilon_{J/\psi})}$$

Extracted from 2D fit

Nuclear modification factor:

$$R_{\text{AA}}^{J/\psi} = \frac{\mathcal{L}_{pp}}{\langle T_{\text{AA}} \rangle \cdot N_{\text{MB}} \cdot \Delta \text{cent}} \left(\frac{N_{J/\psi}^{\text{PbPb}}}{N_{J/\psi}^{\text{pp}}} \right)$$

Measurement of J/ ψ R_{AA}

Measured number of signal events:

$$N_{J/\psi} = \frac{N_{J/\psi}^{\text{raw}}}{(\mathcal{A}_{J/\psi} \times \epsilon_{J/\psi})}$$

Extracted from 2D fit

Nuclear modification factor:

$$R_{\text{AA}}^{J/\psi} = \frac{\mathcal{L}_{pp}}{\langle T_{\text{AA}} \rangle \cdot N_{\text{MB}} \cdot \Delta_{\text{cent}}} \left(\frac{N_{J/\psi}^{\text{PbPb}}}{N_{J/\psi}^{\text{pp}}} \right)$$

p-p integrated luminosity ($28.0 \pm 0.6 \text{ /pb}$)

Measurement of J/ ψ R_{AA}

Measured number of signal events:

$$N_{J/\psi} = \frac{N_{J/\psi}^{\text{raw}}}{(\mathcal{A}_{J/\psi} \times \epsilon_{J/\psi})}$$

Extracted from 2D fit

Nuclear modification factor:

$$R_{\text{AA}}^{J/\psi} = \frac{\mathcal{L}_{pp}}{\langle T_{\text{AA}} \rangle \cdot N_{\text{MB}} \cdot \Delta_{\text{cent}}} \left(\frac{N_{J/\psi}^{\text{PbPb}}}{N_{J/\psi}^{\text{pp}}} \right)$$

p-p integrated luminosity ($28.0 \pm 0.6 / \text{pb}$)

nuclear overlap function
($5.6 \pm 0.2 / \text{mb}$, centrality-integrated)

Measurement of J/ ψ R_{AA}

Measured number of signal events:

$$N_{J/\psi} = \frac{N_{J/\psi}^{\text{raw}}}{(\mathcal{A}_{J/\psi} \times \epsilon_{J/\psi})}$$

Extracted from 2D fit

Nuclear modification factor:

$$R_{\text{AA}}^{J/\psi} = \frac{\mathcal{L}_{pp} \cdot N_{J/\psi}^{\text{PbPb}}}{\langle T_{\text{AA}} \rangle \cdot N_{\text{MB}} \cdot \Delta_{\text{cent}}} \left(\frac{N_{J/\psi}^{\text{PbPb}}}{N_{J/\psi}^{\text{pp}}} \right)$$

nuclear overlap function
(5.6 ± 0.2 /mb, centrality-integrated)

p-p integrated luminosity (28.0 ± 0.6 /pb)
number of equiv. min. bias
events ($(2.37 \pm 0.05) \times 10^9$)

Measurement of J/ ψ R_{AA}

Measured number of signal events:

$$N_{J/\psi} = \frac{N_{J/\psi}^{\text{raw}}}{(\mathcal{A}_{J/\psi} \times \epsilon_{J/\psi})}$$

Extracted from 2D fit

Nuclear modification factor:

$$R_{\text{AA}}^{J/\psi} = \frac{\mathcal{L}_{pp}}{\langle T_{\text{AA}} \rangle \cdot N_{\text{MB}} \cdot \Delta_{\text{cent}}} \left(\frac{N_{J/\psi}^{\text{PbPb}}}{N_{J/\psi}^{\text{pp}}} \right)$$

nuclear overlap function
(5.6 ± 0.2 /mb, centrality-integrated)

number of equiv. min. bias
events ($(2.37 \pm 0.05) \times 10^9$)

p-p integrated luminosity (28.0 ± 0.6 /pb)
Fraction of minimum bias
events within centrality range
([20%, 50%] → 30%)

Measurement of J/ ψ R_{AA}

Nuclear modification factor:

$$R_{\text{AA}}^{\text{J}/\psi} = \frac{\mathcal{L}_{pp}}{\langle T_{\text{AA}} \rangle \cdot N_{\text{MB}} \cdot \Delta\text{cent}} \left(\frac{N_{\text{J}/\psi}^{\text{PbPb}}}{N_{\text{J}/\psi}^{\text{pp}}} \right)$$

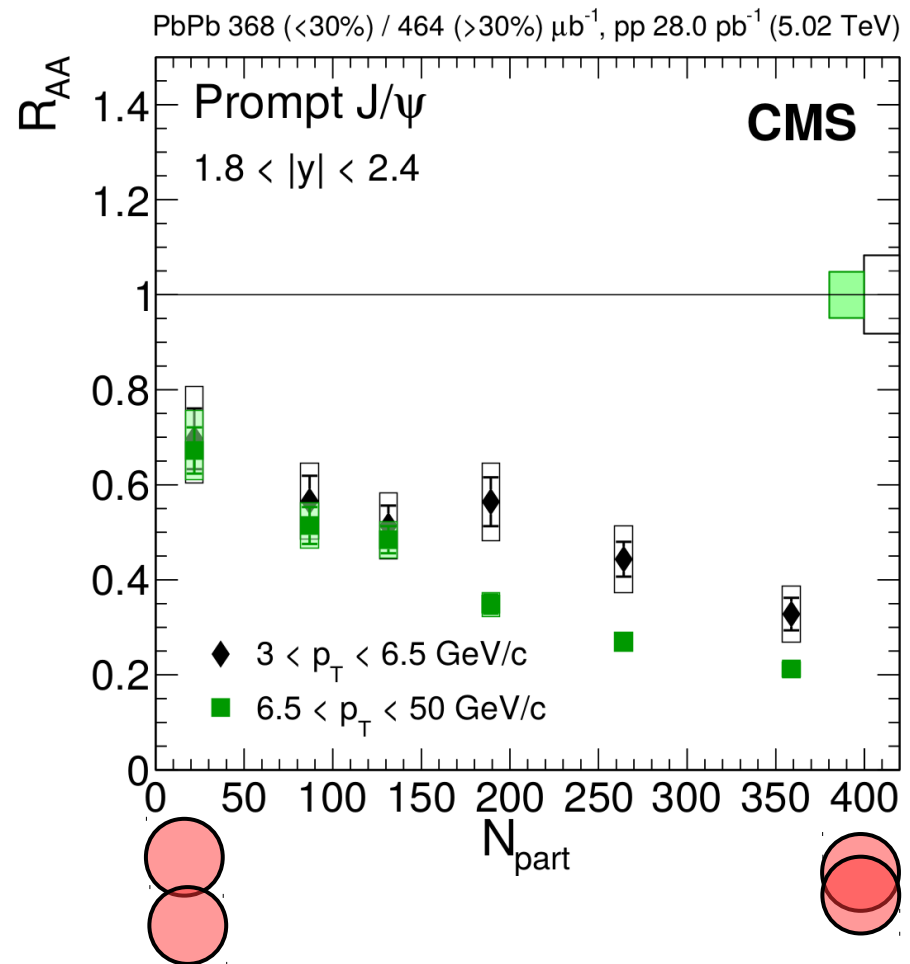
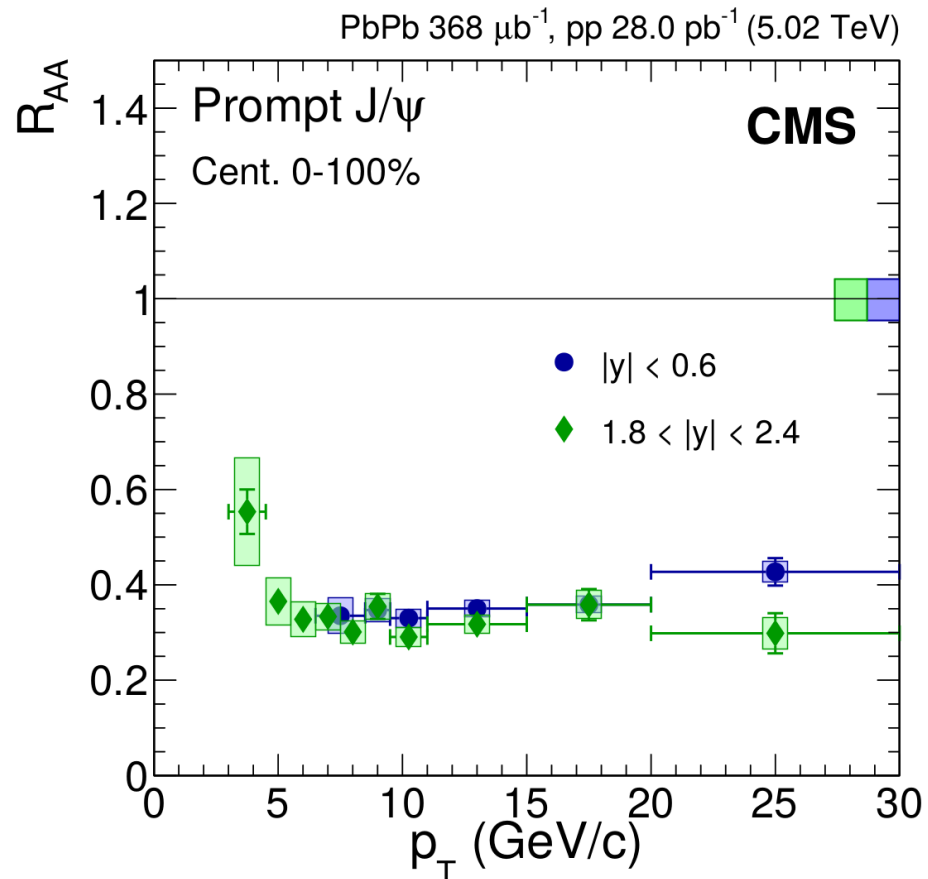
Source of uncertainty	Relative uncertainty	
	Prompt [%]	Nonprompt [%]
Efficiency	3.6 - 16.7	3.6 - 16.6
Invariant mass parametrization	0.5 - 3.4	0.9 - 3.3
Decay length parametrization	2.0 - 10.6	1.7 - 23.7
Luminosity		2.3
Number of minimum bias events		2
Nuclear overlap function T _{AA}		2 - 16

Outline

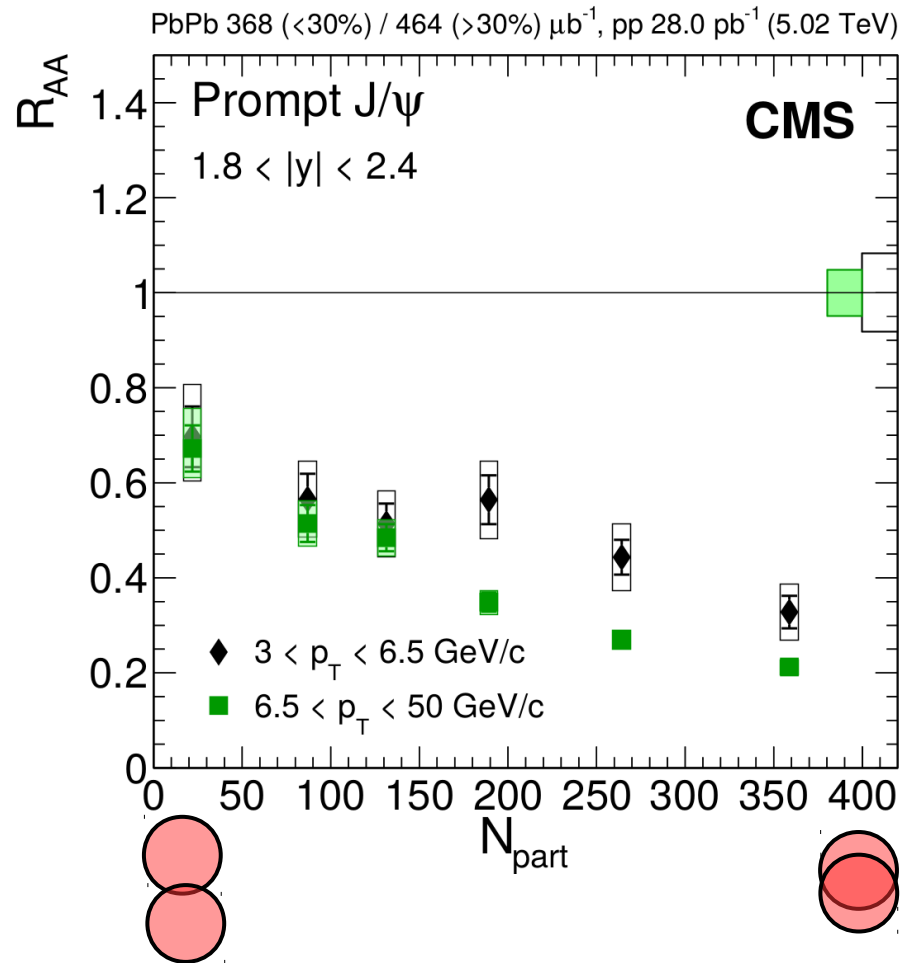
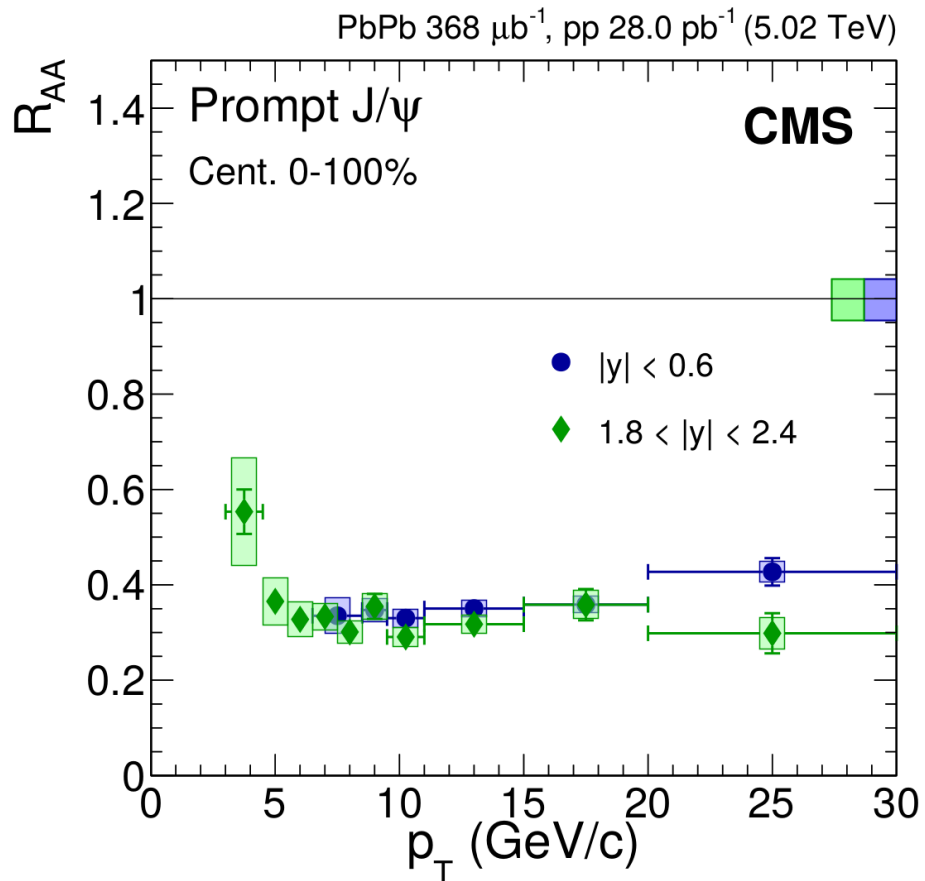
- Theoretical context
- The CMS detector at the LHC
- W-boson production in p-Pb at 8.16 TeV
 - Introduction
 - Analysis
 - Results
- Charmonium production in Pb-Pb at 5.02 TeV
 - Introduction
 - Analysis
 - Results
- Conclusions



Prompt J/ ψ R_{AA}: Low p_T

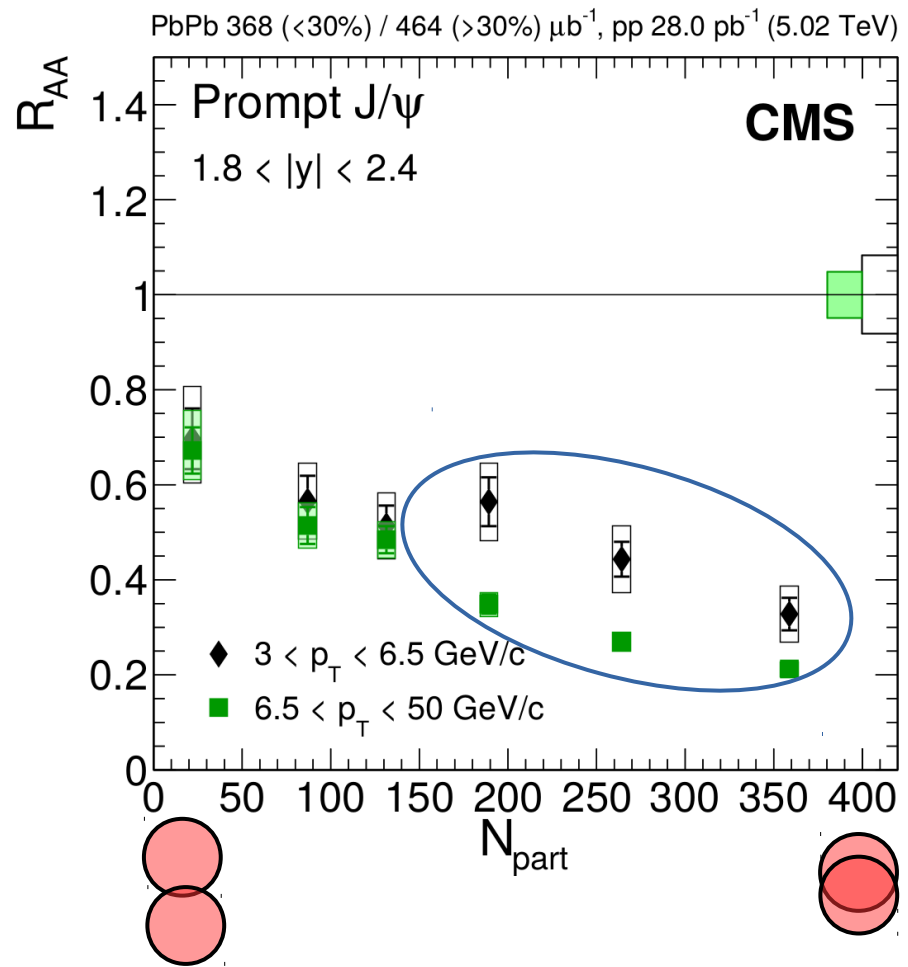
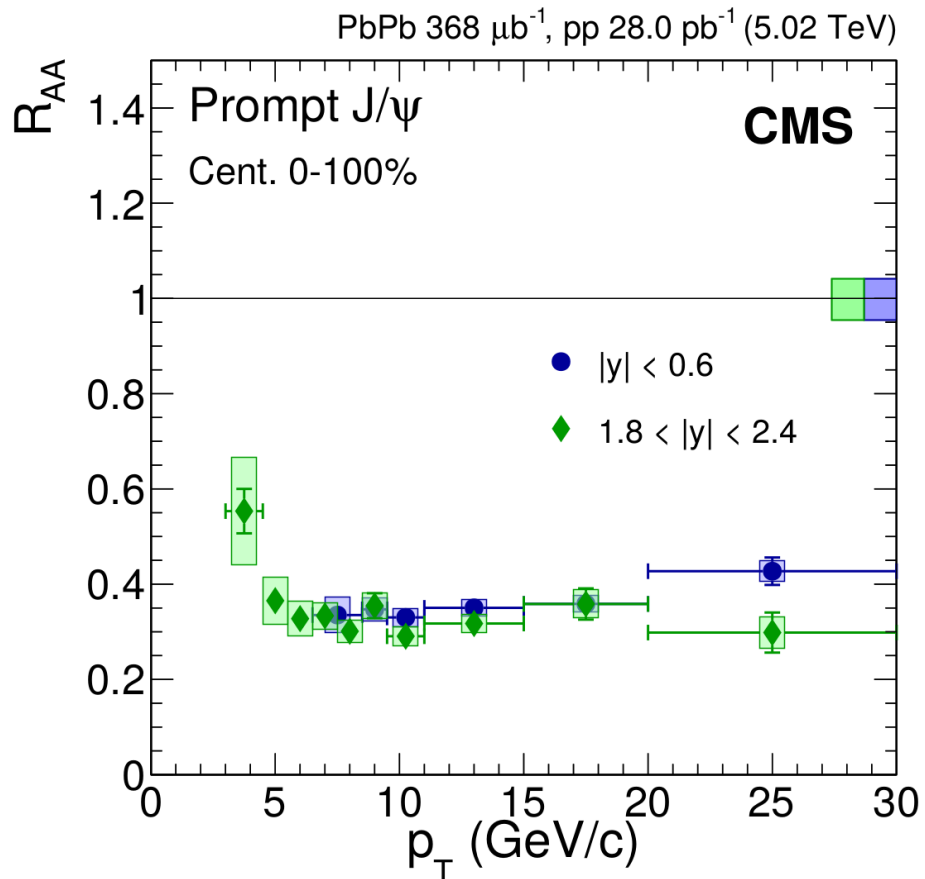


Prompt J/ ψ R_{AA}: Low p_T



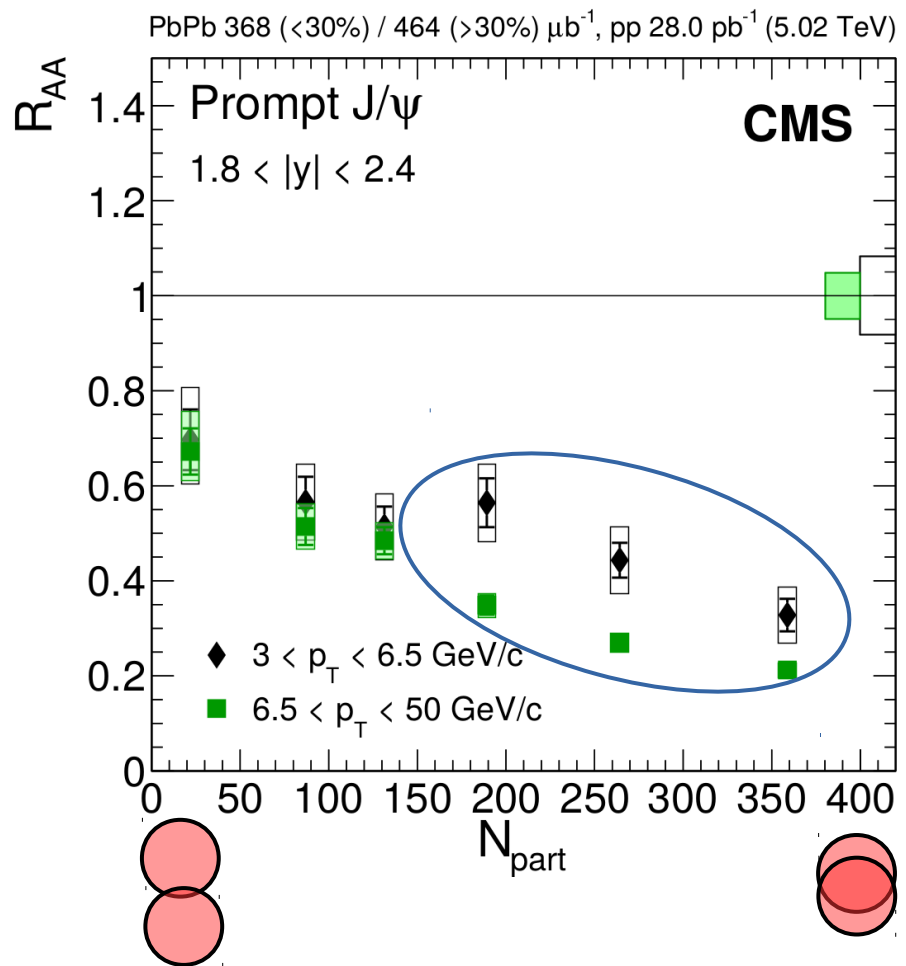
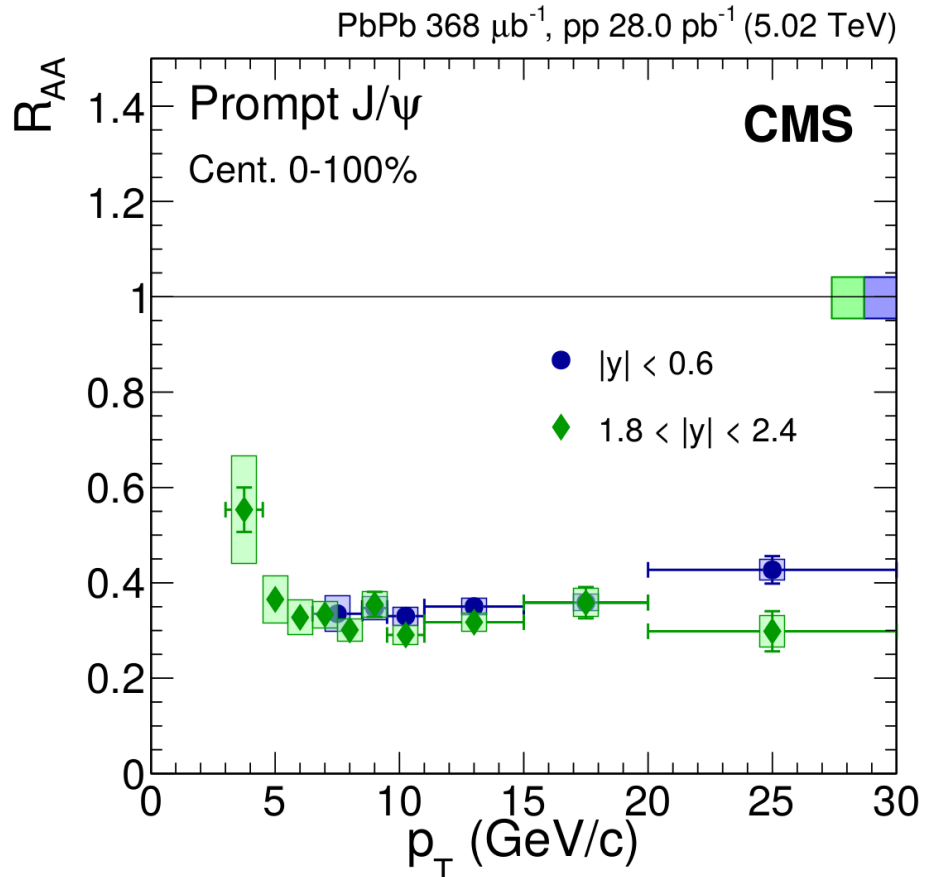
- Similar p_T trend for different rapidities bins

Prompt J/ ψ R_{AA}: Low p_T



- Similar p_T trend for different rapidities bins
- Less suppression at low p_T in central events (cent < 30%)

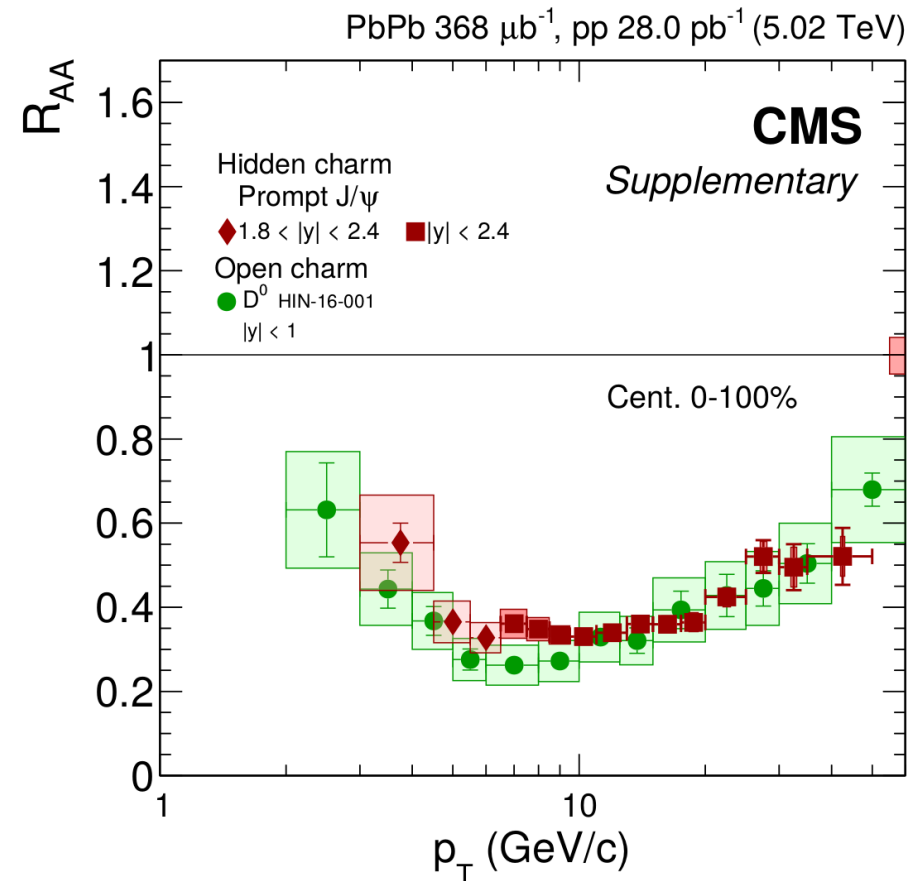
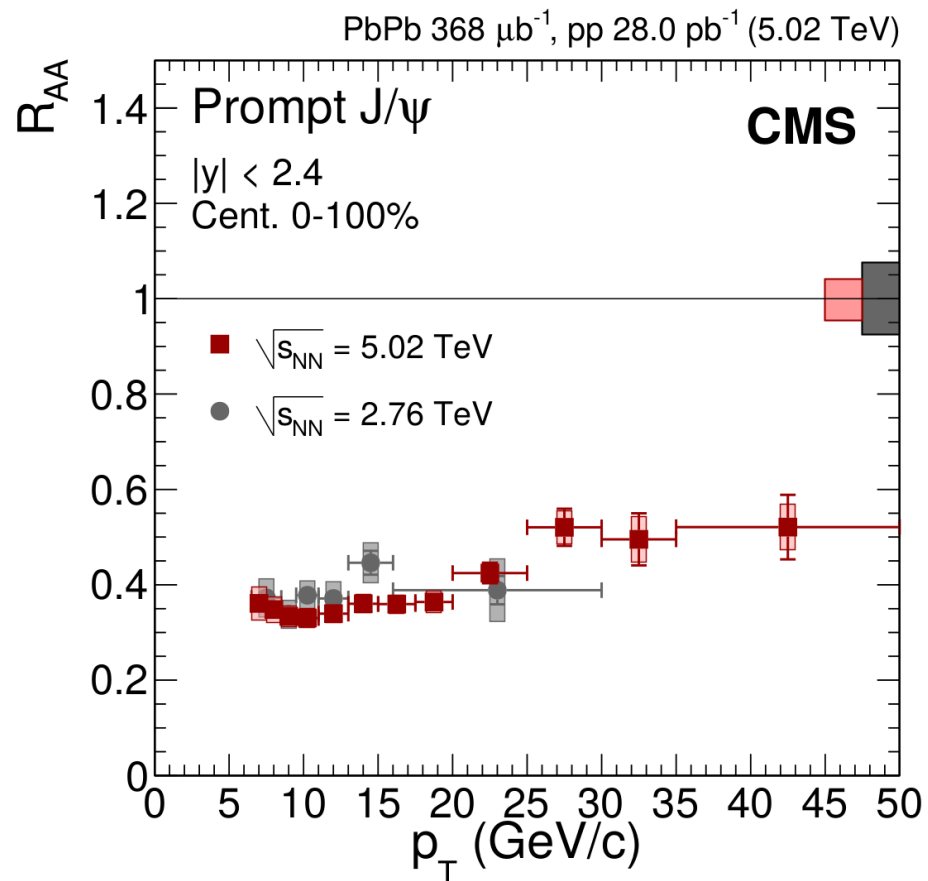
Prompt J/ ψ R_{AA}: Low p_T



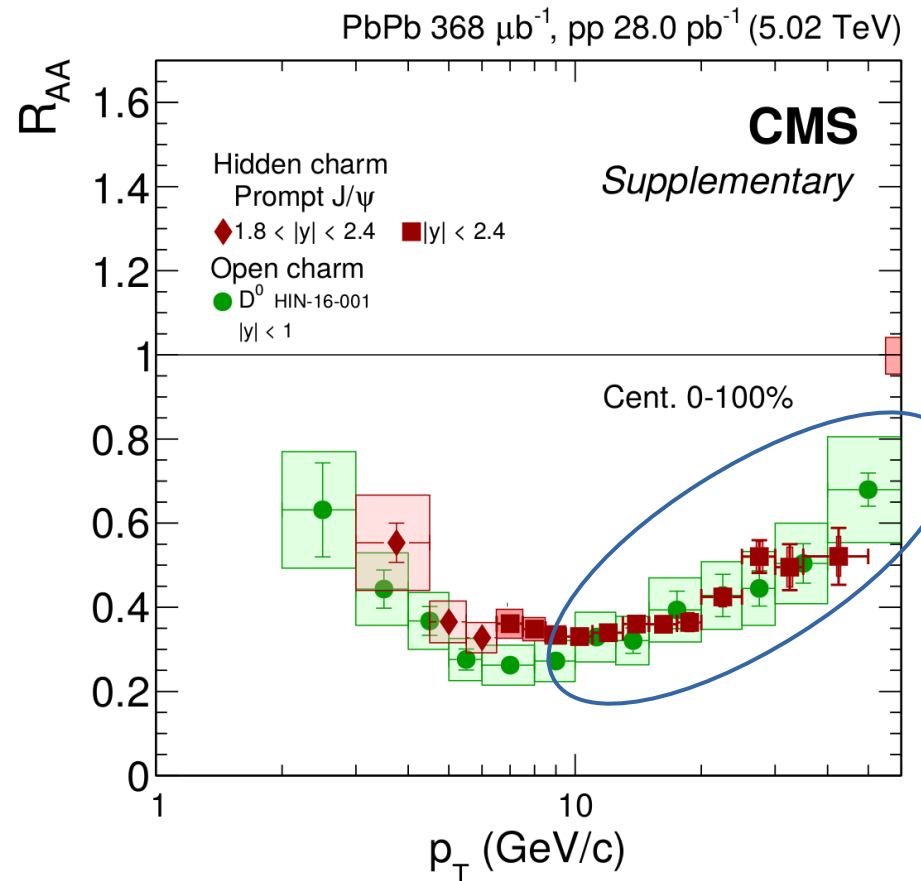
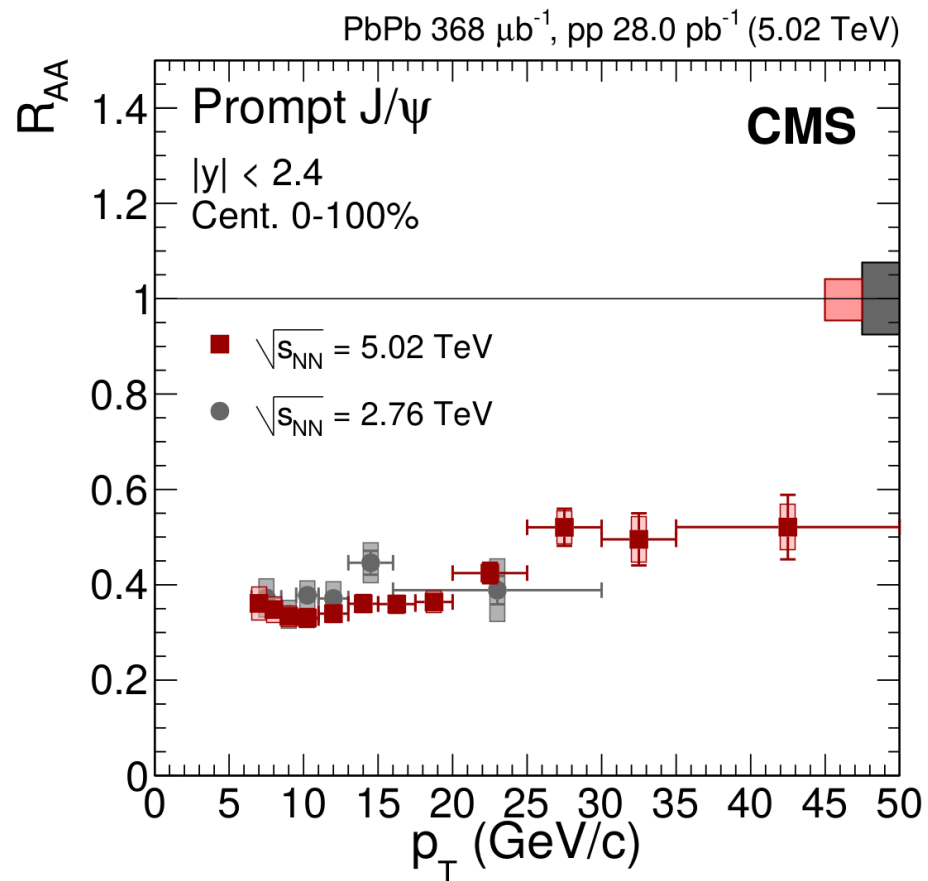
- Similar p_T trend for different rapidities bins
- Less suppression at low p_T in central events (cent < 30%)

Regeneration of J/ ψ at p_T \gtrsim 3 GeV/c ?

Prompt J/ ψ R_{AA}: High p_T

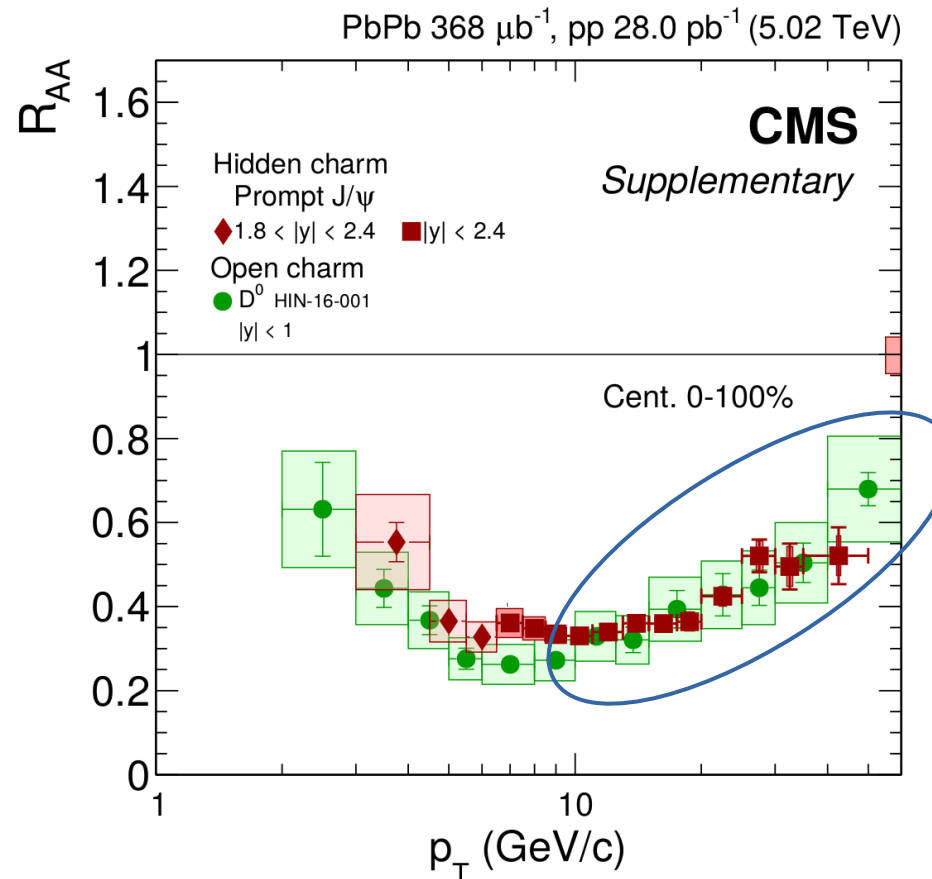
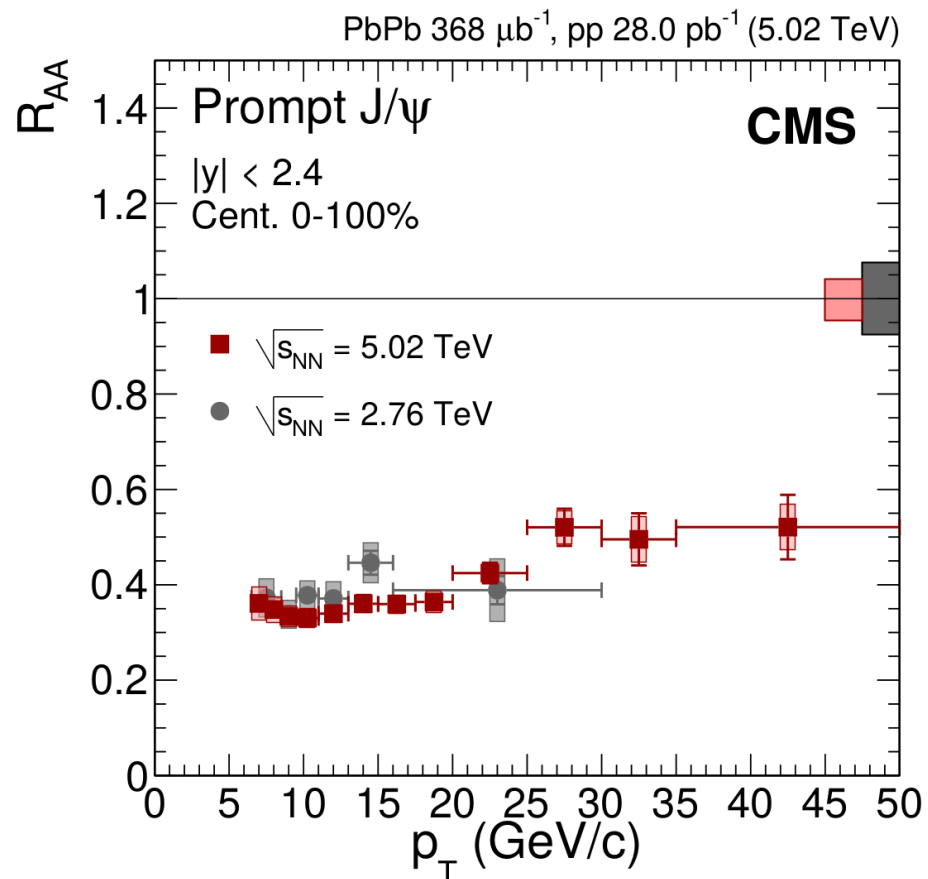


Prompt J/ ψ R_{AA}: High p_T



- Similar level of suppression between prompt J/ ψ and D⁰ mesons

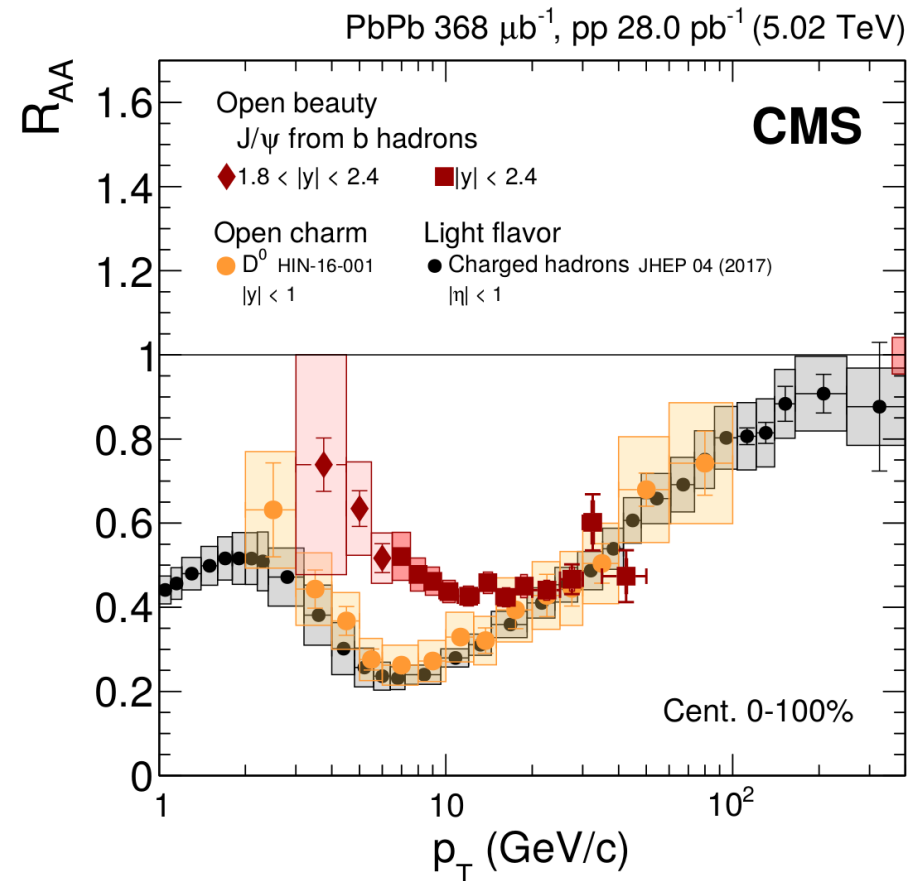
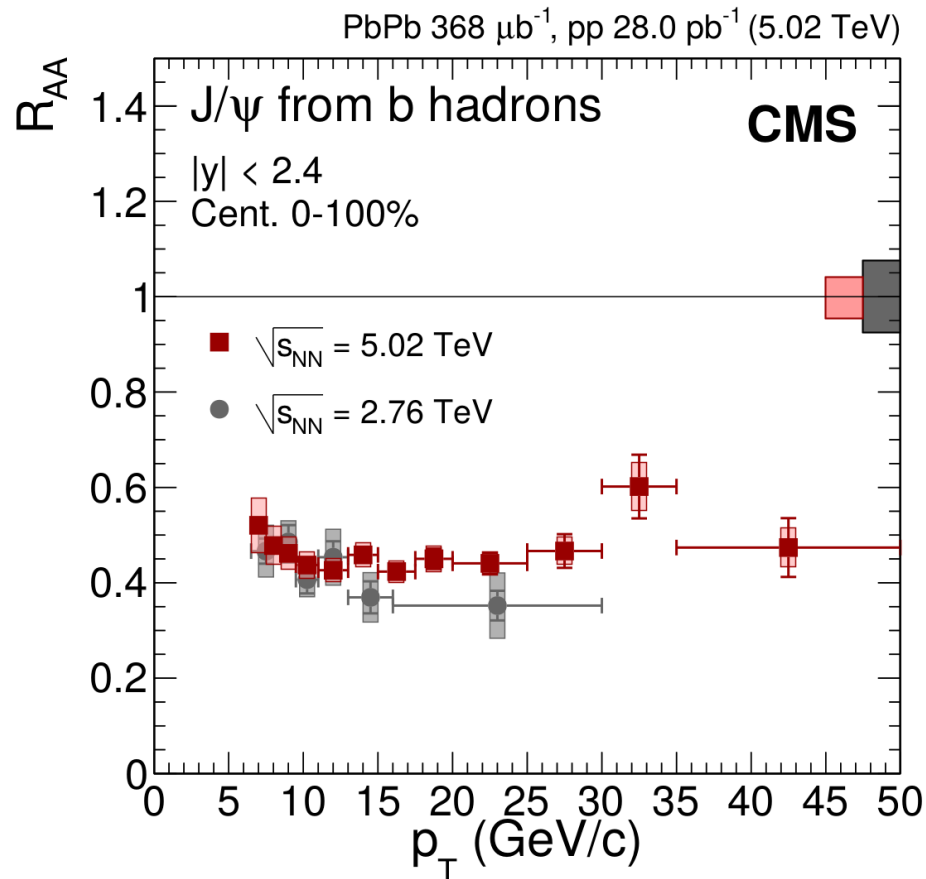
Prompt J/ ψ R_{AA}: High p_T



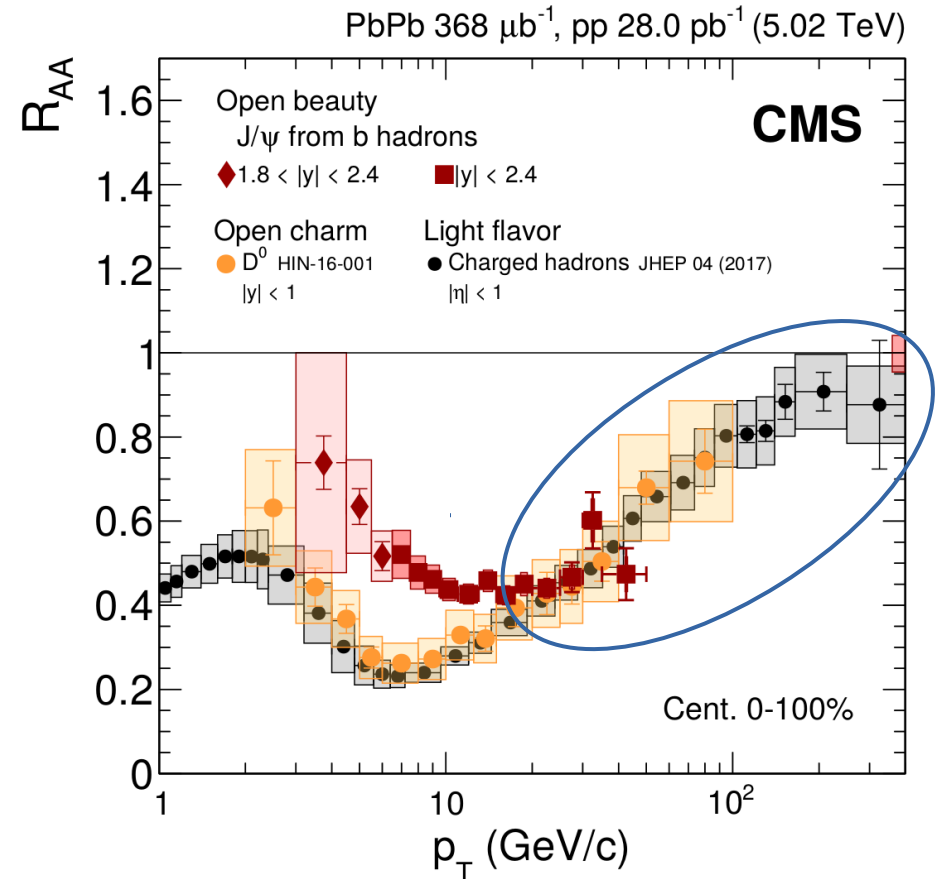
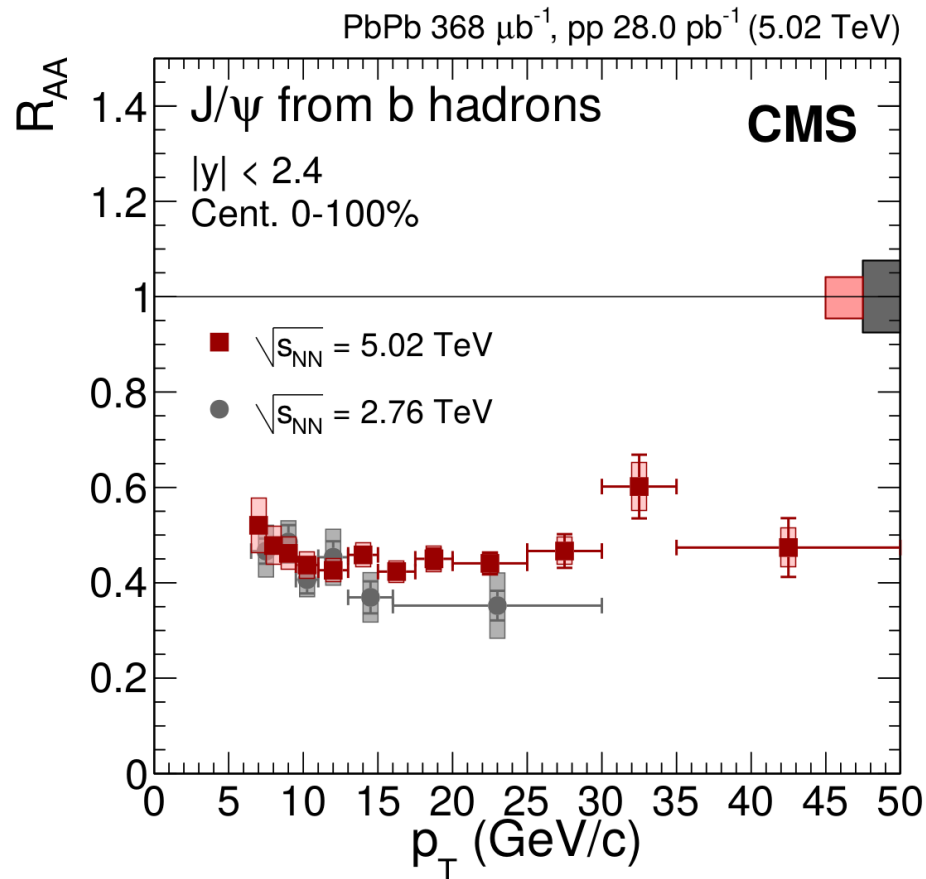
- Similar level of suppression between prompt J/ ψ and D⁰ mesons

Contribution from E_{loss} on J/ ψ ?

Nonprompt J/ ψ R_{AA}

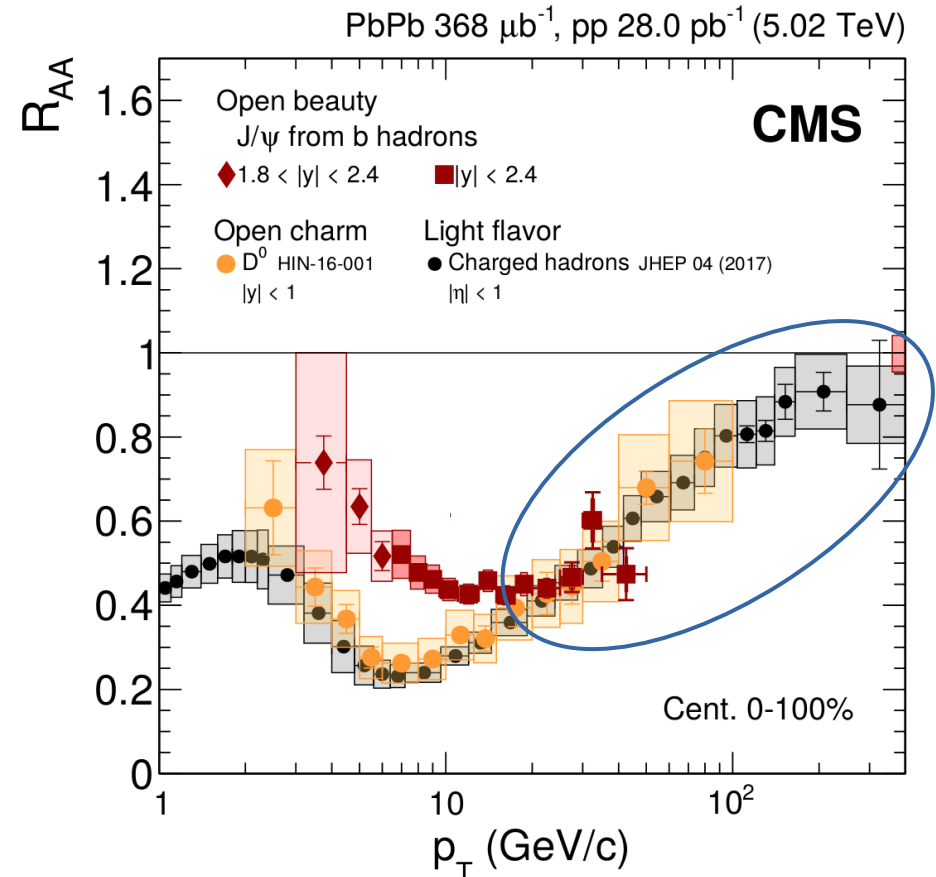
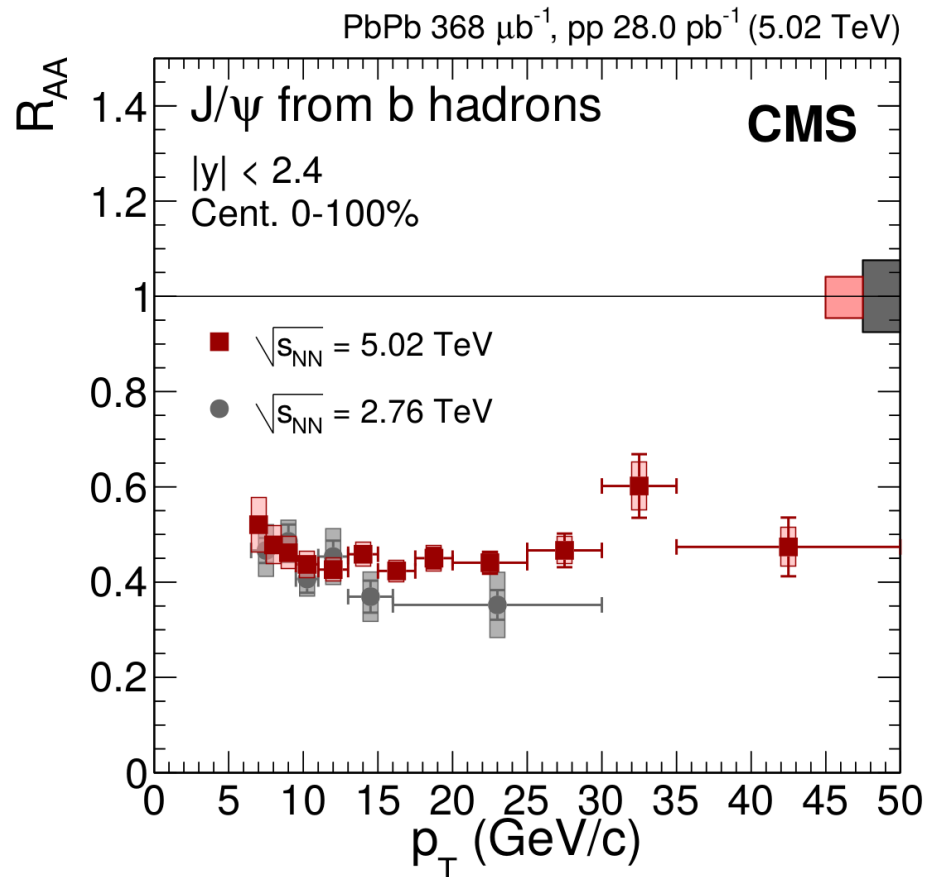


Nonprompt J/ ψ R_{AA}



- Similar suppression between nonprompt J/ ψ , D⁰ mesons and charged hadrons at high p_T

Nonprompt J/ ψ R_{AA}



- Similar suppression between nonprompt J/ψ, D⁰ mesons and charged hadrons at high p_T

Universal flavor dependence of E_{loss} at high p_T ?

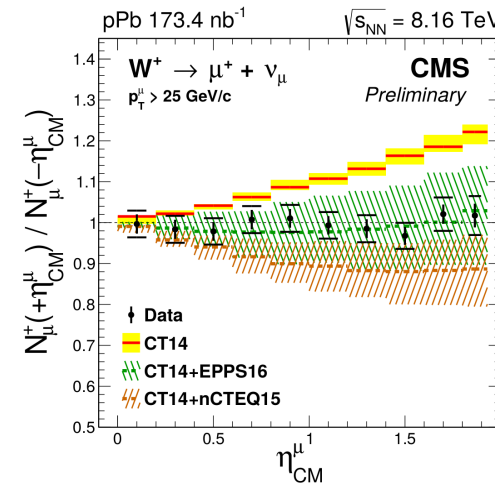
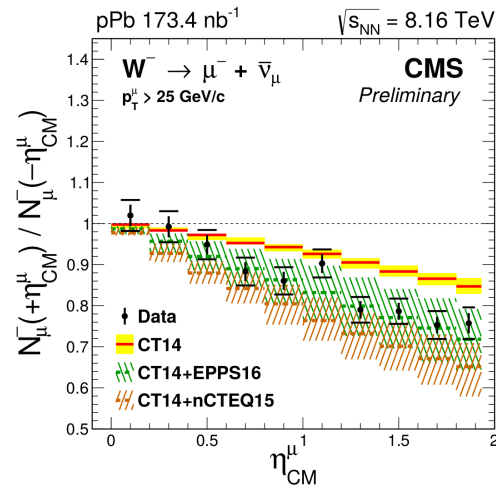
Outline

- Theoretical context
- The CMS detector at the LHC
- W-boson production in p-Pb at 8.16 TeV
 - Introduction
 - Analysis
 - Results
- Charmonium production in Pb-Pb at 5.02 TeV
 - Introduction
 - Analysis
 - Results
- Conclusions



Conclusion

Probing **nuclear PDF**: W bosons in p-Pb collisions

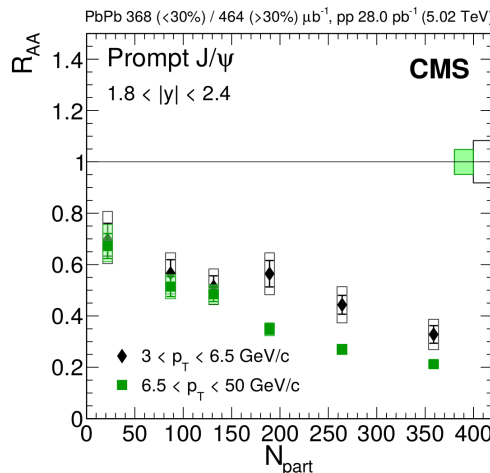


Presented in

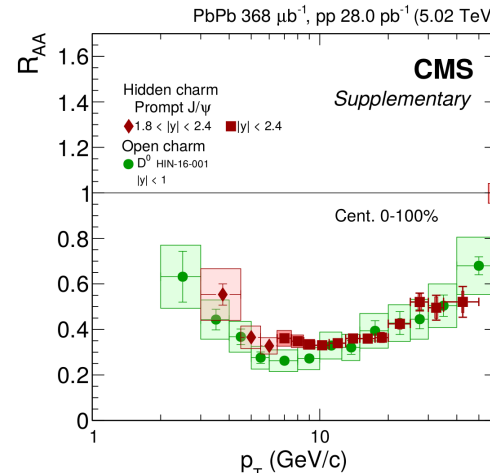
- ICHEP 2018
- QM 2018

- Observation of nuclear modifications of the (anti) quark PDFs

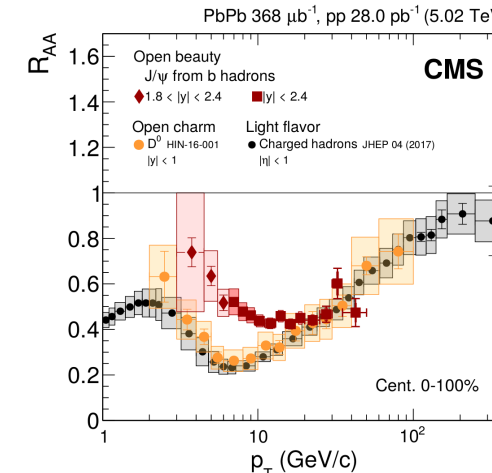
Probing **QGP effects**: J/ ψ mesons in Pb-Pb collisions



Suppression and regeneration of J/ ψ



Contribution of E_{loss} on J/ ψ ?



Universal flavor dependence of E_{loss}?

Published in

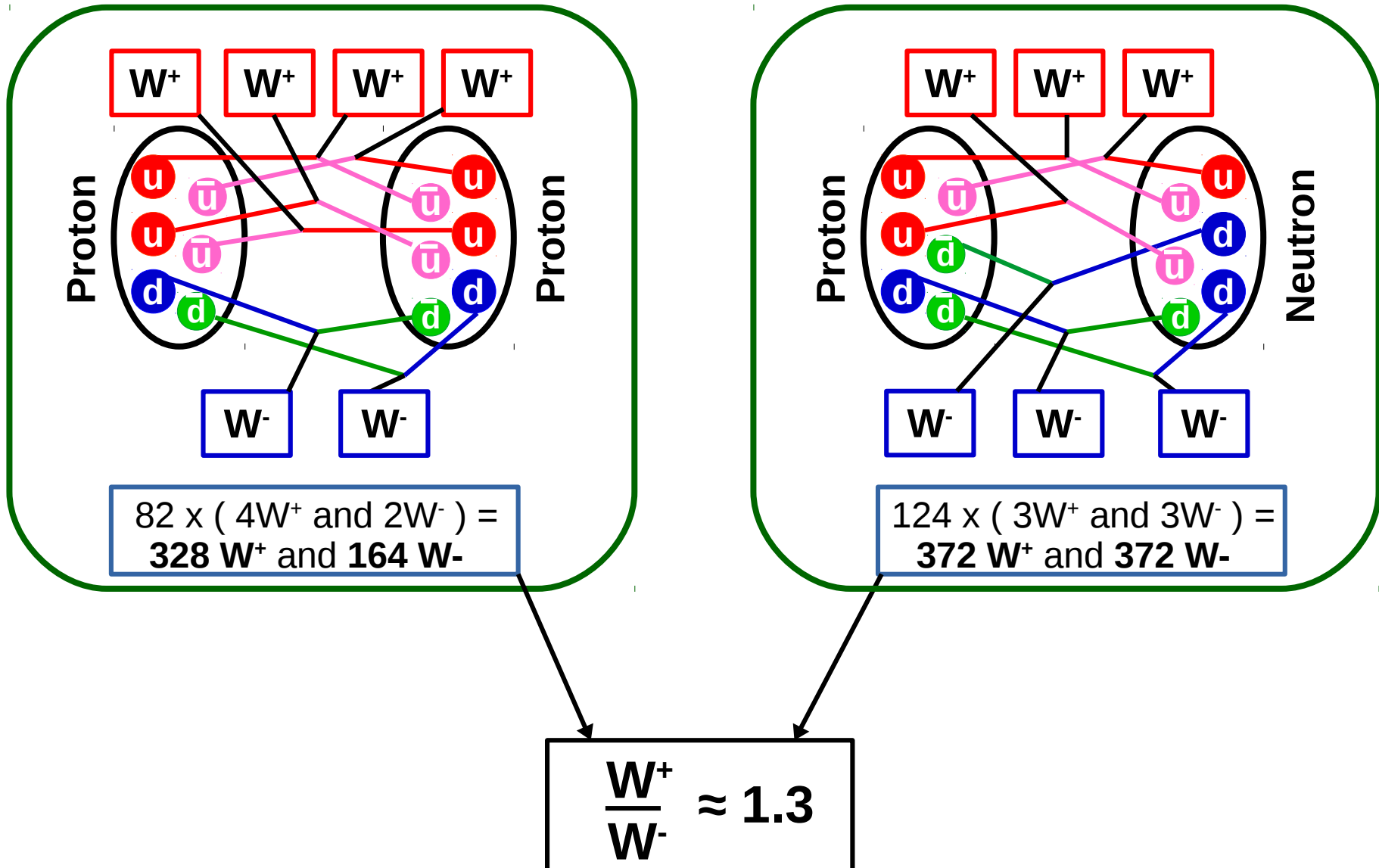
- Eur. Phys. J. C 78 (2018) 509

Thank you for your attention!

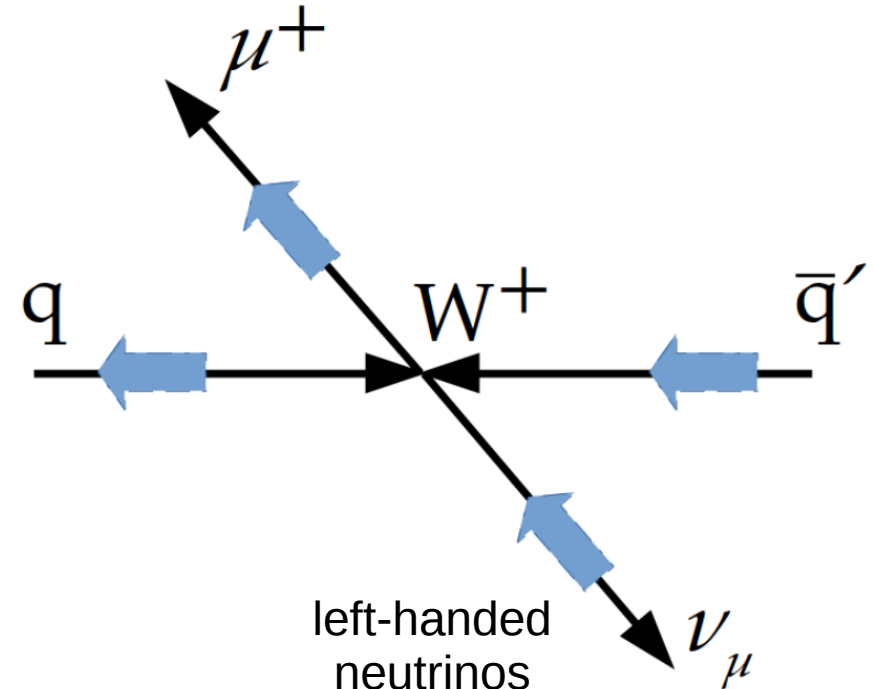
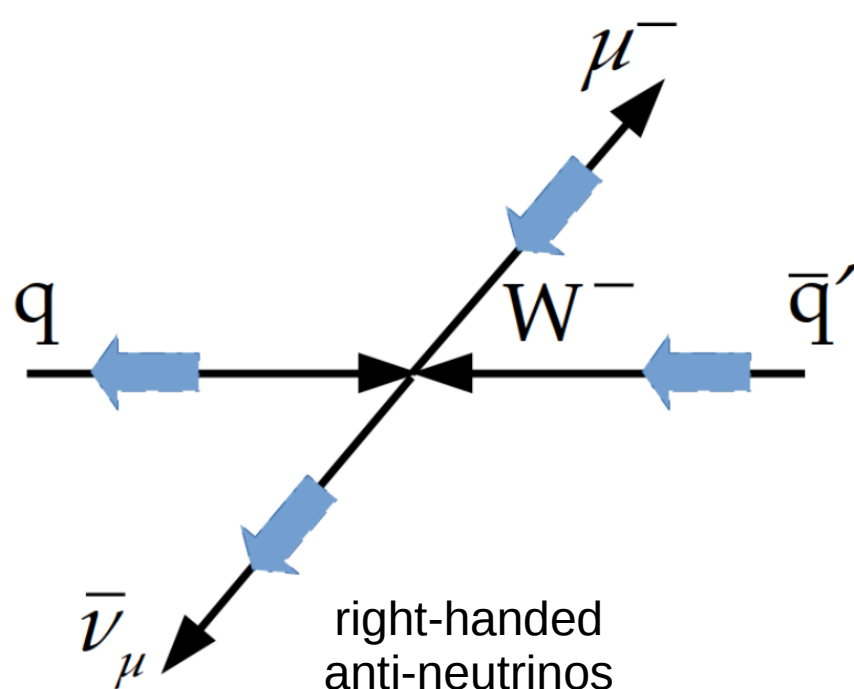


BACKUP

W-boson production in p-Pb



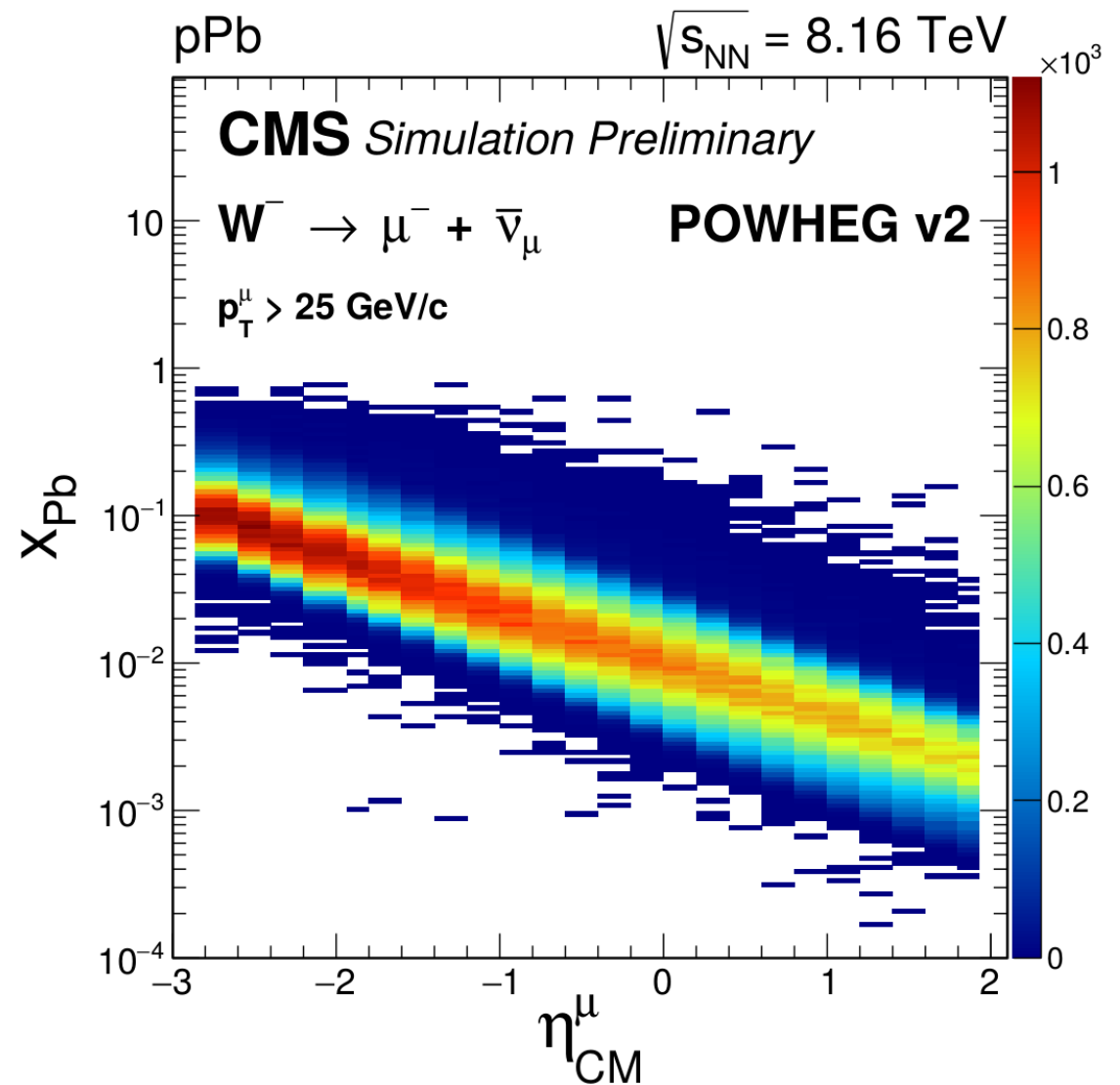
W-boson muonic decay



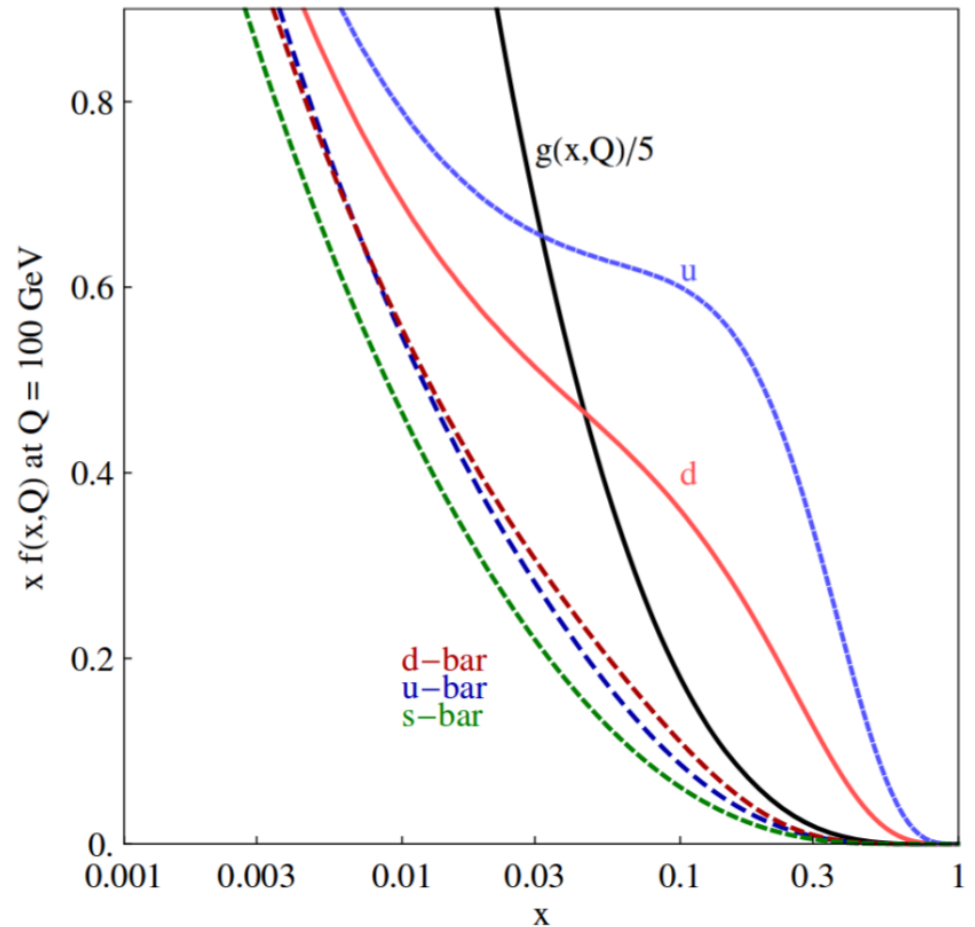
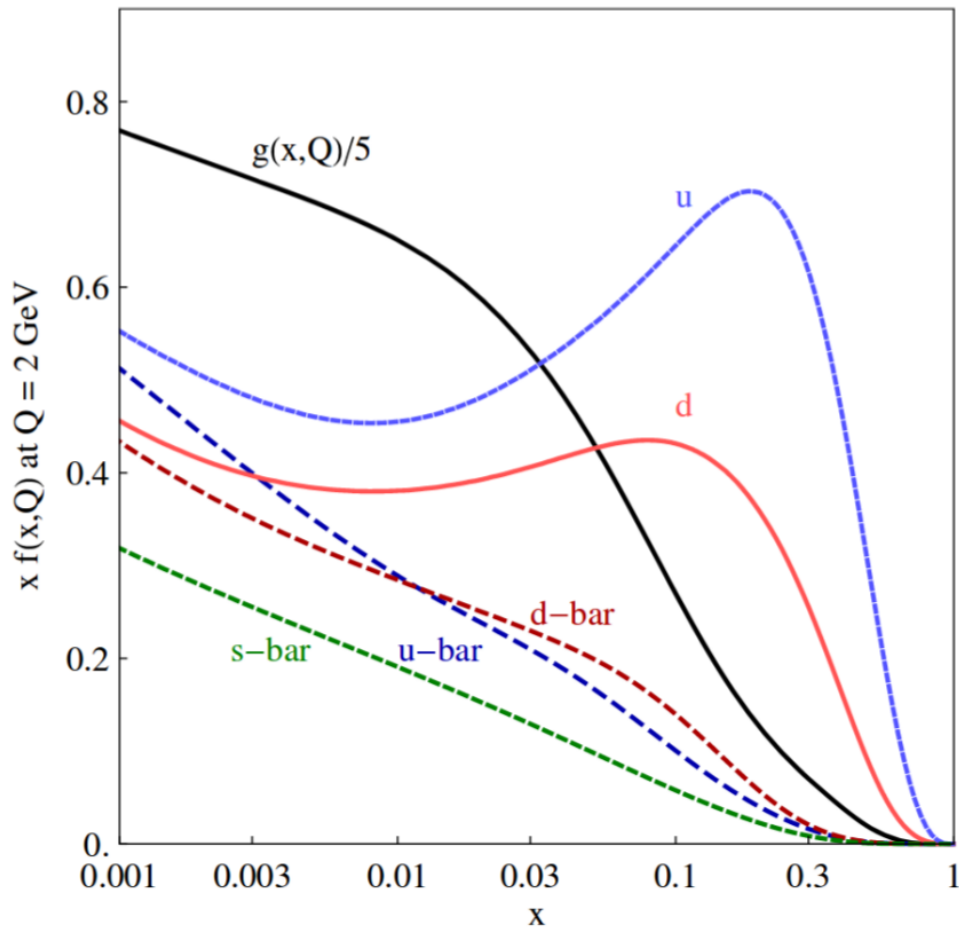
The black arrows represent the particle direction of motion whereas the blue arrows correspond to its spin

Bjorken-x vs muon η

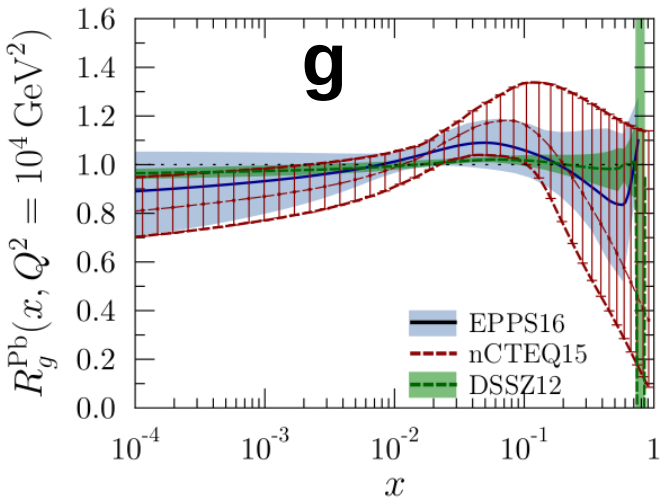
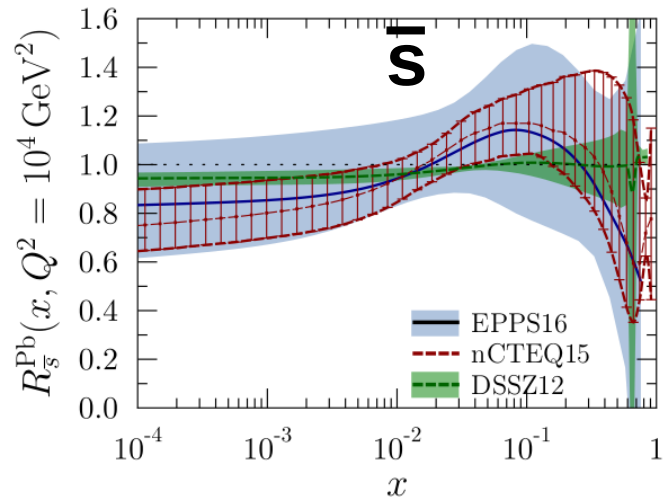
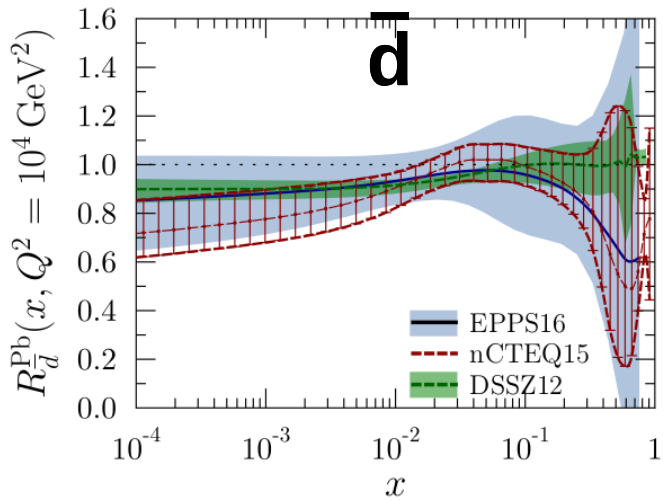
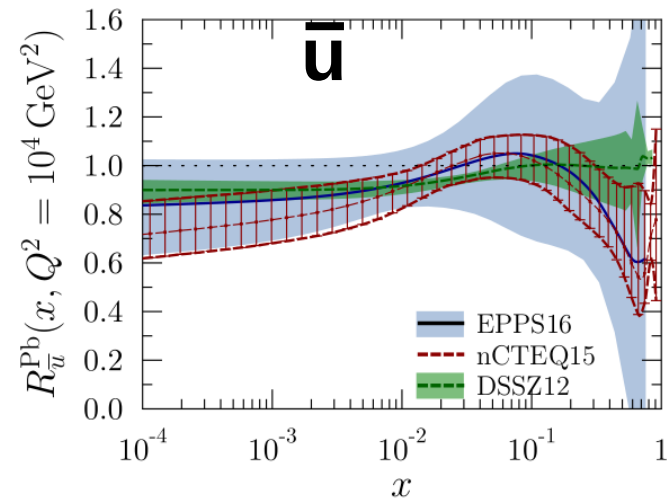
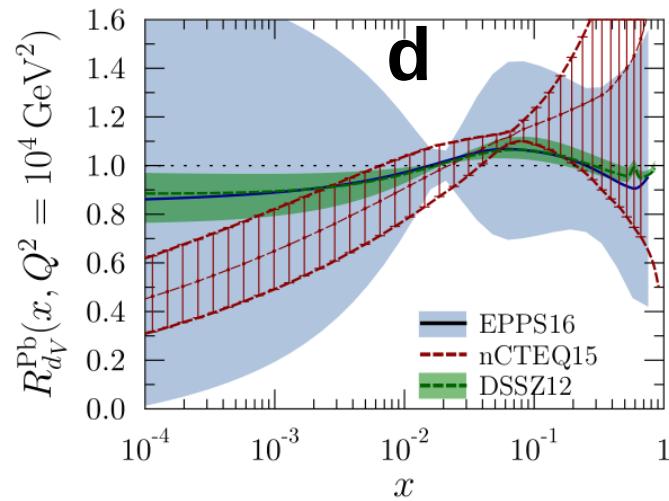
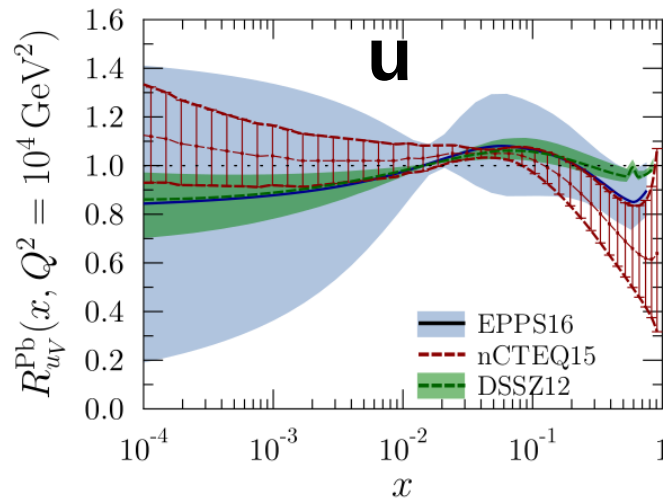
$$x_{\text{Pb}} \approx \frac{M_W}{\sqrt{s_{\text{NN}}}} \exp(-\eta_{\text{CM}}^\mu)$$



CT14 PDF set



Nuclear PDF sets

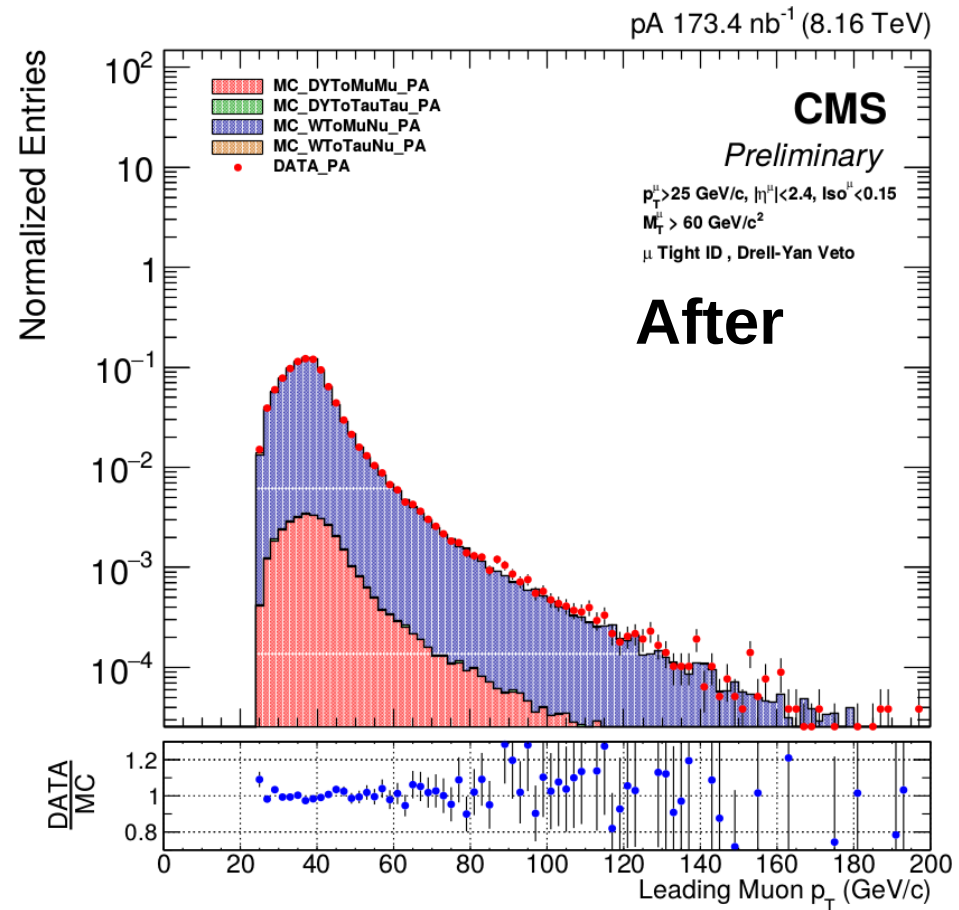
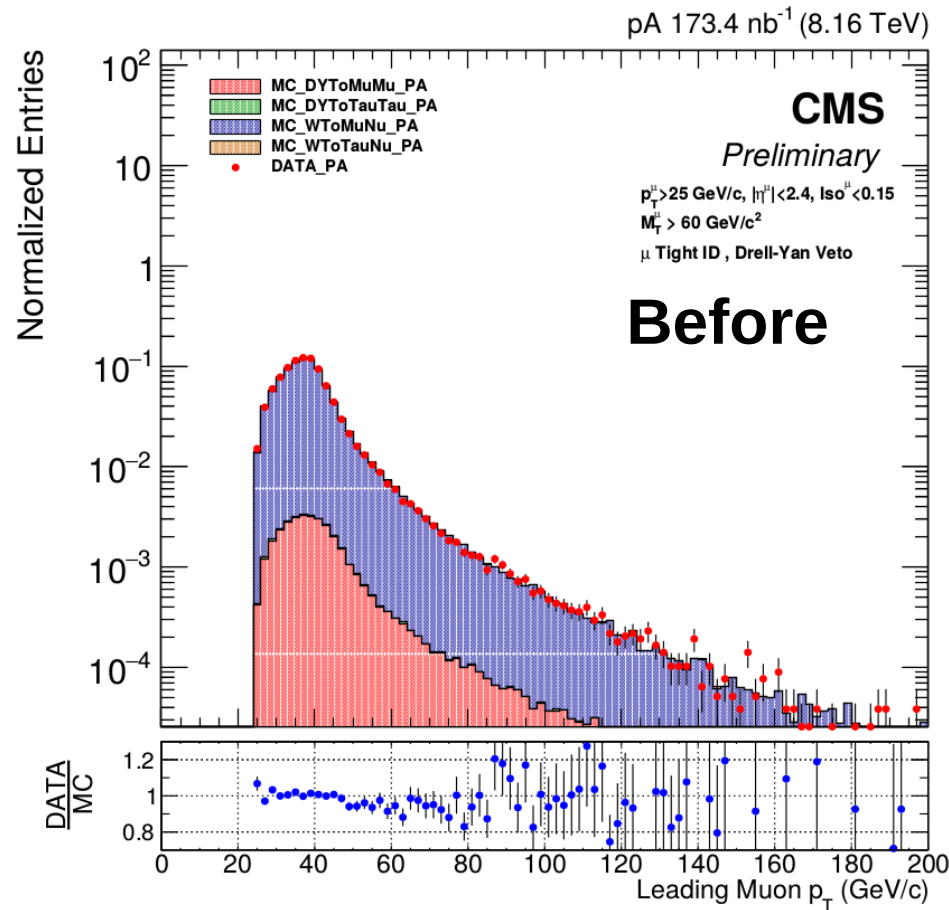


Nuclear PDF sets

nPDF	EPS09	EPPS16	nCTEQ15
Order	NLO	NLO	NLO
Fit	nucler modification	nuclear modification	nuclear PDF
Baseline PDF	CTEQ6	CT14	
Free parameters	15	20	17
Data points	929	1811	708
EMC DY dileptons in p-A	Yes	Yes	Yes
RHIC pions in d-A	Yes	Yes	Yes
SLAC l^\pm -A DIS	Yes	Yes	Yes
CHORUS ν -A DIS	No	Yes	No
RHIC DY in π -A	No	Yes	No
LHC dijets in pPb	No	Yes	No
LHC weak bosons in pPb	No	Yes	No

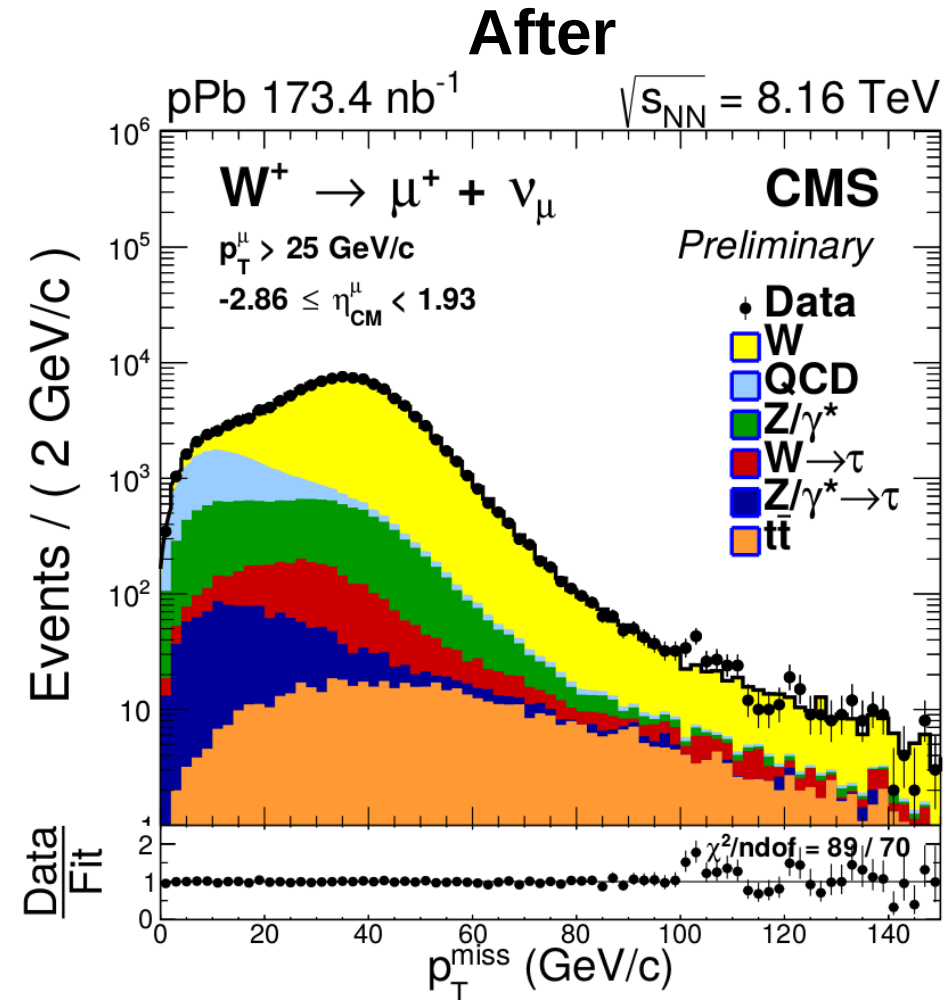
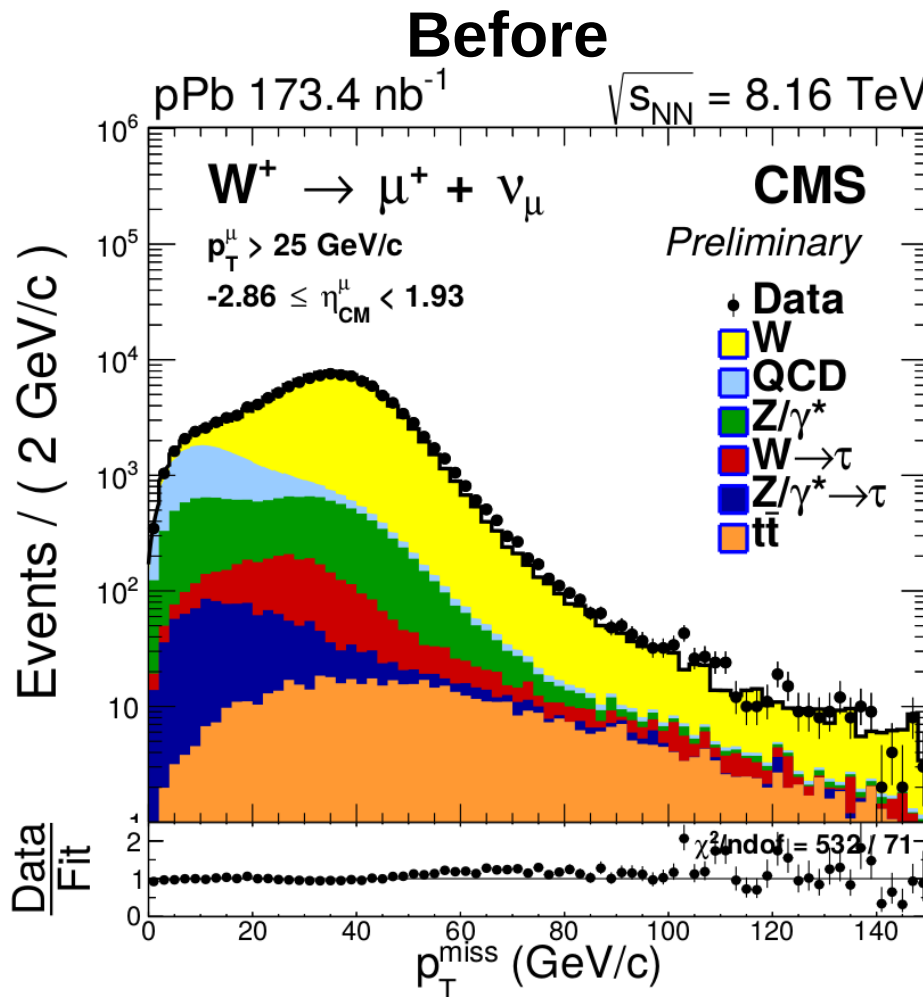
Muon p_T after correction

Impact on muon p_T of applying the weak boson p_T weighing

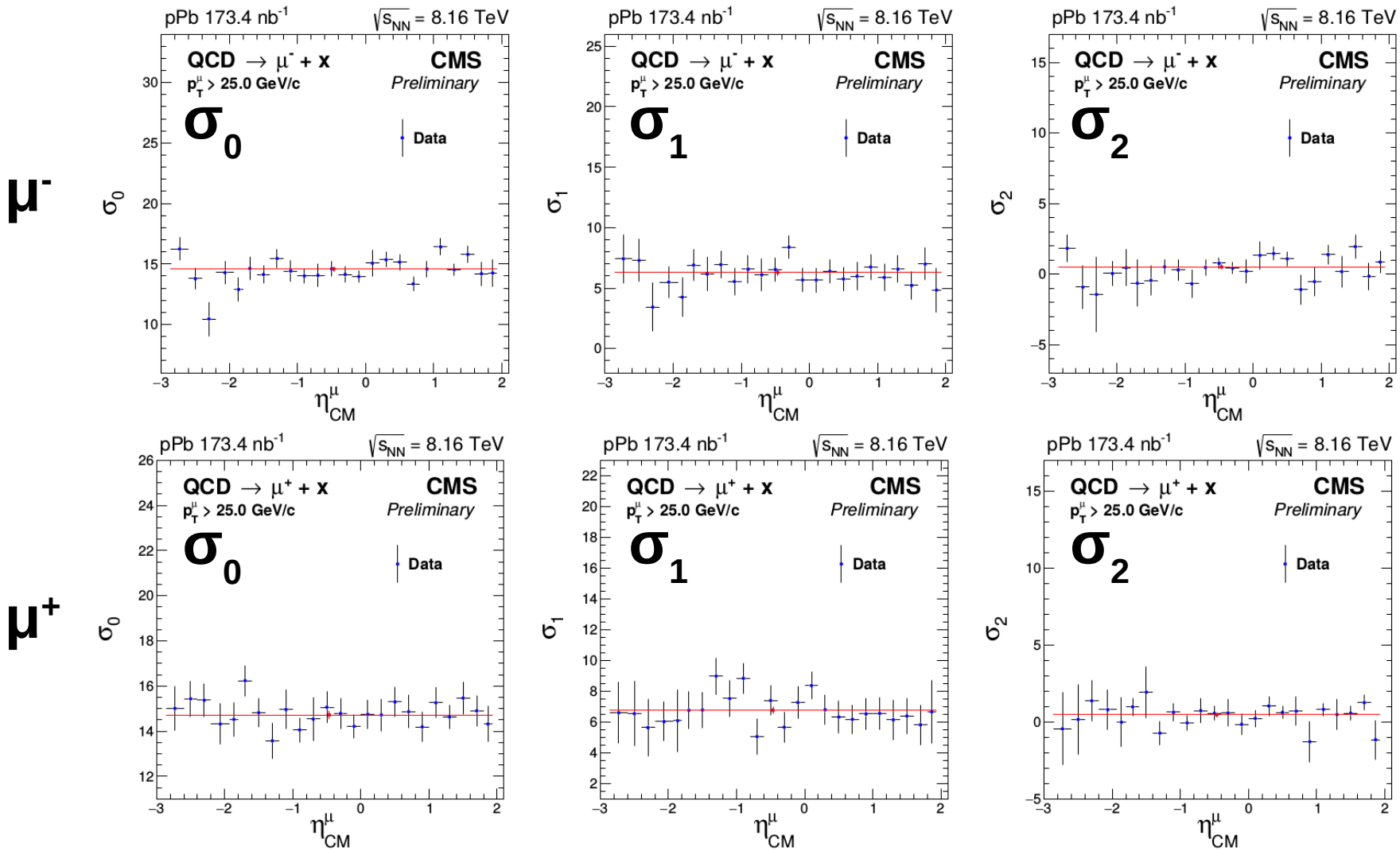


W-boson p_T^{miss} after recoil calibration

Impact on W-boson p_T^{miss} of calibrating the recoil



QCD jet p_T^{miss} parameters vs muon η

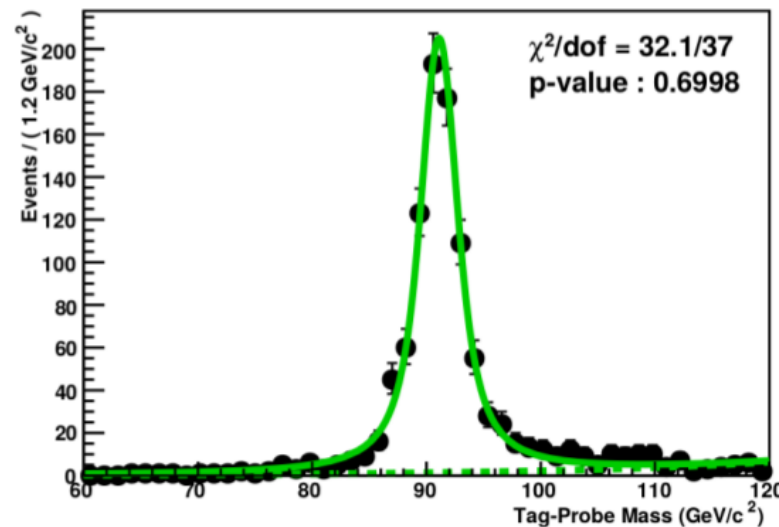


Modified Rayleigh distribution

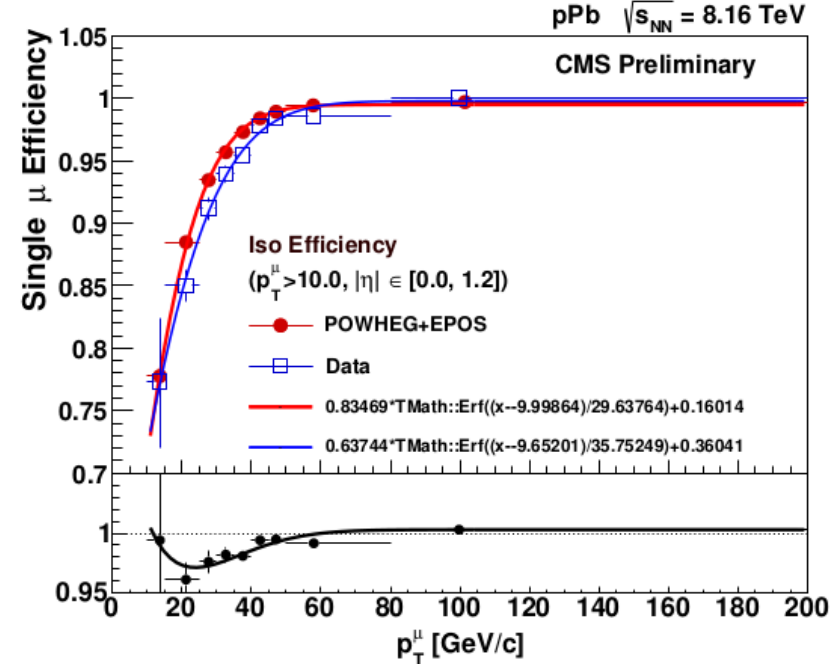
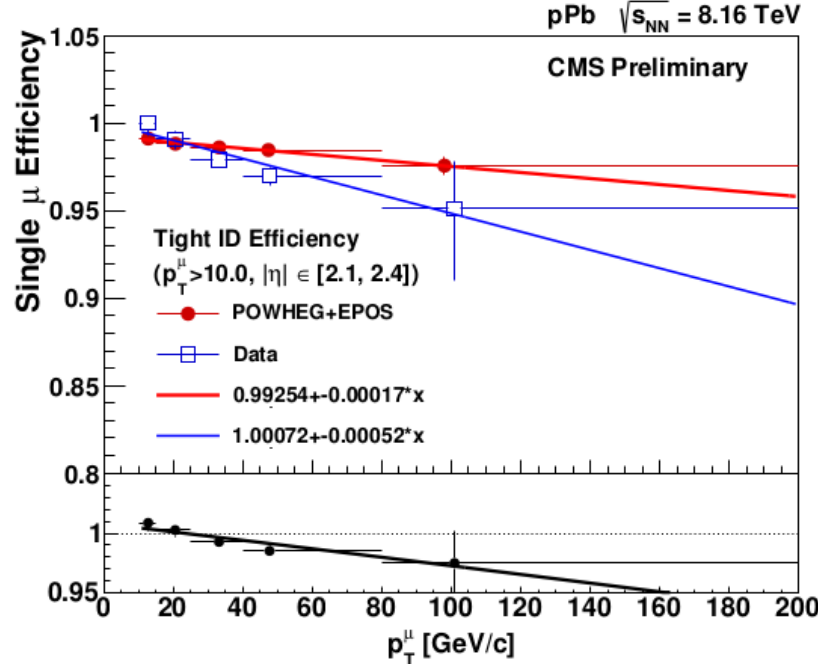
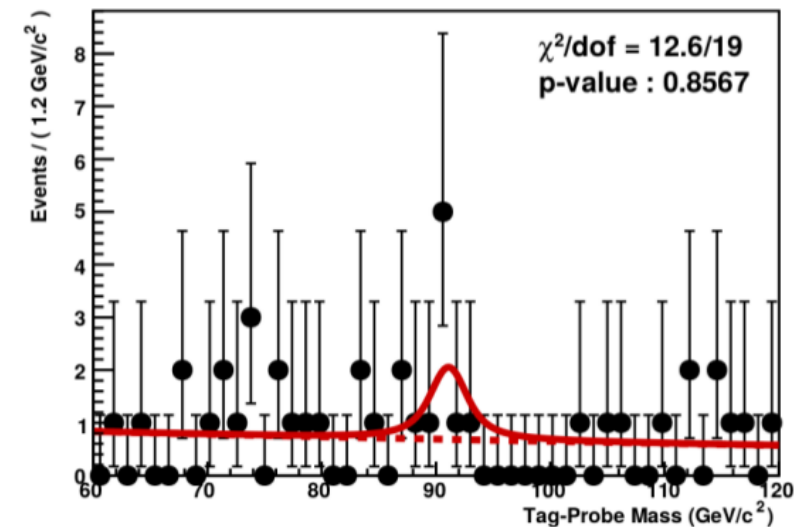
$$p_T^{\text{miss}} \cdot \exp \left(-\frac{(p_T^{\text{miss}})^2}{2(\sigma_0 + \sigma_1 \cdot p_T^{\text{miss}} + \sigma_2 \cdot (p_T^{\text{miss}})^2)} \right)$$

Tag and Probe

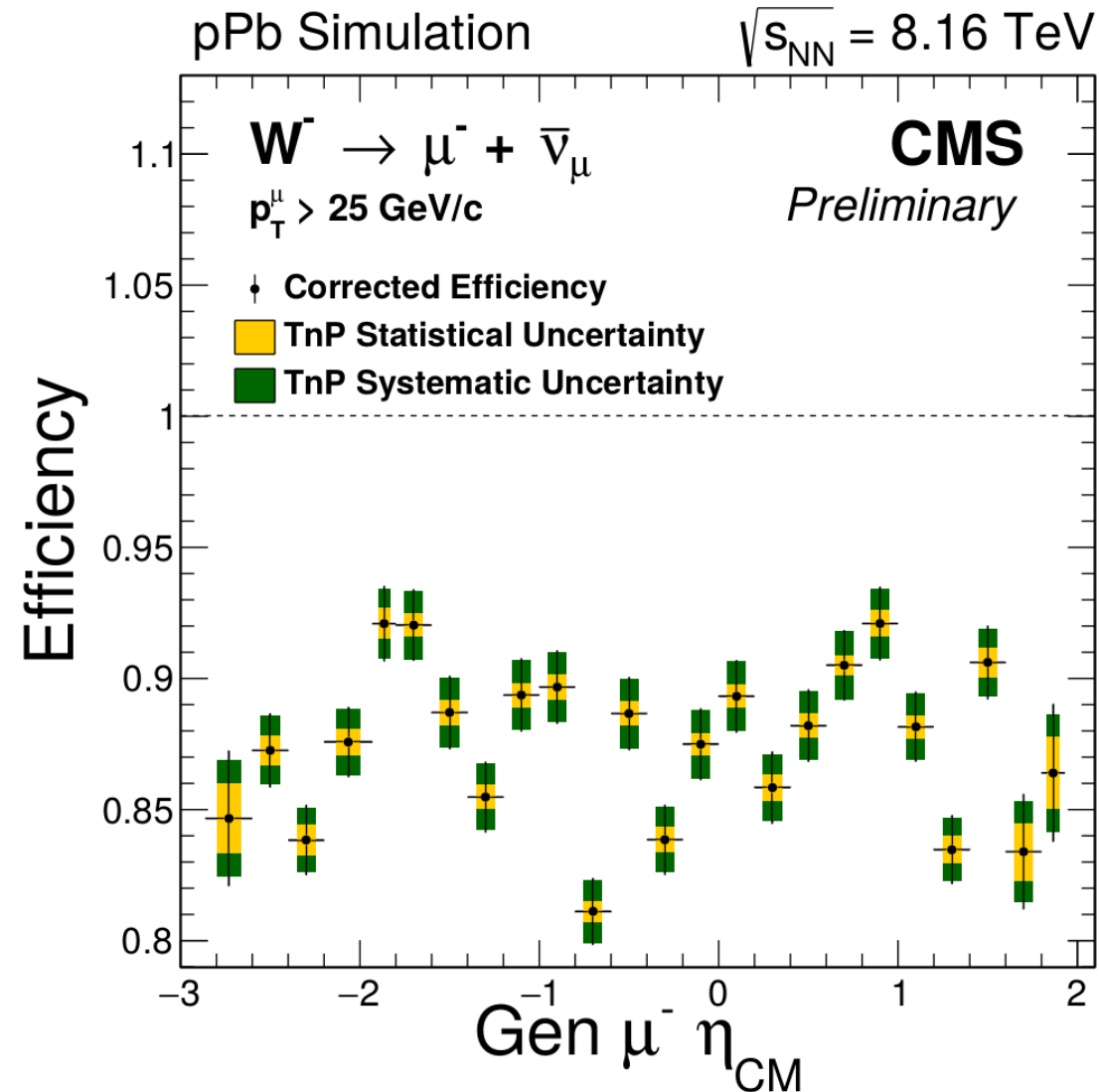
Passing Probes



Failing Probes



Muon efficiency

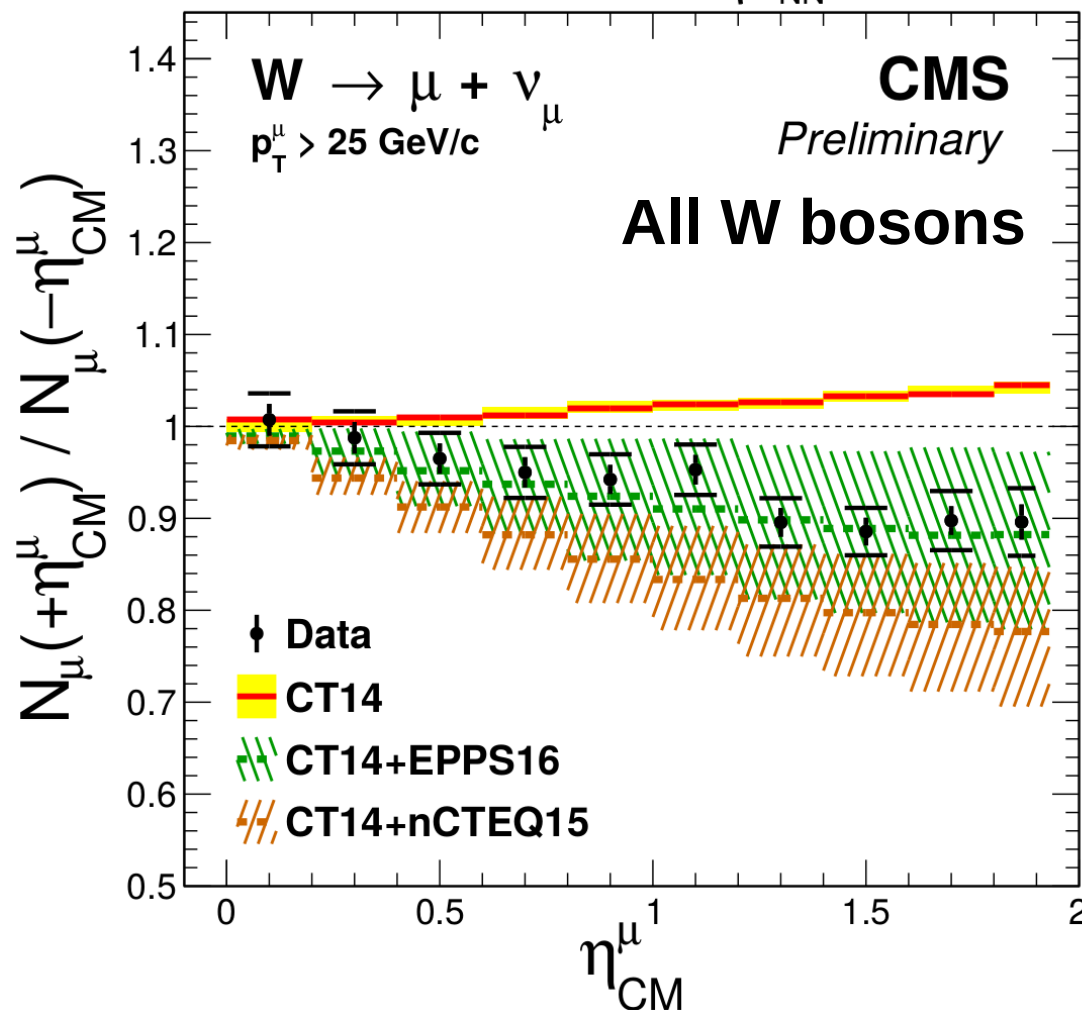


Forward-backward ratio

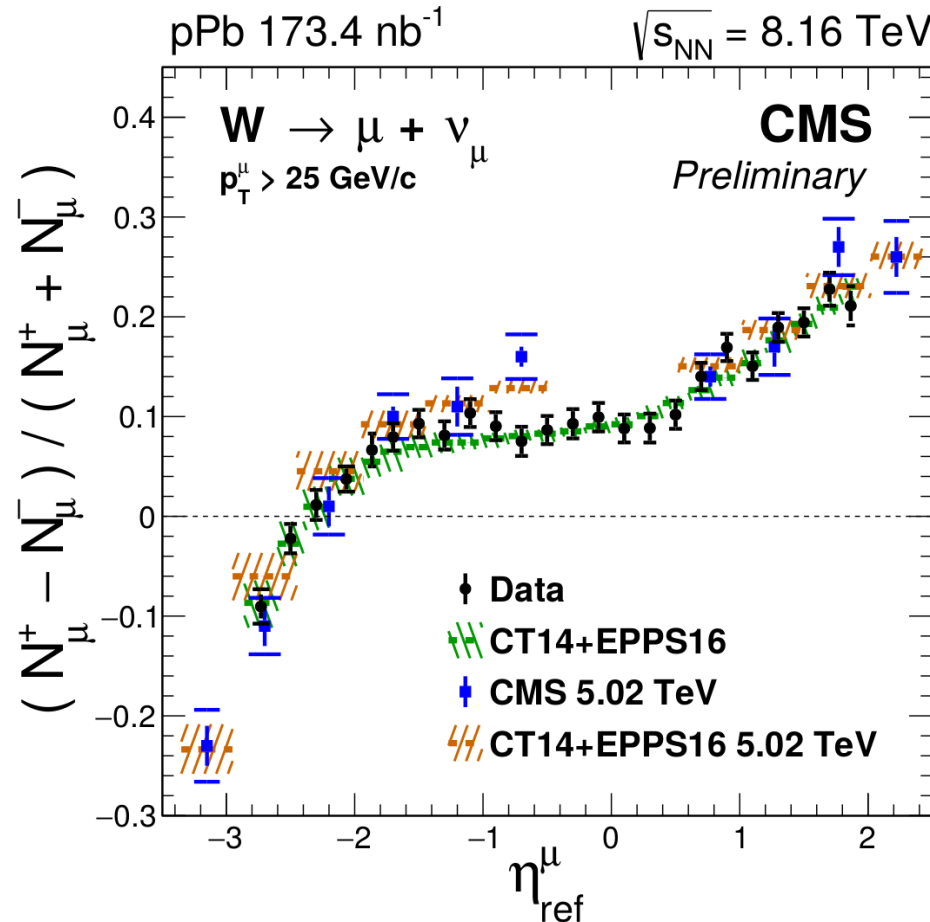
$P(\chi^2) = <0.01\% \text{ CT14} , 90\% \text{ nCTEQ15} , 99\% \text{ EPPS16}$

pPb 173.4 nb⁻¹

$\sqrt{s_{NN}} = 8.16 \text{ TeV}$



Muon charge asymmetry

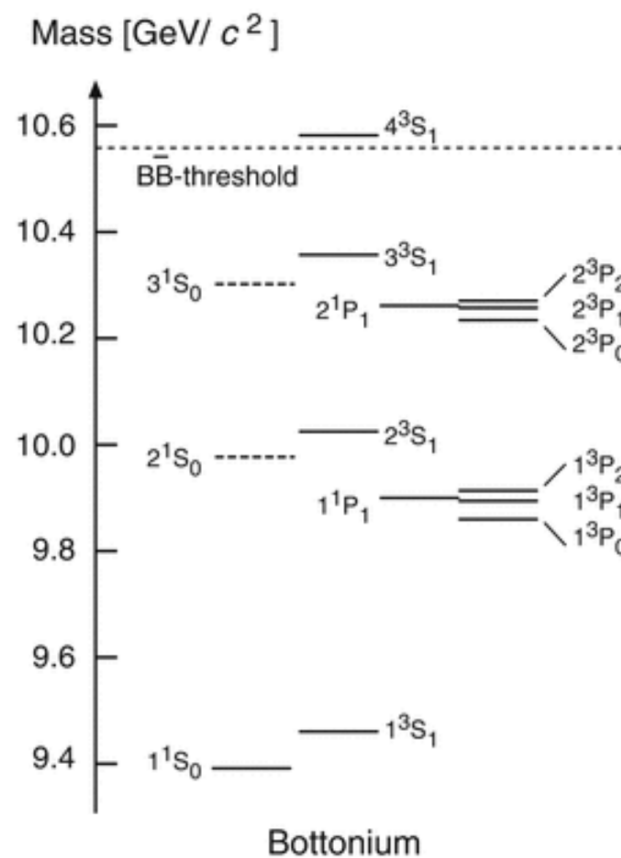
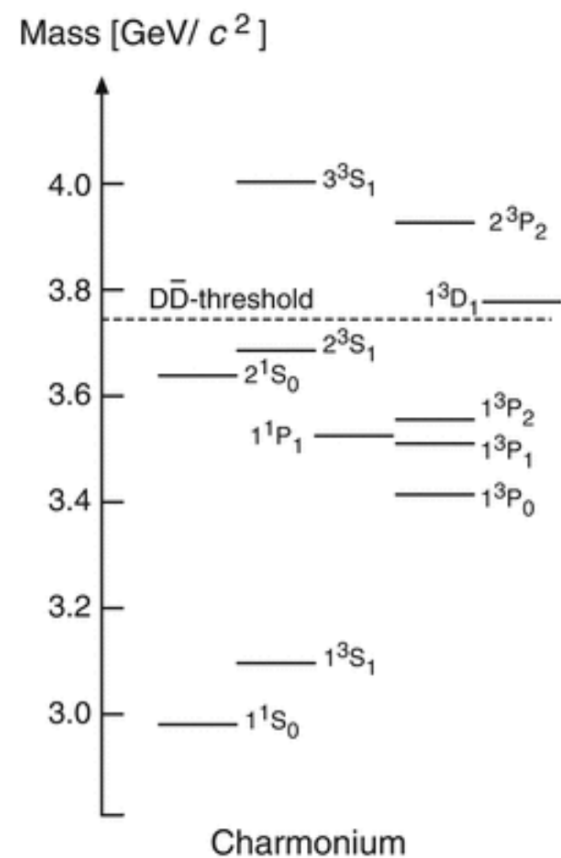


$$\eta_{\text{ref}}^\mu = \eta_{\text{CM}}^\mu \pm \ln \left(\frac{8.16 \text{ TeV}}{\sqrt{s_{NN}}} \right), \eta_{\text{CM}}^\mu \gtrless 0$$

Good agreement between measurement at 8.16 TeV and 5.02 TeV after shifting the η_{CM} taking into account the difference in energy

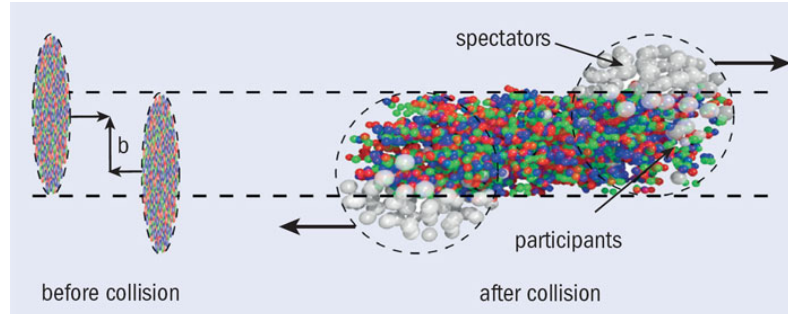
Prompt and nonprompt J/ψ

Quarkonia excited states



Glauber Model

In heavy collisions we need to characterize the size and shape of overlap region

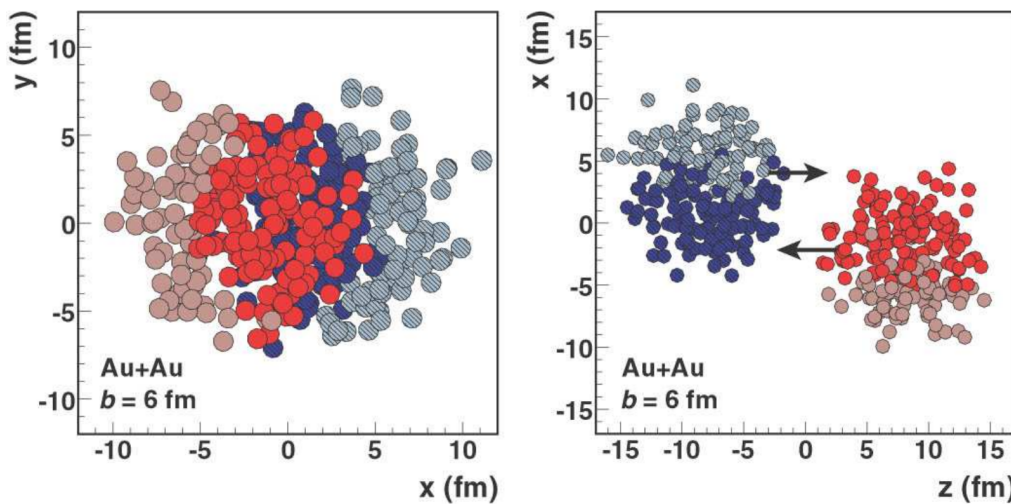


- b = impact parameter
- N_{part} = number of participants
- N_{col} = number of binary collisions

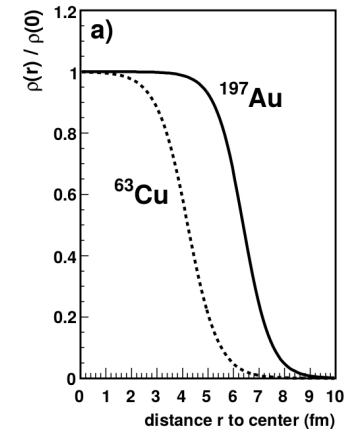
Not possible to be measured experimentally → use **Glauber MC model**

Inputs:

- Inelastic nucleon-nucleon cross section
- Nucleus density profile



$$\rho(r) = \rho_0 \cdot \frac{1 + w(r/R)^2}{1 + \exp\left(\frac{r-R}{a}\right)}$$



- Nucleons distributed with ρ (wood-saxon)
- Impact parameter generated: $d\sigma/db = 2\pi b$
- N-n collision happens if $d \leq \sqrt{\sigma_{\text{inel}}^{\text{NN}}/\pi}$

Acceptance and Efficiency

- Need to correct for the detector acceptance (\mathcal{A}) and efficiency (\mathcal{E}) → use simulations
- Simulated events are weighed to match the y and p_T distributions of J/ψ in data

Acceptance:

$$\mathcal{A}_{J/\psi}(p_T^{\mu\mu}, y^{\mu\mu}) = \frac{N_{\text{gen}, \mu \text{ in CMS}}^{J/\psi \rightarrow \mu^+ \mu^-}(p_T^{\mu\mu}, y^{\mu\mu})}{N_{\text{gen}}^{J/\psi \rightarrow \mu^+ \mu^-}(p_T^{\mu\mu}, y^{\mu\mu})}$$

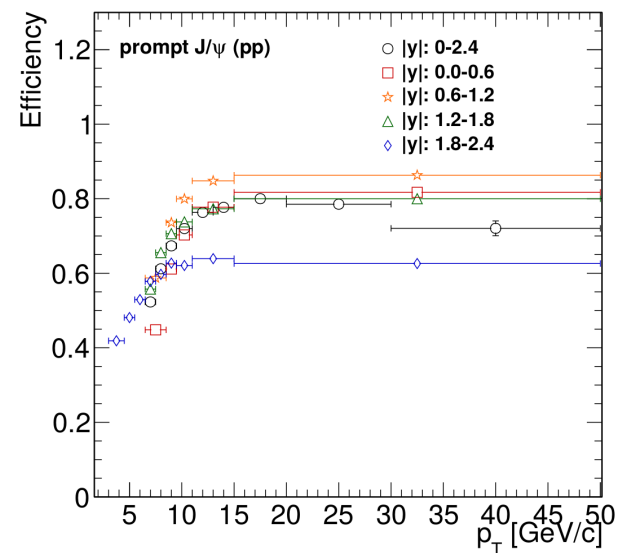
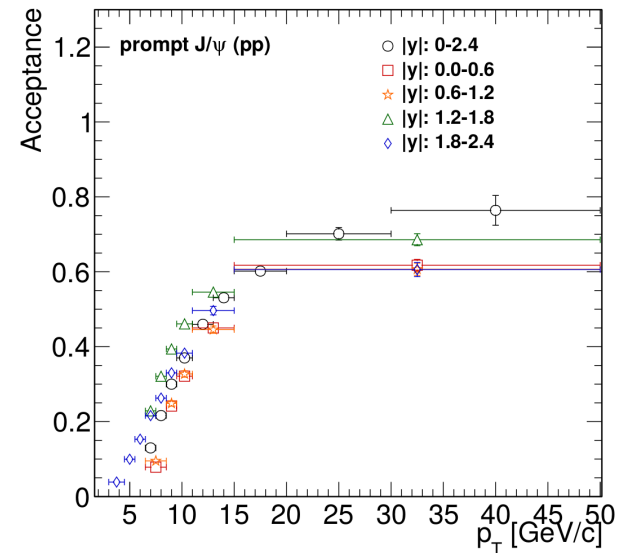
Number of J/ψ mesons
within CMS acceptance

All J/ψ mesons

Efficiency:

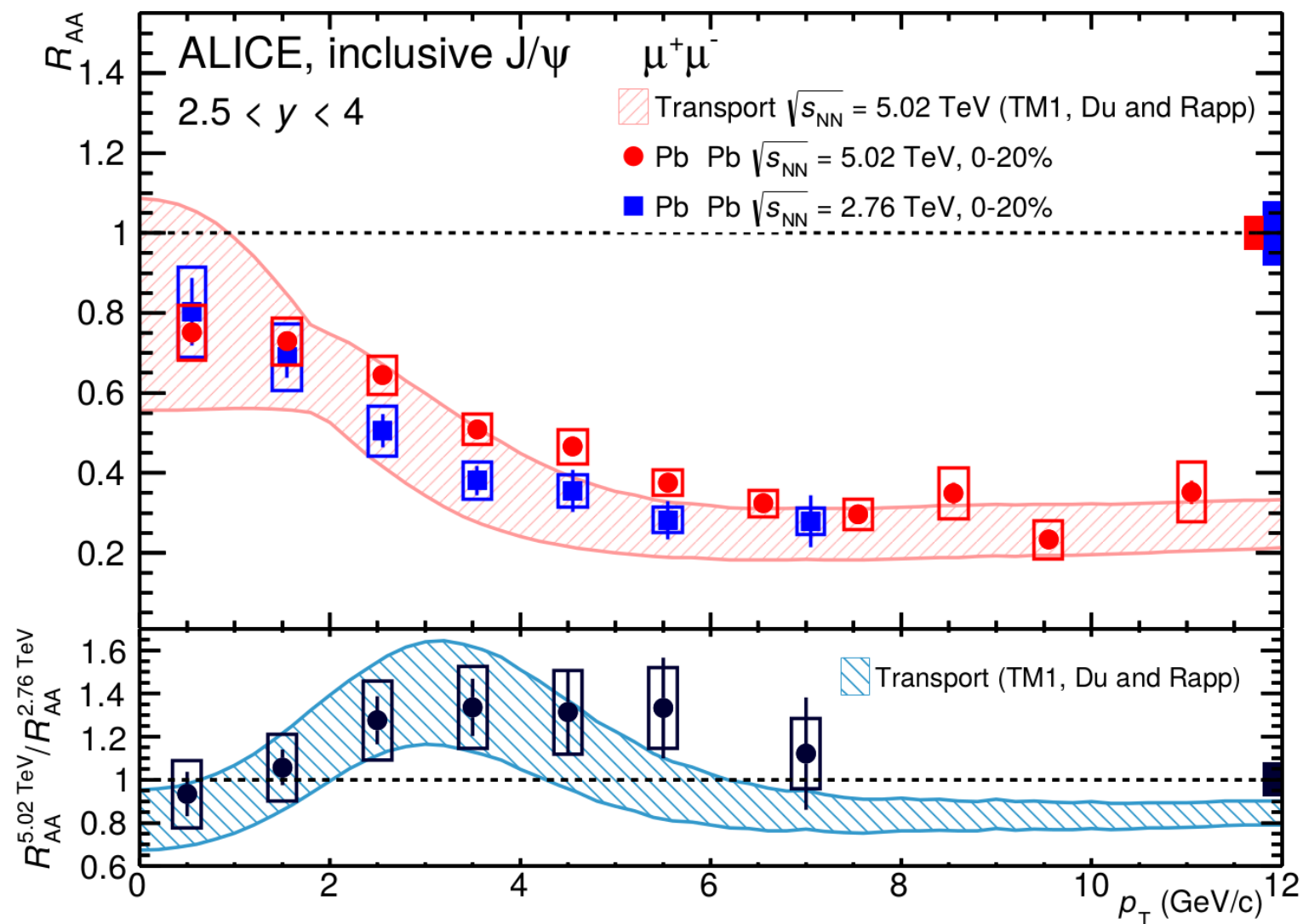
$$\epsilon_{J/\psi}(p_T^{\mu\mu}, y^{\mu\mu}) = \frac{N_{\text{candidate}}^{J/\psi \rightarrow \mu^+ \mu^-}(p_T^{\mu\mu}, y^{\mu\mu})}{N_{\text{gen}, \mu \text{ in CMS}}^{J/\psi \rightarrow \mu^+ \mu^-}(p_T^{\mu\mu}, y^{\mu\mu})}$$

Number of J/ψ mesons
passing analysis cuts



- Correction weights of data / MC muon efficiency ratios (derived with Tag&Probe) applied to J/ψ efficiency

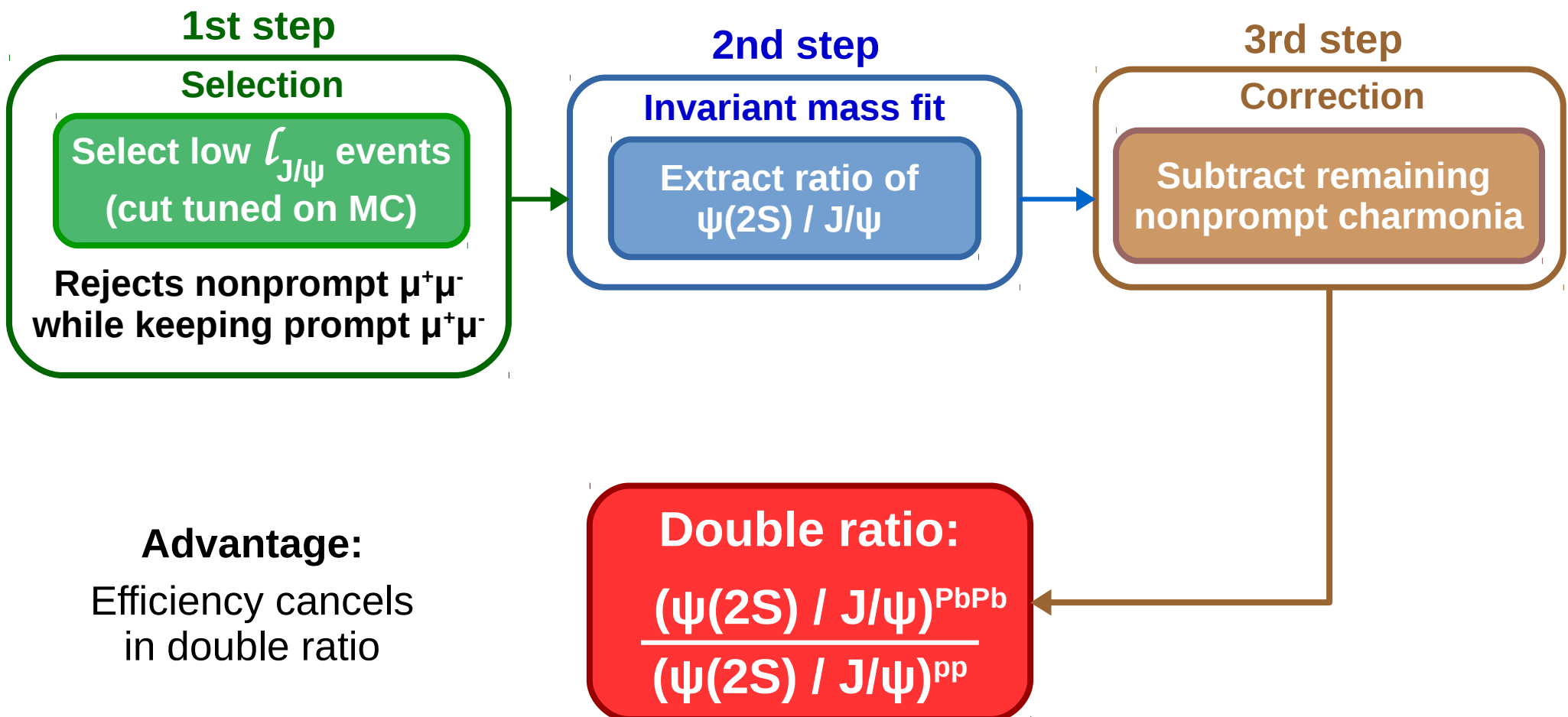
ALICE J/ ψ R_{AA}



Measurement of prompt $\psi(2S)$ / J/ψ double ratio

Measurement of $\Psi(2S) / J/\psi$ double ratio

- Lack of $\Psi(2S)$ statistics in Pb-Pb data → 2D fits not possible
- Use alternative method to separate prompt and nonprompt charmonia



Measurement of $\Psi(2S) / J/\psi$ double ratio

1st step

Selection

Select low $\ell_{J/\psi}$ events
(cut tuned on MC)

Rejects nonprompt $\mu^+\mu^-$
while keeping prompt $\mu^+\mu^-$

2nd step

Invariant mass fit
Extract ratio of
 $\Psi(2S) / J/\psi$

3rd step

Correction

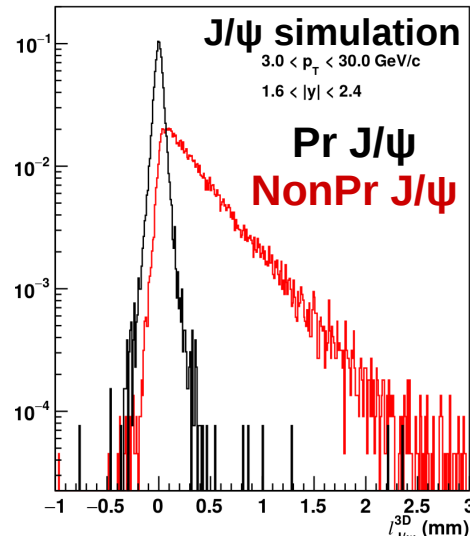
Subtract remaining
nonprompt charmonia

Double ratio:

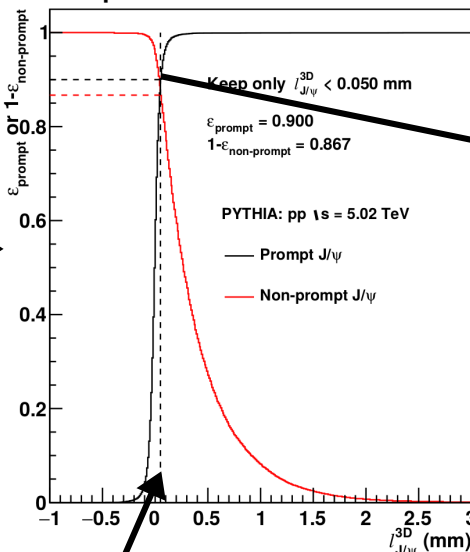
$$\frac{(\Psi(2S) / J/\psi)^{\text{PbPb}}}{(\Psi(2S) / J/\psi)^{\text{pp}}}$$

$\ell_{J/\Psi}$ prompt selection

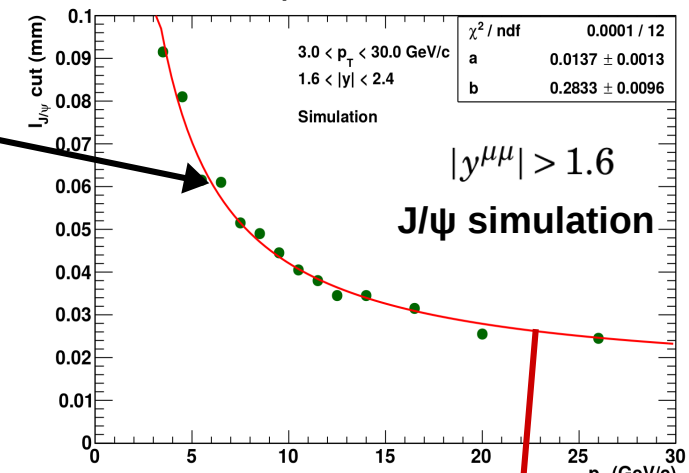
$\ell_{J/\Psi}$ distribution



$\ell_{J/\Psi}$ cut efficiency



$\ell_{J/\Psi}$ cut vs p_T

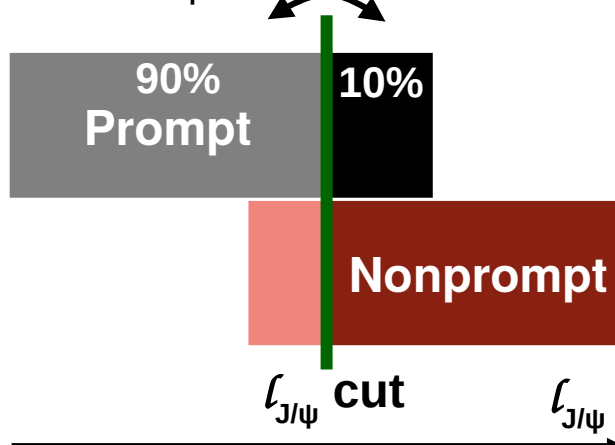


$\ell_{J/\Psi}$ threshold set to keep 90% of prompt J/ψ

$\ell_{J/\Psi}$ cut efficiency depends on p_T

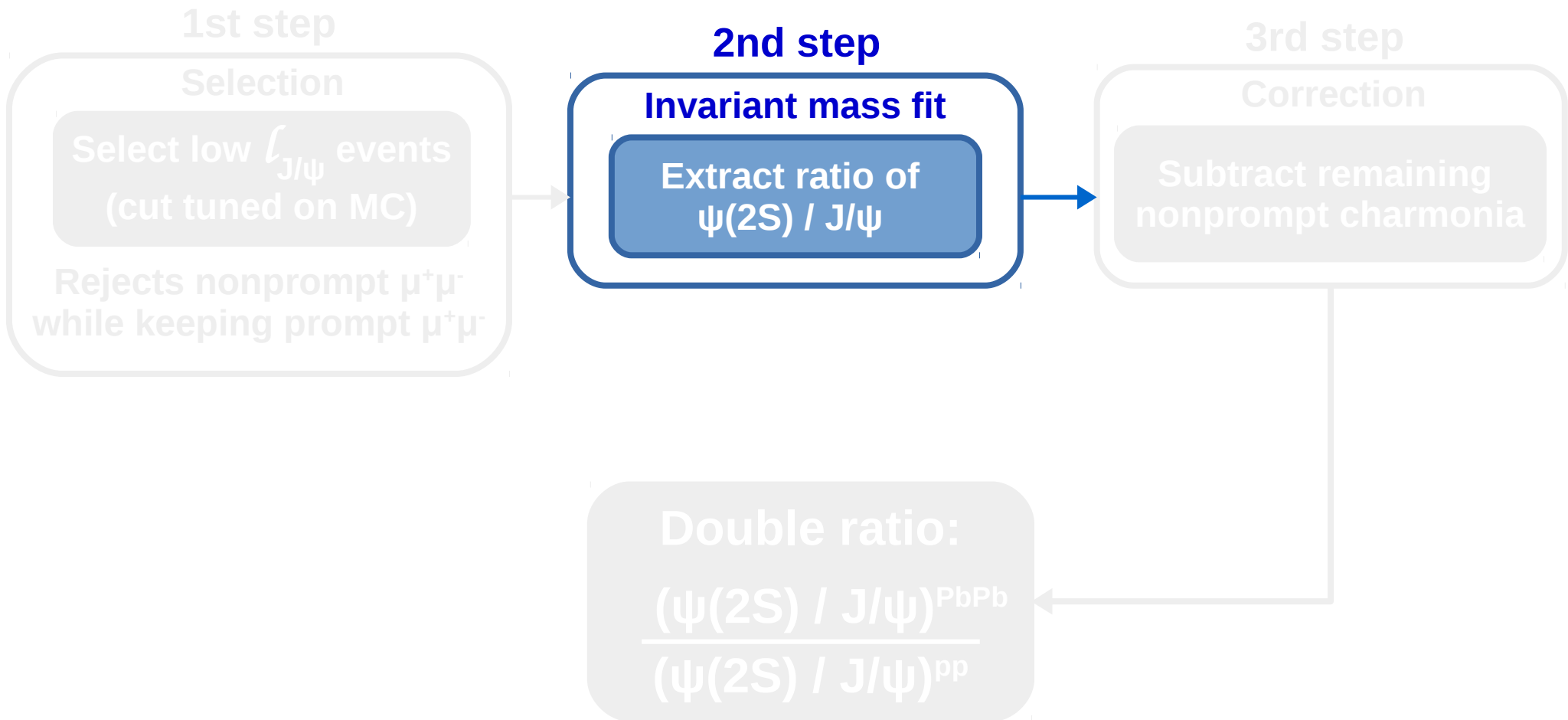
$$l_P(p_T^{\mu\mu}) = a + \frac{b}{p_T^{\mu\mu}}$$

$\ell_{J/\Psi}$ cut efficiency

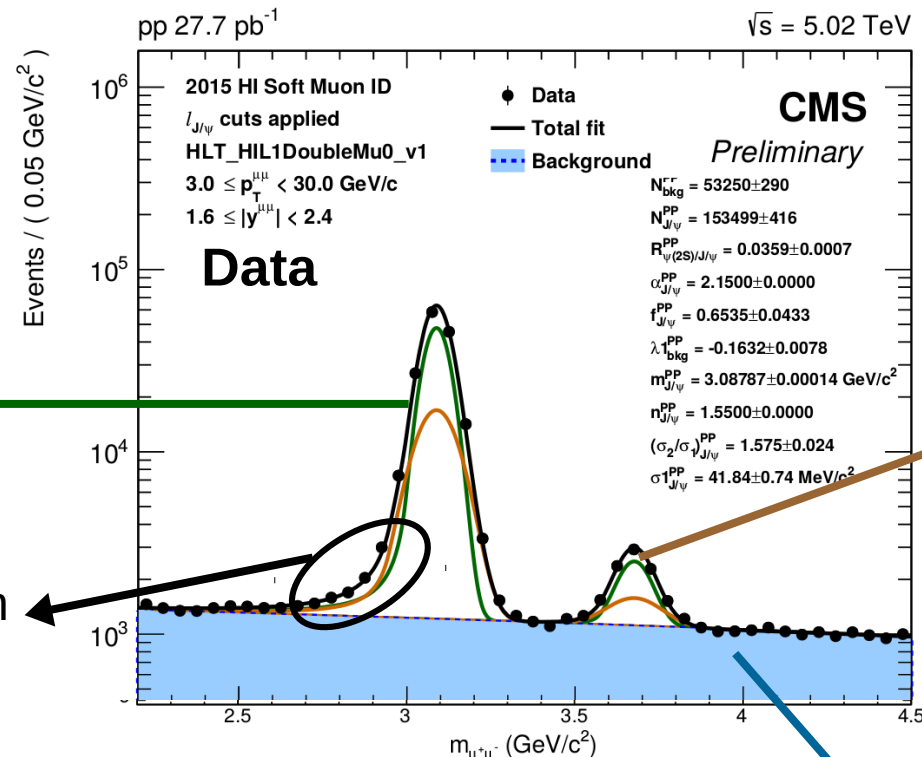


$$\ell_{J/\Psi}[\text{mm}] < \begin{cases} 0.012 + (0.23/p_T^{\mu\mu}[\text{GeV}/c]), & \text{if } |y^{\mu\mu}| \leq 1.6 \\ 0.014 + (0.28/p_T^{\mu\mu}[\text{GeV}/c]), & \text{if } |y^{\mu\mu}| > 1.6 \end{cases}$$

Measurement of $\Psi(2S) / J/\psi$ double ratio



Invariant mass fit



**J/ ψ shape:
2 Crystal Balls**

Tail parameters tuned on
 J/ψ simulation and fixed
on data

**$\psi(2S)$ shape:
2 Crystal Balls**

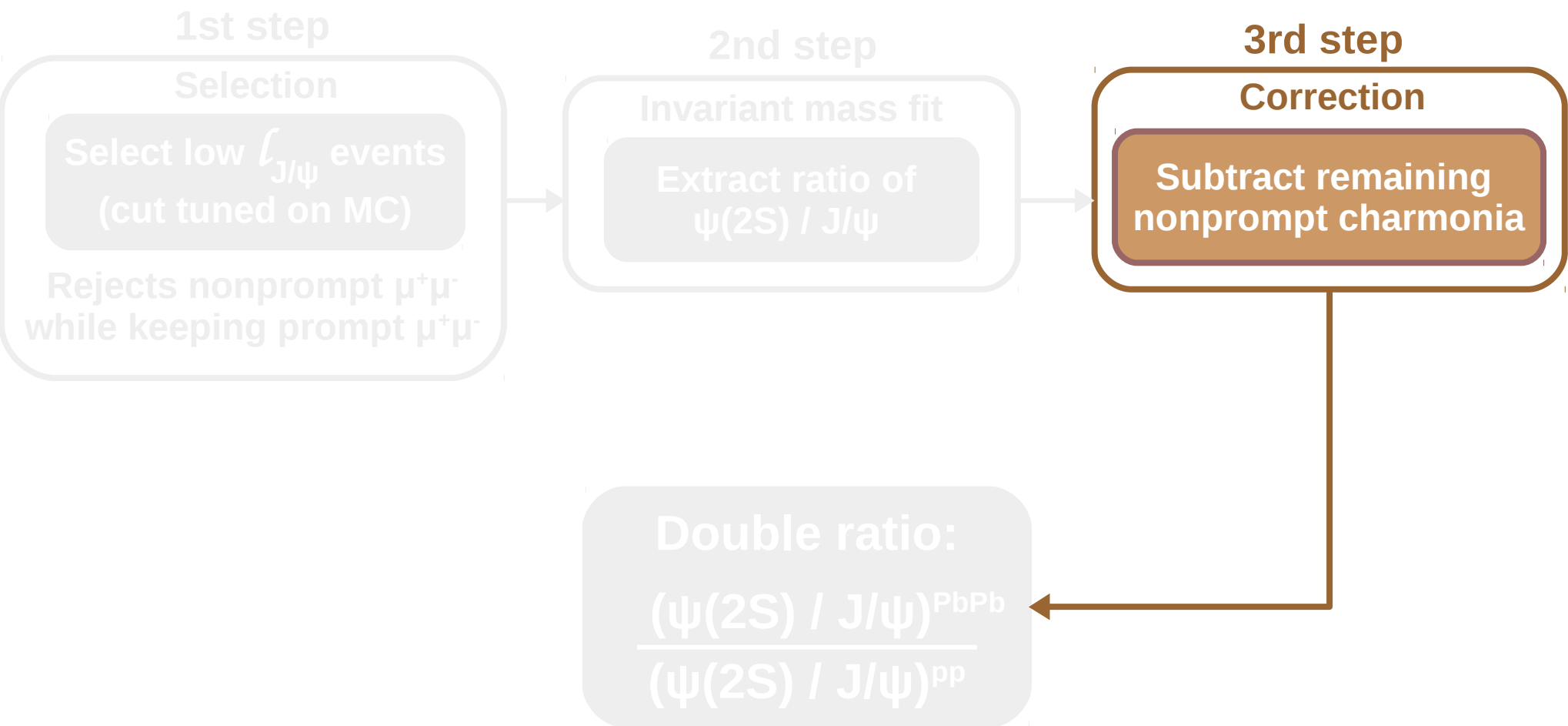
Fixed to J/ψ shape

**Background shape:
Chebyshev polynomial**

- Extract from fit:**
- $N^{J/\psi}$ = number of J/ψ mesons
 - R = ratio of $\psi(2S)$ / J/ψ yields

Best order selected with
Log-Likelihood-ratio test

Measurement of $\Psi(2S) / J/\psi$ double ratio



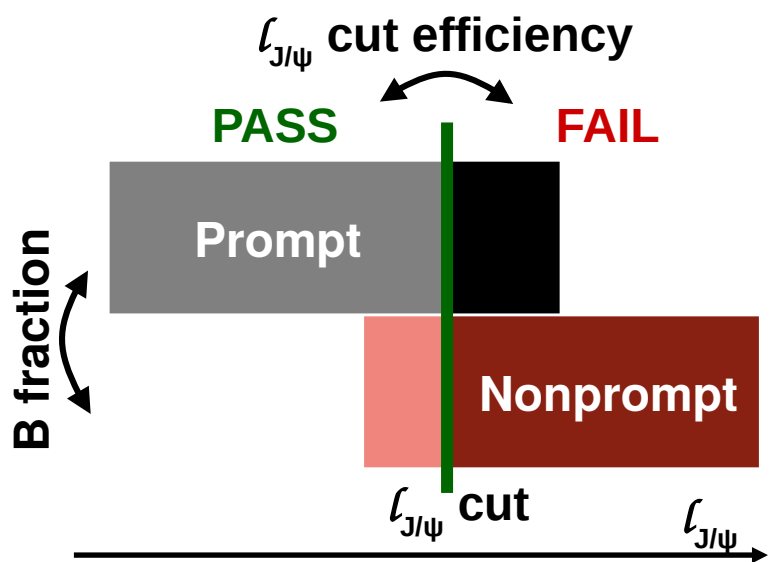
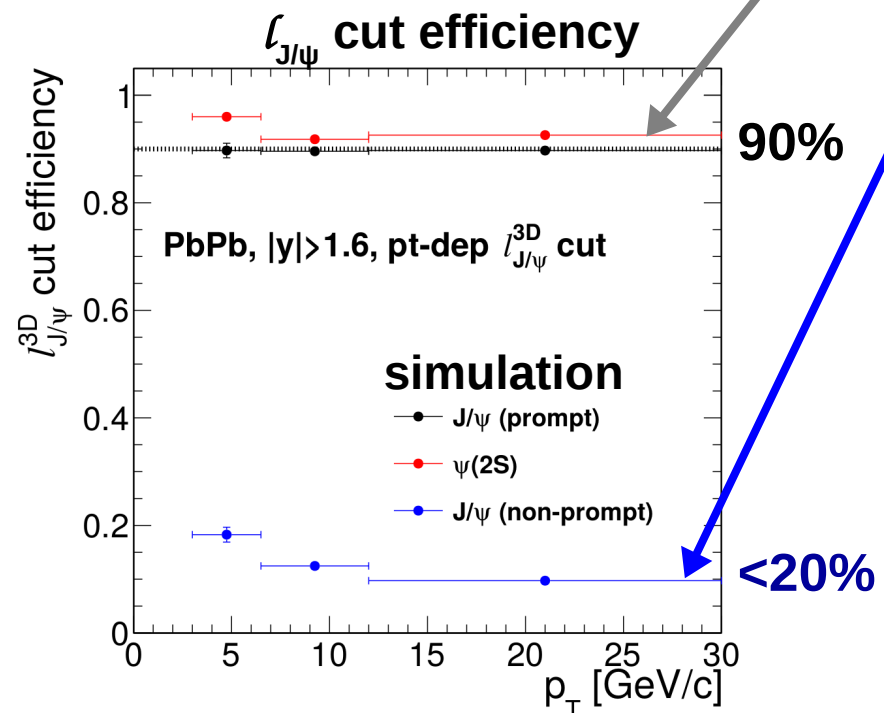
Nonprompt J/ ψ subtraction

Number of charmonia extracted from mass fits
applying $\ell_{J/\psi}$ cut

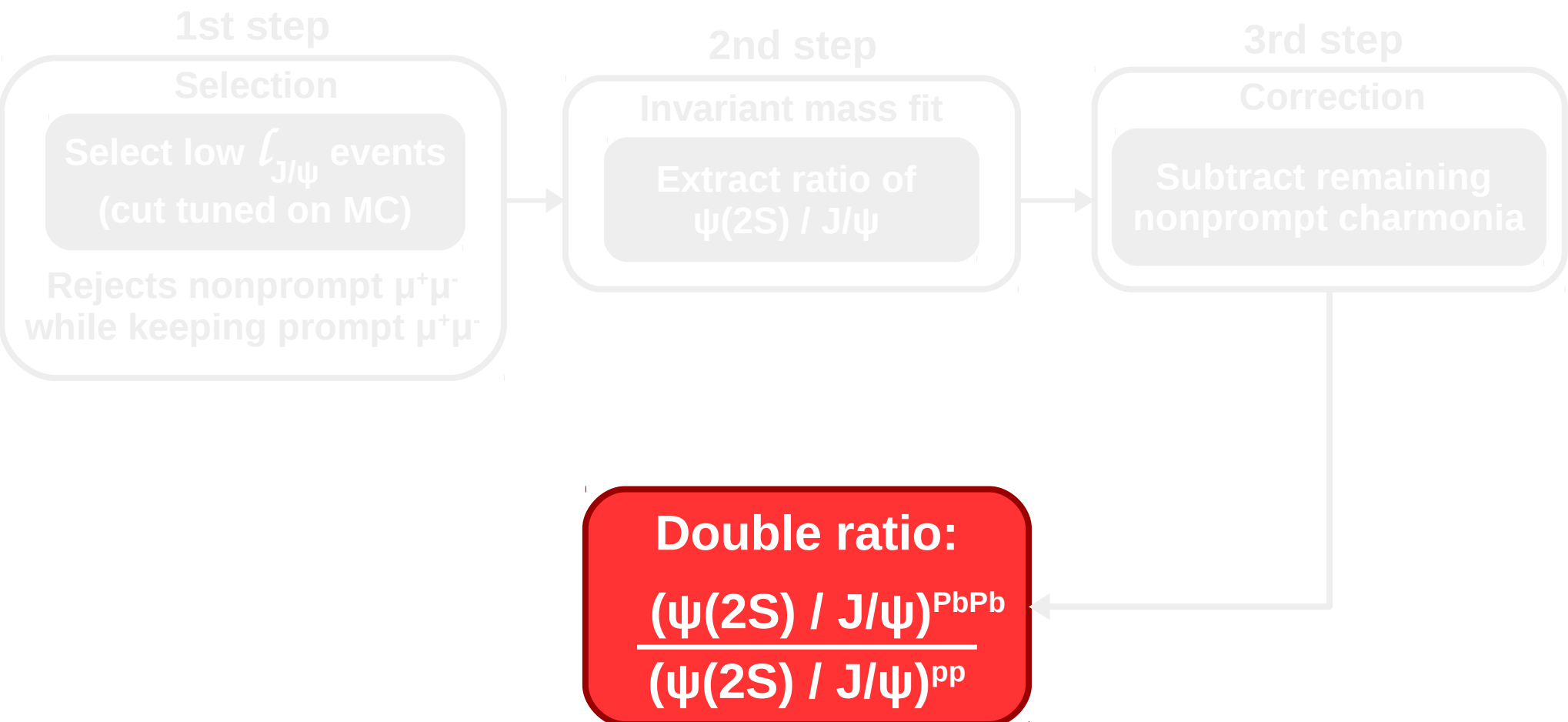
Number of charmonia extracted from mass fits
without $\ell_{J/\psi}$ cut

Number of prompt charmonia

$$N_{\psi}^P = \frac{N_{\psi}^{\text{pass}} - \epsilon_{\psi}^{\text{NP}} \cdot N_{\psi}^{\text{tot}}}{\epsilon_{\psi}^P - \epsilon_{\psi}^{\text{NP}}}$$



Measurement of $\Psi(2S) / J/\psi$ double ratio



Measurement of $\psi(2S)$ / J/ψ double ratio

Double ratio of prompt $\psi(2S)$ over J/ψ meson yields is derived as:

$$\frac{(N_{\psi(2S)}^P/N_{J/\psi}^P)_{\text{PbPb}}}{(N_{\psi(2S)}^P/N_{J/\psi}^P)_{\text{pp}}}$$

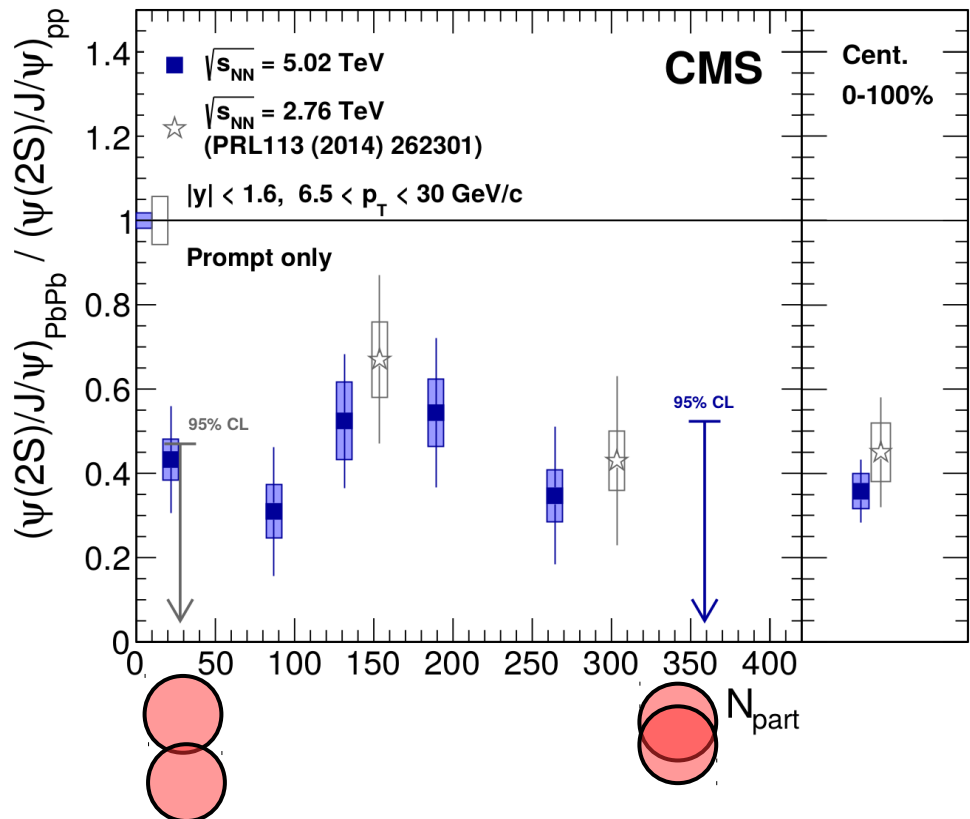
Source of uncertainty	Max. uncertainty
Signal extraction	0.11
Cancellation of efficiencies	0.05
Nonprompt subtraction	0.07

- Signal extraction is the dominant source of uncertainty

$\Psi(2S) / J/\psi$ double ratio

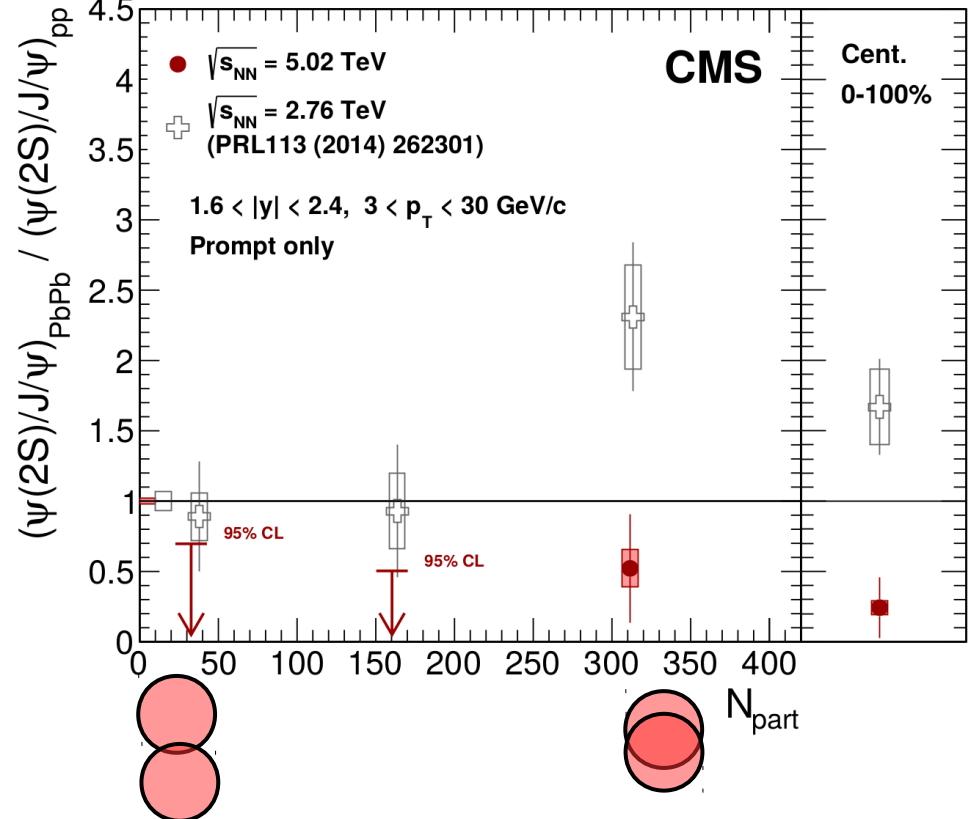
$|y| < 1.6 ; 6.5 < p_T < 30 \text{ GeV}/c$

PbPb $351 \mu\text{b}^{-1}$, pp 28.0 pb^{-1} (5.02 TeV)



$1.6 < |y| < 2.4 ; 3 < p_T < 30 \text{ GeV}/c$

PbPb $351 \mu\text{b}^{-1}$, pp 28.0 pb^{-1} (5.02 TeV)



- $\Psi(2S)$ is more suppressed than J/ψ at 5.02 TeV
- No strong N_{part} dependence at 5.02 TeV
- Double ratio at 5.02 TeV consistently lower than at 2.76 TeV in $1.6 < y < 2.4$, $3 < p_T < 30 \text{ GeV}/c$, especially for most central collisions (~ 3 s.d. in 0-100%)